Technical University of Denmark

DTU

Power Management for Energy Systems

Hovgaard, Tobias Gybel; Jørgensen, John Bagterp; Blanke, Mogens; Larsen, Lars Finn Sloth

Publication date:
2013

Document Version
Publisher's PDF, also known as Version of record

Link back to DTU Orbit

DTU Library
Technical Information Center of Denmark

Power Management for Energy Systems

Tobias Gybel Hovgaard
PhD Thesis, February 2013

Preface

This thesis was prepared at the Department of Applied Mathematics and Computer Science (DTU Compute, formerly known as DTU Informatics) at the Technical University of Denmark with assistance from DTU Elektro and IPU Technology Development, in partial fulfillment of the requirements for acquiring the PhD degree in engineering. The project was funded jointly by Vestas Wind Systems A/S, Danfoss A/S, and the Danish Agency for Science, Technology and Innovation—Ministry of Science, Innovation, and Higher Education of Denmark, under the Industrial PhD program, project 10-078007.

The thesis deals with control methods for flexible and efficient power consumption in commercial refrigeration systems that possess thermal storage capabilities, and for facilitation of more environmental sustainable power production technologies such as wind power. We apply economic model predictive control as the overriding control strategy and present novel studies on suitable modeling and problem formulations for the industrial applications, means to handle uncertainty in the control problems, and dedicated optimization routines to solve the problems involved. Along the way, we present careful numerical simulations with simple case studies as well as validated models in realistic scenarios.

The thesis consists of a summary report and a collection of 13 research papers written during the period Marts 2010 to February 2013. Four are published in international peer-reviewed scientific journals and 9 are published at international peer-reviewed scientific conferences.

Kgs. Lyngby, February 2013

Tobias Gybel Hovgaard

Acknowledgements

It is with gratitude that I look back over my time as Industrial Ph.D. student and think of the many people who have helped me get this far. First and foremost I would like to thank my university supervisor, Assoc. Prof. JOHN BAGTERP JØRGENSEN (DTU Compute), my industrial supervisor Dr. LARS F. S. LARSEN at Vestas Wind Systems A/S, and my co-supervisor Dr. MORTEN JUEL SKOVRUP at IPU Technology Development for the excellent guidance, support and motivation. Their teaching, assistance, and mentoring made this experience extremely satisfying

Also, I would like to thank Prof. STEPHEN P. BOYD at Stanford University, Department of Electrical Engineering, for his hospitality, invaluable guidance, and collaboration during my stay at his department. Working with Prof. Boyd and living in the San Francisco Bay Area for six months was a lifetime experience and I learned so much. Thanks are also extended to the others in the group at Stanford University for allowing me to be part of their work and for fruitful discussions.

I would like to thank my great colleagues at Vestas Wind Systems A/S, at DTU, and (my former colleagues) at Danfoss A/S for contributing to an inspiring working environment and for their interest in this project and the willingness to assist, discuss, and guide when needed. In particular, I want to thank my former boss, initiator of this project, and a great mentor, CLAUS THYBO, for invaluable advice and for being a tremendous source of inspiration. Thanks also go to my fellow Ph.D. student, friend, and collaborator, Rasmus Halvgaard, for joint work and countless discussions. In addition, I would like to give thanks to my four fellow co-founders of the Danish Smart Grid Research Network, for great collaboration, inspiration, and memorable achievements obtained together.

Summary (in English)

In this thesis, we consider the control of two different industrial applications that belong at either end of the electricity grid; a power consumer in the form of a commercial refrigeration system, and wind turbines for power production. Our primary studies deal with economic model predictive control of a commercial multi-zone refrigeration system, consisting of several cooling units that share a common compressor, and is used to cool multiple areas or rooms, *e.g.*, in supermarkets. Substantial amounts of energy are consumed in refrigeration systems worldwide and there is a strong motivation for introducing more energy efficient as well as cost reducing control techniques. At the same time, the power grid is evolving from a centralized system with rather controllable production in the conventional power plants to a much more decentralized network of many independent power generators and a large penetration of renewable, fossil-free energy sources such as solar and wind power. To facilitate such intermittent power producers, we must not only control the production of electricity, but also the consumption, in an efficient and flexible manner. By enabling the use of thermal energy storage in supermarkets, we open up for flexible power consumption schemes with the possibility of reducing operational costs and we develop and demonstrate prototype control technology that creates completely new business opportunities for selling regulating power to the grid. Moreover, this enables a larger penetration of wind energy in the power production and increases the potential market size for wind power generators and other renewable energy sources. Thus, we aim at promoting the use of environmentally sustainable power production technologies while creating new business opportunities for both power consumers and producers of renewable energy.

The second application, wind turbines, takes us to the production side of the power grid. The key concern here is to improve the quality and integrability of power

delivered to the grid from large parks of wind turbines. Our goal is to reduce the fluctuating nature of the power output and to meet tightened demands from the grid by enabling a more intelligent control at both the individual turbine level, at the park controller level, and in cooperation with flexible power consumers or other means of energy storage. The possible interaction and synergies of the two applications are obvious reasons to consider both in this thesis, and as we will see, the similarities in our formulations of the different control problems allow us to apply almost identical techniques despite the lack of immediate similarity.

For control of the commercial refrigeration application as well as the wind turbine application, we propose an economic optimizing model predictive controller, economic MPC. MPC is a feedback control technique that is characterized by its explicit handling of constrained control problems in which a model is used to predict the future behavior of a system along with forecasts of future disturbances. At each time step the values of the control inputs are computed by solving an open-loop finite time optimal control problem over a defined prediction horizon. Only the first step in this optimal open-loop sequence is implemented as a control command. Feedback is obtained by solving the open-loop problem repeatedly, in a receding horizon fashion, as new predictions become available.

Our investigations are primarily concerned with: 1) modeling of the applications to suit the chosen control framework; 2) formulating the MPC controller laws to overcome challenges introduced by the industrial applications, and defining economic objectives that reflect the real physics of the systems as well as our control objectives; 3) solving the involved, non-trivial optimization problems efficiently in real-time; 4) demonstrating the feasibility and potential of the proposed methods by extensive simulation and comparison with existing control methods and evaluation of data from systems in actual operation.

We present contributions on:
- Economic MPC for commercial refrigeration systems, including
  - Linear economic MPC formulations that utilize the flexibility in refrigeration systems to counteract fluctuations in the balance between power consumption and production.
  - Economic MPC with probabilistic constraints, ensuring a robust performance and constraint satisfaction in spite of inaccurate system models and forecasts.
  - Nonlinear economic MPC, reflecting the nonconvexity in the realistic description of temperature dependent efficiencies in the refrigeration cycle.
  - Nonlinear economic MPC with uncertain predictions and the implementation of very simple predictors that use entirely historical data of, *e.g.*, electricity prices and outdoor temperatures.

- Economic MPC for wind turbines, including

  - Optimal steady-state calculation for wind farms.
  - Nonlinear economic MPC for individual turbines.
  - Change of variables and convex formulations of economic MPC for individual turbines.

- Tractable optimization methods for the MPC problems, including

  - Sequential convex programming (SCP) for specific nonconvex problems originating from our studies of commercial refrigeration as well as from our studies concerning wind power.
  - Successful demonstration of the SCP approach on three different problems—the commercial refrigeration system with linear dynamics and constraints and a nonconvex objective, the individual wind turbine with nonlinear dynamics and constraints, and the static optimization of the wind farm with a black-box model.

The major contribution is the formulation of these problems and the demonstrations to show that the SCP method can be used for their solution.

We demonstrate, i.a., substantial cost savings, on the order of 30 %, compared to a standard thermostat-based supermarket refrigeration system and show how our methods exhibit sophisticated demand response to real-time variations in electricity prices. Violations of the temperature ranges can be kept at a very low frequency of occurence inspite of the presence of uncertainty. For the power output from wind turbines, ramp rates, as low a 3 % of the rated power per minute, can be effectively ensured with the use of energy storage and we show how the active use of rotor inertia as an additional energy storage can reduce the needed storage capacity by up to 30 % without reducing the power output.

Resumé (in Danish)

I denne afhandling beskriver vi regulering og styring af to forskellige industrielle app-likationer, der befinder sig i hver sin ende af elnettet; en elforbruger i form af et kom-mercielt køleanlæg, og vindmøller til elproduktion. Vores hovedstudier fokuserer på økonomisk modelprædiktiv regulering af et kommercielt multizonekøleanlæg bestående af flere kølenheder forbundet til en fælles kompressor, som har det formål at ned-køle adskillige rum eller områder, f.eks. i et supermarked. Betydelige mængder energi bliver brugt af køleanlæg verden over, og der er derfor et stærk incitament for at introducere mere energieffektive og omkostningsreducerende reguleringsteknikker. Samtidig undergår elnettet en forandring fra et centralt system med en relativt reg-ulerbar produktion i de konventionelle kraftværker til et langt mere decentraliseret netværk af uafhængige energiproducerende enheder, hvor en stærkt stigende andel af elektriciteten kommer fra vedvarende, fossilfrie energikilder såsom sol og vinen-ergi. For at muliggøre integrationen af store mængder af disse mere uregelmæssige elproducenter, er det ikke længere tilstrækkeligt (eller muligt) kun at styre elproduk-tionen, og vi må i langt højere grad også styre elforbruget til at være både effektivt og fleksibelt. Ved at muliggøre brugen af termisk energilagring i supermarkeder vil vi åbne muligheder for et fleksibelt elforbug, som kan reducere driftsomkostningerne for køleanlægget, og vi udvikler og demonstrerer prototype-reguleringsteknologier, som skaber helt nye forretningsmuligheder, hvor fleksibiliteten kan sælges til elnet-tet som regulerende effekt. Denne fleksibilitet åbner desuden for, at vindenergi kan dække en endnu større del af elproduktionen, og udvider derved markedspotentialet for vindmøller og andre vedvarende energikilder. Med vores arbejde sigter vi altså mod at facilitere brugen af miljømæssigt bæredygtige metoder til energiproduktion og samtidig skabe nye forretningsmuligheder for både elforbrugere og producenter af vedvarende energi.

Vores sekundære fokus i denne afhandling, vindenergi, bringer os til produktionssiden af elnettet. Formålet er her at forbedre kvaliteten og integrerbarheden af strøm leveret til elnettet fra store vindmølleparker. Målet med dette studie er at reducere den fluktuerende natur, som typisk præger vindmøllegenereret strøm, og dermed leve op til strengere krav for tilslutning til elnettet. Dette kan opnås ved at introducere en mere intelligent reguleringsstrategi både i den enkelte vindmølle, på parkstyringsniveau og i samarbejdet med fleksible elforbrugere eller andre typer energilagring. Denne mulige interaktion og synergi mellem de to systemer, som vi betragter i dette projekt, er i sig selv en grund til, at vi inkluderer begge sider af sagen, og som vi skal se, kan de forskellige reguleringsproblemer formuleres med så store ligheder, at vi kan anvende stort set identiske metoder til at løse dem på trods af den umiddelbare mangel på sammenfald.

Vi foreslår en økonomisk optimerende modelprædiktiv regulator (kendt som economic model predictive control eller blot, economic MPC) til at håndtere reguleringen af såvel køle- som vindmølleapplikationen. MPC er en feedback-reguleringsteknik, som er karakteriseret ved dens eksplicitte håndtering af styring til dynamiske systemer med begrænsninger (constraints), hvortil en model, der kan forudsige systemets fremtidige opførsel, benyttes sammen med forudsigelser af fremtidige forstyrrelser. Til hvert tidsskridt beregnes reguleringsvariablene ved at løse et optimalt reguleringsproblem over en given horisont. Resultatet af dette er en optimal åbensløjfesekvens af reguleringsvariable, hvoraf kun det første skridt implementeres. Feedback bliver implementeret ved at løse open-sløjfe problemet igen og igen i en rullende horisont-facon, i takt med at nye forudsigelser bliver tilgængelige.

Vores undersøgelser fokuserer primært på: 1) modellering af de virkelige systemer så de er kompatible med den valgte reguleringsarkitektur, 2) formulering af MPC-reguleringslove, som løser de særlige udfordringer der, følger med de industrielle applikationer og fastlæggelse af økonomiske mål, således at disse afspejler både fysikken bag systemerne såvel som vores definerede reguleringsformål, 3) effektiv realtidsberegning af de implicerede, ikke-trivielle optimeringsproblemer, og 4) demonstration af gennemførligheden og potentialet ved vores foreslåede metoder gennem udførlige simuleringer og sammenligninger med de eksisterende reguleringsmetoder samt data fra systemer i drift.

Vi præsenterer vores bidrag på følgende områder:

- Økonomisk MPC til kommercielle køleanlæg, herunder

    - Lineære økonomisk optimerende MPC-formuleringer der udnytter fleksibiliteten i køleanlæg til at modvirke ubalancer mellem elforbrug og -produktion.

    - Økonomisk MPC med probabilistiske begrænsninger, der sikrer robust ydelse og robust overholdelse af begrænsningerne på trods af upræcise systemmodeller og forudsigelser.

– Ulineær økonomisk MPC, der afspejler de ikke-konvekse elementer i de temperaturafhængige effektiviteter i køleprocessen.

– Ulineær økonomisk MPC med usikre forudsigelser samt implementeringer af simple prædiktionsmetoder, som udelukkende baseres på historiske data af fx. elpriser og udendørstemperaturer.

- Økonomisk MPC til vindmøller, herunder

  – Beregning af optimale statiske driftspunkter for vindmølleparker.

  – Ulineær økonomisk MPC for individuelle møller.

  – Skift af variable og konvekse formuleringer af økonomisk MPC for individuelle møller.

- Implementerbare optimeringsmetoder for MPC-problemerne, herunder

  – Sekventiel konveks programmering (SCP) for de specifikke ikke-konvekse problemer, der opstår i vores studier af kommercielle køleanlæg såvel som i vores studier af vindenergi.

  – Succesfuld demonstration af SCP-tilgangen på tre forskellige problemer— det kommercielle kølesystem med lineær dynamik og begrænsninger, men med en ikke-konveks objektfunktion, den individuelle vindmølle med ulineær dynamik, begrænsninger, og objektfunktion, og den statiske optimering af vindmølleparkdriftspunkter, hvor kun en "black-box"-model er tilgængelig.

Vores hovedbidrag er formuleringen af disse reguleringsproblemer samt demonstrationer, der viser hvordan vores SCP-metode kan bruges til løsning af disse.

Vi demonstrerer bl.a. betydelige omkostningsbesparelser i størrelsesordenen 30 %, sammenlignet med standard termostatstyrede supermarkedskøleanlæg og viser desuden, hvordan vores metode udviser sofistikeret priselastisk forbrug overfor realtids variationer i elpriserne. På trods af usikkerheder i systemet kan overskridelser af temperaturgrænserne begrænses til meget lave forekomstrater. For vindmøller kan effektændringer i strømmen effektivt begrænses til 3 % af møllens nominelle effekt pr. minut, når vi udnytter tilknyttet energilagring, og vi demonstrerer, hvordan den nødvendige lagerkapacitet kan reduceres med op til 30 % uden at reducere den producerede mængde energi ved en aktiv udnyttelse af rotorens inerti som ekstra energilager.

List of publications

International journals

The following papers were published in international journals during the project period. They constitute the main contributions of the Ph.D. project and we advice the reader to pick up on the specific details in the papers after reading the summary report.

[A] Tobias Gybel Hovgaard, Lars F. S. Larsen, Kristian Edlund and John Bagterp Jørgensen. Model predictive control technologies for efficient and flexible power consumption in refrigeration systems. *Energy, the International Journal, 44, pp. 105–116, 2012.*

[B] Tobias Gybel Hovgaard, Lars F. S. Larsen, Morten Juel Skovrup and John Bagterp Jørgensen. Optimal Energy Consumption in Refrigeration Systems - Modelling and Non-Convex Optimisation. *The Canadian Journal of Chemical Engineering, 90 (6), pp. 1426–1433, 2012.*

[C] Tobias Gybel Hovgaard, Lars F. S. Larsen, John Bagterp Jørgensen and Stephen Boyd. Nonconvex Model Predictive Control for Commercial Refrigeration. *International Journal of Control, 86 (8), pp. 1349–1366, 2013.*

[D] Tobias Gybel Hovgaard, Stephen Boyd and John Bagterp Jørgensen. Model predictive control for wind power gradients. *Wind Energy, 2013.* In press.

Peer-reviewed conferences

In addition to the papers listed before, the following peer-reviewed conference contributions were also published during the project period.

[E] Tobias Gybel Hovgaard, Lars F. S. Larsen, Kristian Edlund and John Bagterp Jørgensen. The Potential of Economic MPC for Power Management. *Proc. of the 49th IEEE Conference on Decision and Control—CDC, pp. 7533–7538, 2010.*

[F] Tobias Gybel Hovgaard, Kristian Edlund and John Bagterp Jørgensen. Economic MPC for Power Management in the Smart Grid. *Proc. of the 21st European Symposium on Computer Aided Process Engineering—ESCAPE 21, pp. 1839–1843, 2011.*

[G] Tobias Gybel Hovgaard, Lars F. S. Larsen, Morten J. Skovrup and John Bagterp Jørgensen. Power Consumption in Refrigeration Systems - Modeling for Optimization. *Proc. of the 4th International Symposium on Advanced Control of Industrial Processes—AdConIP, pp. 234–239, 2011.*

[H] Tobias Gybel Hovgaard, Lars F. S. Larsen and John Bagterp Jørgensen. Robust Economic MPC for a Power Management Scenario with Uncertainties. *Proc. of the 50th IEEE Conference on Decision and Control and European Control Conference—CDC-ECC, pp. 1515–1520, 2011.*

[I] Tobias Gybel Hovgaard, Lars F. S. Larsen and John Bagterp Jørgensen. Flexible and Cost Efficient Power Consumption using Economic MPC - A Supermarket Refrigeration Benchmark. *Proc. of the 50th IEEE Conference on Decision and Control and European Control Conference—CDC-ECC, pp. 848–854, 2011.*

[J] Tobias Gybel Hovgaard, Lars F. S. Larsen, Morten J. Skovrup and John Bagterp Jørgensen. Analyzing Control Challenges for Thermal Energy Storage in Foodstuffs. *Proc. of the IEEE International Conference on Control Applications (CCA), part of 2012 IEEE Multi-Conference on Systems and Control—MSC, pp. 956–961, 2012.*

[K] Tobias Gybel Hovgaard, Lars F. S. Larsen, John Bagterp Jørgensen and Stephen Boyd. Fast Nonconvex Model Predictive Control for Commercial Refrigeration. *Proc. of the 4th IFAC Nonlinear Model Predictive Control Conference—NMPC, pp. 514–521, 2012.*

[L] Tobias Gybel Hovgaard, Lars F. S. Larsen, John Bagterp Jørgensen and Stephen Boyd. Sequential Convex Programming for Power Set-point Optimization in a Wind Farm using Black-box Models, Simple Turbine Interactions, and Integer

Variables. *Proc. of the 10th European Workshop on Advanced Control and Diagnosis — ACD, pp. 1–8, 2012.*

[M] Tobias Gybel Hovgaard, Lars F. S. Larsen, John Bagterp Jørgensen and Stephen Boyd. MPC for Wind Power Gradients—Utilizing Forecasts, Rotor Inertia, and Central Energy Storage. *Proc. of the 12th European Control Conference— ECC, pp. 4071–4076, 2013.*

Contents

Part I

Summary Report: Introduction and Background

Introduction

In this chapter, we put the project into a context by describing the trends and challenges from the global electricity systems that motivate our work. We give numbers and figures to illustrate the need for new solutions to control of power consumers and producers and explain why, *e.g.*, supermarket refrigeration systems can play an important role in the future power system. We briefly motivate our choice of method and give references to related work. In addition, we describe the objective of this research project along with our hypotheses and a short summary of both academic as well as industrial contributions from our work. Finally, we give the outline for the remainder of this thesis.

1.1 Global energy challenges

As a remedy for meeting the global energy challenges of satisfying growing demands, securing sufficient energy sources, and reducing climate changes, an increasing amount of electricity from fairly intermittent energy sources, such as solar and wind is installed and more is planned for the coming years. With this large penetration of renewable energy, we must not only control the production, but also the consumption of electricity, in an efficient, flexible and proactive manner. Various types of power consumers possess capacities that can be used to shift the load in time if exploited intelligently in the control system. Such applications include refrigeration,

heating, electrical vehicles, and some industrial processes, to mention a few. We elaborate more on this in Chapter 2.

1.2   Commercial refrigeration

Supermarket refrigeration consumes considerable amounts of energy worldwide. In Denmark around 4500 supermarkets consume more than 600,000 MWh annually. This corresponds to approximately 2 % of the entire electricity consumption in the country. The goods in the refrigerated units make up a large capacity in which energy can be stored in the form of "coldness". However, the hysteresis control policy most commonly used today does not exploit this. In this thesis, we succesfully investigate how a large potential for energy and cost reductions exists, if the system load is distributed inteligently over time in a more cost-optimal way. In addition, this flexibility can render the refrigeration system a flexible power consumer. Such flexibility will be an essential feature in a future smart power grid. An average U.S. supermarket consumes in total around 56 kWh/ft^2 of electricity per year, but as illustrated in Figure 1.1(b), some supermarkets are significantly more energy intensive than this. Typically 43% goes to refrigeration. With an average supermarket size around 4000 m^2 (43,000 ft^2) and electricity prices for industrial consumption around 0.127 USD/kWh (average for USA in 2012) the annual average cost for refrigeration is USD 131,500 per supermarket. In Denmark, supermarkets are generally smaller, and this number is around USD 30,000. Thus, if we can save 30% on the costs related to refrigeration, an average supermarket saves almost USD 40,000 yearly, or 13% of the total electricity bill. Because the profit margins of supermarkets are so thin, on the order of 1 percent, the U.S. Environmental Protection Agency (EPA) estimates that USD 1 in energy savings is equivalent to increasing sales in the supermarket by USD 59. For a major chain, improvements that cut energy costs by 13 percent could yield tens of millions of dollars in added profit [Ene08].

1.3   Wind energy

In Denmark around 30 % of the electricity consumption is produced by wind power as of today. Wind power plants (WPP) consist of many individual wind turbines that share a common power output to the grid and are placed in the close vicinity of each other. Wind power plants seem to be the most promising renewable source of electricity today, and their share of the total electricity production is expected to increase notably. Dedicated rule sets (grid codes) regulate the connection of WPPs to transmission and distribution levels of the power grid, mainly concerning, *e.g.*, power

(a) Electricity use in typical supermarkets.

(b) Distribution of energy intensity in supermarkets.
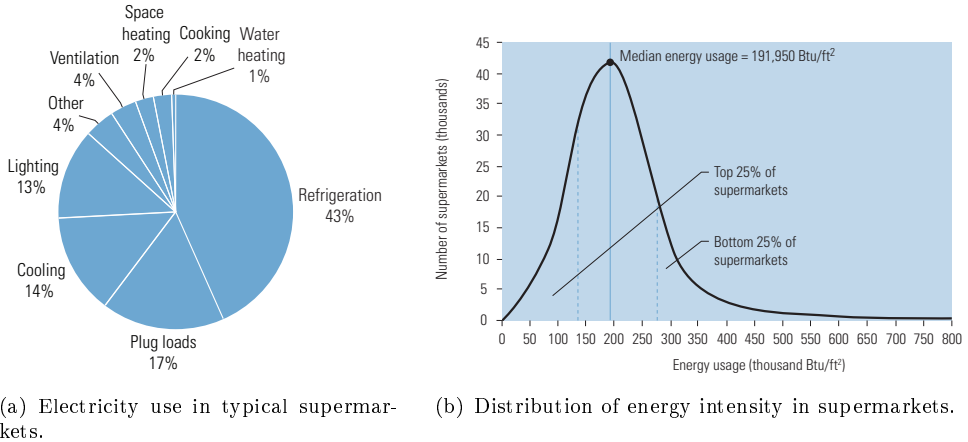
Figure 1.1: Supermarket energy consumption in the U.S. Source: [Ene08]. 1000 Btu ≈ 293 W

controllability and power quality. One of the regulation functions required is a power gradient constraint that limits the maximum rate-of-change of non-commanded variations in the power output from the WPP to the grid. We effectively demonstrate that our techniques for facilitating flexible power consumption in, *e.g.*, refrigeration systems, can play a major role in coordination with the control of WPPs. Consequently, the need for adding expensive storage technologies, in order to live up to tightened grid codes, can be reduced. Hereby, we improve the integrability of wind power in the grid, by reducing its fluctuating nature. As we can achieve this without degrading the power production, we succeed in increasing the potential market size for wind power. Figure 1.2 illustrates the fluctuating nature of wind power. This fluctuating behaviour makes it a challenge to integrate large amounts of wind energy on the power grid.

1.4   Model predictive control

During the last 30 years, model predictive control (MPC) for constrained systems has emerged as one of the most successful methodologies for control of industrial processes [GPM89, BM99, QB03]. Traditionally, MPC is designed using objective functions penalizing deviations from a given set-point. MPC based on economic performance functions that directly address minimization of the operational costs is an emerging methodology known as economic optimizing MPC [RA09, DAR11, AAR12, RAB12, Grü13]. Economic MPC addresses the concerns of controlling a
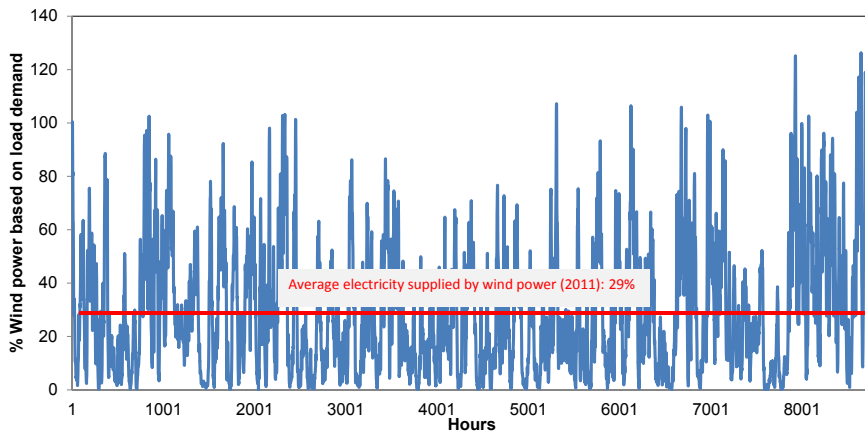
(a) % wind power of full load demand for a full year (2011).
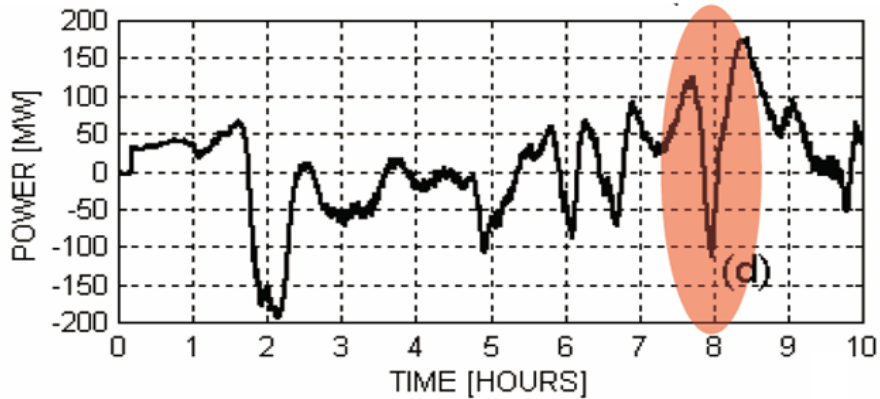
(b) Example power imbalance for 400MW wind farm. The red area shows a fluctuation from -100 MW to +175 MW of the expected production within 15–20 min.

Figure 1.2: Wind power fluctuations in Denmark. Source: Dong Energy

system influenced by a number of disturbances which we can predict (with some uncertainty) over a time horizon into the future, obeying certain constraints, while minimizing the cost of operation. We provide novel formulations and prove that this scheme is well suited and can be adapted to tackle our control problems, *i.e.*, flexible power consumption for commercial refrigeration systems, and reduced power gradients for wind turbines. Textbooks and publications with good introductions to MPC include, *e.g.*, [CB99, ML99, RM09, Mac02].

1.5 Thesis objective

This thesis addresses applications of economic MPC algorithms to enable cost efficient and flexible control of commercial refrigeration systems. Our objectives are to add value to commercial refrigeration and to facilitate more wind energy on the power grid, by developing new functionalities. We do this by investigating control strategies that both minimize the local cost of ownership of, *e.g.*, a supermarket refrigeration system, and at the same time prepare the application to play an important role as a flexible power consumer in the future power grid with increased penetration of intermittent renewable energy sources. In addition, we take a small step to the production side of the power grid by investigating how similar control strategies and the synergies of co-controlling flexible power consumers can improve the integrability of wind power on the grid.

In the project the primary objective was to exploit load shedding in refrigeration systems using economic MPC to obtain a cost efficient operation. Our hypothesis is that *it is possible to develop an optimizing control scheme that schedules the operation of a multi-zone refrigeration system according to weather, price, and load profiles such that an overall energy and cost efficient operation is obtained without violating the requirements to the cooling quality. This would be achieved by utilizing the possibility for storing energy as thermal energy in the refrigeration system. Furthermore, we expect that this will considerably lower the operational cost compared to current control solutions, as well as enable flexible power consumption to benefit the power grid.* Subsidiary, our objective is to coordinate the control of large WPPs and the interaction with energy storage consisting of flexible power consumers. We do this within the framework of economic MPC. Our hypothesis is that *an optimal control scheme that takes predicted wind speed into account can be developed to control a group of wind turbines such that the power output to the grid obey tightened demands to power quality at the lowest possible cost. This is achieved by utilizing the rotational inertia in the individual turbines as well as by co-control of flexible consumers, directly or through, e.g., price signals.*

1.6 State of the art

In this section, we provide an overview of the state of the art and give some references to important literature in the different fields that we will addresses in this thesis. The collection of papers, written during the project, is included in full in Part III of this thesis. As each paper contains the literature studies and references relevant to the specific paper, the reference list in this chapter is not exhaustive, and we refer the reader to those given in the papers as well.

1.6.1 Refrigeration and demand response

We present a novel formulation of economic MPC for the control of a commercial refrigeration system. The goal is to minimize the cost of energy and to allow the system to offer flexibility in terms of demand response to the power grid. Previous and concurrent works have dealt with similar topics and *e.g.*, [CSGSH11, AHP12] review the use of thermal energy storage and the expected importance of MPC in such demand response schemes. Different means of utilizing demand response in a smart grid setting have been investigated in an increasing number of publications, *e.g.*, [AEG⁺10, HHS10, SG11, MGKFGL11], for other kinds of applications with a built-in capability for energy storage such as plug-in electric vehicles and heat pumps. The demand response in relation to price elasticity is described in [Kir03], and [PSF12] analyzed different demand side management strategies. For facilitation of wind generated electricity by price optimized thermal storage, works like *e.g.*, [FFC⁺11] exist. MPC is increasingly being considered to control both refrigeration and power systems, see, *e.g.*, [LGT06, LTR07, SCLdP08, SDE08, ER08, EBJ11, BD11], and the use of load shifting capabilities to reduce total energy consumption have been applied in, *e.g.*, [VH01, BW09, OPJ⁺10a]. Predictive control and optimization for energy cost reductions in vapor compression cycles have been investigated for building temperature regulation too. [MQSX12] considered time of use pricing in that context and [OPJ⁺10b, MBH⁺12, MKDB12] all used weather predictions to optimize the energy efficiency.

1.6.2 Wind energy and power quality

We demonstrate how model predictive control using forecasts of the wind speed can improve the quality of power delivered from wind turbines to the grid. Our study utilizes rotor inertia and energy storage to ensure sufficiently low rates of change on the power output. Other works considered the means of grid support in wind turbines too, *e.g.*, [KNJ⁺11, Tar12] where turbine inertia was used for frequency

response and power oscillation damping. In, *e.g.*, [KH06, BS07, SSD$^+$12, BST$^+$13] the benefits, economics, and challenges of using different means of storage, *i.e.*, batteries, hydrogen, flywheels etc., in combination with wind power were investigated and in, *e.g.*, [STR11] a Lithium-iron-phosphate battery was used to achieve power forecast improvement and output power gradient reduction for wind power. Optimization of the wind farm control level is a topic of increasing interest, too. In, *e.g.*, [HSIB06, PJ09, SJB11, MMR11, SWK12] different control aspects of the wind park controller, such as power maximization, load reduction, wind field and turbulence modeling, and active/reactive power control for the power grid connection, are considered.

1.6.3 Economic MPC

In many applications, the classical approach to achieving overall economic objectives, is to divide the planning and the control into two layers. The first layer performs a steady-state economic optimization of the plant's variables and sends set-points to the second layer. Typically, MPC in the second layer serves the purpose of guiding the plant's transient state to the set-point, rejecting dynamic disturbances that enter the system. *While the classical approach has shown great versatility and has seen widespread application, there are an increasing number of problems for which dynamic economic performance is crucial and the hierarchical separation of economic analysis and control is either inefficient or inappropriate* [RAB12]. The idea of optimizing dynamic economic performance directly is not new. Infinite horizon control problems with unbounded costs were first considered in the field of economics in the 1920s [CHL91]. Theoretical analysis of economic model predictive control for continuous processes began with stability proofs based on convexity for linear systems and convex objectives in, *e.g.*, [RA09]. Average asymptotic cost guarantees and average constraints were demonstrated in. *e.g.*, [AR10] and Lyapunov-based stability proofs for nonconvex systems were provided in [DAR11, ARA11, AAR12]. An analysis of performance in the absence of any terminal constraints or penalties is presented in, *e.g.*, [Grü13]. Economic MPC has been applied to a growing variety of continuous processes and is increasingly being considered to control both refrigeration and power systems [SCLdP08, EBJ11, BD11]. Recently, economic MPC has been applied to power management on a smart grid, too (see, *e.g.*, [HGL12, HPMJ12, MQSX12] and the papers in Part III).

1.6.4 Optimization algorithms

This thesis also addresses a tailored optimization routine that allows our proposed MPC controller to conduct the computations sufficiently fast for real-time implementation. The need for computationally efficient optimization in MPC applied to

systems with either fast sampling or limited computational resources is a major research topic. In [DBS$^+$02] a direct multiple shooting method was presented, capable of solving an nonlinear MPC (NMPC) problem with 42 differential states and 122 algebraic states over 20 control intervals in 10 s and in [WB10] a quadratic MPC problem with 12 states, 3 controls, and a horizon of 30 intervals was solved in 5 ms using warm-starting. Another approach to real-time MPC is the explicit methods as reported in, *e.g.*, [ZJM08] where the technique was used in combination with online optimization for solving QPs under restrictions on the computational time. [GJT07] gives an extension to explicit NMPC. However, it was reported that it is troublesome to ensure stability if the problem is nonconvex, and in addition, the explicit methods are not suitable for larger problems due to extremely large state-spaces. Approaches to parallel implementation of MPC algorithms for real-time execution were shown in, *e.g.*, [JCKL11] where a problem with 32 states, 16 inputs and 10 control intervals was solved in 344 ms on an FPGA. For further reviews of numerical methods for solution of real-time optimal control problems in NMPC see, *e.g.*, [DFH09]. A wide range of algorithms for numerical optimization exists in the literature. These include, methods for linear or quadratic programs, *e.g.*, state-elimination, Riccati-iterations, first-order methods, active-set, and interior-point algorithms, as well as extended LQ, and explicit formulations [BMDP02, Jør05, NW06]. Other methods address nonlinear optimization, *e.g.*, single-shooting, multiple-shooting, and simultaneous algorithms [Bie07, BBB$^+$01, DFH09, ZB09]. For the interested reader, we refer to the literature, *i.a.*, the references given here. Optimization routines that include embedded convex optimization have recently become more available to non-experts by the introduction of the automatic code generators such as FORCES [Dom12, DZZ$^+$12], FiOrdOs [Ull11], or CVXGEN [MB12]. In this work, we use the latter of these alternatives to produce super fast customized solvers.

1.7   Thesis contributions

As this project is accomplished in close collaboration between the two companies (Vestas and Danfoss) and the universities (primarily the Technical University of Denmark, and for some sub-projects, Stanford University), our contributions and value creation are relevant to both industry and academia, of course with different significance depending on the specific outcomes. The vision is that: *by enabling the use of energy storage in supermarkets, we open up the possibility of reducing operational costs and create completely new business opportunities for selling regulating power to the grid. Moreover, this enables a larger penetration of wind energy in the power production and increases the potential market size for wind turbine generators and other renewable energy sources. Thus, we aim at promoting the use of environmental sustainable power production technologies while creating new business opportunities.* The industrial contributions from this project are primarily:

- A novel control scheme based on economic MPC for control of a supermarket refrigeration system.

- Transferring and adaption of modern control technologies (economic MPC) from academia and other fields of the industry to solve specific and evolving needs identified for both power consumers and power producers in the electricity grid (*e.g.*, energy efficiency, cost reductions, flexibility, power quality).

- Demonstration by simulation of the applicability of our methods for industrial applications (with their challenges, *e.g.*, uncertainty, vast variety of systems, limited computational power).

- Reduction of the computational complexity, rendering it possible to implement the methods on an industrial hardware platform.

- Proving the potential of the proposed methods, by evaluating realistic and verified models and inputs for simulation of real scenarios (*e.g.*, savings calculated from real supermarket data, temperatures, and electricity prices).

- Demonstration of economic MPC combined with novel computation approaches to be a top candidate methodology for handling current and future smart grid challenges.

Several of these are naturally overlapping with contributions to the academic community and have been published in several control specific, peer-reviewed journals and conferences (see papers [A]-[M]). Our main research contributions to academia have a common thread in terms of formulating, modeling, and rephrasing theoretic results and methods to the extend where they can be applied to control of real-life problems:

- We develop novel algorithms combining fast MPC with economic MPC and demonstrate this novel approach on a commercial refrigeration system and for the control of a wind turbine.

- We formulate and adapt the methodology of probabilistic constraints for economic MPC of dynamic systems with uncertain model parameters.

- We successfully provide new formulations of the objective function which reflect economic costs related to operating the systems, while explicitly including a type of ancillary services known as primary regulating power. We formulate this non-standard MPC problem such that a generic non-linear optimization tool can be applied.

- We show novel tailored optimization methods capable of solving the non-linear and non-convex problems involved. One method is a simple add-hoc solution separating the problem over the variables and our second method is a

more meticulous sequential convex programming (SCP) approach. The latter is tested extensively for performance and robustness and is proven to be well suited for implementation on industrial hardware.

- We demonstrate a non-trivial change of variables for one of the wind turbine control problems, allowing us to solve this problem super fast and efficient.

We address these substantial industrial and academic contributions throughout parts II–III of this thesis, providing both a summary report and a number of reviewed papers that we have published throughout the project period.

1.8   Thesis outline

The thesis is divided into three parts. The first two parts compose a summary report which is meant to give a coherent overview of the main results and contributions of the thesis. We provide motivating background information on the problems dealt with and their context. The third part comprises 13 research papers prepared during the project period. The contents of each paper are summarized briefly in the following:

Paper A was published in the international journal, *Energy* in 2012. The paper presents studies on economic model predictive control of a supermarket refrigeration system for both cost efficient operation and for offering flexible power consumption as a service to the power grid. We use a generic nonlinear optimization tool to solve the nonconvex problems. In addition, robustifying means in terms of chance-constraints are introduced.

Paper B was published in the *Canadian Journal of Chemical Engineering* in 2012. The paper describes a model of the supermarket refrigeration system which is sufficiently simple for optimization while preserving a very accurate description of the power consumption. Furthermore, we present an optimization routine which overcomes the nonconvex objective function by splitting the problem in the independent variables. We compare the solution with the solution from a generic optimization tool.

Paper C was published in the *International Journal of Control* in 2013. In the paper, we extend our previous studies on price and load responsive control of a supermarket refrigeration system. We use a very realistic system model, which we have verified with dedicated experiments and data from supermarkets in actual operation and we use historic data for electricity spot prices, and outdoor temperatures for a selected location in Denmark. We implement very simple predictors, and we allow for uncertain heat loads affecting the system. A main

focus of this paper is application of an efficient, dedicated, sequential convex programming method that allows for real-time implementation, even with little computational power available.

Paper D is to appear in the international journal *Wind Energy* in 2013. We consider the operation of a wind turbine and a connected energy storage device. The controller takes varying wind speed into account and has the goal of maximizing the total energy generated while respecting limits on the time derivative (gradient) of power delivered to the grid. We use the turbine inertia as an additional energy storage device and we show that by a novel change of variables we can transform the problem from a nonlinear one, to one with linear dynamics and convex constraints. Thus, the problem can be solved for its global optimum with very efficient methods.

Paper E was presented at the *49th IEEE Conference on Decision and Control* in 2010. The paper describes our investigations on economic model predictive control for a small portfolio of controllable power producers together with a large cold storage (a power consumer). The system is approximated with a linear model and the economic MPC is a linear program (LP). An exogenous signal from all non-controllable producers (*e.g.*, wind power) and consumers affect the system and we utilize the refrigeration system's flexibility to counteract fluctuations.

Paper F was presented at the *21st European Symposium on Computer Aided Process Engineering* in 2011. In the paper we describe further development on the case study in the previous paper and introduce the initial studies on chance-constraints to deal with uncertainties in forecasted disturbances.

Paper G was presented at the *4th International Symposium on Advanced Control of Industrial Processes* in 2011. The paper describes our work on building a suitable dynamic model of the refrigeration system. We introduce a nonconvex objective function in order to provide a realistic description of the power consumption function and show two approaches to solve the resulting optimization problem.

Paper H was presented at the *50th IEEE Conference on Decision and Control and European Control Conference* in 2011. It presents our robust formulation of linear economic model predictive control. We use chance-constraints reformulated as second-order cone constraints to deal with the uncertainty in both forecasted disturbances and in the system models. A finite impulse response model with uncertain coefficients describes the system in order to make it compatible with the robust formulation.

Paper I was presented at the *50th IEEE Conference on Decision and Control and European Control Conference* in 2011. The paper describes our results with a

generic nonlinear optimization code for price and temperature optimized operation of the refrigeration systems. We give details on the reformulation of the objective function. This objective function is formulated such that the controller enables the refrigeration system to participate in the regulating power market by offering the flexible power consumption as an ancillary service.

Paper J was presented at the *IEEE International Conference on Control Applications (CCA), part of 2012 IEEE Multi-Conference on Systems and Control* in 2012. In the paper, we present our dedicated experiments to identify key parameters for use in the refrigeration system model and we show how observers for the unknown food temperatures can be constructed. The second part of the paper introduces the term "active thermal mass" which is a measure of the amount of thermal storage potential that can be utilized in a specific foodstuff on a specific timescale. We present both a generic analysis and details for selected typical foodstuffs.

Paper K was presented at the *4th IFAC Nonlinear Model Predictive Control Conference* in 2012. The main focus of the paper is the application and algorithmic details of the sequential convex optimization methods that was developed as a part of the work that was also published in paper C.

Paper L was presented at the *10th European Workshop on Advanced Control and Diagnosis* in 2012. In the paper, we consider optimization of power set-points to a large park of wind turbines that influence each other through the wind field. The presented approach uses a sequential optimization method, similar to the one introduced in some of our previous papers, to deal with challenges such as black-box models of the system, integer variables, and nonlinear dynamics.

Paper M was presented at the *European Control Conference 2013*. Like in paper D, the goal is to operate a wind turbine and a connected energy storage device to maximize the total energy output while keeping the time derivative (gradient) of power delivered to the grid sufficiently small. Our approach in this paper is to keep the natural control variables in the optimization problem which we solve using a sequential convex programming method.

1.8.1   Organization of the summary report

The remainder of the summary report is constructed as follows. In Chapter 2, we provide background, context, and motivation for the research objectives defined for this project. The following two chapters give the control relevant dynamic models used for controller design in our studies. In Chapter 3, we delve into the supermarket refrigeration system and show dynamics, constraints, and objectives as well as a linear simplification. Chapter 4 provides the necessary details of the models used

for wind turbines and WPPs. We give sufficient details and parameters to allow for reconstruction of most of our results. We give an overview of the work done on economic MPC and discuss our choice of method in Chapter 5.

In Part II, we summarize the main contributions from this project. In Chapter 6, we describe our price and temperature response functionality for the refrigeration system. This chapter also deals with offering the flexible power consumption in refrigeration systems to the market for ancillary power services. Chapter 7 deals with different means to robustifying the MPC against uncertainties in model parameters and forecasts. In particular we consider so-called probabilistic constraints for linear systems and a simpler back-off method for use with the more complex models. In addition, we present very simple predictors that provide our controller with forecasts based entirely on historical data. In Chapter 8, we describe the different optimization methods that we have applied throughout this project. They range from standard linear and quadratic solvers over a generic non-linear optimization tool to our tailored SCP method. Finally, in Chapter 9, we demonstrate how economic MPC and coordination with means of energy storage can ensure certain limits on the rate of change for the power output from wind farms. In addition to fulfilling tight demands in a cost optimal way, we demonstrate how the total power output from a WPP can be maximized using sequential optimization. We give conclusions and perspectives in Chapter 10.

Smart grids

This chapter outlines the challenges and new possibilities that are emerging for both consumers and producers on the electricity grid. We briefly describe why the smart grid is a very hot topic, we give our definition of the smart grid, and describe the smart grid concept used in this work. Furthermore, we explain why wind power is both a very popular source of renewable energy while causing rather large concerns about stability and power balances. We also introduce the idea of flexible power consumption and intelligent demand response. This is a key element of our investigations in this thesis, as well as for the power grid in general.

2.1 Power grid operation

The current power grid has evolved into a very stable and reliable system with uptime close to 100 % in most western countries. However, the global energy challenge for the future is at least threefold; to satisfy the growing demands, secure sufficient energy sources, and meet the challenges of climate changes and pollution.

The supply chain for electricity is significantly different from most other products in terms of inventory and storage. There are limited possibilities for effective storage of electricity and most options are intractable due to relatively high costs. Conse-

Figure 2.1: The future smart grid is tomorrow's green, flexible and intelligent power system - a power system where the generation, transport and consumption of power is linked intelligently.

quently, balancing the production and the consumption of electricity at all times is an important task. With a dominance of conventional coal and gas fired power plants on the grid, the balance responsible parties have become good at planning the operation of these rather controllable production types and the security of supply is very high. This paradigm of predicting the electricity consumption and planning the production accordingly is, however, changing. For several reasons, goals have been set by many governments to increase the penetration of renewable energy sources and to phase out fossil fuels. Besides preparing us for a time where these conventional energy sources are sparser and sparser, more renewable energy on the power grid helps us reduce our CO_2 emissions, limits the global warming effects, and makes us more independent of oil and gas producing countries. A consequence of the greater penetration of renewable energy is that we start to shut down conventional power plants. The downside of this is that we lose a lot of the traditional flexibility and controllability that we are relying on today. As the renewable power production, in most cases, is subject to the vagary of the weather, there is a need for a new paradigm in which we predict the power production (instead of the consumption) and control part of our consumption to match accordingly.

In contrast to the current rather centralized power generation system, the electricity grid will be a network of many independent power generators. The future intelligent

power grid, that incorporates all these, is often referred to as the smart grid. The Danish transmission system operator (TSO) give the following definition of smart grids: *"Intelligent electrical systems that can integrate the behavior and actions of all connected users—those who produce, those who consume and those who do both—to provide a sustainable, economical and reliable electricity supply, efficiently"* [Ene11]. This definition is rather common, so we adopt it in our work. Figure 2.1 sketches some of the energy sources and devices that are linked closely together in the future electricity system. In a smart grid, the consumers will be able to interact with the power system and generation through automated and intelligent control of their electrical appliances. In this way, they can act as resources for the power system.

2.2 Renewable energy sources

Renewable energies such as wind, solar, tidal, and hydro power promise to be an important source for the future power generation. They are safe, clean and plentiful and unlike conventional fuels, renewable energies are permanently available in almost every country in the world. Of the renewable technologies, wind power currently has the potential to make the largest impact. In Denmark the political ambitions are to increase the share of wind power to 50 % of the electricity consumption by 2020 and to fully cover the energy supply by renewable energies in general in 2050 [DMoCB12].

The fluctuating nature of wind power introduces several challenges to reliable operation of the power systems. During the first two decades of wind turbines being connected to the public grid (1980-2000), a fairly strong grid was assumed and the turbines and controls were simple. With the increasing wind power penetration today, modern wind power plants (WPP) must be equipped with power electronics converters that are designed to fulfill increasingly demanding requirements (grid codes) to power quality and reliability (see, *e.g.*, [MPdH06, CW08]). This alone can, however, not make the electricity sector capable of handling the massive amount of wind power that is planned. As a consequence, the demand side of the grid is expected to play a key role in this transformation.

Today, the electricity price is found in the market by auctions. These auctions make the supply and demand curves intersect and the most expensive power source that must be put in play to fulfill the demand, sets the price. This works today without any elasticity in the consumption due to the elasticity in the production price. Different producers such as wind, coal, gas, nuclear, etc. have different marginal prices on production. But, as long as the wind turbines are installed and the wind is available, the marginal cost of increasing the energy production from wind turbines, is basically zero. Consequently, the elasticity on the production side will almost disappear with a high wind penetration. Thus, to maintain stable electricity prices, elasticity on the

(a) Marginal electricity price on production.   (b) Today: little flexibility in consumption.
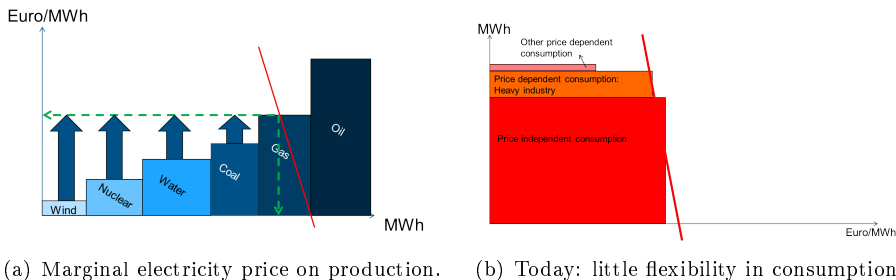
Figure 2.2: Basic demand and supply curves decide the electricity prices. Source: Danske Commodities

consumption side is required. Figure 2.2 illustrates the supply and demand curves for the electricity market today.

2.3 Flexible power consumption

As we are installing a large number of wind turbines, there is a need for a more intelligent and flexible energy system. Intelligent electricity meters and time-controlled electricity-consuming appliances, including the millions of flexible electric devices that consumers will have in future, are some of the means to make electricity consumption more flexible. *"Electricity consumption and generation in Denmark is set to change significantly in the coming years. Electricity customers will demand new services as they replace oil-fired burners with electric heat pumps and traditional petrol-powered vehicles with electric vehicles and plug-in hybrid vehicles. The electricity sector should be ready to provide these services with the same high level of delivery quality as today. This should occur in a situation where electricity generation is increasingly derived from renewable energy."* [DE10].

Energy storage technologies, which enable intelligent demand response, are being explored throughout the world as a component of absorbing electricity in times of excess production from wind turbines and for providing ancillary services to the power system. The need for change dictated from the developments in the surrounding socio-technical landscape create a new window of opportunity for making profit and reducing costs. A new business of selling flexibility to the power grid arises as this inevitably will be a service of increasing value. And as power prices are expected to fluctuate much more, a new potential in shifting power consumption in time to reduce costs and increase efficiency, appears. Meanwhile, technical research areas that enable this kind of advanced control to be distributed to a large number of applications

have come to a stage of maturity where they can be moved from laboratories to real applications. Modern technologies such as computational power of low-cost processors available to the broad industry, availability of low-cost sensors, high-quality prediction methods, and advanced control techniques clear the way for these new features to be implemented. Apart from the technology the lack of good business models is still an obstacle for exploiting these flexibilities. Throughout this project, we have aimed at showing the economical potential. The development of the enabling technology and the necessary business models must, however, go hand in hand.

Several technologies, that are already in place today, possess a potential flexibility. If these flexibilities are exploited intelligently and combined over several units they can benefit the balancing of the power market to a great extent. Many systems have the potential to deliver ancillary services to the grid while optimizing their own local costs of operation. These applications include, but are not limited to, residential and office heating and air-conditioning (see, *e.g.*, [OPJ+12, MKDB12]), plug-in electric vehicles (*e.g.*, [WLT+11, HPM+12]), some types of heavy industry [SK12], and commercial refrigeration in, *e.g.*, supermarkets and warehouses as we concentrate on in this thesis. The majority of such applications can easily offer flexibility for fast ancillary services that work on time scales of seconds to minutes and up to hours. For some applications, day/night or other longer intraday load shifts might even be possible. However, non of the typical demand response applications can uphold a certain regulating power forever and, *e.g.*, seasonal variations must be covered my other means (*e.g.*, strong transmission lines, pumped hydro power, bio gasification, etc.) The following section gives a brief summary of the regulating power services used in Denmark today.

In this work, we assume that we have a forecast of the electricity price available. This forecast can reflect the real spot price or be made up by some aggregator in order to promote a certain demand response. How to create such signals is, however, a study on its own which is outside the scope of this thesis.

2.3.1   Regulating power

Figure 2.3 shows the different types of regulating power services that are used the balance the power grid today. In the event of frequency deviations, the primary reserve regulation must ensure that the balance between production and consumption is restored, stabilizing the frequency at close to, but deviating from 50 Hz. Primary reserve regulation is automatic and provided by production or consumption units which, by means of control equipment, respond to grid frequency deviations. It is supplied at frequency deviations of between 20 and 200 mHz within 15–30 seconds. It must be possible to maintain the regulation for a maximum of 15 minutes. The secondary reserve serves two purposes. One is to release the primary reserve which has been activated, *i.e.*, restore the frequency to 50.00 Hz. The other purpose is
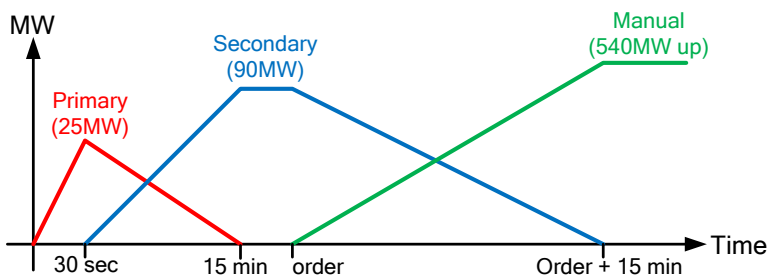
Figure 2.3: Regulating power services in West Denmark.

to restore any imbalances caused by major operational disturbances that cannot be handled by the primary reserves. Secondary reserve regulation is also automatic and provided by production or consumption units. It must be possible to supply the reserve requested within 15 minutes and maintain the regulation continuously. Alternatively, continuous reserve can be supplied by a combination of units. The manual reserve is used to restore system balance on the longer time scale. The reserve is activated from the TSO's control center by manually ordering upward and downward regulation from the relevant suppliers, primarily production units. Primary reserves get a payment for being available while other regulating services are paid according to the actual amounts that are activated. In some of our studies, we explicitly consider primary regulating power by letting the supermarket refrigeration system prepare itself for automatic activation.

Commercial Refrigeration

In this chapter, we describe the refrigeration process and the dynamic model of a commercial multi-zone refrigeration system. Such systems can include supermarkets, warehouses, or air-conditioning. We describe the thermodynamics, the constraints of the system, and the function reflecting the economic cost of operating the plant. In addition, we show how simplified linear models, that are suitable for conceptual studies, can be derived. Section 3.8 give a full set of parameters for the model.

3.1 Models

The model presented in this chapter describes a system with multiple cold rooms in which a certain temperature for the stored foodstuff has to be maintained [LIZW07]. We describe the temperature dynamics and the energy cost of the system using SI units throughout. Energy flows and power consumption are in Watts, temperatures are in degrees centigrade, pressures are in Pascal, enthalpies are in J/kg, and instantaneous electricity prices are in EUR/W. This fixes the units of all quantities used.

Figure 3.1 illustrates a refrigeration system with one cold storage room and one frost room connected to the system. The refrigeration system utilizes a vapor compression

cycle in which a refrigerant circulates in a closed loop consisting of a compressor, an expansion valve and two heat exchangers, an evaporator in the cold storage room, as well as a condenser/gas cooler located in the surroundings. When the refrigerant evaporates, it absorbs heat from the cold reservoir which is rejected to the hot reservoir. According to the 2nd law of thermodynamics, the evaporation temperature $T_e(t)$ (of the refrigerant at the pressure $P_e(t)$) has to be lower than the temperature in the cold reservoir $T_{air}(t)$ and the condensation temperature has to be higher than the temperature at the hot reservoir $T_a(t)$, in order to sustain the heat transfer from cold room to the surroundings. Low pressure refrigerant, with the pressure $P_e(t)$, from the outlet of the evaporator is compressed in the compressors to a high pressure $P_c(t)$ at the inlet to the condenser to increase the saturation temperature. In these expressions t denotes time. To lighten notation, we will drop the time argument (t) in time-dependent functions in the sequel.

Usually, several cold storage rooms, *e.g.*, display cases, connect to a common compressor rack and condensing unit. Because of this, the individual display cases see the same evaporation temperature, but each unit has its own inlet valve for individual temperature control. Figure 3.2 shows a simplified diagram for a one-unit refrigeration cycle.

3.2 Temperature dynamics in a cold room

We use a first principles model and describe the dynamics in the cold room by simple energy balances. An energy balance for the temperature of the foodstuff $T_{food}(t)$ yields the differential equation,

$$m_{food}c_{p,food}\frac{dT_{food}}{dt} = \dot{Q}_{food-air},$$

where $\dot{Q}_{food-air}(t)$ is the energy flow from the air in the cold room to the foodstuff, m_{food} is the (assumed constant) mass of food, and $c_{p,food}$ is the constant specific heat capacity of the food. The temperature of the air in the cold room $T_{air}(t)$ satisfies the differential equation,

$$m_{air}c_{p,air}\frac{dT_{air}}{dt} = \dot{Q}_{load} - \dot{Q}_{food-air} - \dot{Q}_e.$$

$\dot{Q}_e(t)$ is the applied cooling capacity (energy absorbed in the evaporator), $\dot{Q}_{load}(t)$ is the heat transfer from the surroundings to the air, m_{air} is the constant mass of air in the cold room, and $c_{p,air}$ is the constant specific heat capacity of the air. We describe the heat flows using Newton's law of cooling,

$$\dot{Q}_{food-air} = k_{food-air}(T_{air} - T_{food}),$$
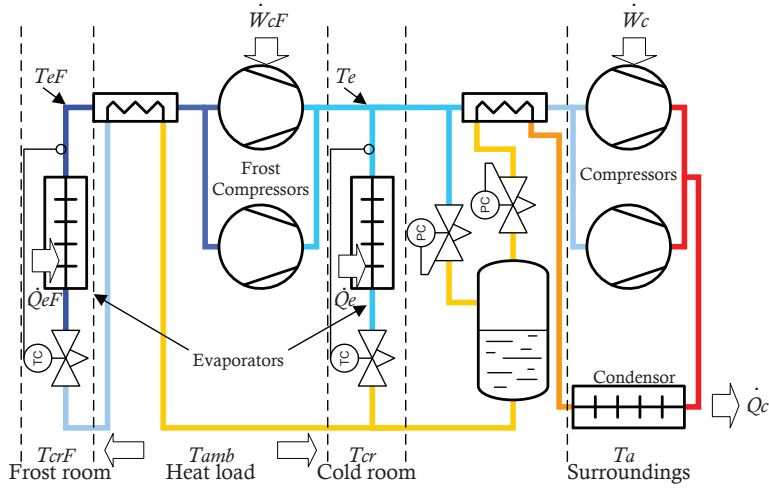
Figure 3.1: Schematic layout of basic refrigeration system.

$$\dot{Q}_{\text{load}} = k_{\text{amb}-\text{cr}}(T_{\text{amb}} - T_{\text{air}}) + \dot{Q}_{\text{dist}},$$

where $k_{\text{food}-\text{air}}$ and $k_{\text{amb}-\text{cr}}$ are the constant overall heat transfer coefficient between two media, $T_{\text{amb}}(t)$ is the temperature of the ambient air which puts the heat load on the refrigeration system, and $\dot{Q}_{\text{dist}}(t)$ is a disturbance to the load (*e.g.*, an injection of heat into the cold room). The cooling capacity satisfies

$$\dot{Q}_{\text{e}} = k_{\text{evap}}(T_{\text{air}} - T_{\text{e}}),$$

where k_{evap} is the heat transfer coefficient of the evaporator that varies with the filling of the evaporator. The filling of the evaporator is manipulated by another control system. This low level control loop ensures that the desired cooling capacity $\dot{Q}_{\text{e}}$ is obtained. The temperature dynamics are, with this choice of variables, entirely linear. The continuous time 2nd-order state space description is given as

$$\dot{x} = Ax + Bu + Ed,$$

with

$$x = \left[\begin{array}{c} T_{\text{air}} \\ T_{\text{food}} \end{array} \right], \quad u = \left[\begin{array}{c} \dot{Q}_{\text{e}} \end{array} \right], \quad d = \left[\begin{array}{c} T_{\text{amb}} \\ \dot{Q}_{\text{dist}} \end{array} \right],$$

and

$$A = \left[\begin{array}{cc} -\frac{k_{\text{food}-\text{air}} + k_{\text{amb}-\text{cr}}}{m_{\text{air}} c_{\text{p,air}}} & \frac{k_{\text{food}-\text{air}}}{m_{\text{air}} c_{\text{p,air}}} \\ \frac{k_{\text{food}-\text{air}}}{m_{\text{food}} c_{\text{p,food}}} & -\frac{k_{\text{food}-\text{air}}}{m_{\text{food}} c_{\text{p,food}}} \end{array} \right], \quad B = \left[\begin{array}{c} -\frac{1}{m_{\text{air}} c_{\text{p,air}}} \\ 0 \end{array} \right],$$

$$E = \left[\begin{array}{cc} \frac{k_{\text{amb}-\text{cr}}}{m_{\text{air}} c_{\text{p,air}}} & \frac{1}{m_{\text{air}} c_{\text{p,air}}} \\ 0 & 0 \end{array} \right].$$
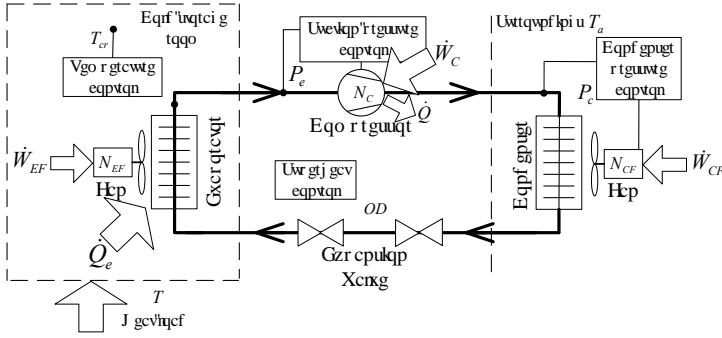
Figure 3.2: Simplified schematic for a supermarket refrigeration system with one cold room.

The system matrix A has 2 real, distinct and negative eigenvalues λ_i, $i = 1, 2$, and the system has 2 time constants given by $\tau_i = -1/\lambda_i$. We give numerical values of the time constants for three typical units in Section 3.8. We can take advantage of this linear description of the system dynamics when designing both dedicated optimization algorithms and methods for system identification.

3.3   Constraints

We would like the food temperatures to satisfy the inequalities

$$T_{\text{food,min}} \leq T_{\text{food}} \leq T_{\text{food,max}},$$

where $T_{\text{food,min}}$ and $T_{\text{food,max}}$ are a given allowable range given for each of the individual units. In addition, two constraints that cannot be violated are given by the nature of the system,

$$0 \leq \dot{Q}_{\text{e}} \leq k_{\text{evap,max}}(T_{\text{air}} - T_{\text{e}}),$$

$$0 \leq \dot{W}_{\text{c}} \leq \dot{W}_{\text{c,max}},$$

where $k_{\text{evap,max}}$ is the constant overall heat transfer coefficient from the refrigerant to the air when the evaporator is completely full and $\dot{W}_{\text{c,max}}$ is the constant limit on maximum energy consumption in the compressors.

3.4 Energy cost

The work done in the compressor, denoted $\dot{W}_c(t)$, dominates the power consumption in the system. It can be expressed by the mass flow of refrigerant $\dot{m}_{\mathrm{ref}}(t)$ and the change in energy content. We describe energy content by the enthalpy of the refrigerant at the inlet and at the outlet of the compressor ($h_{ic}(t)$ and $h_{oc}(t)$, respectively). These enthalpies are refrigerant-dependent functions of T_e and $P_c = P_c(T_a)$ (T_a is outdoor temperature) as denoted in (3.1). They are computed using, *e.g.*, the software package REFEQNS [Sko00b], which models the thermodynamical properties of different refrigerants, or by using data sheets for the refrigerant. Another compressor sits between the frost evaporator and the suction side of the other compressors, as seen in Figure 3.1. This compressor decreases the evaporation temperature for the frost part of the system to a lower level. We can describe the work in the frost compressor by identical equations but the pressure at its outlet is determined by the evaporation temperature for the cooling part. The mass flow through the frost compressor adds to the flow through the cooling compressors. We use the subscript F to denote variables related to the frost part. We describe $\dot{W}_c$ as

$$\dot{W}_c = \frac{\dot{m}_{\mathrm{ref}}\left(h_{oc}(T_e, P_c) - h_{ic}(T_e)\right)}{\eta_{is}(P_c/P_e)(1 - \eta_{\mathrm{heat}})}, \tag{3.1}$$

where the isentropic efficiency $\eta_{is}(t)$ is a function mapping the pressure ratio over the compressor into compression efficiency and η_{heat} is a constant heat loss (in per cent) from the compressor. The mass flow is determined as the ratio between cooling capacity and change of enthalpy over the evaporator ($h_{oe}(t) - h_{ie}(t)$):

$$\dot{m}_{\mathrm{ref}} = \frac{\sum_i \dot{Q}_e, i}{h_{oe}(T_e) - h_{ie}(P_c)} + \dot{m}_{\mathrm{refF}},$$

$$\dot{m}_{\mathrm{refF}} = \frac{\sum_j \dot{Q}_{eF}, j}{h_{oe}(T_{eF}) - h_{ie}(P_c)},$$

for $i = 1, \ldots, \#$ of refrigerated units and $j = 1, \ldots, \#$ of frost units.

The efficiency function η_{is} can be found in several ways. We used data from first principles thermodynamic calculations to fit a model of the form

$$\eta_{is}(\alpha) = c_1 + c_2\alpha + c_3\alpha^{1.5} + c_4\alpha^3 + c_5\alpha^{-1.5},$$

where $c_1, \ldots, c_5$ are constant parameters. We found this approximation to be accurate within 1 %. Figure 3.3 shows η_{is} versus the pressure ratio $\alpha = P_c/P_e$.

We describe the instantaneous energy cost of operating the system by multiplying power consumption by the real-time electricity price $p_{el}(t)$. The energy cost C over
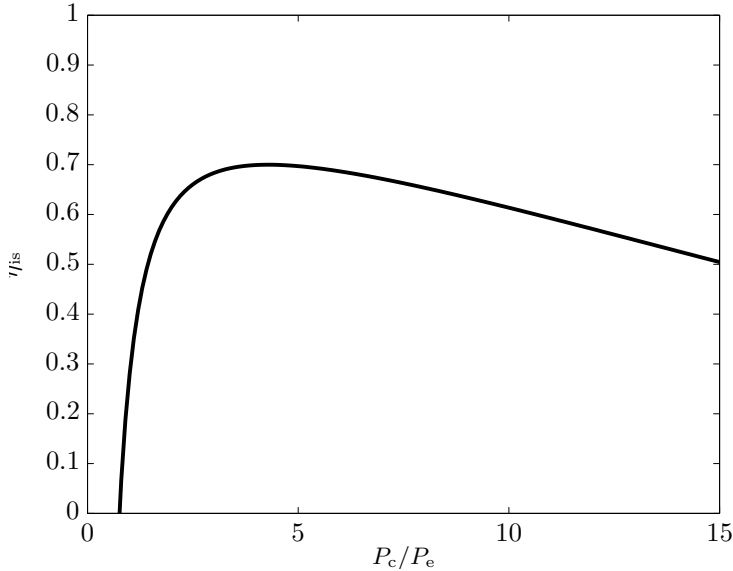
Figure 3.3: Isentropic efficiency of the compressor as a function of the pressure ratio P_c/P_e.

the period $[T_0, T_{\text{final}}]$ is

$$C = \int_{T_0}^{T_{\text{final}}} p_{\text{el}} \left(\dot{W}_c + \dot{W}_{cF} \right) dt.$$

Whereas the system dynamics can be described with linear relations, we found that the nonlinearities in the cost of energy, especially due to the temperature dependent efficiency of the work done in the compressor, are quite severe. Thus, for realistic reflection of the cost reduction potentials, we must model these terms rather accurately.

3.5 Control

Manipulated variables Our controller manipulates the cooling capacity $\dot{Q}_e$ in each zone and the evaporation temperatures T_e and T_{eF}. The latter two are common for the entire refrigeration part and the entire frost part, respectively. In practice this is achieved by setting the set-points for inner control loops which operate with a high sample rate (compared to our control). This fast local control system allows us to ignore the complex and highly nonlinear behavior in the gas-liquid mixture in the evaporator.

Measured variables The controller bases its decisions on measurements of air and food temperatures in each unit, on the known current outdoor temperature and electricity price, and on the predicted future values of the latter two. The heat disturbances are unknown and regarded as stochastic variables.

3.6 Thermostat control

Today, most display cases and cold rooms are controlled by a thermostat. This means that maximum cooling is applied when the cold room temperature reaches an upper limit and shut off when the lower limit is reached. The advantage of this control policy is that it is simple and robust. The disadvantages, however, include: a high operating cost since the controller is completely unaware of system efficiency and electricity prices, no capability of demand response, and no specific handling of disturbances.

3.7 Linear simplification and model reduction

For the more conceptual studies in this thesis, we use a simplified linear model. We lump the food and air temperatures into a common cold room temperature $T_{cr}(t)$, that satisfy the following energy balance

$$mc_p \frac{dT_{cr}}{dt} = \dot{Q}_{load} - \dot{Q}_e,$$

with

$$\dot{Q}_{load} = k_{amb-cr}(T_{amb} - T_{cr}),$$
$$\dot{Q}_e = k_{cr-e}(T_{cr} - T_e).$$

The combined thermal mass for the cold room is denoted by mc_p. The evaporation temperature of the refrigerant T_e can be controlled by the compressor work and must satisfy $T_{cr} \geq T_e$. This is the only manipulable variable in this model. The constants k denote the heat transfer coefficients. m and c_p are the mass and the overall specific heat capacity of the combined refrigerated goods and air. The power consumed by the refrigeration system is due to the work performed by the compressors. We use the linear relation: $W_c = \eta \dot{Q}_e$. η is the coefficient of performance that we for simplification assume constant and independent of the temperatures. The constraints are

$$T_{cr,min} \leq T_{cr} \leq T_{cr,max}$$
$$0 \leq T_{cr} - T_e \leq \infty$$

In addition to these constraints, we enforce the evaporation temperature (T_e) to be between specified limits and to respect some rate of change constraints.

This model has entirely linear dynamics, constraints and cost function (the work in the compressor) and can be used when formulations compatible with, *e.g.*, linear programming are desired. However, the model is quite simplified, especially the assumption for W_c. Still, the resulting dynamics are well suited for illustrating the conceptual case.

3.8   A set of selected parameters

We have collected data from supermarkets actually in operation in Denmark and from dedicated lab experiments (see Section 3.9 for further details). From these data, typical parameters such as time constants, heat loads, temperature ranges, capacities, and normal control policies have been estimated for three very different units; a milk cold room, a vertical shelving display case and a frost storage room. These units differ widely in load, mass of goods, and temperature demands. The refrigeration system that we monitored uses CO_2 as refrigerant. CO_2 is getting increasingly popular for supermarket refrigeration since it is non-poisonous and non-flammable and since several governments put restrictions on the usage of conventional HFC refrigerants. We use calculations of the power consumption capable of handling both sub- and super-critical operation of the CO_2 system. Table 3.1 gives the key parameters for the system. Table 3.2 shows examples of the different types of units, the total energy storage potential for each unit, and their time constants according to the state space description in Section 3.2. We note how the dominating time constant is much larger than the other time constant in all cases.

3.9   Model verification

The model of the refrigeration system builds on first principles from thermodynamics and on the advanced heat exchanger modeling described in *e.g.*, [KE11]. In the latter, and in the reference therein the models have been verified with real commercial components. We follow the definitions established in the literature, *e.g.*, [DIB96] as well. In Paper J, we demonstrate how to setup a dedicated experiment in a lab environment to estimate the parameters in our model and to design an observer for the food temperatures in the refrigeration system. Figure 3.4 shows the schematic and a picture of the setup used. As we describe in the paper, we use a grey-box identification method to estimate the parameters. We use separate data sets for

Unit 1: Milk cooler		
$m_{\text{food}}c_{\text{p,food}}$	550.0	kJ/K
$m_{\text{air}}c_{\text{p,air}}$	80.0	kJ/K
$k_{\text{amb}-\text{cr}}$	8.0	W/K
$k_{\text{food}-\text{air}}$	45.0	W/K
$k_{\text{evap,max}}$	135.0	W/K
$T_{\text{food,min}}$	1.0	°C
$T_{\text{food,max}}$	4.0	°C
Unit 2: Vertical display		
$m_{\text{food}}c_{\text{p,food}}$	395	kJ/K
$m_{\text{air}}c_{\text{p,air}}$	100.0	kJ/K
$k_{\text{amb}-\text{cr}}$	11.0	W/K
$k_{\text{food}-\text{air}}$	80.0	W/K
$k_{\text{evap,max}}$	170.0	W/K
$T_{\text{food,min}}$	2.0	°C
$T_{\text{food,max}}$	3.0	°C
Unit 3: Frost room		
$m_{\text{food}}c_{\text{p,food}}$	775	kJ/K
$m_{\text{air}}c_{\text{p,air}}$	50.0	kJ/K
$k_{\text{amb}-\text{cr}}$	2.3	W/K
$k_{\text{food}-\text{air}}$	19.0	W/K
$k_{\text{evap,max}}$	88.0	W/K
$T_{\text{food,min}}$	-22.0	°C
$T_{\text{food,max}}$	-18.0	°C
Common		
c_1	0.844	
c_2	-0.014	
c_3	-0.003	
c_4	8.97e-06	
c_5	-0.547	
T_{amb}	20.0	°C
$T_{\text{e,min}}$	-12.0	°C
$T_{\text{eF,min}}$	-35.0	°C
Compressor heat loss (η_{heat})	15	%

Table 3.1: Key parameters for the refrigeration system with three selected units.

UNIT 1: MILK COOLER

$\tau_1 = 0.4$ h
$\tau_2 = 25$ h
$\Delta T_{\mathrm{food}} m_{\mathrm{total}} c_{\mathrm{p,total}} = 1890$ kJ

UNIT 2: VERTICAL DISPLAY

$\tau_1 = 0.25$ h
$\tau_2 = 13$ h
$\Delta T_{\mathrm{food}} m_{\mathrm{total}} c_{\mathrm{p,total}} = 495$ kJ

UNIT 3: FROST ROOM

$\tau_1 = 0.6$ h
$\tau_2 = 110$ h
$\Delta T_{\mathrm{food}} m_{\mathrm{total}} c_{\mathrm{p,total}} = 3300$ kJ

Table 3.2: Examples of different units, their time constants in hours, and the total amount of energy stored when the temperature is changed from $T_{\mathrm{food,max}}$ to $T_{\mathrm{food,min}}$.

(a) Refrigerated display case with indications of energy flows, measurements and defined control volumes for air temperatures.

(b) The experiment setup in the lab.
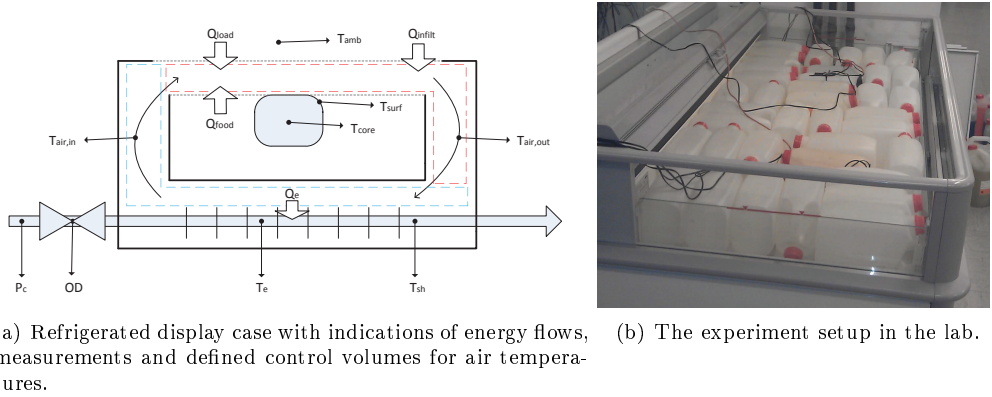
Figure 3.4: Dedicated experiment for estimation of key parameters.

training and for test of the fitted model. Figure 3.5 shows the validation set resulting in a very good fit with the experimental data and thus, validating the structure of the model. We use the Matlab function `idnlgrey` which implements numerical optimization to minimize a weighted norm of the prediction error—the difference between the measured output and the predicted output of the model. The method uses a model of the system as a set of first-order nonlinear differential equations:

$$\frac{dx(t)}{dt} = F(t, x(t), u(t), \Theta),$$

$$y(t) = H(t, x(t), u(t), \Theta),$$

where F and H are arbitrary linear or nonlinear functions (as given for the system in Paper J), t is the time, x, u, and y are the state vector, the input vector, and the output vector, respectively, and Θ is a vector of parameters to be estimated. The data set includes a time series of measured values for the input and output vectors and the estimation becomes more accurate for larger numbers of data samples.

In addition, we use extensive data sets monitored from supermarkets in real operation to adjust our model to fit different types and sizes of units. All this serve the purpose of ensuring that the dynamics, energy losses, and energy storage potentials are reflected correctly in the model that we use for our studies. To the best of our knowledge, this is the case for the advanced model presented in the previous sections, whereas the linear simplification of the power consumption is entirely conceptual, as already described. Figure 3.5 shows a data set from the validation of our model and in Figure 3.6, we show an example from a supermarket in operation.
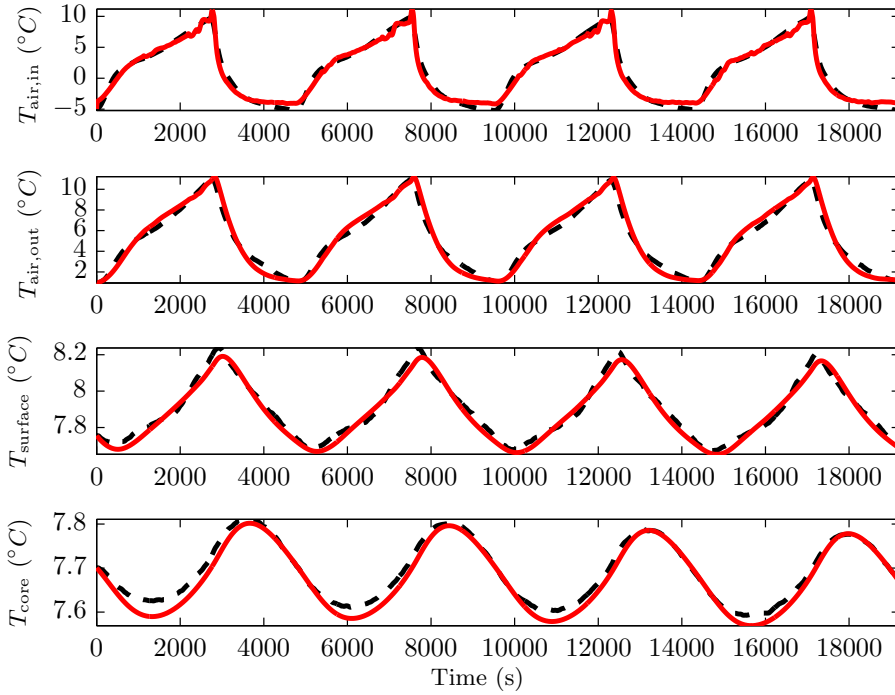
Figure 3.5: Model verification. The dashed lines show the measurements and the red solid lines show the estimated values from our model. The data are from a dedicated experiment with sensors at the surface and in the core of some simulated foodstuff.
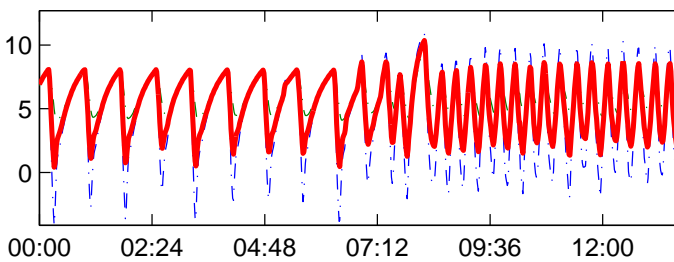
Figure 3.6: Data series showing the air temperature ($°C$) in a refrigerated unit from a supermarket in operation vs. the hour. Note the change in load from night to daytime when the store opens around 8 o'clock.

Food item	$\rho \cdot$ **Cp** $\cdot$ **V**	ESP, 15 min	ESP, 2 hours	ESP, 12 hours
50-g ham	121	11	75	NA
500-g ground beef, frozen	850	76	486	NA
1-kg solid meat, frozen	1,729	167	1,034	NA
Fresh egg	183	25	128	NA
Whole chicken, frozen	5,928	414	2.881	NA
500-g ground beef	1,569	79	513	1,397
1-L cow's milk	3,917	157	1,124	3,408
1-kg vegetables, frost	1,494	356	1,267	NA
2-L fruit juice	7,710	463	2,544	6,862
100-L milk in rack	400,876	4,009	20,044	88,193

Table 3.3: Energy storage potential (ESP) for different foodstuffs, sorted by Biot number, given for three different timescales. Energies are in J/K and the $\rho \cdot Cp \cdot V$ column gives the maximum storage potential.

3.10 Active thermal mass in foodstuffs

Depending on the timescale, the energy storage potential is not directly given by the thermal mass (total mass times the specific heat capacity) in a refrigerated unit. Since only fractions of the stored mass might be affected by the changes in surrounding temperature, we propose to introduce the term "active thermal mass". The active thermal mass is the part of the total energy storage potential in a specific item that can be utilized when temperature changes of given durations are applied. Hence, it depends on item size, properties such as thermal conduction and surface heat transfer, and on the timescale (frequency) of the temperature changes. The relevance of applying load shifting strategies on different timescales depends on the active thermal mass for the specific foodstuffs. In Paper J, we present an analysis regarding this for different typical food items and we generalize the analysis using the two properties Biot and Fourier number. The analysis reveal a large variation among different foodstuffs and different ways of packing the items. As reproduced in Table 3.3, we find that most food items can be used for load shifting of up to 2 h duration and a few even up to 12 h, but with very different degrees of utilization with respect to the maximum potential for the items. Consequently, we would recommend to make the thermal mass $m_{\text{food}}c_{\text{p,food}}$ depend on the frequency of intended energy storage in future studies.

3.11 Challenges

A refrigeration system is influenced by a number of disturbances which we can predict (with some uncertainty) over a time horizon into the future. Cooling is the primary purpose of refrigeration systems and the main challenge is to guarantee an unaltered

quality of cooling and food safety when changing the control strategy. Some disturbances, like customers who remove goods, are difficult to predict accurately and consequently safety margins on the temperatures must be maintained. Another challenge is the vast variety of refrigeration systems installed, making it a hard task to come up with generic models suitable for off-the-shelf usage in model based control schemes of such systems. Even though we do not deal with this topic explicitly in this thesis, we would expect some kind of online adaptability of the models to accompany our control techniques in practical applications.

CHAPTER 4

Wind Power

In this chapter, we provide sufficient background and model details needed to understand the parts of this thesis that deal with control of wind turbines and wind power plants/farms. We use very generic models that are mostly developed and verified by others and made publicly available. For this reason, we will refrain from reproducing all the details in this chapter. Instead, we give an overview, describe our simplifications and assumptions, and state the relevant references.

4.1 Models

4.1.1 Wind turbine

For individual turbines, we use the NREL 5MW wind turbine model for simulations. The model and all parameters are openly available and are described in detail in, *e.g.*, [JBMS09, GSK+10]. For studies concerning control of single turbines and for reflecting the inertia in the rotational motion of the turbines, we use a representation of the model in the controller which is a slightly simplified version as described here. Table 4.1 provide the key parameters and Figure 4.2 show the power coefficient table for the NREL 5MW model. Figure 4.1 illustrates a simple mechanical structure of a wind turbine.
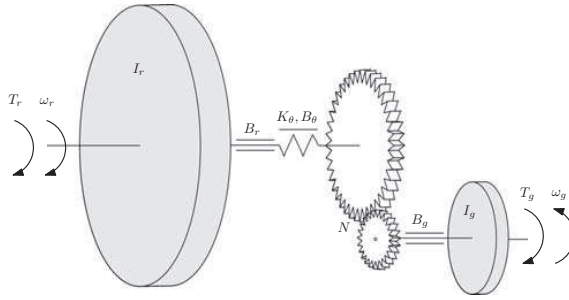
Figure 4.1: The mechanical structure of a simplified wind turbine.

We model the turbine, transmission, and generator as a single rotational system, with generator speed $\omega_{\mathrm{g}}(t)$ in rad/s, and rotor speed $\omega_{\mathrm{r}}(t) = \omega_{\mathrm{g}}(t)/N$ in rad/s. N is the gear ratio of the transmission. We let J_{g} and J_{r} denote the inertias of the generator and rotor, respectively, and we let $J = J_{\mathrm{g}} + J_{\mathrm{r}}/N^2$ denote the equivalent inertia at the generator shaft. Neglecting losses and shaft torsion (as opposed to, *e.g.*, [HHP12, MPN12]), the dynamics is given by

$$J\dot{\omega}_{\mathrm{g}}(t) = T_{\mathrm{r}}(t)/N - T_{\mathrm{g}}(t), \tag{4.1}$$

where $T_{\mathrm{g}}(t)$ is the generator (back) torque and $T_{\mathrm{r}}(t)$ is the rotor torque from the wind, in Nm. The generator speed and torque must lie within given bounds:

$$\omega_{\mathrm{g,min}} \leq \omega_{\mathrm{g}}(t) \leq \omega_{\mathrm{g,max}},$$

$$0 \leq T_{\mathrm{g}}(t) \leq T_{\mathrm{g,max}}.$$

$$\dot{T}_{\mathrm{g,min}} \leq \dot{T}_{\mathrm{g}}(t) \leq \dot{T}_{\mathrm{g,max}}.$$

The rotor torque $T_{\mathrm{r}}(t)$ is a function of rotor speed $\omega_{\mathrm{r}}(t)$, wind speed $v(t)$ (in m/s), and the blade pitch angle, denoted $\beta(t)$ (by convention in degrees). The blade pitch angle must satisfy

$$\beta_{\mathrm{min}} \leq \beta(t) \leq \beta_{\mathrm{max}}.$$

The rotor with radius R, extracts the mechanical power from the wind, denoted P_{w},

$$P_{\mathrm{w}}(t) = \omega_{\mathrm{r}}(t)T_{\mathrm{r}}(t) = \frac{1}{2}\rho A C_{\mathrm{P}}(v(t), \omega_{\mathrm{r}}(t), \beta(t))v(t)^3,$$

where ρ is the air density, $A = \pi R^2$ is the swept rotor area, and C_{P} is the coefficient of power. The coefficient of power is a function of wind speed, rotor speed, and blade pitch, typically given by a lookup table, found from aerodynamic simulations or tests. Figure 4.2 shows the C_{P}-table for the model we use. The generator produces power $P_{\mathrm{g}}(t)$, given by

$$P_{\mathrm{g}}(t) = \eta_{\mathrm{g}}T_{\mathrm{g}}(t)\omega_{\mathrm{g}}(t),$$
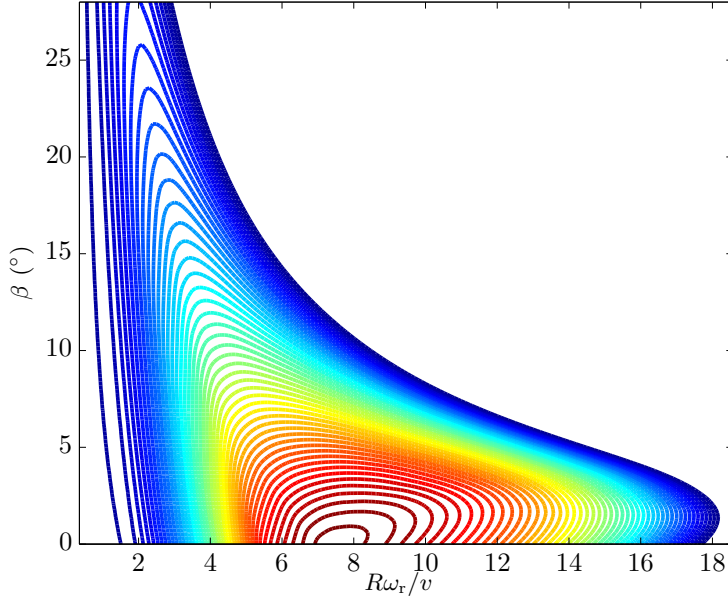
Figure 4.2: Coefficient of power C_P. The peak power coefficient is 0.482.

where $\eta_g \in [0, 1]$ is the generator efficiency. This power is constrained by

$$P_{\min} \leq P_g(t) \leq P_{\text{rated}},$$

where P_{rated} is the rated power of the generator.

4.1.2   Simple energy storage

We include a very simple model that illustrates some kind of energy storage that can be connected to a wind farm. We let $Q(t)$ denote the state-of-charge of the energy storage device, in J. With a small charge and discharge loss, the dynamics of $Q(t)$ is

$$\dot{Q}(t) = P_{\text{chg}}(t) - \eta_{\text{loss}} \left| P_{\text{chg}}(t) \right|,$$

where $P_{\text{chg}}(t)$ is the charge rate, in W. (Negative $P_{\text{chg}}(t)$ means discharging.) $\eta_{\text{loss}} \in [0, 1]$ is the loss in per cent. Charge rate and state-of-charge are limited by

$$P_{\text{chg,min}} \leq P_{\text{chg}}(t) \leq P_g(t),$$

and

$$0 \leq Q(t) \leq Q_{\max}.$$

NREL 5MW WIND TURBINE MODEL			
Rated power	P_{rated}	5	MW
Generator inertia	J_{r}	35,444,067	$kg \cdot m^2$
Generator efficiency	η_{g}	94.4	%
Generator rated speed	$\omega_{\text{g,rated}}$	123	rad/s
Max. generator torque	$T_{\text{g,max}}$	47,403	Nm
Rotor inertia	J_{g}	534	$kg \cdot m^2$
Rotor radius	R	63	m
Gear ratio	N	97	
Min. blade pitch	β_{min}	0	°
Max. blade pitch	β_{max}	90	°
Cut-In, Rated, Cut-Out wind speed	v	3, 11.4, 25	m/s

Table 4.1: Key parameters for the NREL 5MW model used for individual turbines
in this thesis.

Finally, the power supplied to the grid is

$$P_{\text{grid}}(t) = P_{\text{g}}(t) - P_{\text{chg}}(t).$$

4.1.3   Wind farms

Practical considerations and perhaps more importantly, the desire to reduce the cost
of wind energy, favor the formation of a large number of wind turbines in wind farms,
or wind power plants (WPP), as opposed to production in single wind turbines located
far from each other [JT09]. Due to the common power output to the grid, which is
shared by all the turbines in the WPP, and due to the mutual coupling of the turbines
through the wind fields flowing in between them, a park controller that distributes
the set-points to the individual turbines is added. A detailed model of a wind farm is
very complicated since it includes the fluid dynamics of the turbulent wind fields that
propagate through the farm, how the wind fields are affected by the behavior of each
single turbine, as well as by the texture of the surface of the ground. For this reason,
several simplified models that aim at capturing only the features that are important
for control, exist in the literature, *e.g.*, [MR11]. In our studies, we use a quasi-static
wind farm flow model developed in [BW10a] for simulation. It specifies in real time
the wind speed plus the tower bending moment, the blade bending moment, the rotor
shaft torque and the aerodynamic power of each turbine in a wind farm as a function
of ambient wind speed, wind direction, turbulence intensity and power set-points to
each turbine. The farm model has been validated against real measurement data from
ECNs Wind turbine Test site Wieringermeer (EWTW) [BW10b] and implemented in
Matlab in [SBW11]. Figure 4.3 illustrates the structure of the model. The wind farm

consists of turbines using the NREL 5MW model. As the farm model is entirely work that has been done by others and as it has been documented elsewhere, we choose not to go into details with it here.

In the controller design, we use the same model, but treat it as a black-box, *i.e.*, one that can be used to evaluate the outputs (*e.g.*, local wind speeds, local power production, local wind deficits, etc.) for any given values of the parameters (such as ambient wind speed and direction, power set-points, etc.). We do not attempt to implement analytic expressions that are related to first-principles models of the plant, in any way. The farm model has the following basic input/output interface for a farm with n turbines

$$[P, V, D, \Sigma_{\mathrm{add}}, M_{\mathrm{t}}, M_{\mathrm{b}}, M_{\mathrm{s}}] = f_{\mathrm{farm}}(v_0, \sigma_0, P_{\mathrm{s}}, x, y).$$

The capital letters $\{P, V, D, \Sigma_{\mathrm{add}}, M_{\mathrm{t}}, M_{\mathrm{b}}, M_{\mathrm{s}}\}$ denote n-length vectors that for each turbine in the farm give the produced power, local wind speed, wind deficit, added turbulence (velocity standard deviation), bending moment for the tower, bending moment for the blades, and bending moment for the shaft in the drive train. The inputs are ambient wind speed (v_0), ambient turbulence (velocity standard deviation) (σ_0), an n-length vector with power set-points (P_{s}), and two n-length vectors with the coordinates (topology) of the turbines (x, y). In addition, we have,

$$[p_i, d_i, \sigma_{\mathrm{add}_i}, m_{\mathrm{t}_i}, m_{\mathrm{b}_i}, m_{\mathrm{s}_i}] = f_{\mathrm{turbine}}(v_i, \sigma_i, p_{\mathrm{s}_i}),$$

for a single turbine, using local wind speed, v_i, local turbulence, σ_i, and power set-point, p_{s_i}, as inputs, where i is the turbine number. The outputs are identical to the outputs from the farm model but with only a single quantity each, related to the specific turbine in question. Thus, f_{turbine} describes the local variables for a turbine without including interactions in the farm while f_{farm} includes these and work on the farm level.
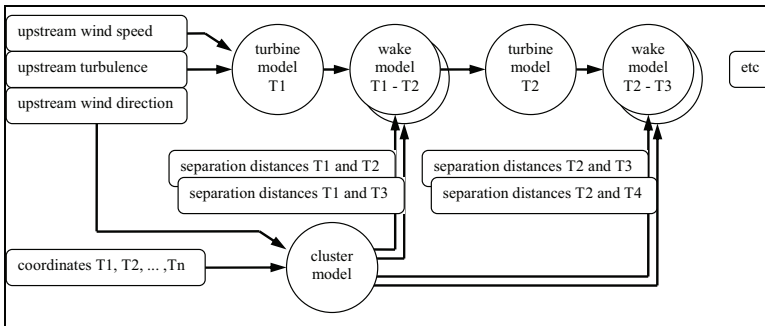
Figure 4.3: Block diagram of the wind farm model [BW10a].

For representing the turbine interactions in our controller, we have introduced a simple linear relationship. We can describe the local wind speed at each turbine as the ambient wind speed minus a linear combination of the deficits (wind speed reduction in m/s directly after a turbine, d_i) caused by all other turbines, with the coefficients depending on mutual distance and the relative angle to the wind direction. Likewise, turbulence levels (velocity variance, σ_i^2) at each turbine are the sum of the ambient turbulence (velocity variance, σ_0^2) and a linear combination of the turbulence added by all other turbines ($\sigma_{\text{add},i}^2$). $i \in 1, 2 \ldots, n$ is the turbine number in a farm consisting of n turbines. From the farm model, we estimate two coupling matrices, W_d and W_t, such that,

$$
\begin{bmatrix} v_1 \\ v_2 \\ \vdots \\ v_n \end{bmatrix} = v_0 - W_\text{d} \begin{bmatrix} d_1 \\ d_2 \\ \vdots \\ d_n \end{bmatrix},
$$

$$
\begin{bmatrix} \sigma_1^2 \\ \sigma_2^2 \\ \vdots \\ \sigma_n^2 \end{bmatrix} = \sigma_0^2 + W_\text{t} \begin{bmatrix} \sigma_{\text{add},1}^2 \\ \sigma_{\text{add},2}^2 \\ \vdots \\ \sigma_{\text{add},n}^2 \end{bmatrix}.
$$

We use an ℓ_1-norm sparsifying regularizer to emphasize the strong relations in the couplings and to promote sparse matrices.

The turbines are not able to produce power from wind speeds below a certain level. However, it might not be optimal on the farm level to downgrade upwind turbines in order to leave enough wind speed to keep all turbines in the row spinning. Turning off one or more of the turbines can be a better solution, and we introduce binary variables, $\{u_i\}_{i=1}^n$ such that the power in each turbine is constrained by

$$
P_{\min} u_i \leq p_i \leq P_{\text{rated}} u_i.
$$

In addition, the power is constrained by the available power in the wind p_{w_i}, which we find by maximizing f_{turbine} over the power set-point.

As illustrated in the two previous sections, it is possible to consider the control of a single turbine without including the interaction in the wind field. However, the wind farm controller can be combined with the single turbine MPC that we present in this thesis. This would include the effect of the wind field. In this case the optimal set-points would impose upper limits on power constraints for each turbine.

4.1.4   Control

The goal of the controller for the simplified turbine model is to choose the generator torque $T_g(t)$ and the blade pitch angle $\beta(t)$ (and the charge rate $P_{chg}(t)$ if storage is included), subject to the constraints described. The objective is to maximize the power output and obey rate-of-change constraints on the power delivered to the grid. In our studies, we compare the results with a nominal controller that has the sole objective of extracting as much power from the wind as possible at any time instant. There is no storage attached to the nominal controller as the goal is to send all the available power directly to the grid.

Traditionally, the rotor speed of modern wind turbines is controlled for tracking the tip-speed ratio ($\text{TSR}(t) = R\omega_r(t)/v(t)$) such that maximum power is extracted. This is done according to the table in Figure 4.2 while obeying constraints on the maximum rotational speed. However, due to the inertia of the rotating masses in the turbine, there is a potential for improving the quality of the power output by actively letting the rotor speed deviate from the optimal setting. This might of course come at a cost of slightly reduced power output. In, *e.g.*, [KNJ$^+$11, Tar12] turbine inertia is used for frequency response and power oscillation damping.

For our wind farm study, the goal is to compute the optimal distribution of power set-points to the individual turbines so that the total power output is maximized for a given wind speed and direction. We compare the optimal power set-points with a local "greedy" controller that aims at maximizing the power production in each single turbine with no knowledge of the interactions in the farm.

4.2   Challenges

We have several objectives to consider for the wind turbines. The first is the total energy E over the period,

$$E = \int_0^T P_{grid}(t) \, dt,$$

which we want to maximize. For the WPP, P_{grid} is the sum of power over the number of turbines. Secondly, we can add a penalty (which we wish to minimize) for violating a target maximum value of power rate of change, G (in W/s):

$$R_{pen} = \int_0^T (|\dot{P}_{grid}(t)| - G)_+ \, dt,$$

where $(b)_+ = \max(b, 0)$.

For the wind farm optimization we only focus on combined power output, *i.e.*, maximization of the sum P_{total} over the vector P

$$P_{\text{total}} = \sum_{i=1}^{n} p_i.$$

The optimizer manipulates the vector P_{s} with power set-points p_{s} for each turbine.

Contrary to the refrigeration systems, the model parameters for the individual wind turbines are pretty accurately known. However, the models describing the wind fields and the interaction between the turbines in the farm are quite simplified. Like the refrigeration systems, wind turbines are affected by disturbances, primarily the wind. Even though wind prediction methods have improved a lot the forecasts are still somewhat uncertain and it can be a challenge to obey the constraints on, *e.g.*, load, speed, and power output.

Economic Model Predictive Control

In this chapter, we motivate the choice of economic model predictive control as our preferred control strategy throughout the thesis. Furthermore, we introduce our general formulation of the economic model predictive control problem.

5.1   Choice of methods

In the control challenges, we have described in the previous sections concerning both refrigeration systems and the selected aspects of wind power, several similarities exist. The systems are constrained by physical/mechanical limitations as well as limits imposed by different desires to control performance such as upholding certain cold room temperatures or obeying power ramp rates defined in the grid codes. In addition, the control problems are multivariate with several independent and dependent variables that are hard (or impossible) to separate into single-input-single-output control loops. MPC has gained a lot of popularity in the process industry due to its natural and explicit handling of multivariable constrained optimal control problems. Besides its capability to handle constrained control problems, another reason for choosing MPC is its ability to easily incorporate predictions and forecasts from, *e.g.*, weather services, electricity markets, power balance responsible parties, etc. For the applications
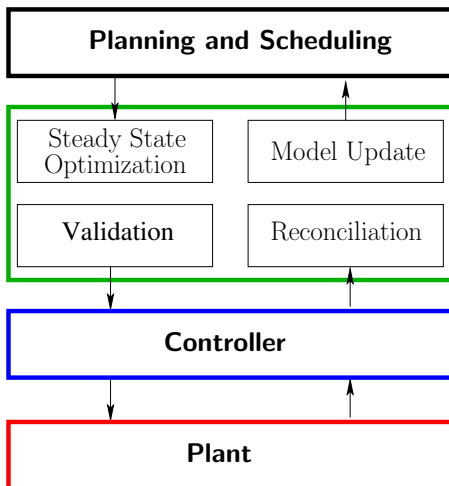
Figure 5.1: Two layer structure: The steady-state layer optimizes steady state
model and passes optimal set-points to the dynamic layer. The con-
troller in the dynamic layer tracks the set-points using, *e.g.*, a linear
MPC. Source: [RAB12].

we consider in this project, we do not aim at tracking certain set-points or trajecto-
ries but merely at minimizing an economic cost, or likewise maximizing the profit,
related to operating the system. Economic optimizing MPC provides a straightfor-
ward and natural framework for formulating economic objectives for the controller
that are directly related to the real costs and are easy to understand. Often, MPC
is used to regulate a system to a steady-state. But for the energy systems that we
consider, a steady-state is not existing, or it is at best periodic over the day, week,
or year. A traditional least-squares approach, that regulates the system towards a
defined trajectory, can of course be combined with an economic optimizing strategy.
In this case, the economic objectives would be used to compute an optimal trajectory
offline while the goal of the tracking controller (*e.g.*, an LQG controller) would be
to follow the trajectory. This setup is illustrated in Figure 5.1. By implementing
economic MPC with the economic objectives explicitly in the dynamic layer, and
without a precalculated steady-state target, we allow the system to exploit potential
economic improvement opportunities that arise during the operation. We can regard
this as a way of increasing the frequency of calculating the optimal steady-states.
This formulation also has an advantage when we include the stochastic elements of
the system. As the open-loop optimization might not be optimal in the presence of
uncertainty, a more frequent computation of the optimization problem can be supe-
rior. Consequently, the two layer structure in Figure 5.1 is merged into only one layer
in our formulations.

5.2   Performance vs. complexity

The best choice of method is often a balance between performance and complexity. The increase in performance must motivate the increase in complexity. As MPC is traditionally considered an advanced control method that may require online solution of optimization problems, we aim at simplifying our models and implementations to avoid unnecessary complexity. Thereby, we demonstrate the feasibility for industrial implementations. Complexity can be in terms of both modeling, implementation and computational effort. With our natural constraints and objectives directly inspired from the physics of the systems, our efficient optimization routine for nonconvex problems, and with the disposal of today's computing power and tools for embedded optimization codes, we remove important barriers for applying MPC. Figure 5.2 schematically illustrates the trade-off between complexity and performance of a control method. When we replace the rather simple control strategies, that are currently implemented in the industrial applications, with a more complicated method such as MPC, we expect to improve the performance of the system up to at least some significant level. The challenge is to achieve this while keeping the complexity on a tractable level. For economic MPC, control performance is primarily in terms of cost of operation as well as constraint satisfaction. In this work, we prove that the expected potential for increased performance exists, and we demonstrate that the complexity induced by our methods can be reduced to render implementation on industrial applications feasible.
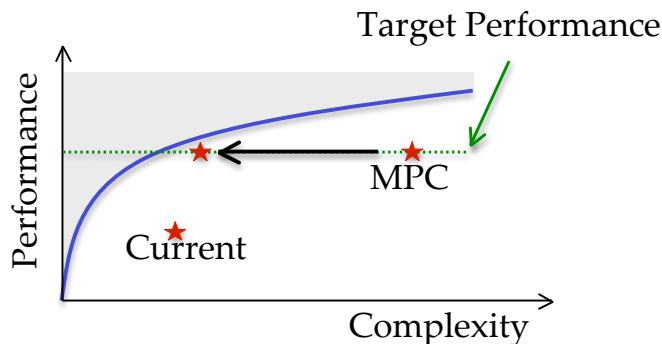
Figure 5.2: Performance vs. complexity going from the current control scheme to MPC to specialized MPC. Goal: Minimize complexity for a given performance. Source: [MJBZ07]

5.3   Deterministic and stochastic systems

The explicit use of a system model in MPC is an obvious advantage. However, due
to the lack of exact knowledge of system parameters and/or unmodeled high order
dynamics, the system model can also introduce uncertainty into the solution. Several
means for robustifying the MPC formulations exist in the literature and in this thesis
we will apply a couple of these—a rather advanced probabilistic formulation of the
constraints, and a simpler method introducing safety margins to the limits. Both,
utilize the property that the constraints related to a desired performance in MPC
generally, do not have to be fulfilled at all times. In the implementations, we mostly
base the control design on deterministic systems. We assume that the separation
principle applies and use the certainty equivalence for designing our deterministic
controllers (see, *e.g.*, [Bre02]). We do not consider the design of observers, *e.g.*, a
Kalman filter, in this thesis, although such state estimators would normally be part
of the feedback loop in a real application. We handle the stochasticity in a heuristic
manner, and obtain robustness by tuning. Furthermore, we must remember that
feedback (or recourse) resolves a lot and the optimization problem solved in each
MPC step is nothing but a heuristic for computing a good control. The quality of
closed-loop control with MPC is generally good even without accurate knowledge.
Figure 5.3 exemplifies that the reduced risk in robust methods typically comes at the
price of a lower expected profit compared to a non-robust strategy, e.g. a certainty
equivalent strategy. However, the induced cost from severe violations (*e.g.*, damaged
foodstuffs, break down of equipment, and power imbalance penalties) in our appli-
cations, necessitate some trade-off to be made. In spite of this, we expect that the
introduction of our advanced control strategies can reduce the variance on the system
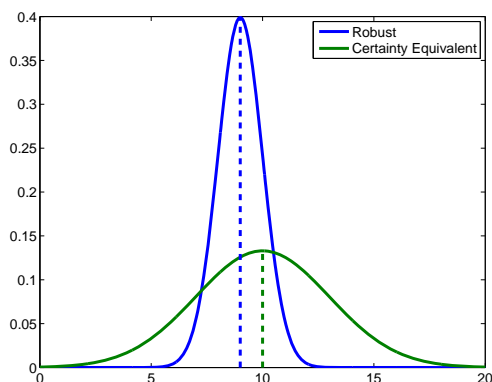
Figure 5.3: Sketch of the distribution of the profit for two strategies. A robust
strategy has lower variance and typically also lower mean value than
non-robust strategies such as a certainty equivalent strategy.

outputs sufficiently to allow for operation closer to the constraints.

5.4 Economic MPC formulation

As in traditional MPC, the economic MPC controller is implemented in a receding horizon manner, where an optimization problem over N time steps (the control and prediction horizon) is solved at each step. The result is an optimal input sequence for the entire horizon, out of which only the first step is implemented [RM09, Mac02]. The term economic MPC indicates that the objective has no relation to stabilization of tracking problems, which are predominant in the MPC literature [Grü13]. "Standard" MPC, adopts a stage cost that need not be directly related to the economic cost incurred during plant operation. This cost is conveniently chosen to be minimal at the desired set-point [RA09, AAR12]. Figure 5.4 illustrates the receding horizon principle for the standard MPC. However, [MAS80, Sko00a] states that the objective in the synthesis of a control structure is to translate the economic objectives into process control objectives. This is explicitly implemented in economic MPC where the cost incurred for plant operation is used directly as a stage cost in the MPC optimization.

In recent literature [DAR11, AAR12], steady-state stability and performance of economic MPC schemes have attracted much attention, *e.g.*, by means of suitable Lyapunov techniques. In our formulations of economic MPC, we do not consider steady-states or target set-points, since such are not natural for the energy systems we consider. For instance, our controller for the supermarket refrigeration systems aims at minimizing the electricity cost of operation. This cost relates to the energy consumption but we do not aim specifically at minimizing this, nor do we focus on tracking certain temperatures in the cold rooms as long as they stay within certain ranges. In addition, we do not deal specifically with stability issues as we use rather long prediction and control horizons to overcome this in all our formulations. Also, *e.g.*, [Grü13] shows how generalization of conditions from standard stabilizing MPC without terminal constraints can ensure convergence towards the optimal state and approximately optimal transient behavior.

For our formulation of economic MPC, we use discrete time, constrained systems in the form

$$x_{k+1} = f(x_k, u_k, d_k),$$

$$h(x_k, u_k, d_k) \leq 0,$$

where x describes the dynamical states of the system, u is the manipulable inputs and d is a (predictable) disturbance, with $k \in \{0, 1, \ldots, N\}$. In general, the system dynamics $f(x_k, u_k, d_k)$ and/or the set of constraints $h(x_k, u_k, d_k)$ can be either linear
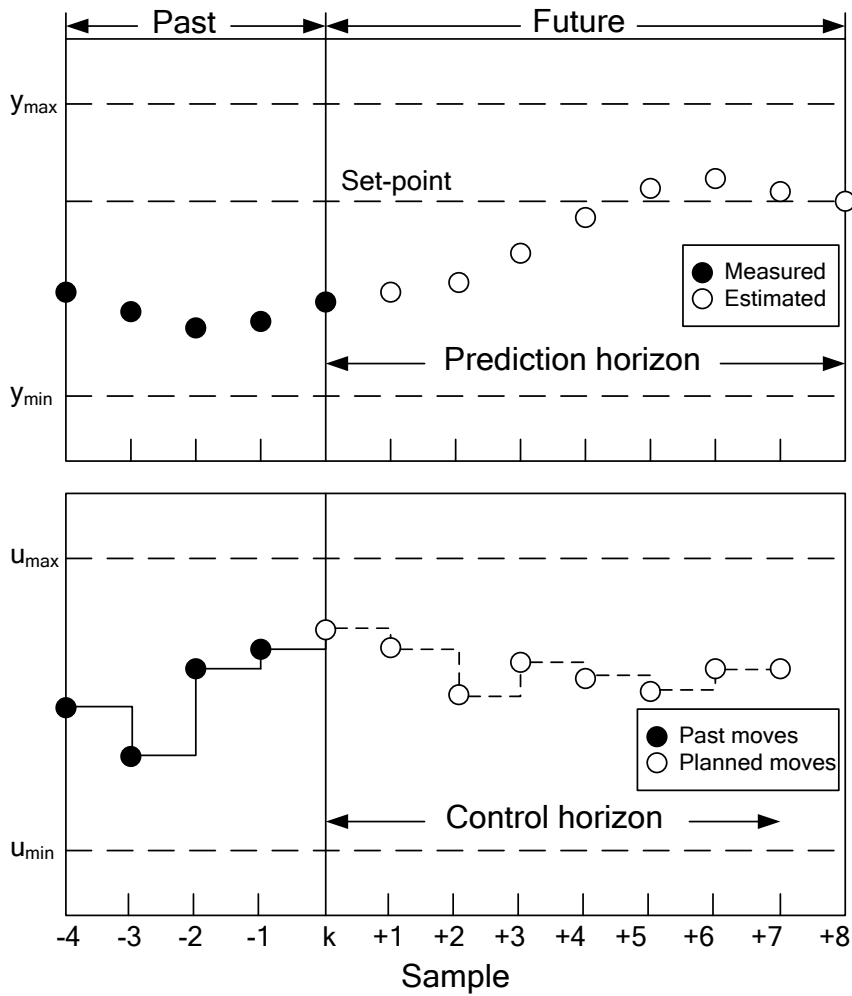
Figure 5.4: Sketch of one step in the closed-loop MPC trajectory for a standard tracking MPC.

or non-linear. Both functions are directly derived from the differential equations and the constraints that we presented in the modeling chapters (3–4), by applying, *e.g.*, a zero-order hold to the continuous time variables. For all cases in this thesis regarding the supermarket refrigeration systems, we chose the variables such that both f and h are linear and convex functions. For the wind power problems, we distinguish between one approach in which we accept the dynamics as nonlinear, and a reformulation that renders the problem fully convex.

In addition, we specify an economic stage cost function $L(x_k, u_k, d_k)$ from the economic objectives that we define for both systems in the modeling chapters. L is not confined to be neither linear nor convex in the general case. This economic stage cost differs from the stage cost in tracking problems, which is typically formulated as a weighted least-squares type of cost

$$L_{\text{tracking},k} = Q\|x_k - x_{\text{sp}}\|_2^2 + R\|u_k - u_{\text{sp}}\|_2^2,$$

where $(x_{\text{sp}}, u_{\text{sp}})$ is the desired set-point and Q and R are constant weights. While working with the commercial refrigeration systems, we found that the efficiency of the refrigeration cycle is highly nonlinear and dependent on both the manipulable variables and the disturbances. Thus, for realistic studies, we accepted the objective function L as nonconvex in most of our work. This case, with linear dynamics and constraints but a nonconvex cost, is rather special and we exploit this when developing our methods. We also use an entirely linear simplification of the problem which allows us to perform some of the more conceptual feasibility studies in this thesis.

The goal of the economic MPC is to implement a feedback law, $u_k = \mu(x_k, d_k)$, so that the system remains feasible while the cost

$$\sum_{k=0}^{N} L(x_k, u_k, d_k) + L_N(x_N),$$

over the control and prediction horizon N, is minimized. Within this framework, we formulate all control problems in the thesis. Our work primarily contributes to this field by demonstrating actual usage for real systems—from formulation and adaption of realistic dynamical models, over modifications of robust variants to economic MPC, to dedicated optimization techniques that can facilitate the soundness of practical implementations. As such, economic MPC is the overall theme for our project and we will go more into detail with the contributions to the field as we describe the applications throughout the remainder of this thesis.

Part II

Summary Report: Main Contributions

Flexible Power Consumption in Commercial Refrigeration

In this chapter, we highlight the scientific contributions related to flexibility of commercial refrigeration by using economic MPC.

6.1 Scientific contributions

The common subject for Papers A, E, and I (and partially for Papers C, F, and K as well) is the investigation of model predictive control technologies that enable flexible power consumption, *i.e.*, ability to shift the system load in time, in supermarket refrigeration systems. With the exception of papers E and F, in which a direct control scheme is applied, we do this so that the local cost of operation of the refrigeration systems is optimized at the same time. We assume that a price signal is available in order to do this. In all our studies, we observe the main purpose of supermarket refrigeration; namely, to keep the foodstuffs within safe temperature ranges.

6.2 Linear economic MPC

In Papers E and F, we present conceptual studies using the linear model (see Section 3.7). We investigate the potential of utilizing the refrigeration systems' flexibility to counteract imbalances in a simple power plant portfolio consisting of two conventional power plants with different capacities, slew rate limitations and costs, a large controllable cold room, and a net power demand signal formed by combining the effect of all uncontrollable consumers and producers. The latter can be exemplified by wind power production and to reflect rapid changes in the wind speed, we construct the net power demand signal with sudden steps. For this scenario, we define a central control directly controlling all units. The subsystems are dynamically independent but they are coupled through a supply-demand constraint. Our studies extend the power plant examples used in [EBJ11] and with the addition of our simplified refrigeration system, the entire system can still be modeled in a form compatible with the economic MPC for linear systems.

In this section, we use the simplified linear model with constant efficiency, as presented in Section 3.7. We discretize this model and formulate the economic MPC as a linear program. The matrices A, B, C, D, C_z, D_z, E, F, and F_z describe the linear, discrete-time state space model.

$$\text{minimize}_{\{x,u,y,z\}} \quad \sum_{k \in \mathcal{T}} c_y' y_k + c_u' u_k \tag{6.1a}$$

$$\text{subject to} \quad x_{k+1} = Ax_k + Bu_k + Ed_k \quad k \in \mathcal{T} \tag{6.1b}$$

$$y_k = Cx_k + Du_k + Fd_k \quad k \in \mathcal{T} \tag{6.1c}$$

$$z_k = C_z x_k + D_z u_k + F_z d_k \quad k \in \mathcal{T} \tag{6.1d}$$

$$u_{\min} \leq u_k \leq u_{\max} \quad k \in \mathcal{T} \tag{6.1e}$$

$$\Delta u_{\min} \leq \Delta u_k \leq \Delta u_{\max} \quad k \in \mathcal{T} \tag{6.1f}$$

$$z_{\min} \leq z_k \leq z_{\max} \quad k \in \mathcal{T} \tag{6.1g}$$

with $\mathcal{T} \in \{0, 1, \ldots, N\}$. The cost of the economic MPC is a linear function of the manipulable inputs, u_k, and the outputs, y_k. In this case the cost is only related to producing power and is thus solely dependent on the manipulable inputs, u_k (here the power set-point to the two power plants), and $c_y = 0$. The manipulable inputs, u_k, are constrained by the input constraints (6.1e) and (6.1f). The outputs, z_k, are limited by the output constraints (6.1g). We assume that the economic MPC is feasible, i.e. that the initial state, x_0, and the disturbances, $\{d_k\}_{k=0}^N$, are such that the feasible manipulable variables, $\{u_k\}_{k=0}^N$, can bring the system to satisfy the output constraints (6.1g).

Figure 6.1 reproduces some of the results from this study, showing, *e.g.*, how the cold room temperature is pulled down to its lower limit after the sudden drop in power
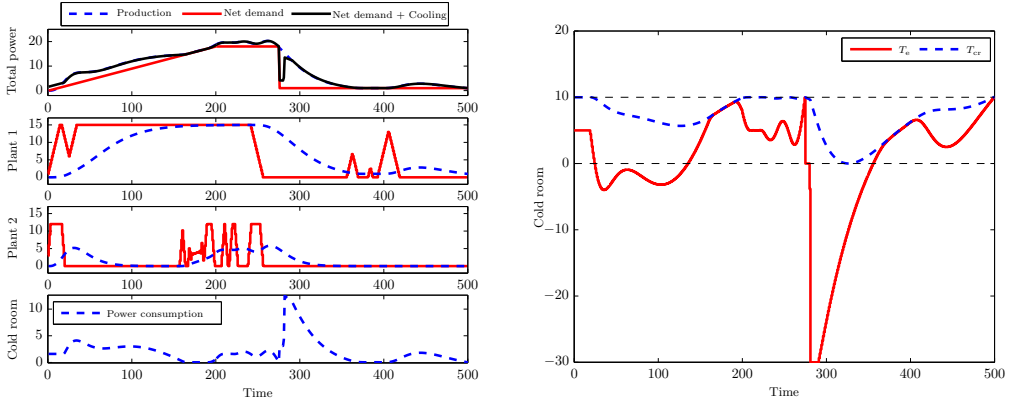
(a) Power productions from the two power plants (dotted blue) and their power set-points (solid red). "Total Power" is total power production (dotted blue), the net demand (with (solid black) and without (solid red) the consumption for refrigeration.)

(b) Temperature in the cold room T_{cr} and the control signal for the refrigeration system T_e. $T_{cr,min}$ and $T_{cr,max}$ are shown with dotted black.

Figure 6.1: Simulation of simple power generation problem with two power plants and one cold room. The open-loop profile is shown. On the upper left plot the power production coincide with the total demand (the black line) except immediately after the drop in net demand.

demand. By doing so, the excess power produced in the power plants is absorbed and the power demand from the refrigeration system can be reduced at a later time, resulting in a total saving for the entire scenario. We also investigate the correlation between total thermal mass in the cold room and potential savings. This gives the trend illustrated in Figure 6.2.

These studies demonstrate that economic MPC for refrigeration systems is able to provide a more flexible power consumption. This flexibility is obtained by utilizing the thermal storage capability by solving a centralized economic MPC problem. We reveal the viability and a potential of applying such a method. However, we base the analysis on rather simplified models and disregarded practical limitations of the method such as: 1) how to solve the centralized optimization problem as the number of subsystems grows large in a realistic power portfolio, and 2) how to make the solution robust as the optimum of an LP is an extreme point of the feasible region, which implies that even small perturbations in the data or the disturbances may change the optimal solution dramatically [RR00]. Furthermore, the control signal to one of the power plants in Figure 6.1(a) is too aggressive. This behavior must be regularized in the formulation.
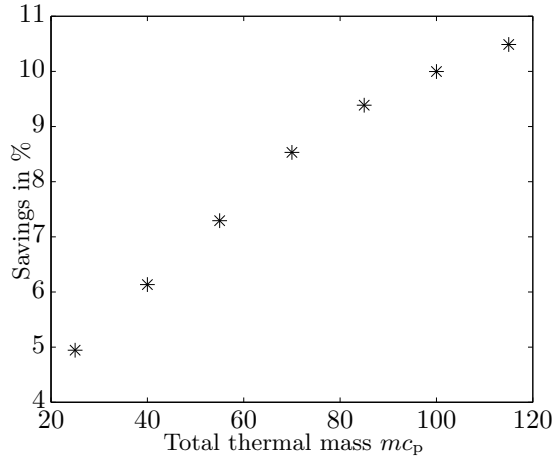
Figure 6.2: Savings compared to non-controllable load for different values of mc_p

6.3   Cost optimal price and load response

In this section, we create a local cost optimizing controller for the supermarket refrigeration system, as opposed to the centralized solution summarized above. The control strategy is still economic MPC, with a cost function reflecting entirely economic objectives, but in this case it is decoupled from the production side by electricity price signals or predictions of these. In addition, we use the forecasted outdoor temperatures to take the varying efficiency of the thermodynamic cycle into account. In Papers A, C, I, and K this is the recurring scope. The major concern in Papers C and K is the dedicated optimization method which we will describe in more detail in Section 8.4. The overall motivation in these papers too, is the price responsive flexible power consumption and we will highlight the main results in this section.

In the studies the objective is to minimize the term C which we introduced in Section 3.4. C is the sum of the instantaneous energy cost of operating the system (the product of power consumption W and real-time electricity price p_{el}) for the control horizon $[T_0, T_{final}]$:

$$C = \int_{T_0}^{T_{final}} p_{el} \left(\dot{W}_c + \dot{W}_{cF} \right) dt.$$

In all three papers, we use slight variations of the full model described in Chapter 3. We consider cases with three very different refrigerated units attached to the same compressor and condenser system. The study include one frost unit with high thermal capacity and low load, and two fridges—one with relatively low thermal capacity and a high load and another with a higher capacity and smaller load. The units all

have different temperature ranges. This is to reflect the composition in actual super-markets. All parameters, dynamics and constraints for this system are included in the full model description in Chapter 3. The model dynamics and the constraints are linear but, as C is nonconvex in the controllable variables Q_e and T_e, the optimization problem is nonconvex.

In Papers A and I, we assume perfect knowledge of the predictions (outdoor temperature and electricity price). We use electricity prices from NordPool's hourly el-spot price for a period of one month. There is a clear trend in these data for each 24-h period. Therefore, for each hour of the day, we compute the average and use this 24-h signal as the electricity price. Likewise, we use temperature readings from the Danish Meteorological Institute covering the same month. From these, we estimate the intra-day variations by a sinusoid with a 24-h period and a phase shift such that it peaks a couple of hours after noon. The amplitude is $3°C$. We do not include any unknown disturbances such as unpredictable heat loads on the units. These assumptions lead to a prescient scenario with full knowledge which is of course a crude simplification. However, the slow dynamics of the refrigeration system allow us to sample at a very slow rate (once every 32 minutes) as there is no stochastic elements to affect the system in this case. Hereby, we can limit the computational burden of the non-trivial optimization problem by covering a prediction horizon of 16 h with just $N = 30$ samples. The constrained optimal control problem to be solved is non-linear and nonconvex. We use ACADO [HFD10], a generic nonlinear optimal control code, to solve the problem.

In Paper B, we analyze the structure of the optimization problem and conclude that a unique minimum exists within the feasible region. This suggests that a nonlinear optimization tool, such as ACADO, will find the optimal solution. The downside is still the computational complexity. For the problems presented here, ACADO needs more than 4 minutes per MPC step to compute the solution (on a 2.8GHz Intel Core i7). In Papers C and K, as well as in Section 8.4, we address computational methods to reduce the time needed to compute a solution for the nonconvex constrained optimal control problem.

Figure 6.3 shows the simulated refrigeration system using the outdoor temperature and electricity price trajectories to optimize the cost. We clearly observe how the cold room temperatures are pulled down when there is a combination of low price and high efficiency (low outdoor temperature) between 3 and 5 o'clock. The smaller dips in the price at other times result in less energy being stored in the refrigeration system. Here we have magnified the amplitude of the electricity price by a factor of four to reflect a scenario with variable taxes instead of the flat-rate fees on electricity consumption. With this price structure, the cost savings are above 30 % for the scenario considered.
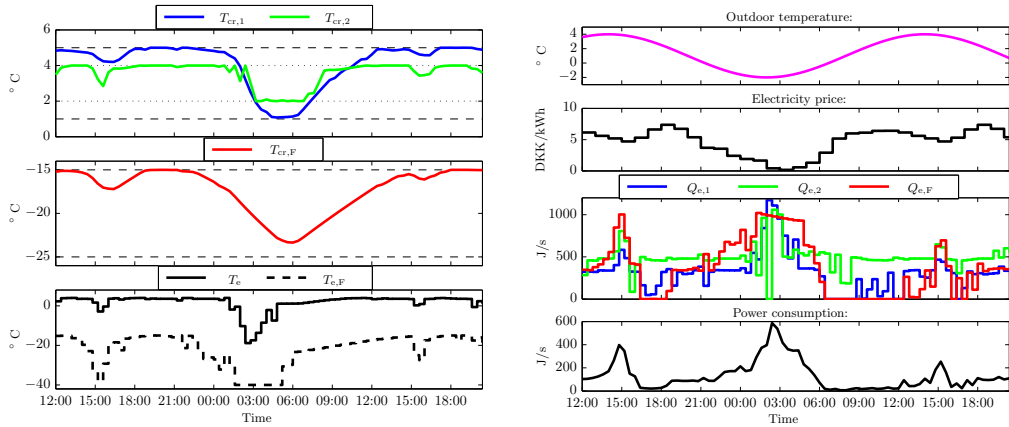
(a) Temperatures for the cold rooms ($T_{cr,1}$ and $T_{cr,2}$), the frost room ($T_{cr,F}$), and the evaporation temperatures (T_e and $T_{e,F}$).

(b) Disturbances, cooling capacities ($Q_{e,1}$, $Q_{e,2}$, and $Q_{e,F}$), and total power consumption.

Figure 6.3: Simulation showing how variations in outdoor temperature and electricity prices are exploited by utilization of thermal storage.

6.3.1 Realistic simulations

In Papers C and K, we demonstrate our method for a realistic model, with a full year simulation and 15 minute time periods, using historical electricity prices and weather data, as well as random variations in thermal load. In addition, we implement very simple predictions of the outdoor temperatures and the electricity prices for the chosen prediction horizon. Only past values of such parameters can be available to the controller and we incorporate predictors that can provide a sufficiently good estimate of the disturbances using a series of past measurements. We use historical data to train these predictors. Section 7.3 and Papers C and K describe the details and the accuracy of our simple predictors. With randomly occurring load disturbances, it is not possible to guarantee that the temperatures are always within the range, so in lieu of imposing the constraints, we encode the temperature constraints as a set of soft constraints and tune the back-offs and penalties so that violations of the constraints are very infrequent. Refer to the formulation of the soft constraint and back-offs in Section 7.2, where we define an additional term in the objective function, V, that we want to minimize in order to impose the temperature constraints. In section 8.4, we will describe our SCP optimization routine which allows us to carry out such extensive testings of the method in a realistic setting, in just a couple of minutes.

(a) Control by thermostat.   (b) Control by MPC.
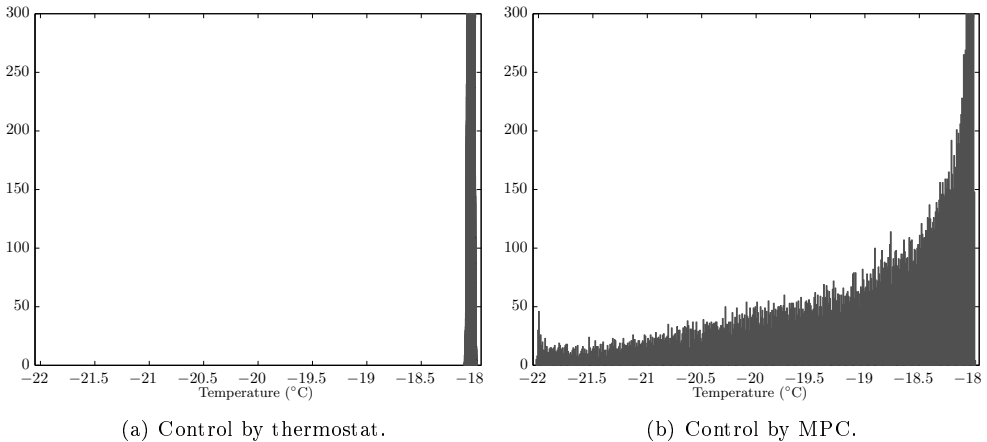
Figure 6.4: Temperature distribution for selected unit. Simulation over the full year 2010.

In the sequel, we report some of the most interesting results from the full year simulation in Paper C. Figure 6.4 illustrates resulting temperature distributions for a selected unit for both control by the conventional thermostat and by MPC. While both control policies tend to keep the temperatures close to the upper limit most of the time, we observe how the MPC controller makes use of the entire range for storing coldness. Figure 6.5 shows the total cooling energy applied to all three units plotted as a function of the electricity price at the time of use. We observe no correlation between energy consumption and electricity prices when the thermostat controls the refrigeration system while we see a clear tendency to apply more cooling at times with low prices, and vice versa, if we employ the proposed MPC scheme. Figure 6.6 compares the cost-per-period distribution for the system controlled by thermostat and by MPC, respectively. We observe savings on the order of 30 % for the simulations covering a full year (2010). We find that the extra savings gained by having the full information available instead of using the simple predictors are in the order of 1-2 %. Therefore, more complicated predictors are not needed. The papers present additional results from this study.

6.4   Regulating power

In Papers A and I, we present an extension of the study of flexible power consumption. We consider other incentives for load shifting than those already mentioned and
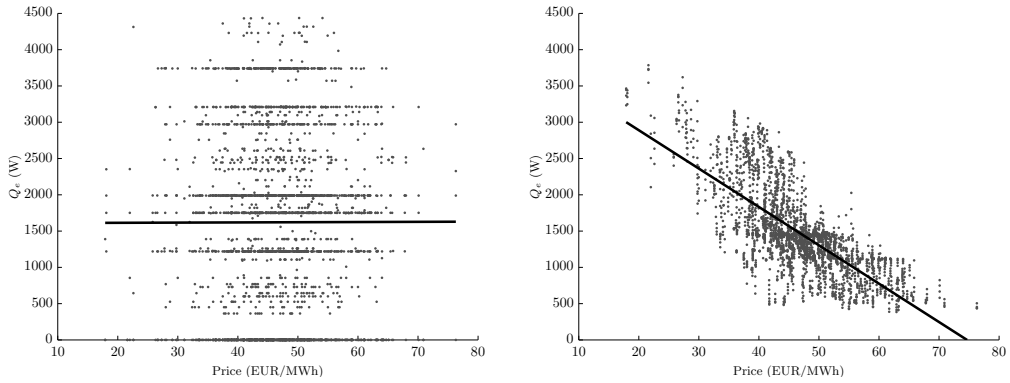
(a) Control by thermostat. The solid line is a linear fit with almost zero slope.

(b) Control by MPC. The solid line is a linear fit with a slope of -53 W/(EUR/MWh).

Figure 6.5: Illustration of demand response in systems controlled by MPC vs. thermostat control.
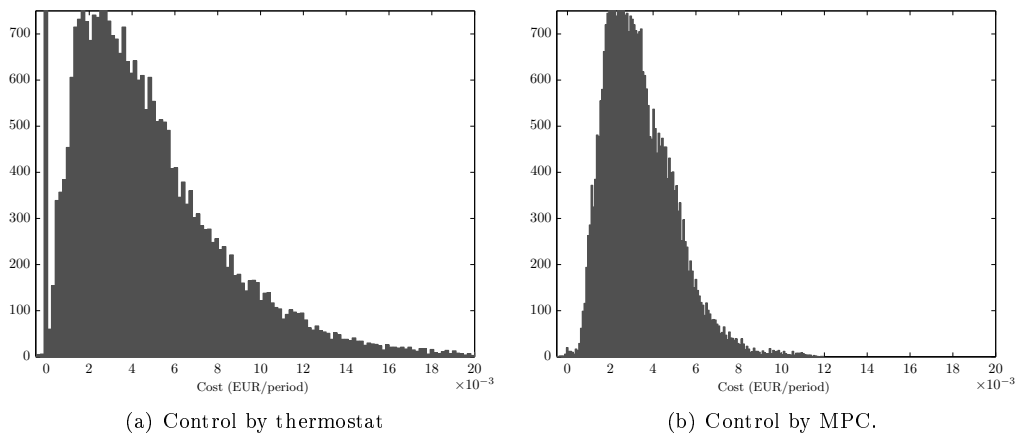
(a) Control by thermostat

(b) Control by MPC.

Figure 6.6: Distribution of cost-per-period. Simulation over the full year 2010.

formulate a framework in which the supermarkets can participate in the primary reserve market. Primary reserves are the fastest acting spare production capacity or consumption that is made available in advance to the TSO in return for an availability payment. The reserves are at the disposal of the TSO and can be activated to regulate the electricity system up, down or both. Up-regulating power corresponds to increased production or reduced consumption. Down-regulating power corresponds to decreased production or increased consumption. Activation of the primary reserve is automatic and linearly frequency-dependent in the range ± 200 mHz. Activation is maintained for up to 15 min (typically 2–3 min) and must be fully restored after 15 min.

We can derive functions for the amount of cooling capacity that can be released as up-regulating power or extra cooling capacity that can be applied for down regulation for a period of 15 min for any initial temperature level T_{cr}. Maximum up-regulating power is the decrease in compressor work W by reducing the cooling capacity with

$$\dot{Q}_{\mathrm{reg}\div} = (T_{\mathrm{cr,max}} - T_{\mathrm{cr}})\frac{m \cdot C_{\mathrm{p}}}{900s},$$

and similar, maximum down-regulating power is the increase in compressor work by increasing the cooling capacity with

$$\dot{Q}_{\mathrm{reg}+} = (T_{\mathrm{cr}} - T_{\mathrm{cr,min}})\frac{m \cdot C_{\mathrm{p}}}{900s}.$$

$\dot{Q}_{\mathrm{reg}\div}$ and $\dot{Q}_{\mathrm{reg}+}$ are constrained by the constraints on maximum cooling capacity and compressor work. We introduce new decision variables $\alpha_\div \in [0;1]$ and $\alpha_+ \in [0;1]$, which are the amounts of available up- or down-regulating power that are actually offered to the grid. By this, we can add the following two terms to the objective of the optimization problem

$$\sum_{k=0}^{N} -C_{\mathrm{upreg}_k} W_{\mathrm{c},k}(\alpha_{\div,k}\dot{Q}_{\mathrm{reg}\div,k}, T_{\mathrm{e}}, P_{\mathrm{c}}),$$

$$\sum_{k=0}^{N} -C_{\mathrm{downreg}_k} W_{\mathrm{c},k}(\alpha_{+,k} \cdot \dot{Q}_{\mathrm{reg}+,k}, T_{\mathrm{e}}, P_{\mathrm{c}}),$$

where C_{upreg} and C_{downreg} are the disposal payments for up- and down-regulating reserves. Figure 6.7 shows an example similar to Figure 6.3 but with the new cost function and a scenario of disposal payments downloaded from Nordpool along with the electricity spot price. We do not show actual activation of regulating power but make the refrigeration system prepare itself for offering the most beneficial amount of regulating services at any given time. This simulation reveals an additional saving of around 50 % compared to the case where only the electricity spot price is used for optimization. With an increasing penetration of intermittent wind energy, the value
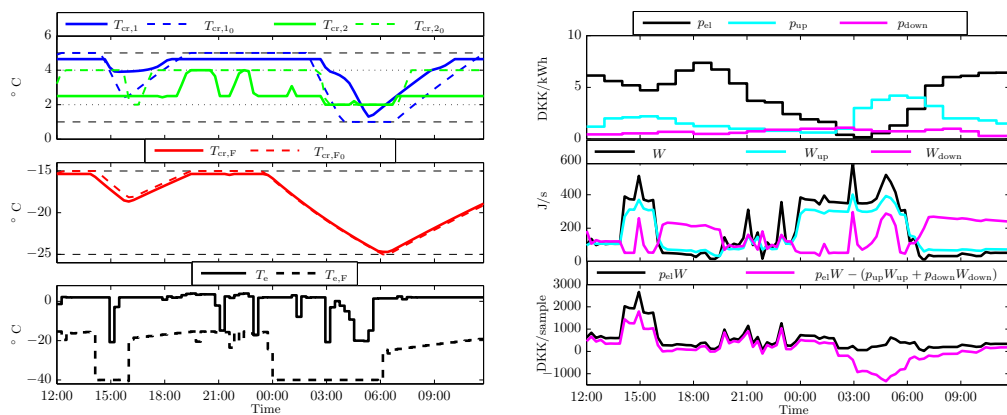
(a) Temperatures for the cold rooms ($T_{cr,1}$ and $T_{cr,2}$), the frost room ($T_{cr,F}$), and the evaporation temperatures (T_e and $T_{e,F}$).

(b) Prices (spot price p_{el}, up-reg p_{up}, down-reg p_{down}), powers (consumption W, up-reg W_{up}, down-reg W_{down}) and costs (nominal and after disposal payment.

Figure 6.7: Simulation showing how the flexible consumption is utilized for offering regulating power to the balancing market. The cold room temperatures for an optimization utilizing only the electricity spot price over the same period are shown (denoted with subscript 0) to illustrate the difference.

of regulating reserves is expected to increase [MNPW⁺10]. Thus, not only the need for regulating power, but also the incentives to participate in the regulating power market increase in the future.

6.5 Summary

In this chapter, and in the related papers, we demonstrate a significant potential for cost savings by using economic MPC to exploit the variations in prices and in the system's efficiency. In addition, we show how flexibility can be sold as a service to the grid in return for an availability payment. In our studies, we do not include actual activation of the flexibility but focus entirely on making it available while guaranteeing optimal operation for the refrigeration system. It is very likely that an activation in a real implementation will take the MPC temporarily out of play while delivering the up or down regulation of which the MPC has ensured the availability. Following the activation the MPC will kick in again and bring the system back to optimal operation. In all cases, we assume that "good" price signals, electricity price and/or regulating power prices, are available online. This is of course a prerequisite for the presented methods to work.

Uncertain Forecasts and Models

The optimal solution to a deterministic optimization problem is not always optimal, nor feasible, in the stochastic case. Therefore, we describe means to handle uncertainties in both the forecasts and in the models of the system. We investigate an extension to the linear economic MPC that provides robust performance in the presence of both forecast and model uncertainties. This method is similar to [OPJ+10a] where energy consumption for climate control is minimized under influence of uncertain weather predictions. Our extension is that, we use a finite impulse response (FIR) formulation of the system models that allows us to handle model uncertainties within the same framework of probabilistic constraints. The computational burden is significant when the constraints are treated as probabilistic constraints and solved as a second-order cone program. Consequently, for the fast solutions using sequential convex programming (Papers C and K), we back off from the constraints so that much simpler computations are neeeded.

7.1 Chance constrained economic MPC

In many applications, probability distributions can be quantified for the uncertainty. If this information is ignored (e.g. by defining worst-case costs and invoking con-

straints over all uncertainty realizations) it can lead to conservative results. In Papers A and H, we use assumptions of the uncertainty belonging to certain distribution functions and define the confidence level (probability) that the constraints in the MPC should hold with. This approach is similar to the work in, *e.g.*, [VHSB01, OJM08]. [BCH98] and [LVBL98] demonstrate that probabilistic linear constraints can be written as deterministic second-order cone (SOC) constraints that are convex provided the probability involved is greater than 0.5. We demonstrate this for the simple linear power portfolio example.

To have a system which is linear in the model parameters, we define the system model in FIR form:

$$y_k = b_k + \sum_{i=0}^{k} H_i u_{k-i}, \ H_i = \begin{cases} D & for \ i = 0 \\ CA^{i-1}B & for \ i > 0 \end{cases}$$

where y and u are the outputs and inputs, respectively. H are the impulse response coefficients, and b is a bias term. The matrices A, B, C, and D define the standard discrete time state space model. This form is very handy for formulating the constraints as probability constraints. as the uncertain elements (impulse response coefficients) are multiplied with the decision variables.

With this model, we define a stochastic optimization problem (boldface variables are uncertain)

$$\begin{aligned}
\text{minimize} \quad & E\left\{ \sum_{k=0}^{N} \mathbf{c_k}' u_k \right\}, \\
\text{subject to} \quad & u_{\min} \leq u_k \leq u_{\max}, \\
& \text{Prob}\left\{ \mathbf{y_k} \geq \mathbf{r_k} \right\} \geq 1 - \alpha, \quad \alpha \in [0; 0.5], \\
& \mathbf{y_k} = b_k + \sum_{i=1}^{k} \mathbf{H_i} u_{k-i} + \sum_{i=1}^{k} \mathbf{H_{D,i}} \mathbf{d_{k-i}},
\end{aligned}$$

where $\mathbf{c}$ is the cost on the control variables, $\mathbf{r}$ is the net power demand trajectory, $\mathbf{d}$ is a disturbance (outdoor temperature), and $1 - \alpha$ is the confidence level for the supply-demand constraint. The distributions of the uncertain elements are given by

$$\begin{aligned}
&1) \ \ \mathbf{c_k} \sim N(\bar{c}_k, \sigma_c^2) \quad & 2) \ \ \mathbf{r_k} \sim N(\bar{r}_k, \sigma_r^2) \\
&3) \ \ \mathbf{H_i} \sim N(\bar{H}_i, \Sigma_H^2) \quad & 4) \ \ \mathbf{H_{D,i}} \sim N(\bar{H}_{D,i}, \Sigma_H^2), \\
&5) \ \ \mathbf{d_k} \sim N(\bar{d}_k, \sigma_d^2)
\end{aligned}$$

where 1) and 2) are forecast uncertainties, 3) and 4) describe model uncertainties while 5) is uncertainty in the disturbances. We can reformulate the probability constraint as a deterministic counterpart. The uncertain model descriptions and disturbances lead to second-order cone constraints, while an uncertain power demand signal just adds a back-off to the constraint. These two cases can of course easily be combined. We solve the problem with the constraint $Prob\left\{ \mathbf{y_k} \geq r_k \right\} \geq 1 - \alpha$ reformulated as its deterministic counterpart. The result is a constraint on the following
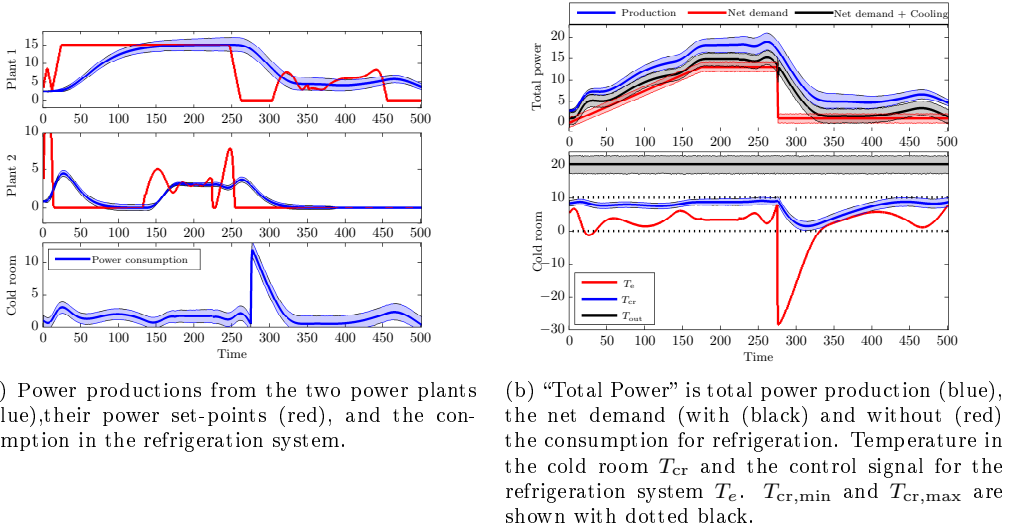
(a) Power productions from the two power plants (blue),their power set-points (red), and the consumption in the refrigeration system.

(b) "Total Power" is total power production (blue), the net demand (with (black) and without (red) the consumption for refrigeration. Temperature in the cold room T_{cr} and the control signal for the refrigeration system T_e. $T_{cr,min}$ and $T_{cr,max}$ are shown with dotted black.

Figure 7.1: Simulation of simple power generation problem with two power plants and one cold room. $\alpha = 0.05$, $H_i \sim N(\bar{H}_i, 0.0055^2)$, $r_k \sim N(\bar{r}_k, 0.7071^2)$. Outdoor temperature: $T_{out} \sim N(\bar{T}_{out}, 1.7321^2)$. The shaded bands show the 95 % confidence interval from 10,000 random instances.

form

$$\Phi^{-1}(\alpha) \left\| \Sigma^{1/2} \begin{bmatrix} U_{\text{past}} \\ U \end{bmatrix} \right\|_2 + \bar{y}_k \geq r_k.$$

Σ is a covariance matrix, Φ^{-1} is the cumulative distribution function (CDF) of a zero mean unit variance Gaussian random variable, U_{past} is the vector of past inputs and U is the vector of future inputs. The constraint has the form of a second order cone. Paper A provides the remaining details on the reformulated constraints.

For the power plant portfolio scenario, that we considered in Chapter 6, we formulate the constraints on the cold room temperature as well as on balancing supply and demand as probability constraints. These are rephrased into SOC constraints and we use the high-level optimization tool Yalmip [Löf08] to solve the second order cone program (SOCP). Figure 7.1 illustrates the trajectories from the optimizer. Notice the confidence intervals, shown as shaded areas around each of the trajectories in Figure 7.1. The solid lines are the expected outcomes, while the shaded areas are created by 10,000 simulations with random instances of the noise descriptions. The 95 % percentile is used both in the SOCP formulation and for plotting the shaded areas. We observe how the amount of back-off from the boundaries is just enough to account for the 95 % confidence interval of the uncertainty descriptions for the

system. Two drawbacks of this method are: 1) it is confined to economic MPC with entirely linear or quadratic dynamics, constraints and objectives, and 2) the implementation with SOCP solvers can be computationally demanding and make the real-time implementation on industrial hardware debatable.

7.2   Simple robust economic MPC

The key topic for Papers C and K is related to the speed of computation. To be able to implement the methods on industrial hardware, the computations and memory requirements of the algorithms must be modest. Besides, speed of computation is also an important concern for the ability to make extensive simulations with a reasonable little time consumption. For this purpose, we deemed the chance-constraint/SOCP method too slow. But, as the study in Papers C and K include randomly occurring heat loads as well as far from perfect predictions, we cannot guarantee that the temperatures are always in the feasible range. In the papers, we add back-offs $\epsilon_{\text{back-off}}$ to the food temperature inequalities

$$T_{\text{food,min}} + \epsilon_{\text{back-off,min}} \leq T_{\text{food}} \leq T_{\text{food,max}} - \epsilon_{\text{back-off,max}}.$$

[LP96, MCS$^+$10], among others, discuss the use of back-offs to ensure constraint satisfaction. The back-off should account for both the time variations, the statistical variations, as well as the possible bias terms from model errors. While systematic methods to choose the sufficient amounts of back-off exist, we choose to tune the back-offs in a heuristic manner using trial and error with realistic simulations. The variances of the outputs are also important since a lower variance lets us decrease the back-off (see, *e.g.*, [MCS$^+$10]). For imposing the constraints, we encode them as a set of soft constraints, *i.e.*, as a term added to the cost function,

$$V = \int_{T_0}^{T_{\text{final}}} \rho_{\text{soft,max}}(T_{\text{food}} - T_{\text{food,max}})_+ + \rho_{\text{soft,min}}(T_{\text{food,min}} - T_{\text{food}})_+ dt,$$

where $(a)_+ = \max\{a, 0\}$. This objective term penalizes violations of the temperature range constraints. We choose the positive constants $\rho_{\text{soft,max}}$, $\rho_{\text{soft,min}}$, $\epsilon_{\text{back-off,min}}$, and $\epsilon_{\text{back-off,max}}$ so that violations are very infrequent in closed-loop operation. Due to the speed of our optimizer, this is possible to do by extensive Monte Carlo sampling. With this formulation, we ensure a feasible problem even in the presence of uncertain loads. In our studies, we find that less than $0.1°$C back-off is often sufficient to reduce violations of the limits to occur only 0.5–1 % of the time. We verify this, *e.g.*, with histograms of the temperatures, as illustrated in Figure 6.4.

7.3   Simple predictors for MPC

The economic MPC formulations require a forecast of the exogenous variables such as the outdoor temperatures and the electricity prices for the chosen prediction horizon. We can choose to assume full knowledge of such future values or go for a more realistic implementation where only past values of the parameters can be available to the controller. In this section, and in Papers C and K, we describe a forecast system and the involved predictors. With this, we compute a sufficiently good estimate of both electricity prices and outdoor temperatures, using a series of past measurements. As the predicted values obviously are not accurate, we must deal with the uncertainty in the optimization problem as described in the previous section. The contribution from this section and the previous is primarily to illustrate how well extremely simple predictors can work with economic MPC in closed-loop. We use the fact that the optimization problem is nothing but a heuristic for computing a good control and that the quality of closed-loop control with MPC is generally good without solving each problem accurately with full knowledge.

We use predictors that are simple to find from historical data and require extremely little computational effort in the real-time closed-loop implementation. We use the historical training data set to construct typical days that describe the mean daily variation for each month in the year. If, *e.g.*, price is sampled every hour, we get 24 data points for each one of the 12 months. We compute a smooth baseline covering all 365 days in a year using linear interpolation of two adjacent months. For the entire historical data set, we calculate the residual (difference between baseline and historical data) and compute a residual predictor by solving the convex optimization problem

$$\text{minimize} \quad \sum_{k=1}^{K} \left\| [R_{k-n}, \ldots, R_k] X - [R_{k+1}, \ldots, R_{k+N}] \right\|_2^2 + \lambda \left\| X \right\|_1,$$

for X, where K is the number of data points in the training data set, n is the number of past data points used for prediction, N is the number of future data points that we want to predict, X is the $n + 1 \times N$ predictor matrix and R are the residuals. The ℓ_1 regularization on the predictor, with positive parameter λ, yields a sparse predictor matrix [BV04]. By cross-validation with the test data set, we choose λ to minimize the validation error. We can compute the predictions online in each time increment by first predicting the N future residuals from the n past residuals (n past measurements subtracted the baseline) and adding these to the baseline of the corresponding time window.

In Paper C, we evaluate the prediction error from this method, *e.g.*, by plotting the mean absolute error as a function of prediction horizon and by showing histograms of the prediction error 1, 4, 12, and 24 h ahead in time. We train with data sets covering from 1 January 2007 until 31 December 2009 and the simulation/test set covers the entire year of 2010. Over the horizon, the mean absolute prediction error of

(a) Electricity price.   (b) Outdoor temperature.
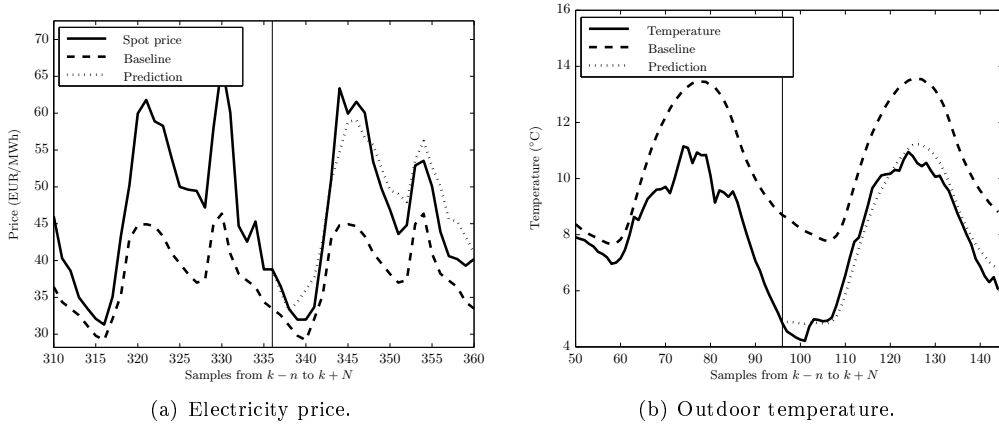
Figure 7.2: Measurements, baseline and prediction for a randomly chosen point of time, k. The vertical line indicates k and everything to the left of that point are past measurements used for prediction while the predictions are shown to the right of the line.

the outdoor temperature increase from 0 (at $N = 0$) to around 1.8°C (at $N = 24$h), and the mean absolute prediction error of the electricity price increase from 0 (at $N = 0$) to around 5.5EUR/MWh (at $N = 24$h).

We show an example with baseline, predicted values, and real measurements for a randomly chosen point of time in Figure 7.2 and give more details in the papers.

Optimization Methods Applied to Commercial Refrigeration

The implementability of economic MPC on industrial hardware depends critically on the computation efficiency of the optimization algorithms as well as on the formulation of the optimization problem. In this chapter, we address the optimization formulations and selected optimization algorithms. For the optimization algorithms, we restrict ourselves to mainly proof-of-concept studies of publicly available optimization software.

In our first conceptual studies concerning the refrigeration systems, we aim at formulating the problem (system dynamics, constraints, and objectives) to obtain a fully linear optimization problem that can be solved by well-established, efficient tools. Next, we make the studies more realistic, to actually prove the feasibility and to clear the way for first implementations on industrial hardware, and we use a full thermodynamic model of the refrigeration system—accepting nonlinearities and nonconvexity. With the formulation of economic MPC as a nonlinear and nonconvex constrained optimal control problem, we consider several solution methods: 1) we apply a generic tool to solve the optimization problems directly, 2) we perform a small study separating the problem in the variables to bring it back to the form of the linear optimization, 3) we develop a tailored sequential convex programming ap-

proach for solving the nonconvex optimization. Out of these, we consider the SCP to be the most promising for price and load flexible consumption by MPC in commercial refrigeration systems, as it accurately models, *e.g.*, the temperature dependent efficiencies while being more than fast enough to run in real-time even with limited computational resources. Below, we summarize all these methods.

8.1   Linear and quadratic optimization

With the simplified model, we can formulate the economic MPC for commercial refrigeration as the linear program stated in (6.1). Linear programming (LP) solvers have been refined to a great extent over the last decades and are now available in both free and commercial editions. Tools like Matlab, also include LP capabilities for rapid prototyping and recent developments on solvers for linear programming directly address economic MPC formulations [SEF+13]. Thus, economic MPC solutions employing LPs can be implemented reliably and computationally efficient for most applications. Furthermore, the LPs can easily be decomposed in case the central optimization problems grow too big (*e.g.*, dual decompositions [Sca09] and Dantzig-Wolfe decomposition [EBJ11]). In Papers E and F, we entirely apply LP solvers included with Matlab and/or a faster FORTRAN implementation that was available to us [Jør05]. When we include soft constraints with an ℓ_2 penalty on violating the constraints, the problem becomes a quadratic program (QP) for which similar reliable optimization tools are available.

In general, we can formulate all the dynamic optimization problems in this class using the QP form

$$
\begin{aligned}
\text{minimize}_x \quad & f(x) = \tfrac{1}{2}x^T Q x + c^T x, \\
\text{subject to} \quad & A_{\text{ineq}} x \le b_{\text{ineq}}, \\
& A_{\text{eq}} x = b_{\text{eq}}.
\end{aligned}
$$

x and c are column vectors and Q is a symmetric matrix that must be positive semidefinite for the problem to be convex. If Q is zero the problem is an LP.

A problem with linear programming in control, is that the optimal point is always at an extremum of the feasible set. Hence, the solution is not very robust against uncertainty. Our robustification of the linear economic MPC via chance constraints in Papers A and H requires solvers capable of handling second order cone programs. Such solvers are according to our experiences much less computationally efficient.

8.2 Nonlinear optimization tools

A range of generic optimization tools that are capable of handling nonlinear problems exist. Many of those use generic formulations of, *e.g.*, sequential quadratic programming (SQP) [BT95]. For the studies in Papers A and I involving the nonconvex objective terms, we choose to apply the toolkit ACADO to solve the optimization problems. "*ACADO Toolkit is a software environment and algorithm collection for automatic control and dynamic optimization. It provides a general framework for using a great variety of algorithms for direct optimal control, including model predictive control, state and parameter estimation and robust optimization*" [HFD10].

With linear dynamics and constraints, we solve the more general dynamic optimization problem

$$
\begin{aligned}
\text{minimize}_x \quad & g(x, d), \\
\text{subject to} \quad & A_{\text{ineq}} x \leq b_{\text{ineq}}, \\
& A_{\text{eq}} x = b_{\text{eq}},
\end{aligned}
$$

where $g(x, d)$ is the nonconvex function of the variables x and the exogenous inputs d. For the refrigeration system, $g(x, d)$ is the energy cost of operation C, which we defined in Section 3.4.

From the analysis in Paper B (see also Figure 8.1), we know that a unique minimum can be found within the feasible region of the optimization problems for the commercial refrigeration. Thus, we believe without further validation, that the solution found in ACADO is the optimal solution. This method works really well for testing our concepts. Furthermore, implementation with ACADO is straightforward and as new features in ACADO now enable code generation for exporting tailored embedded solvers [HFD11] this approach might also get applicable for practical implementations. However, we did not try this feature and in our studies, we find this implementation too slow. For the price and load response summarized in Section 6.3, ACADO uses more than 4 minutes to compute each MPC step with a prediction and control horizon of 30 increments (16 h) on a 2.8GHz Intel Core i7. Adding the regulating power capability as in Section 6.4 increases the computation time with at least a factor of three.

8.3 Separation of variables

In Papers B and G, we present a small study with the aim to solve the MPC problem with the accurate refrigeration model but using standard LP and QP solvers as in Section 8.1. To do this, we omit the isentropic efficiency of the compressor and fit first order polynomials (with the coefficients α_1, β_1, α_{21}, α_{22}, and β_2) for the enthalpy
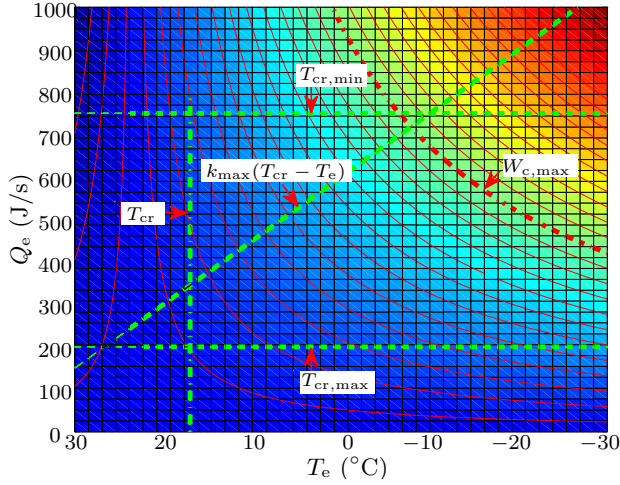
Figure 8.1: Illustration of the feasible region for a single refrigerated unit, with color and contours indicating the work done in the compressor. The arrows indicate from which side of the lines the area is constrained.

differences to describe the compressor work on the simpler form

$$W_c = \dot{Q}_e \frac{\alpha_{21}T_e + \alpha_{22}P_c + \beta_2}{\alpha_1 P_c + \beta_1}.$$

We propose an optimization routine in which we separate the problem over the variables $\dot{Q}_e$ and T_e. We fix T_e to a feasible initial guess and solve the optimization problem for $\dot{Q}_e$. We keep the linear constraints and formulate the first objective function as

$$g(\dot{Q}_e) = \sum_{k=1}^{N} p_{el,k} \dot{Q}_{e,k} \frac{\alpha_{21}T_e + \alpha_{22}P_{c,k} + \beta_2}{\alpha_1 P_{c,k} + \beta_1}.$$

This is a the linear program

$$
\begin{aligned}
\text{minimize}_{\dot{Q}_e} \quad & C_1^T \dot{Q}_e, \\
\text{subject to} \quad & A_{\text{ineq}} x \leq b_{\text{ineq}}, \\
& A_{\text{eq}} x = b_{\text{eq}},
\end{aligned}
$$

where C_1 combines all the constant terms. Next, we can fix $\dot{Q}_e$ to the solution from the first optimization and solve the problem for T_e. P_c is a constant vector in time and $\dot{Q}_e$ is the optimal cooling capacity found as the solution to the linear program above. We formulate the objective function as

$$g(T_e) = \sum_{k=1}^{N} c_{el,k} \dot{Q}_{e,k} \left(\frac{\alpha_{21}}{\alpha_1 P_{c,k} + \beta_1} T_{e,k} + \frac{\alpha_{22}P_{c,k} + \beta_2}{\alpha_1 P_{c,k} + \beta_1} \right).$$

The last term is constant with respect to T_e and can be omitted in the optimization problem. The optimization problem is again a linear program

$$
\begin{aligned}
\text{minimize}_{T_e} \quad & C_2^T T_e, \\
\text{subject to} \quad & A_{\text{ineq}} x \leq b_{\text{ineq}}, \\
& A_{\text{eq}} x = b_{\text{eq}},
\end{aligned}
$$

where C_2 combines all the constant terms. From Figure 8.1, we can verify the sequence of optimizing over $\dot{Q}_e$ first. Solving the two linear programs is much more efficient than performing one solve with a generic tool. If the solution is feasible, we are done at this point. However, the constraint on $W_{c,\max}$ includes both decision variables and can only be checked after they have been computed. Thus, if violations occur, we must limit the solution at those points and rerun the two optimization problems. Some iteration can be necessary in order to remove all violations.

We test this method for some simple scenarios and compare with the solution obtained with ACADO. In these cases the solutions are almost identical. In spite of this, we did not find any way to prove the optimality of this separation technique. Also, to be able to separate the optimization problem in the first place, we had to make some simplifications by fitting the polynomials for enthalpy differences and finally, the limit-and-rerun procedure is a bit add-hoc for solving this problem. On the other hand, solving the repeated LPs involved can be done with much greater reliability and speed than solving the nonlinear problem as it is.

8.4 Sequential convex programming

In Papers C and K, we propose a variation on model predictive control to achieve the goal of minimizing the total energy cost, using real-time electricity prices, while obeying temperature constraints on the zones. Our formulation (choice of variables) results in an optimization problem with linear constraints, but an objective function that is nonconvex (see the model in Section 3.4). To handle this nonconvexity, we propose a sequential convex optimization method, which typically converges in fewer than 5 or so iterations. Instead of a generic SQP (or other) method, we use a sequential convex programming (SCP) method, in which the objective is approximated by a convex function in each iteration; the equality and inequality constraints, which are convex, are preserved, giving us the speed and reliability of solvers for convex optimization [BV04]. Our method, like SQP, involves the solution of a sequence of (convex) quadratic programs (QPs), but differs very much in how the QPs are formed. In SQP, an approximation to the Lagrangian of the problem is used; the linearization required in each step can end up dominating the computation [DSD11]. In our SCP method, the convexification step needed in each iteration is straightforward. Unlike SQP, our method does not exhibit terminal quadratic convergence, but since our

method converges in practice in just a handful of iterations, this does not seem to be an issue, at least in this application.

We express the energy cost function C using the coefficients of performance, COP, ($\eta_{\mathrm{COP}}(t)$ and $\eta_{\mathrm{COP,F}}(t)$ respectively),

$$C = \int_{T_0}^{T_{\mathrm{final}}} p_{\mathrm{el}} \left(\frac{1}{\eta_{\mathrm{COP}}} \dot{Q}_{\mathrm{e}} + \frac{1}{\eta_{\mathrm{COP,F}}} \dot{Q}_{\mathrm{eF}} \right) dt.$$

$\eta_{\mathrm{COP}}(t)$ and $\eta_{\mathrm{COP,F}}(t)$ are complicated functions of the outdoor temperature and of the controllable variables $\dot{Q}_{\mathrm{e}}$ and T_{e}. For any given values of these variables we can, however, compute the coefficients of performance. We solve the optimization problem iteratively using convex programming, replacing the nonconvex cost function C with a convex approximation,

$$\hat{C}^i = \int_{T_0}^{T_{\mathrm{final}}} p_{\mathrm{el}} \left(\frac{1}{\hat{\eta}_{\mathrm{COP}}^i} \dot{Q}_{\mathrm{e}} + \frac{1}{\hat{\eta}_{\mathrm{COP,F}}^i} \dot{Q}_{\mathrm{eF}} \right) dt,$$

where $\hat{\eta}_{\mathrm{COP}}^i$ and $\hat{\eta}_{\mathrm{COP,F}}^i$ are calculated for the ith iteration using $\dot{Q}_{\mathrm{e}}^{i-1}$ and T_{e}^{i-1} found in the previous iteration. Thus, in each iteration, we solve a convex optimization problem, which can be done very reliably and extremely quickly. Our approximation in each step is simple and natural: We use the coefficient of performance calculated for the last iteration trajectory. To avoid oscillations from iteration to iteration we add proximal regularization (penalizing large deviations from the solution found in the previous iteration)

$$\varphi_{\mathrm{prox}} = \rho_{\mathrm{prox}} \sum_{k=0}^{N-1} \| \dot{Q}_{\mathrm{e}}^k - \dot{Q}_{\mathrm{e}}^{k,\mathrm{prev}} \|_2^2,$$

where the superscript 'prev' indicates that it is the solution from the previous iteration and ρ_{prox} is a constant weight chosen to damp large steps in each iteration. Furthermore, we add a quadratic penalty on the rate-of-change of $\dot{Q}_{\mathrm{e}}$,

$$\varphi_{\mathrm{roc}} = \rho_{\mathrm{roc}} \sum_{k=1}^{N-1} \| \dot{Q}_{\mathrm{e}}^k - \dot{Q}_{\mathrm{e}}^{k-1} \|_2^2.$$

This regularization term serves two purposes: it improves the convergence of the sequential programming method, and also discourages rapid changes or switches in compressor levels, which helps reduce wear and tear of the compressor. Adding the two regularization terms to the linear objective formed by $\hat{C}+V$, results in a QP which we must solve once in each iteration. V imposes the soft temperature constraints as we showed in Section 7.2.

Algorithm 1 outlines the method. We define the set Ω as all $(\dot{Q}_{\mathrm{e}}, T_{\mathrm{e}})$ that satisfy the system dynamics and the constraints from Chapter 3. Paper C gives further algorithmic details, concerns and evaluations.

Algorithm 1 Iterative optimization with nonconvex objective.

Initialize
    $\dot{Q}_e^0$, T_e^0, and $i = 1$.
Compute
    $\hat{\eta}_{COP}^i$ and $\hat{\eta}_{COP,F}^i$, as functions of $\{\dot{Q}_e, T_e\}^{i-1}$ and T_a.
Solve
    minimize $\hat{C}^i + V + \varphi_{prox} + \varphi_{roc}$,
    subject to $(\dot{Q}_e^i, T_e^i) \in \Omega$,
                        $T_{food}^{T_{final}, i} = (T_{food,min} + T_{food,max})/2$,
Update
    $\dot{Q}_e^i$, T_e^i, and $i = i + 1$
Repeat until convergence.

Recent advances in convex optimization allow for convex QPs to be solved at millisecond and microsecond time-scales. We use CVXGEN [MB12] to generate a custom embedded solver for ultra fast computation of each convex QP in the sequential approach. With this implementation the optimization problems solve in the order of a handful of milliseconds per MPC step which is more than fast enough for real-time implementation. We use a prediction horizon of 24 hours, with non-equidistant sampling. The first 6-hour interval is sampled every 15 minutes, followed by the second 6-hour interval sampled every 30 minutes, and the last 12-hour interval is sampled every hour. This gives us a total of 48 values to describe the 24-hour period. Several software packages for fast, embedded optimization of convex QPs exist, including the beforementioned code-generation feature in ACADO and tools like FORCES [Dom12, DZZ+12] or FiOrdOs [Ull11] that are all publicly available.

8.5   Summary

The SCP technique presented, prove to be really efficient and inspired by this, we choose to implement variations of it to solve the wind power problems considered within the scope of this project. In the case of the commercial refrigeration system, one feature that makes the SCP method work extremely well, is the ability to formulate the system as mostly linear and convex. We have all nonlinearities boiled down to one factor, the efficiency, which we choose to regard as a constant in each iteration. For the wind power problems, this is not the case, however, we demonstrate that the method can still be applied. Thus, an important contribution from this thesis is the successful application of the SCP approach to solve economic MPC problems for a range of specific industrial systems. We elaborate on the SCP implementations for the wind power problems in Chapter 9.

CHAPTER 9

Wind Power on the Grid—Two selected aspects

In this chapter, we focus our attention on two aspects from the production side of the power grid, more specifically, from the control of wind power plants (WPP). We present results related to economic MPC for 1) dynamic operation of a wind turbine and a connected local electrical storage device or other deferrable load, and 2) static optimization for a farm of wind turbines. For the single turbine, we take varying wind speed into account, with the goal of maximizing the total energy generated while respecting limits on the time derivative (gradient) of power delivered to the grid. On the farm level, we consider the static problem of finding the optimal power set-points to the individual wind turbines in the farm at given wind conditions. Our motivation for these investigations is twofold: 1) We see several profitable synergies with our contributions to the control of supermarket refrigeration. This is both in terms of applying similar economic optimizing predictive control strategies and in terms of directly utilizing the flexibility from, *e.g.*, supermarket refrigeration to balance fluctuating wind power production. 2) We aim at controlling wind power so it can be seen as a part of the solution for a reliable and efficient future power grid, instead of being considered as the cause of the problem of balancing electricity supply and demand.

9.1   Utilizing storage for ensuring power gradients

A main challenge with wind power is its fluctuating nature that can make it problematic to stabilize the power grid. To minimize this risk, a technical document (the Grid Code (GC)) sets out the rules, responsibilities and procedures governing the operation, maintenance and development of the power system. It is a public document periodically updated with new requirements and it differs from operator to operator. Countries with large amounts of wind power have issued dedicated GCs for its connection to transmission and distribution levels, focused mainly on power controllability, power quality and fault ride-through capability [IHSC07, SS09]. Particularly, Denmark establishes some of the most demanding requirements regarding active power control [Elt04]. One of the regulation functions required, is a power gradient constraint that limits the maximum rate-of-change of non-commanded variations in the power output from the WPP to the grid. As of today, this constraint is softened if the power production in the WPP drops due to the lack of wind. This is merely out of necessity and the GCs are expected to tighten further regarding this requirement. Ensuring slow power gradients reduces the risk of instability in the grid, allows the TSO time for counteracting the change, and improves the predictability of power output, enabling the WPP owner to put less conservative bids on the power market.

Energy storage strikes the major problems of wind power. However, the additional cost of batteries or other types of energy storage is usually the showstopper, at least as the market is today. We have shown how thermal capacity, *e.g.*, in supermarket refrigeration, can be utilized for flexible power consumption and it is very likely that such techniques can play a major role instead of adding expensive battery technologies.

In our studies, we use the turbine inertia as an additional energy storage device, by varying the turbine's rotational speed over time, and coordinate the flows of energy from the wind to the grid and to/from the storage. This is based on our findings in Papers D and M. We utilize predictive control with forecasts of the wind speed to ensure very low power gradients e.g., less than 3 % of the rated power per minute. The papers and Chapter 4 elaborate on the model of the turbine. Also, recall the penalty (which we wish to minimize) for violating a target maximum value of power rate of change, G (in W/s):

$$R_{\mathrm{pen}} = \int_0^T (|\dot{P}_{\mathrm{grid}}(t)| - G)_+ \, dt,$$

where $(b)_+ = \max(b, 0)$, which is subtracted from the overall economic objective of

maximizing the amount of energy delivered to the grid

$$E = \int_0^T P_{\mathrm{grid}}(t)\, dt.$$

The two terms in the objective function form a bi-criterion. The trade-off between these terms can be regarded as a mean-covariance trade-off, similar to the trade-off applied in the Markowitz portfolio optimization problem [MT00, Mar12]. In these studies, we disregard the interconnection of the turbines through the wind field. This is the focus of a study that we present in Section 9.2.

9.1.1   Dynamic model formulation

The system dynamics are nonlinear, and the constraints and objectives are not convex functions of the control inputs. Consequently, the resulting optimal control problem is difficult to solve for its global optimum. In Paper D, we show how the optimal control problem can be formulated as a convex optimal control problem, $i.e.$, one with linear dynamics convex constraints, and a concave objective functional (to be maximized). The trick is a novel change of variables, to work with power flows and energies solely. This implies that the problem can be solved globally, in a computationally efficient and reliable way. In our formulation, we choose the quantities

$$P_{\mathrm{g}}(t), \quad P_{\mathrm{grid}}(t), \quad P_{\mathrm{chg}}(t), \quad P_{\mathrm{w}}(t), \quad Q(t), \quad K(t),$$

over the time interval $0 \le t \le T$. $K(t) = (J/2)\omega_{\mathrm{g}}(t)^2$ is the kinetic energy stored in the rotational motion and $P_{\mathrm{w}}(t) = T_{\mathrm{r}}(t)\omega_{\mathrm{r}}(t)$ is the power extracted from the wind. The rotor speed can be expressed in terms of the kinetic energy as

$$\omega_{\mathrm{r}}(t) = (1/N)\sqrt{(2/J)K(t)}.$$

We express the dynamics of the turbine in terms of the kinetic energy as

$$\dot{K}(t) = J\omega_{\mathrm{g}}(t)\dot{\omega}_{\mathrm{g}}(t) = \omega_{\mathrm{g}}(t)\left(\frac{T_{\mathrm{r}}(t)}{N} - T_{\mathrm{g}}(t)\right) = P_{\mathrm{w}}(t) - P_{\mathrm{g}}(t)/\eta_{\mathrm{g}},$$

which is a linear differential equation relating K, P_{w}, and $P_{\mathrm{g}}(t)$. The limits on rotor speed can be expressed as limits on kinetic energy, as

$$(J/2)\omega_{\mathrm{g,min}}^2 \le K(t) \le (J/2)\omega_{\mathrm{g,max}}^2,$$

and the generator torque is

$$T_{\mathrm{g}}(t) = \frac{P_{\mathrm{g}}(t)}{\eta_{\mathrm{g}}\sqrt{(2/J)K(t)}}.$$

so the generator torque constraints translate into

$$0 \le P_{\mathrm{g}}(t) \le \eta_{\mathrm{g}}\sqrt{(2/J)K(t)}T_{\mathrm{g,max}},$$

which is a convex constraint on $P_{\mathrm{g}}(t)$ and $K(t)$, since $\sqrt{(2/J)K(t)}$ is a concave function of $K(t)$. We define the available wind power, as a function of wind speed and kinetic energy,

$$P_{\mathrm{av}}(v, K) = \max_{\beta_{\min} \le \beta \le \beta_{\max}} \Phi(v, (1/N)\sqrt{(2/J)K}, \beta)v^3,$$

where

$$\Phi(v(t), \omega_{\mathrm{r}}(t), \beta(t)) = (1/2)\rho A C_{\mathrm{P}}(v(t), \omega_{\mathrm{r}}(t), \beta(t)).$$

By definition, we have

$$P_{\mathrm{w}}(t) \le P_{\mathrm{av}}(v(t), K(t)), \tag{9.1}$$

which states that the extracted wind power cannot exceed the maximum available power. As β varies over its range, the extracted power varies from 0 to P_{av}. In other words, by blade pitch control, we can vary the extracted power from 0 up to the maximum available power. We define the function $\Psi(v, K, P_{\mathrm{w}})$ as the value of β that gives the extracted power P_{w}. For the constraint (9.1) to be convex, for each wind speed v, P_{av} must be a concave function of K. This is the case with realistic coefficient of power models, as explained in Paper D. We use piecewise linear approximations to implement P_{av} in the controller.

9.1.2 Optimization problem

We solve the optimal control problem for a single turbine using the convex formulation:

$$
\begin{aligned}
&\text{maximize} \quad E - \lambda R_{\mathrm{pen}}, \\
&\text{subject to} \\
&\qquad \text{constraints defined in Chapter 4,} \\
&\qquad \text{and in the convex formulation above,}
\end{aligned}
\tag{9.2}
$$

where the variables are P_{g}, P_{grid}, P_{chg}, P_{w}, Q, and K (all functions of time). The optimization uses an initial state of the dynamic variables $K(t)$ and $Q(t)$ as well as known, or estimated, wind speeds for the interval. We allow for overspeed up to 150 % of the rated speed but penalize this in the objective function so that it is infrequent and only happens when needed for ensuring the power gradient constraint. For details, see Paper D.

9.1.3   Simulation results

Figure 9.1 shows the output from the optimizer for a selected scenario where the wind speed drops from 12 m/s to 10 m/s over a period of 20 s. This equals a drop in available power (given in per unit (pu), *i.e.*, normalized by P_{rated}) from around 1.2 pu to 0.7 pu. Figure 9.1 illustrates that the turbine operates at its maximum rated power whenever possible, *i.e.* in the period 0–80. Up to sample 80, all the power is sent to the grid and nothing is directed to the storage. Around sample 80, the controller prepares for the predicted reduction in available power by diverting more and more power to the storage. This is done in order to follow the commanded gradient on the power delivered to the grid while adjusting for the new level of available power after the decrease in wind speed. Shortly before the wind speed changes, we see that P_{w} increases. This extra power is used to spin up the rotor speed such that the rotational energy can be used to prolong a higher power generation in the generator when the wind speed drops. Note, how this cuts off the peak of the needed storage capacity. As we allow for overspeed of the rotor, we find that the intelligent utilization of rotational inertia can cut off up to 30 % of the need for storage capacity. In addition, this very local and fast acting type of storage can have other benefits in terms of reducing high frequency power fluctuations to the storage. In this simulation, we assume perfect knowledge of the predicted wind speed.

9.1.4   MPC with wind data and forecasts

We show simulations with real wind data series measured at the Danish wind turbine test site Høvsøre in 2004. The controller bases its decisions on a prediction of future wind speeds. We use the predictions generated in [NMS04, NM04] by modern continuous time formulations of the predictors. The predictors use upstream wind speed information from other turbines or measurements located several hundred meters in front of the turbine. For the simulations in this section, we implement an economic optimizing model predictive controller to address the closed-loop control of a single wind turbine. Our controller repeatedly solves the optimal control problem in (9.2). Consequently, the aim is to maximize the power delivered to the grid while obeying the strict requirements to power gradient constraints. This objective function relates to maximizing the profit within the limits of mechanical as well as regulated constraints. In paper D, we provide simulations with three different wind scenarios and Figure 9.2 illustrates one of the three scenarios which covers 215 minutes of operation with a significant drop in wind speed. Figure 9.2 illustrates the wind scenario (measurement and prediction), the wind speed prediction error, power delivered to the grid, and the distribution of power gradients. We compare our controller to the nominal controller in the full Simulink model for the NREL 5MW wind turbine [JBMS09, GSK$^+$10]. This turbine delivers all the power it produces directly
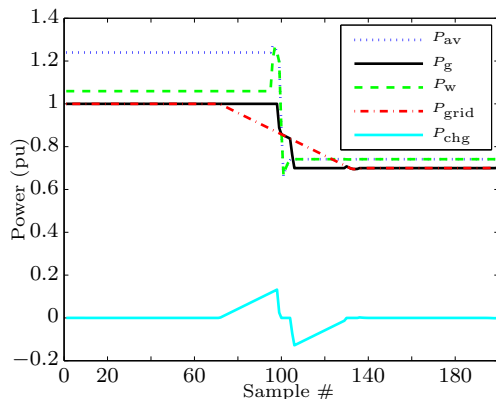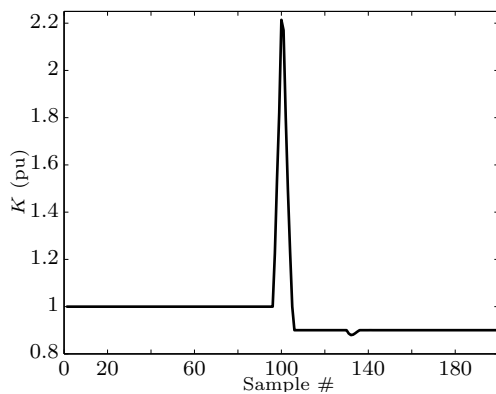
(a) Power flows normalized by P_{rated}.

(b) Kinetic energy, $K(t)/K_{\text{rated}}$.
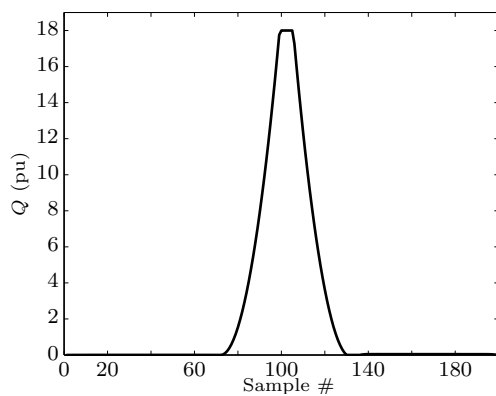
(c) State of charge, $Q(t)/P_{\text{rated}}$.

Figure 9.1: Test of power gradient satisfaction. We use pu as the unit for all quantities and let the wind speed drop from 12 m/s to 10 m/s linearly from sample 99 to 101.

to the grid and the pitch and generator torque control is based on gain-scheduled PI controllers that track optimal set-points given as look-up tables. Figure 9.2 show how the heavy fluctuations in power delivered to the grid almost disappear with our MPC controller. We see a much smoother power signal which is supported by the histograms that clearly show how the rate of change of the power (with a few exceptions) is limited to the $\pm3\%$/minute range that we allow in the problem formulation. This comes at a cost of just a 0.42% reduction in total energy delivered to the grid.

9.1.5   SCP for wind power gradients

In Paper M, we solve the same problem without transforming the problem into a convex optimal control problem. Instead, we choose to solve the optimization problem iteratively using convex programming, replacing the nonconvex terms with convex approximations. In each iteration, i, we perform a first-order Taylor expansion of the nonconvex parts around the operating point found in iteration $i-1$, estimating the derivatives that involve table look-ups by perturbing the parameters. Thus, in each iteration we solve a convex optimization problem. This algorithm is inspired by our work with the refrigeration system (Section 8.4) and is thus closely related to that SCP method. In this case, we also add proximal regularization tuned to damp large steps from iteration to iteration. We refer the reader to the paper for the algorithmic details of this implementation. When initialized with the trajectory from the nominal controller, the proposed method generally converges in 5–10 iterations. In MPC, however, the open-loop trajectory from the previous run of the optimizer, shifted one time step, is an excellent guess on the next solution and is well suited for warm-starting the algorithm. Using this warm start initialization, the method generally just need a couple of iterations to converge. The results are almost identical to those produced by the convex formulation above. It is clear that the change of variables, rendering the problem convex, is far superior to the SCP method in all cases where it is applicable (for obvious computational reasons as well as for reliability). Still, the SCP approach appear to be quite efficient for this application as well.

9.2   Power maximization for wind farms

In this section, we compute a static economic MPC that operates a wind farm such that the combined power production is maximized for a given wind speed. Extracting maximum power from each wind turbine in a WPP in a greedy manner does not always result in maximal power output for the entire farm. Accordingly, a wind farm controller is needed to fully exploit the potential of the installed capacity and to reduce wear and tear of the mechanical structures [PJ09]. Examples of wind farms in
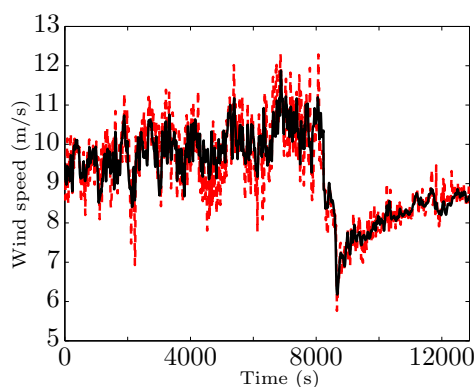
(a) Measured wind speed (dashed red) and pre-
dicted wind speed (solid black).
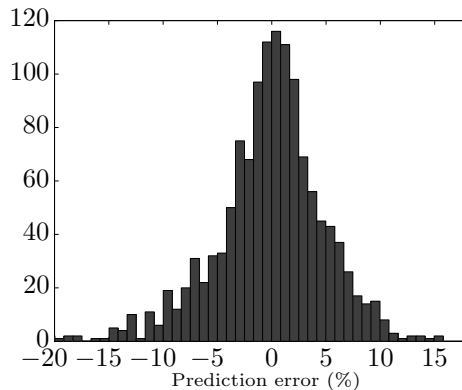
(b) Wind speed prediction error in per cent
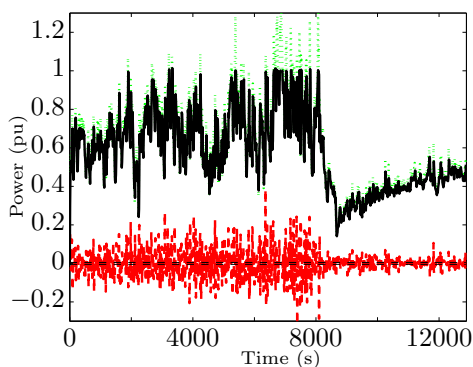
(c) Nominal controller: P_{grid} (solid black),
max P_{av} (dotted green), and ΔP_{grid}/sample
(dashed red).
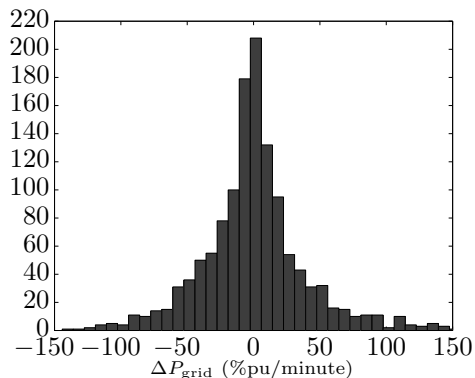
(d) Nominal controller: Power gradient in per
cent of rated power per minute.
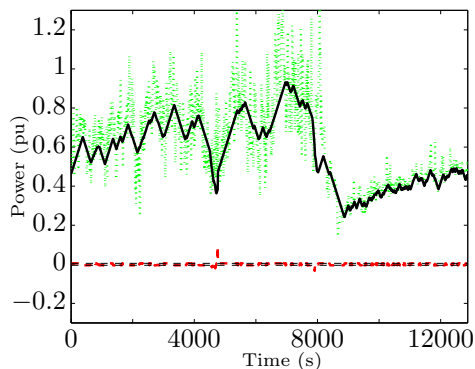
(e) MPC controller: P_{grid} (solid black), max P_{av}
(dotted green), and ΔP_{grid}/sample (dashed red).
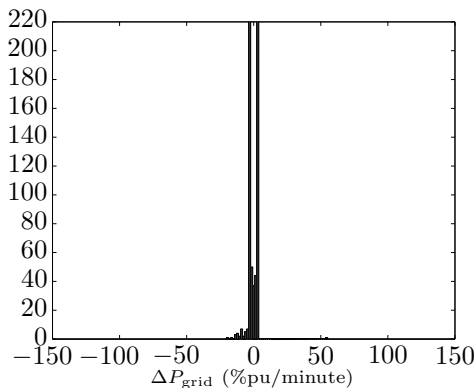
(f) MPC controller: Power gradient in per cent of
rated power per minute.

Figure 9.2: Closed-loop simulation of MPC controller with a real wind scenario.

Denmark can have yearly productions around 600 GWh (Horns Rev I) and up to 1600 GWh (Anholt). Typically, the power sales price is guaranteed to be at a fixed level for around 10 years of operation. The prices vary from around 44.25 EUR/MWh (Horns Rev I) to around 140.85 EUR/MWh (Anholt). With such production levels and power prices, an average change in power output of just 1 % changes the yearly revenue by 0.265–2.253 million EUR. Thus, slight improvements in the average extracted power can have a significant impact on the economics of operating the wind farm.

9.2.1 Problem formulation

In Paper L, we present a method to provide optimal steady-state operating points for several turbines in a WPP. The novelty in our paper is that we use very little knowledge and as few analytic expressions as possible for formulating the optimization problem. We adopt the wind farm model that was derived in [BW10a] and validated in [BW10b], together with our simple linear turbine interaction models (see Section 4.1.3), and use it as a black-box model. In spite of the lack of analytic expressions for this model, we can evaluate the outputs (*e.g.*, local wind speeds, local power production, local wind deficits, etc.) rather quickly for any given values of the parameters (such as ambient wind speed and direction, power set-points, etc.). By perturbing this model, we approximate the derivatives needed. We use an SCP approach in which we solve a series of the approximated (convex) problems until convergence. Due to the mechanical design, wind turbines cannot extract power from arbitrarily low wind speeds. This introduces on/off, or integer, variables into the optimization problem. We chose to implement these in the framework of sequential convex optimization as well, using a relaxation of the binary constraints and linear approximations to penalize deviations from 0 or 1. This is combined with a rounding routine to ensure strictly binary variables. When the approximated binary variables do not converge to either zero or one, we force the lowest ones to zero and repeat the optimization. If some of the approximated binary variables still deviate from either zero or one, the procedure is repeated. As we demonstrate in the paper, this is a major contribution from this study.

9.2.2 Optimization problem

Our objective function has three terms. The primary objective is to maximize the sum of power outputs from the entire WPP. The second is a penalty φ_{int} (which we want to minimize) on the integer variables deviating from either 0 or 1, and the third term φ_{prox} is a proximal regularization to damp oscillatory behavior that can occur due to several radically different solutions of the power set-points having almost the

same outcome in the objective function. Thus, in each iteration k we solve

$$
\begin{aligned}
\text{maximize} \quad & P_{\text{total}}^k + \varphi_{\text{prox}} + \varphi_{\text{int}}, \\
\text{subject to} \quad & (\hat{p}_i^k, \hat{v}_i^k, \hat{\sigma}_i^k) \in \Omega, \ i = 1 \ldots n, \\
& (\hat{u}_i^k, \hat{\eta}_{\text{int},i}^k) \in \Omega_{\text{int}}, \ i = 1 \ldots n.
\end{aligned}
$$

where '$\hat{\ }$' indicate that this is the approximation we obtain in the iteration. With the constant, negative, weight ρ_{prox}, we have

$$
\varphi_{\text{prox}} = k\rho_{\text{prox}} \| [p_1, p_2, \ldots, p_n]^{k-1} - [p_1, p_2, \ldots, p_n]^k \|_\infty,
$$

Likewise, ρ_{int} is a constant, negative, weight. We define

$$
\varphi_{\text{int}} = \rho_{\text{int}} \sum_{i=1}^{n} \eta_{\text{int},i},
$$

and

$$
\eta_{\text{int},i} \leq \left(u_i^{k-1}\right)^2 - u_i^{k-1} + \left(2u_i^{k-1} - 1\right)\left(u_i^k - u_i^{k-1}\right).
$$

The right hand side of the last equation is a linearization of $(u_i^2 - u)$ around the point u_i^{k-1}. We define the set Ω_{int} as all $(u_i, \eta_{\text{int},i}), \ i = 1 \ldots n$ that satisfy $0 \leq u_i \leq 1$ and the constraint on $\eta_{\text{int},i}$ shown above. Furthermore, the set Ω contains all $(p_i, v_i, \sigma_i), \ i = 1 \ldots n$, that satisfy the power constraints, and the farm interaction model. In each iteration, the farm model is evaluated at the operating point found in the previous iteration and with small perturbations, in order to find linear first-order approximations of the available power p_{w_i}, the wind deficit d_i, and the wind turbulence σ_i, for each turbine in the farm.

9.2.3   Results

In Figure 9.3, we show the resulting power set-points for a small wind farm with four turbines in a row parallel to the wind direction. As described in Chapter 4, we benchmark our method against a "greedy" control scheme. The figures show the comparison of the two methods. The differences in produced power P_{total}, for the two control strategies, are reported in the captions. The cases shown in the figure reveal huge improvements but we should point out that these are quite special scenarios. In the illustrated scenarios, the optimal power set-point distribution can keep more of the turbines above the cut-off level. The cut-off level is the minimum amount of power that the turbine can produce due to mechanical constraints. If the power set-point is below the cut-off level, the turbine does not produce any power. In the more general case, the improvement is usually around 2 %. We give further results on the optimization and on the approximate integer constraints in Paper L.

(a) $v_0 = 6.9\text{m/s}$. Improvement: 80 %

(b) $v_0 = 6.99\text{m/s}$. Improvement: 50 %
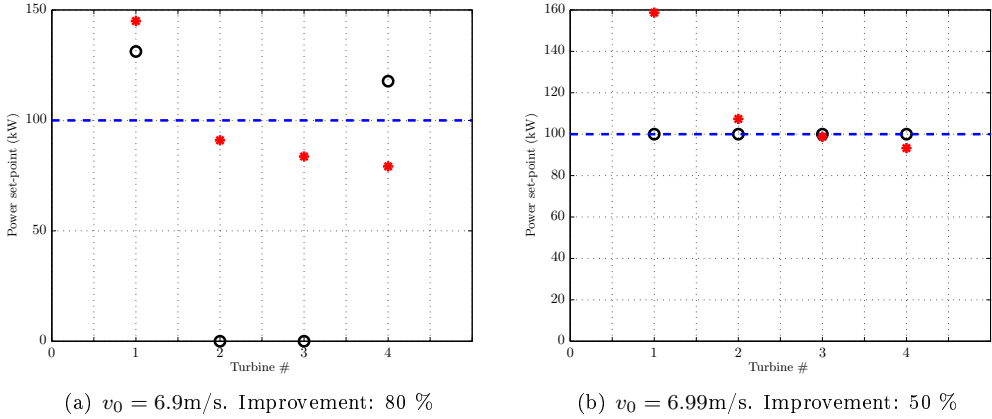
Figure 9.3: Test of power set-point optimization (blue circles) vs. "greedy", individual turbine control (red stars) for small farm. The dotted blue line is the cut-off ($P_{\min}$).

9.3 Summary

In this chapter, we demonstrate how the distribution of individual power set-points to the turbines in a wind farm can be optimized for given wind speeds and directions using only very little information about the complicated dynamics that couple the turbines mutually. On the individual turbine level, we successfully show how model predictive control can utilize both rotor inertia and external sources of energy storage to ensure strict requirements on the power rate-of-change. An important contribution to the control of individual turbines, is our change of variables that results in a convex formulation that we can solve very efficiently. It would be a natural extension to combine the farm level controller with the individual turbine MPC, however, this is outside the scope of this thesis.

CHAPTER 10

Conclusions and Perspectives

In this thesis, we have looked at problems in the design and implementation of economic model predictive control policies for two industrial applications: Commercial refrigeration and power production by wind turbines. For the refrigeration systems, the goal is to enable flexible and efficient power consumption, and for the wind turbines, we aim at improving power quality and integrability to the grid. In this section, we offer some concluding remarks, possible extensions, and directions for future research.

Compared to our vision, which is repeated below, we have come a long way. *Our vision is that, by enabling the use of energy storage in supermarkets, we open up the possibility of reducing operational costs and create completely new business opportunities for selling regulating power to the grid. Moreover, this enables a larger penetration of wind energy in the power production and increases the potential market size for wind turbine generators and other renewable energy sources. Thus, we aim at promoting the use of environmental sustainable power production technologies while creating new business opportunities.*
We show that this is indeed feasible and present promising methods to overcome many of the challenges that we face when implementing such advanced control methods on the commercial refrigeration and the wind turbine systems. In addition to accomplishing successful feasibility studies for our methods on these specific applications, we show the techniques and first steps that pave the way for real commercial implementations. We demonstrate a potential for significant savings in operating

costs and reveal promising means, for both the power consumer side and for the producers of wind power. By economic MPC, we counteract some of the problematic features of intermittent, renewable energy sources on the power grid. In line with our hypothesis, we demonstrate that intelligent utilization of the possibility for storing energy as thermal energy in the refrigeration system can lower the operational cost considerably, compared to current control solutions, as well as enable flexible power consumption that can benefit the power grid. We show that economic MPC is indeed an appealing method to enable this functionality.

10.1   MPC for commercial refrigeration

In Chapter 6 and in Papers A, E, I, C, F, and K, we describe model predictive control technologies that enable flexible power consumption in supermarket refrigeration systems. We provide solutions that make active use of the thermal energy stored in the systems. By controlling the thermal energy storage, we optimize the cost of operation with respect to, *e.g.*, price signals and outdoor temperature predictions while observing the specified temperature ranges for safe food storage. We have extended this study to include primary regulating power which is a type of flexibility that can be sold to the balance responsible parties on the power grid. In the future, other types of regulating power, or new ways of making and communicating incentives for flexible power consumption, can be tested with the refrigeration systems. Furthermore, our method is not confined to refrigeration systems and we believe that it can be adapted to control other applications that hold some thermal (or other kind of) storage capabilities as a bi-product of the original intent with the systems. This could be, but is not limited to, air-conditioning, heat pumps, district heating, ice banks, plug-in electric vehicles, hydrogen storage, gasification, or batteries.

10.2   Robust economic MPC

A considerable challenge in these methods is the accuracy of the system models and of the forecasted disturbances. In our work we have put a lot of effort into posing the problems and the models as simple as possible, focusing on the important dynamics and details only. In particular, simple control oriented models are needed for the supermarket refrigeration systems where rather generic controllers are used for a vast variety of systems and configurations today. We expect that the implementations of our proposed controllers should be performed concurrently with some online system identification of the key parameters in the system. In Chapter 7 and in Papers A, H, and C, we address a couple of approaches to make the MPC formulation more

robust against uncertain and inaccurate knowledge. We give a formulation of chance-constraints with FIR models of the system, that explicitly incorporates knowledge about the probability distributions of uncertainty in both forecasts and impulse response coefficients in the system model. The main disadvantage of the presented approach is the need for second-order cone constraints. A fast solver that exploits the structure of an MPC problem with SOC constraints would be a good future step in the direction of proving the practical implementation of this method. In addition, such a solver should export embedded solvers for that class of optimization problems, too. Another drawback is that we must have the probability density functions for the uncertainty at hand in order to compute the SOC constraints. With the work in Paper C, we show that a much simpler approach with extensive sampling for tuning of safety margins on the constraints and of the penalties associated with soft constraints can work well in practice.

10.3 Optimization and sequential convex programming

Our first results in this thesis focus on linear formulations that can be solved using LP or QP (or SOCP in the case of chance-constraints) optimization tools. To extend this, we use generic nonlinear optimization tools to solve a problem with a less simplified nonconvex objective function. In Chapter 8 and in Papers C and K, we provide an efficient solution for the more realistic nonlinear and nonconvex description of the refrigeration system and the economic objectives. Our SCP method successfully computes real-time solutions for the nonlinear systems. In this project, we have tested this approach on both the commercial refrigeration system, on a dynamic wind turbine control problem, as well as for a static optimization of the wind farm power set-points. Thus, we demonstrate the method on at least three different problems with good results. Implementation of such methods directly on the embedded processors in commercial systems is a natural and interesting next step.

10.4 MPC for wind power

The results presented in Chapter 9 and in Papers D and M, successfully show that an economic optimizing MPC approach, very similar to the one we developed for the supermarket refrigeration systems, can play an important role in the control of wind turbines, especially for reducing the undesirable fluctuating nature of wind power. The synergies between flexible power consumers, *e.g.*, refrigeration systems as in this thesis, and fluctuating power producers is a very interesting field of future research.

In this thesis, we have only scratched the surface of this field. Our studies reveal how well cognate techniques can be used to control both the consumption and the production side of the power grid. The studies in this thesis point to the potential for future co-control of such applications. Another important observation is that by a novel change of variables, we are able to rely entirely on very robust, efficient, and well-proven convex optimization methods to solve the wind power gradient problem. Paper D demonstrates this.

10.5   Perspectives and future work

There are many directions to explore for further improvement of the methods presented in this thesis. One immediate need is development of prototypes and extensive real-life testing to definitively prove the economic potential, evaluate the potential for a higher penetration of renewable energy sources, and judge the robustness. Such tests are needed to finally decide if more sophisticated methods such as chance-constraints or the like must be pursued in future research. Models, tuning and verification of robustness and performance are challenges that now limit the implementation of MPC. In some cases, simpler control strategies for online implementation might be possible to extract by analyzing the behavior of the MPC in simulations. If this simpler method can mimic the MPC in most operating conditions and provide, say 80 % of the performance, overview and benchmarking studies of such approaches can be of interest. Furthermore, one can evaluate the worst case scenarios for the specific application before implementing more advanced handling of robustness. This might not always lead to overly conservative control strategies and should therefore be considered at first.

For the method to be applicable for a real refrigeration system, there is at least one missing link at the moment. When we transform the system description, we assume that the cooling capacity can be controlled directly. However, in reality a valve at the inlet to the evaporator controls the filling and the flow of refrigerant (the superheat temperature) and a simple conversion between cooling capacity and valve opening must be added. Future work on dedicated, tailored optimization routines for the non-trivial problems that arise in our MPC formulations would be interesting directions as would a combination with and test of some of the alternatives for exporting embedded, customized solvers, that we have mentioned in this thesis. Alternative approaches such as a change of variables to convert the problems into standard forms are also of interest.

As of today, the lack of suitable business models, reward schemes, tax structures, and other incentives is a show stopper for moving a lot of the smart grid technologies, including parts of the schemes developed in this project, to a commercial setting

outside the research communities. We are certain that policy makers and the creation of attractive business cases must go hand-in-hand with the technology. We believe that these changes inevitable will be driven by the energy challenges of satisfying the growing demands, securing sufficient energy sources, and meeting the challenges of climate changes and pollution. Hence, research in the enabling technologies will continuously play an important role in the years to come. In the meantime, companies can develop and brand products to be "Smart Grid Ready" just as our TVs for a while have been marked with "HD Ready".

Bibliography

[AAR12]   D. Angeli, R. Amrit, and J. Rawlings. On average performance and
            stability of Economic Model Predictive Control. *Automatic Control,
            IEEE Transactions on*, 57(7):1615–1626, 2012.

[AEG+10]   S. L. Andersson, A. K. Elofsson, M. D. Galus, L. Göransson, S. Karls-
            son, F. Johnsson, and et al. Plug-in hybrid electric vehicles as regu-
            lating power providers: Case studies of Sweden and Germany. *Energy
            policy*, 38(6):2751–2762, 2010.

[AHP12]   A. Arteconi, N. J. Hewitt, and F. Polonara. State of the art of thermal
            storage for demand-side management. *Applied Energy*, 93(0):371–389,
            2012.

[AR10]   D. Angeli and J. B. Rawlings. Receding horizon cost optimization and
            control for nonlinear plants. In *Proc. of the 8th IFAC Symposium on
            Nonlinear Control Systems* , pages 1217–1223, 2010.

[ARA11]   R. Amrit, J. B. Rawlings, and D. Angeli. Economic optimization
            using model predictive control with a terminal cost. *Annual Reviews
            in Control*, 35(2):178–186, 2011.

[BBB+01]   T. Binder, L. Blank, H. G. Bock, R. Bulirsch, W. Dahmen, M. Diehl,
            T. Kronseder, W. Marquardt, J. P. Schlöder, and O. v. Stryk. In-
            troduction to Model Based Optimization of Chemical Processes on
            Moving Horizons. In M. Grötschel, S. O. Krumke, and J. Rambau,
            editors, *Online Optimization of Large Scale Systems: State of the Art*,
            pages 295–340. Springer, 2001.

[BCH98]   S. Boyd, C. Crusius, and A. Hansson. Control applications of nonlin-
            ear convex programming. *Journal of Process Control*, 8(5-6):313–324,
            1998.

[BD11]   M. B. Blarke and E. Dotzauer. Intermittency-friendly and high-
            efficiency cogeneration: Operational optimisation of cogeneration with
            compression heat pump, flue gas heat recovery, and intermediate cold
            storage. *Energy*, 36(12):6867 − 6878, 2011.

[Bie07]   L. T. Biegler. An overview of simultaneous strategies for dynamic
            optimization. *Chemical Engineering and Processing: Process Intensi-
            fication*, 46(11):1043–1053, 2007.

[BM99]   A. Bemporad and M. Morari. Robust model predictive control: A
            survey. *Robustness in Identification and Control*, pages 207–226, 1999.

[BMDP02]   A. Bemporad, M. Morari, V. Dua, and E. N. Pistikopoulos. The ex-
            plicit linear quadratic regulator for constrained systems. *Automatica*,
            38(1):3–20, 2002.

[Bre02]   C. Brezinski. *Computational aspects of linear control*, volume 1.
            Springer, 2002.

[BS07]   M. Black and G. Strbac. Value of Bulk Energy Storage for Managing
            Wind Power Fluctuations. *IEEE Transactions on Energy Conversion*,
            22(1):197–205, march 2007.

[BST+13]   C. Budischak, D. A. Sewell, H. Thomson, L. Mach, D. E. Veron, and
            W. Kempton. Cost-Minimized Combinations of Wind Power, Solar
            Power and Electrochemical Storage, Powering the Grid up to 99.9%
            of the Time. *Journal of Power Sources*, 225:60–74, 2013.

[BT95]   P. T. Boggs and J. W. Tolle. Sequential Quadratic Programming.
            Acta Numerica, 4:1–51, 1995.

[BV04]   S. Boyd and L. Vandenberghe. *Convex Optimization*. Cambridge
            University Press, 2004.

[BW09]   R. Bush and G. Wolf. Utilities load shift with thermal storage. *Trans-
            mission & Distribution World*, page 12, 2009.

[BW10a]   A. J. Brand and J. W. Wagenaar. A quasi-steady wind farm flow
            model in the context of distributed control of the wind farm. In *Proc.
            of the European Wind Energy Conference (EWEC 2010)*, 2010.

[BW10b]   A. J. Brand and J. W. Wagenaar. Validation of a quasi-steady wind
            farm flow model in the context of distributed control of the wind farm.
            In *The Science of making Torque from Wind (Torque2010)*, 2010.

[CB99]   E. F. Camacho and C. Bordons. *Model predictive control*, volume 303.
              Springer Berlin, 1999.

[CHL91]   D. A. Carlson, A. Haurie, and A. Leizarowitz. *Infinite horizon optimal
              control: deterministic and stochastic systems.* Springer-Verlag, 1991.

[CSGSH11]   E. F. Camacho, T. Samad, M. Garcia-Sanz, and I. Hiskens. Control
              for Renewable Energy and Smart Grids. In T. Samad and A. M. An-
              naswamy, editor, *The Impact of Control Technology, Control Systems
              Society*, pages 69–88. IEEE Control Systems Society, 2011.

[CW08]   J. F. Conroy and R. Watson. Frequency Response Capability of Full
              Converter Wind Turbine Generators in Comparison to Conventional
              Generation. *IEEE Transactions on Power Systems*, 23(2):649–656,
              may 2008.

[DAR11]   M. Diehl, R. Amrit, and J. B. Rawlings. A Lyapunov Function for
              Economic Optimizing Model Predictive Control. *Automatic Control,
              IEEE Transactions on*, 56(3):703–707, 2011.

[DBS$^+$02]   M. Diehl, H. G. Bock, J. P. Schlo, R. Findeisen, Z. Nagy, and F. All-
              göwer. Real-time optimization and nonlinear model predictive control
              of processes governed by differential-algebraic equations. *Journal of
              Process Control*, 12(4):577–585, 2002.

[DE10]   Danskenergi   and   Energinet.dk.   Smart   Grid   in   Denmark.
              http://www.energinet.dk/SiteCollectionDocuments/Engelske%
              20dokumenter/Forskning/Smart%20Grid%20in%20Denmark.pdf,
              2010.

[DFH09]   M. Diehl, H. Ferreau, and N. Haverbeke. Efficient Numerical Meth-
              ods for Nonlinear MPC and Moving Horizon Estimation. In Magni,
              Lalo and Raimondo, Davide and Allgöwer, Frank, editor, *Nonlinear
              Model Predictive Control*, volume 384 of *Lecture Notes in Control and
              Information Sciences*, pages 391–417. Springer Berlin / Heidelberg,
              2009.

[DIB96]   D. P. Dewitt, F. P. Incropera, and T. L. Bergman. *Fundamentals of
              heat and mass transfer.* John Wiley & Sons, New York, 1996.

[DMoCB12]   Energy Danish Ministry of Climate and Building. Energy policy re-
              port 2012. Technical report, Danish Ministry of Climate, Energy and
              Building. Denmark, May 2012.

[Dom12]   A. Domahidi. FORCES: Fast optimization for real-time control on
              embedded systems. http://forces.ethz.ch, October 2012.

[DSD11]   Q. T. Dinh, C. Savorgnan, and M. Diehl. Real-time sequential convex programming for nonlinear model predictive control and application to a hydro-power plant. In *Proc. of the 50th IEEE Conference on Decision and Control and European Control Conference (CDC-ECC)*, pages 5905–5910, 2011.

[DZZ+12]   A. Domahidi, A. Zgraggen, M. N. Zeilinger, M. Morari, and C. N. Jones. Efficient interior point Methods for Multistage Problems Arising in Receding Horizon Control. In *Proc. of the 51th Conference on Decision and Control (CDC)*, pages 668–674, Maui, HI, USA, 2012.

[EBJ11]   K. Edlund, J. D. Bendtsen, and J. B. Jørgensen. Hierarchical model-based predictive control of a power plant portfolio. *Control Engineering Practice*, 19:1126–1136, 2011.

[Elt04]   Eltra/Elkraft/Energinet.dk.   Regulation TF 3.2.5, Wind turbines connected to grids with voltages above 100 kV — Technical regulation for the properties and the regulation of wind turbines.   https://selvbetjening.preprod.energinet.dk/NR/rdonlyres/E4E7A0BA-884F-4E63-A2F0-98EB5BD8D4B4/0/WindTurbinesConnectedtoGridswithVoltageabove100kV.pdf, December 2004.

[Ene08]   EnergyStar. Building Upgrade Manual. Chapter 11: Facility Type: Supermarkets and Grocery Stores . http://www.energystar.gov/index.cfm?c=business.bus_upgrade_manual, 2008.

[Ene11]   Energinet.dk. Potential and opportunities for flexible electricity consumption with special focus on individual heat pumps (in Danish). Technical report, Energinet.dk, The Danish TSO owned by the Danish Climate and Energy Ministry. Denmark, 2011.

[ER08]   M. S. Elliott and B. P. Rasmussen. Model-based predictive control of a multi-evaporator vapor compression cooling cycle. In *Proc. of the American Control Conference*, pages 1463–1468, 2008.

[FFC+11]   P. Finn, C. Fitzpatrick, D. Connolly, M. Leahy, and L. Relihan. Facilitation of renewable electricity using price based appliance control in irelandŠs electricity market. *Energy*, 36(5):2952 − 2960, 2011.

[GJT07]   A. Grancharova, T. Johansen, and P. Tøndel. Computational Aspects of Approximate Explicit Nonlinear Model Predictive Control. In Findeisen, R. and Allgöwer, F. and Biegler, L., editor, *Assessment and Future Directions of Nonlinear Model Predictive Control*, volume 358 of *Lecture Notes in Control and Information Sciences*, pages 181–192. Springer Berlin / Heidelberg, 2007.

[GPM89]   C. E. Garcia, D. M. Prett, and M. Morari. Model predictive control: theory and practice - a survey. *Automatica*, 25(3):335–348, 1989.

[Grü13]   Lars Grüne. Economic receding horizon control without terminal constraints. *Automatica*, 49(3):725âĂŞ–734, 2013.

[GSK$^+$10]   J. D. Grunnet, M. Soltani, T. Knudsen, M. N. Kragelund, and T. Bak. Aeolus Toolbox for Dynamics Wind Farm Model, Simulation and Control. In *Proc. of the European Wind Energy Conference and Exhibition, EWEC*, 2010.

[HFD10]   B. Houska, H.J. Ferreau, and M. Diehl. ACADO Toolkit–An Open Source Framework for Automatic Control and Dynamic Optimization. *Optimal Control Applications and Methods*, 2010.

[HFD11]   B. Houska, H. J. Ferreau, and M. Diehl. An auto-generated real-time iteration algorithm for nonlinear MPC in the microsecond range. *Automatica*, 47(10):2279–2285, 2011.

[HGL12]   H. Hindi, D. Greene, and C. Laventall. Coordinating Regulation and Demand Response in Electric Power Grids: Direct and Price-Based Tracking Using Multirate Economic Model Predictive Control. In Chakrabortty, A. and Ilic, M. D., editor, *Control and Optimization Methods for Electric Smart Grids*, volume 3 of *Power Electronics and Power Systems*, pages 111–131. Springer US, 2012.

[HHP12]   L. C. Henriksen, M. H. Hansen, and N. K. Poulsen. Wind turbine control with constraint handling: a model predictive control approach. *I E T Control Theory and Applications*, 6(11):1722–1734, 2012.

[HHS10]   S. Han, S. Han, and K. Sezaki. Development of an optimal vehicle-to-grid aggregator for frequency regulation. *IEEE Transactions on Smart Grid*, 1(1):65–72, 2010.

[HPM$^+$12]   R. Halvgaard, N. K. Poulsen, H. Madsen, J. B. Jørgensen, F. Marra, and D. E. M. Bondy. Electric vehicle charge planning using Economic Model Predictive Control. In *Proc. of the 2012 IEEE International Electric Vehicle Conference (IEVC)*, 2012.

[HPMJ12]   R. Halvgaard, N. K. Poulsen, H. Madsen, and J. B. Jørgensen. Economic Model Predictive Control for building climate control in a Smart Grid. In *Innovative Smart Grid Technologies (ISGT), 2012 IEEE PES*, pages 1–6, jan. 2012.

[HSIB06]   A. D. Hansen, P. Sørensen, F. Iov, and F. Blaabjerg. Centralised power control of wind farm with doubly fed induction generators. *Renewable Energy*, 31(7):935–951, 2006.

[IHSC07]   F. Iov, A. D. Hansen, P. E. Sørensen, and N. A. Cutululis. A survey of interconnection requirements for wind power. In *Proc. of the Nordic wind power conference (NWPC)*. Risø National Laboratory, 2007.

[JBMS09]   J. M. Jonkman, S. Butterfield, W. Musial, and G. Scott. *Definition of a 5-MW reference wind turbine for offshore system development*. National Renewable Energy Laboratory, Feb 2009.

[JCKL11]   J. L. Jerez, G. A. Constantinides, E. C. Kerrigan, and K. V. Ling. Parallel MPC for real-time FPGA-based implementation. In *Proc. of the 18th IFAC World Congress*, pages 1338–1343, 2011.

[Jør05]   J. B. Jørgensen. *Moving Horizon Estimation and Control*. PhD thesis, Department of Chemical Engineering, Technical University of Denmark, 2005.

[JT09]   K. E. Johnson and N. Thomas. Wind farm control: Addressing the aerodynamic interaction among wind turbines. In *Proc. of the American Control Conference.*, pages 2104–2109, 2009.

[KE11]   Martin Ryhl Kærn and Brian Elmegaard. *Analysis of flow maldistribution in fin-and-tube evaporators for residential air-conditioning systems*. PhD thesis, Technical University of Denmark, 2011.

[KH06]   M. Korpås and A. T. Holen. Operation planning of hydrogen storage connected to wind power operating in a power market. *IEEE Transactions on Energy Conversion*, 21(3):742–749, 2006.

[Kir03]   D. S. Kirschen. Demand-side view of electricity markets. *Power Systems, IEEE Transactions on*, 18(2):520–527, 2003.

[KNJ+11]   T. Knuppel, J. N. Nielsen, K. H. Jensen, A. Dixon, and J. Østergaard. Power oscillation damping controller for wind power plant utilizing wind turbine inertia as energy storage. In *Proc. of the IEEE Power and Energy Society General Meeting*, pages 1–8, 2011.

[LGT06]   D. Leducq, J. Guilpart, and G. Trystram. Non-linear predictive control of a vapour compression cycle. *International Journal of Refrigeration*, 29(5):761 – 772, 2006.

[LIZW07]   L. F. S Larsen, R. Izadi-Zamanabadi, and R. Wisniewski. Supermarket refrigeration system - benchmark for hybrid system control. *Proc. of the European Control Conference*, pages 113–120., 2007.

[Löf08]   J. Löfberg. Modeling and solving uncertain optimization problems in YALMIP. In *IFAC World Congress 2008*, 2008.

[LP96]   C. Loeblein and J. D. Perkins. Economic analysis of different struc-
            tures of on-line process optimization systems. *Computers & Chemical
            Engineering*, 20, Supplement 1:S551–S556, 1996.

[LTR07]   L. F. S. Larsen, C. Thybo, and H. Rasmussen. Potential energy savings
            optimizing the daily operation of refrigeration systems. *Proc. of the
            European Control Conference*, pages 4759–4764, 2007.

[LVBL98]   M. S. Lobo, L. Vandenberghe, S. Boyd, and H. Lebret. Applications
            of second-order cone programming* 1. *Linear Algebra and its Appli-
            cations*, 284(1-3):193–228, 1998.

[Mac02]   J. M. Maciejowski. *Predictive control: with constraints*. Pearson edu-
            cation, 2002.

[Mar12]   H. Markowitz. Portfolio Selection. *The journal of finance*, 7(1):77–91,
            2012.

[MAS80]   M. Morari, Y. Arkun, and G. Stephanopoulos. Studies in the synthesis
            of control structures for chemical processes: Part I: Formulation of the
            problem. Process decomposition and the classification of the control
            tasks. Analysis of the optimizing control structures. *AIChE Journal*,
            26(2):220–232, 1980.

[MB12]   J. Mattingley and S. Boyd. CVXGEN: a code generator for embedded
            convex optimization. *Optimization and Engineering*, 13:1–27, 2012.

[MBH$^+$12] Y. Ma, F. Borrelli, B. Hencey, B. Coffey, S. Bengea, and P. Haves.
            Model Predictive Control for the Operation of Building Cooling Sys-
            tems. *IEEE Transactions on Control Systems Technology*, 20(3):796–
            803, may 2012.

[MCS$^+$10] D. J. Marshman, T. Chmelyk, M. S. Sidhu, R. B. Gopaluni, and
            G. A. Dumont. Economic performance assessment with optimized
            LQG benchmarking in MIMO systems. In *Proc. of the 9th Interna-
            tional Symposium on Dynamics and Control of Process Systems*, pages
            761–766, 2010.

[MGKFGL11] A. Molina-Garcia, M. Kessler, J. A. Fuentes, and E. Gomez-Lazaro.
            Probabilistic characterization of thermostatically controlled loads to
            model the impact of demand response programs. *IEEE Transactions
            on Power Systems*, 26(1):241–251, 2011.

[MJBZ07]   M. Morari, C. Jones, M. Baric, and M. Zeilinger. Multiparamet-
            ric Linear Programming with Applications to Control. http://
            www.kuleuven.be/optec/event/507, 2007. Lecture slides from the
            Fourth Simon Stevin Lecture on Optimization in Engineering, given
            at OPTEC, K.U. Leuven, Belgium.

[MKDB12]   Y. Ma, A. Kelman, A. Daly, and F. Borrelli. Predictive Control for Energy Efficient Buildings with Thermal Storage: Modeling, Stimulation, and Experiments. *IEEE Control Systems Magazine*, 32(1):44–64, feb. 2012.

[ML99]   M. Morari and J. H. Lee. Model predictive control: past, present and future. *Computers & Chemical Engineering*, 23(4):667–682, 1999.

[MMR11]   D. Madjidian, K. Martensson, and A. Rantzer. A distributed power coordination scheme for fatigue load reduction in wind farms. In *Proc. of the American Control Conference*, pages 5219–5224, 2011.

[MNPW⁺10]   S. Meyn, M. Negrete-Pincetic, G. Wang, A. Kowli, and E. Shafieepoorfard. The value of volatile resources in electricity markets. In *49th IEEE Conference on Decision and Control, 2010*, pages 1029–1036, 2010.

[MPdH06]   J. Morren, J. Pierik, and S. W. H. de Haan. Inertial response of variable speed wind turbines. *Electric Power Systems Research*, 76(11):980–987, 2006.

[MPN12]   M. Mirzaei, N. K. Poulsen, and H. H. Niemann. Robust Model Predictive Control of a Wind Turbine. In *Proc. of the 2012 American Control Conference*, pages 4393–4398, 2012.

[MQSX12]   J. Ma, J. Qin, T. Salsbury, and P. Xu. Demand reduction in building energy systems based on economic model predictive control. *Chemical Engineering Science*, 67(1):92–100, 2012.

[MR11]   D. Madjidian and A. Rantzer. A Stationary Turbine Interaction Model for Control of Wind Farms. In *Proc. of the 18th IFAC World Congress*, pages 4921–4926, 2011.

[MT00]   H. M. Markowitz and G. P. Todd. *Mean-variance analysis in portfolio choice and capital markets*, volume 66. Wiley, 2000.

[NM04]   H. A. Nielsen and H. Madsen. Forecasting wind speeds on the minute time-scale using up-stream information. Technical report, Technical University of Denmark, Informatics and Mathematical Modelling, 2004.

[NMS04]   H. A. Nielsen, H. Madsen, and P. Sørensen. Ultra-short term wind speed forecasting. In *Proc. of the European Wind Energy Conference & Exhibition, London*, 2004.

[NW06]   J. Nocedal and S.J. Wright. *Numerical Optimization*. Springer Series in Operations Research and Financial Enginee. Springer, 2006.

[OJM08]   F. Oldewurtel, C. N. Jones, and M. Morari. A tractable approximation of chance constrained stochastic MPC based on affine disturbance feedback. In *47th IEEE Conference on Decision and Control, 2008*, pages 4731–4736, 2008.

[OPJ⁺10a]   F. Oldewurtel, A. Parisio, C. N. Jones, M. Morari, D. Gyalistras, M. Gwerder, and et al. Energy Efficient Building Climate Control using Stochastic Model Predictive Control and Weather Predictions. In *Proc. of American Control Conference 2010*, pages 5100–5105, 2010.

[OPJ⁺10b]   F. Oldewurtel, A. Parisio, C.N. Jones, M. Morari, D. Gyalistras, M. Gwerder, V. Stauch, B. Lehmann, and K. Wirth. Energy Efficient Building Climate Control using Stochastic Model Predictive Control and Weather Predictions. In *Proc of the American Control Conference (ACC)*, pages 5100–5105, 2010.

[OPJ⁺12]   F. Oldewurtel, A. Parisio, C. N. Jones, D. Gyalistras, M. Gwerder, V. Stauch, B. Lehmann, and M. Morari. Use of model predictive control and weather forecasts for energy efficient building climate control. *Energy and Buildings*, 45(0):15–27, 2012.

[PJ09]   L. Y. Pao and K. E. Johnson. A tutorial on the dynamics and control of wind turbines and wind farms. In *Proc. of the American Control Conference*, pages 2076–2089, 2009.

[PSF12]   A. Pina, C. Silva, and P. Ferrão. The impact of demand side management strategies in the penetration of renewable electricity. *Energy*, 41(1):128 – 137, 2012.

[QB03]   S. J. Qin and T. A. Badgwell. A survey of industrial model predictive control technology. *Control engineering practice*, 11(7):733–764, 2003.

[RA09]   J. B. Rawlings and R. Amrit. Optimizing Process Economic Performance Using Model Predictive Control. *Nonlinear Model Predictive Control: Towards New Challenging Applications*, pages 119–138, 2009.

[RAB12]   J. B. Rawlings, D. Angeli, and C. Bates. Fundamentals of economic model predictive control. In *Proc. of the 51th IEEE Conference on Decision and Control*, pages 3851–3861, 2012.

[RM09]   James B. Rawlings and David Q. Mayne. *Model Predictive Control: Theory and Design*. Nob Hill Publishing, 2009.

[RR00]   C. V. Rao and J. B. Rawlings. Linear programming and model predictive control. *Journal of Process Control*, 10(2-3):283–289, 2000.

[SBW11]   M. Soleimanzadeh, A. J. Brand, and R. Wisniewski. A wind farm controller for load and power optimization in a farm. In *Proc. of the IEEE International Symposium on Computer-Aided Control System Design (CACSD)*, pages 1202–1207, 2011.

[Sca09]   Riccardo Scattolini. Architectures for distributed and hierarchical Model Predictive Control — A review. *Journal of Process Control*, 19(5):723–731, 2009.

[SCLdP08]   D. Sarabia, F. Capraro, L. F. S. Larsen, and C. de Prada. Hybrid NMPC of supermarket display cases. *Control Engineering Practice*, 17(4):428–441, 2008.

[SDE08]   C. Sonntag, A. Devanathan, and S. Engell. Hybrid NMPC of a Supermarket Refrigeration System using Sequential Optimization. In *Proc of 17th IFAC World Congress*, pages 13901–13906, 2008.

[SEF+13]   L. E. Sokoler, K. Edlund, G. Frison, A. Skajaa, and J. B. Jørgensen. A Riccati Based Homogeneous and Self-Dual Interior-Point Method for Linear Economic Model Predictive Control. In *Proc. of the IEEE Multi-conference on Systems and Control*, page to appear, 2013.

[SG11]   H. Saele and O. S. Grande. Demand response from household customers: Experiences from a pilot study in norway. *IEEE Transactions on Smart Grid*, 2(1):90–97, 2011.

[SJB11]   V. Spudic, M. Jelavic, and M. Baotic. Wind turbine power references in coordinated control of wind farms. *AUTOMATIKA*, 52(2):82–94, 2011.

[SK12]   T. Samad and S. Kiliccote. Smart grid technologies and applications for the industrial sector. *Computers & Chemical Engineering*, 47(0):76–84, 2012.

[Sko00a]   S. Skogestad. Plantwide control: The search for the self-optimizing control structure. *Journal of process control*, 10(5):487–507, 2000.

[Sko00b]   M. J. Skovrup. Thermodynamic and thermophysical properties of refrigerants - software package in borland delphi. Technical report, Department of Energy Engineering, Technical University of Denmark, Kgs. Lyngby, Denmark, 2000.

[SS09]   B. Singh and S.N. Singh. Wind Power Interconnection into the Power System: A Review of Grid Code Requirements. *The Electricity Journal*, 22(5):54–63, 2009.

[SSD+12]   D. I. Stroe, A. I. Stan, R. Diosi, R. Teodorescu, and S. J. Andreasen. Short term energy storage for grid support in wind power applications. In *Proc. of the 13th International Conference on Optimization of Electrical and Electronic Equipment (OPTIM)*, pages 1012–1021, 2012.

[STR11]   M. J. Swierczynski, R. Teodorescu, and P. Rodriguez. Lifetime investigations of a lithium iron phosphate (LFP) battery system connected to a wind turbine for forecast improvement and output power gradient reduction. In *Proc. of the 15th Battcon Stationary Battery Conference and Trade Show*, pages 20.1–20.8, 2011.

[SWK12]   M. Soleimanzadeh, R. Wisniewski, and S. Kanev. An optimization framework for load and power distribution in wind farms. *Journal of Wind Engineering and Industrial Aerodynamics*, 107–108:256–262, 2012.

[Tar12]   G. C. Tarnowski. *Coordinated Frequency Control of Wind Turbines in Power Systems with High Wind Power Penetration*. PhD thesis, Technical University of Denmark, 2012.

[Ull11]   F. Ullmann. FiOrdOs: A Matlab Toolbox for C-Code Generation for First Order Methods. Master's thesis, ETH Zurich, 2011.

[VH01]   G. L. Van Harmelen. The virtual power station targeting residential, industrial and commercial controllable loads. *IFAC Conference on Technology Transfer in Developing Countries - Automation in Infrastructure Creation (DECOM-TT 2000) Proceedings volume from IFAC Conference*, pages 45–48, 2001.

[VHSB01]   D. H. Van Hessem, C. W. Scherer, and O. Bosgra. LMI-based closed-loop economic optimization of stochastic process operation under state and input constraints. In *IEEE Conference on Decision and Control 2001*, volume 5, pages 4228–4233, 2001.

[WB10]   Y. Wang and S. Boyd. Fast Model Predictive Control Using Online Optimization. *IEEE Transactions on Control Systems Technology*, 18(2):267–278, 2010.

[WLT+11]   J. Wang, C. Liu, D. Ton, Y. Zhou, J. Kim, and A. Vyas. Impact of plug-in hybrid electric vehicles on power systems with demand response and wind power. *Energy Policy*, 39(7):4016–4021, 2011.

[ZB09]   V. M. Zavala and L. T. Biegler. Nonlinear Programming Strategies for State Estimation and Model Predictive Control. In Magni, Lalo and Raimondo, Davide and Allgöwer, Frank, editor, *Nonlinear Model Predictive Control*, volume 384 of *Lecture Notes in Control and Information Sciences*, pages 419–432. Springer Berlin / Heidelberg, 2009.

[ZJM08]   M. N. Zeilinger, C. N. Jones, and M. Morari. Real-time suboptimal model predictive control using a combination of explicit MPC and online optimization. In *Proc. of the 47th IEEE Conference on Decision and Control (CDC)*, pages 4718–4723, 2008.

Part III

Papers

Model predictive control technologies for efficient and flexible power consumption in refrigeration systems

Model predictive control technologies for efficient and flexible power consumption in refrigeration systems

Tobias Gybel Hovgaard [a,c,*], Lars F.S. Larsen [a], Kristian Edlund [b], John Bagterp Jørgensen [c]

[a] Danfoss A/S, Nordborgvej 81, DK-6430 Nordborg, Denmark
[b] DONG Energy A/S, Kraftværksvej 53, DK-7000 Fredericia, Denmark
[c] DTU Informatics, Technical University of Denmark, Richard Petersens Plads, Building 321, DK-2800 Kgs. Lyngby, Denmark

ARTICLE INFO

ABSTRACT

Considerable amounts of energy are consumed in supermarket refrigeration systems worldwide. Due to the thermal capacity of refrigerated goods and the rather simplistic control most commonly applied, there is a potential for distributing the system load over time in a more cost-optimal way. In this paper we describe a novel economic-optimizing Model Predictive Control (MPC) scheme that reduces operating costs by utilizing the thermal storage capabilities. A nonlinear optimization tool to handle a non-convex cost function is utilized for simulations with validated scenarios. In this way we explicitly address advantages from daily variations in outdoor temperature and electricity prices. Secondly, we formulate a new cost function that enables the refrigeration system to contribute with ancillary services to the balancing power market. This involvement can be economically beneficial for the system itself, while crucial services can be delivered to a future flexible and intelligent power grid (Smart Grid). Furthermore, we discuss a novel incorporation of probabilistic constraints and Second Order Cone Programming (SOCP) with economic MPC. A Finite Impulse Response (FIR) formulation of the system models allows us to describe and handle model as well as prediction uncertainties in this framework. This means we can demonstrate means for robustifying the performance of the controller.

1. Introduction

To obtain an increasing amount of electricity from intermittent energy sources such as solar and wind, we must not only control the production of electricity, but also the consumption of electricity, in an efficient, flexible and proactive manner. The facilitation of wind generated electricity by price optimized thermal storage has been described in Ref. [1]. In contrast to the current rather centralized power generation system, the future electricity grid will be a network of a very large number of independent power generators. The Smart Grid is the future intelligent electricity grid and is intended to be the smart electrical infrastructure required to increase the amount of green energy significantly. The Danish transmission system operator (TSO) has the following definition of Smart Grids which we adopt in this work: "Intelligent electrical systems that can integrate the behavior and actions of all connected users — those who produce, those who consume and those who do both — in order to provide a sustainable, economical and reliable electricity supply efficiently" [2].

In Denmark around 4500 supermarkets consume more than 550,000 MW h annually. This corresponds roughly to 2% of the entire electricity consumption. The installed cooling capacity equals an electrical wattage ranging from 10 to 200 kW, depending on the supermarket size. Refrigerated goods make up a large capacity in which energy can be stored in the form of "coldness". The hysteresis control policy most commonly used today does not exploit this and a large potential for energy and cost reductions exists. Preliminary investigations have been carried out in Larsen et al. [3], Hovgaard et al. [4], and in this paper we further analyse this in a realistic setting. Furthermore a novel formulation of the cost function enables the supermarket refrigeration system to benefit from the enablement of flexible power consumption.

In this paper we utilize the flexibility of the refrigeration system to offer ancillary demand response to the power grid as regulating power. Different means of utilizing demand response have been investigated in an increasing number of publications, e.g. Andersson et al. [5], Han et al. [6], Saele and Grande [7], Molina-Garcia et al. [8], for plug-in electric vehicles and heat pumps. Kirschen [9] investigated

demand response in general concerning price elasticity and Pina et al. [10] analyzed different demand side management strategies.

Our proposed control strategy is an economic-optimizing model predictive controller, economic MPC. Predictive control for constrained systems has emerged during the last 30 years as one of the most successful methodologies to control industrial processes [11] and is increasingly being considered to control both refrigeration and power systems [12–14]. MPC based on optimizing economic objectives has only recently emerged as a general methodology with efficient numerical implementations and provable stability properties [15–17]. We have previously introduced economic MPC in Hovgaard et al. [18] to control a power management scheme for large power consumers such as supermarket refrigeration systems. The economic MPC has the ability to choose the optimal cooling strategy from predictions of the disturbances. The thermal capacity is utilized to shift the load in time, while keeping the temperatures within certain bounds. These bounds are chosen such that they have no impact on food quality. We exploit the fact that the dynamics of the temperature in the cold room are rather slow, while the power consumption can be changed rapidly. Utilizing load shifting capabilities to reduce total energy consumption has also been described in e.g. Van Harmelen [19], Bush and Wolf [20], Oldewurtel et al. [21]. In the simulations that will be presented in this paper, we use models, parameters and temperatures verified against data logged from real supermarkets, along with electricity prices from the NordPool spot market.

Our cost function is nonlinear in the control variables, but instead of doing any simplification we have chosen a nonlinear solver [22] to run the simulations. The proposed nonlinear economic MPC algorithm is not tractable for industrial hardware with limited computational resources. Hence, the contribution of this paper is to illustrate the optimal solution and maximum potential of our approach. The study is therefore suitable for benchmarking future, more appealing algorithms and not to present a directly implementable controller. However, it should be kept in mind that the slow dynamics of the system allow for long sample times and therefore increased complexity of the controller. Nonlinear programming was used in Ref. [23] to maximize the retailers' profit in a real-time pricing scenario.

In this paper we also propose a reformulation of the underlying optimization problem for the economic MPC that accounts for the ever-present uncertainties in both models and forecasts. Like in Hovgaard et al. [24], we use a small conceptual problem formulated as a linear program to illustrate this method.

Several works exist that consider constrained MPC in the presence of uncertainty [25]. In many applications, distributions can be quantified for uncertainty and if this information is ignored (e.g. by defining worst-case costs and invoking constraints over all uncertainty realizations) it can lead to conservative results, and the need for a stochastic extension to constrained MPC is clear [26]. Taking expected values of the cost provides an obvious way to utilize probabilistic information [27]. However, constraints often admit a probabilistic formulation too, e.g. a variable should not exceed a certain bound with a given probability. Van Hessem et al. [28] and Oldewurtel et al. [29] considered MPC with probabilistic constraints with the cost based on the expected value of a linear function of the states. In the former, the implementation of probabilistic constraints can be conservative due to the use of statistical confidence ellipsoidal approximations, whereas the latter uses affine disturbance feedback. Boyd et al. [30] and Lobo et al. [31] demonstrated that probabilistic linear constraints can be written as second-order cone (SOC) constraints that are convex, provided the probability involved is greater than 0.5. Probabilistic constraints are also introduced in Schwarm and Nikolaou [32] for model uncertainties and in Li et al. [33] for uncertain disturbances. Both

works confined the analysis to open loop optimization, whereas Kassmann et al. [34] used SOCP methods to calculate steady-state targets for MPC under uncertainty. In Shin and Primbs [35] a fast algorithm for MPC with probabilistic constraints was presented. For power management scenarios, e.g. Carrion et al. [36] proposed a risk-constrained stochastic programming for signing day-ahead contracts under uncertain price forecasts and in the work by Parvania and Fotuhi-Firuzabad [37] a stochastic mixed-integer program was proposed for the scheduling of reserves by demand response under forecast uncertainty and random outages of generating units and transmission lines. Refs. [38,39] considered probabilistic approaches for calculating the optimal amount of spinning reserves in a day-ahead market.

This paper is organized as follows. In Section 2 we formulate our economic-optimizing MPC controller. Section 3 describes the physics and models used for the supermarket refrigeration systems as well as the thermal storage capabilities. Furthermore the scenario for a realistic simulation and the corresponding results are presented, utilizing variations in outdoor temperatures and electricity prices. In Section 4 the calculations needed for regulating power are given along with simulations revealing the potential of this addition to the cost function. In Section 5 we explain the different sources of uncertainty and reformulate both the model and forecast uncertainties to fit into solutions with probabilistic constraints. This is followed by a description of the models, assumptions and scenarios used for simulating a simple case study. Future work is outlined in Section 6, and in Section 7 we give conclusions.

2. Economic MPC setup

A supermarket refrigeration system is influenced by a number of disturbances that can be predicted to some degree of certainty over a time horizon into the future. The controller also has to obey certain constraints for the systems, while minimizing the cost of operation. Economic MPC addresses all these concerns. Whereas the cost function in MPC traditionally penalizes a deviation from a set-point, our proposed economic MPC directly reflects the actual costs of operating the plant. This formulation is tractable for refrigeration systems, where we are interested in keeping the outputs (cold-room temperatures) within certain ranges, while minimizing the cost of doing so.

Like in traditional MPC, we implement the controller in a receding horizon manner, where an optimization problem over N time steps (our control and prediction horizon) is solved at each sample. The result is an optimal input sequence for the entire horizon, out of which only the first step is implemented. This procedure is repeated at each sample. The controller aims at minimizing the electricity cost of operation. This cost is related to energy consumption but we do not aim specifically at minimizing the energy consumption, nor do we focus on tracking certain temperatures in the cold rooms. The optimization problem is thus formulated as:

$$\min_{(\mathbf{Q_e},\mathbf{T_e}) \in \Omega} \Phi = \sum_{k=0}^{N-1} C_{el,k} W_c(\dot{Q}_{e,k}, T_{e,k}, T_{a,k}, T_{amb,k}) \qquad (1a)$$

$$\dot{\mathbf{Q}}_\mathbf{e} = \{\dot{Q}_{e,k}\}_{k=0}^{N-1}, \quad \mathbf{T_e} = \{T_{e,k}\}_{k=0}^{N-1} \qquad (1b)$$

where $W_c(\cdot)$ is the energy consumption as described in Section 3 and the feasible set Ω that imposes the system dynamics and constraints is defined in Eqs. (2)–(4). The MPC feedback law is the first move in Eq. (1b).

Often output constraints are soft in MPC, but in this setup, constraints on temperatures and capacity are made hard. In reality, one could formulate a cost on cold-room temperatures outside the allowable range related to the degrading of the foodstuff. This cost would then be the cost on slack variables in a soft constraint. However, firstly it is not realistic that an owner of a refrigeration system will damage the foodstuff, and secondly, estimating bacteria growth in refrigerated food is, in itself, a complicated study. In a stochastic formulation, as the one presented in Section 5, a feasible problem can be guaranteed using probabilistic constraints.

In the above formulation, we assume perfect predictions and therefore we allow the system to go to any extreme point within the feasible region. However, both disturbance predictions and models of the systems are subject to uncertainties that are prone to driving the otherwise optimal solution of the economic MPC to a very undesirable solution. For refrigeration systems, such situations could be too high or too low temperatures in the cold room damaging the foodstuff; emergency shut down of systems due to maximum capacity being exceeded; penalties for not fulfilling regulating power agreements or unnecessarily high operation costs. Consequently, we have formulated a robust economic MPC scheme in Section 5 using probabilistic constraints and assumed knowledge of the probability density functions for stochastic disturbances and impulse response coefficients of the system models [24].

3. Supermarket refrigeration

The supermarket refrigeration systems considered utilize a vapor compression cycle in which a refrigerant is circulated in a closed loop consisting of a compressor, an expansion valve and two heat exchangers, an evaporator in the cold storage room, as well as a condenser/gas cooler located in the surroundings. When the refrigerant evaporates, it absorbs heat from the cold reservoir which is rejected to the hot reservoir. In order to keep the refrigeration cycle flowing with the heat transfers as described here, the evaporation temperature (T_e) has to be lower than the temperature in the cold reservoir (T_{cr}) and the condensation temperature has to be higher than the temperature at the hot reservoir (T_a). Low pressure refrigerant (P_e) from the outlet of the evaporator is compressed in the compressors to a high pressure (P_c) at the inlet to the condenser to increase the saturation temperature. The setup is sketched in Fig. 1, with one cold storage room and one frost room

connected to the system. Usually, several cold storage rooms, e.g. display cases, are connected to a common compressor rack and condensing unit. Because of this, the individual display cases see the same evaporation temperature, whereas each unit has its own inlet valve for individual temperature control.

3.1. Models

The dynamics in the cold room can be described by a simple energy balance:

$$mc_p \frac{dT_{cr}}{dt} = \dot{Q}_{load} - \dot{Q}_e \tag{2}$$

with

$$\dot{Q}_{load} = (UA)_{amb-cr} \cdot (T_{amb} - T_{cr}) \tag{3a}$$

$$\dot{Q}_e = (UA)_{cr-e} \cdot (T_{cr} - T_e) \tag{3b}$$

where UA is the heat transfer coefficient and m and c_p are the mass and the specific heat capacity of the refrigerated goods, respectively. T_{amb} is the temperature of the ambient air which puts the heat load on the refrigeration system. The states and control variables of the system are limited by the following constraints:

$$T_{cr,min} \leq T_{cr} \leq T_{cr,max} \tag{4a}$$

$$0 \leq T_{cr} - T_e \leq \infty \tag{4b}$$

$$0 \leq \dot{Q}_e \leq (UA)_{cr-e,max} \cdot (T_{cr} - T_e) \tag{4c}$$

We define the set Ω as all $(\dot{Q}_e, T_e)$ that satisfy the system dynamics (Eq. (2)) and the constraints given in Eq. (4).

The work done by the compressor dominates the power consumption in the system and can be expressed by the mass flow of refrigerant (m_{ref}) and the change in energy content of the refrigerant. Energy content is described by the enthalpy of the refrigerant at the inlet and at the outlet of the compressor (h_{ic} and h_{oc} respectively). This gives the expression in Eq. (5):

$$\dot{W}_c = \frac{m_{ref} \cdot (h_{oc}(T_e, P_c) - h_{ic}(T_e))}{\eta_{is}(P_c/P_e)} \tag{5}$$
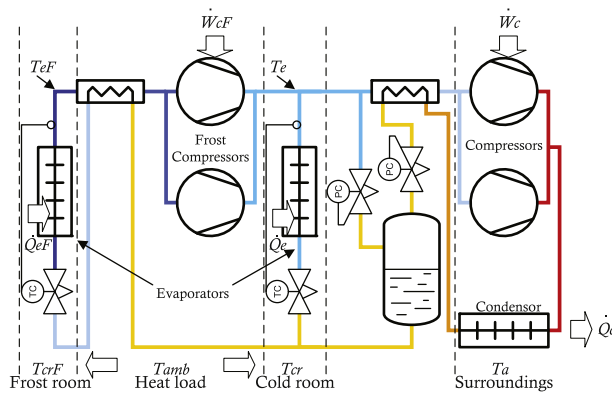

Fig. 1. Schematic layout of basic refrigeration system.

where the enthalpies depend on the evaporation temperature and the condensing pressure, as stated. The mass flow can be determined as the ratio between cooling capacity and change of enthalpy over the evaporator:

$$m_{\text{ref}} = \frac{\dot{Q}_e}{h_{\text{oe}}(T_e) - h_{\text{ie}}(P_c)} \qquad (6)$$

All the enthalpies given here as functions of T_e, P_c or both are nonlinear refrigerant-dependent functions which can be calculated, e.g. by the software package "RefEqns" [40].

In the sequel, we adopt the approximation used for $\dot{W}_c$ in Hovgaard et al. [4], where polynomials are fitted for the enthalpy differences and the isentropic efficiency, η_{is}, is assumed constant within the range of operation. When a frost room is included, an extra compressor system is usually added between the frost evaporator and the suction side of the other compressors. This compressor decreases the evaporation temperature for the frost part of the system to a lower level. The work in the frost compressor is similar to what we have already described, but instead of the condensing temperature, the frost compressor sees the evaporation temperature for the cooling part at its outlet. The mass flow through the frost compressor needs to be added to the flow through the compressors from the cooling. We use the subscript F to denote variables related to the frost part.

For the studies in this paper, we have collected data from several supermarkets actually in operation in Denmark. From these data, typical parameters such as time constants, heat loads, temperature ranges and capacities, in both individual display cases and for the overall system, have been estimated for horizontal display cases, vertical shelving units and frost rooms. Furthermore the running compressor capacity has been monitored and the relation to energy consumption has been found from the data sheets.

3.2. Thermal storage

Today, most display cases and cold rooms in supermarkets are controlled by hysteresis. This means that maximum cooling is applied when the cold-room temperature reaches an upper limit and shut off when the lower limit is reached. This control policy does not exploit the thermal capacity in the refrigerated mass, and energy is consumed randomly when it is needed instead of when it is more favorable. Several factors can, however, make it beneficial to shift the load by keeping the temperatures at a low or high level for some periods. These include variations in outdoor temperature, fluctuating energy prices, times for restocking, and night covers. Obviously several unexploited potentials exist. If peak loads can be predicted, pre-cooling can be applied so that the stored coldness helps reduce the demand at the peak time. As a result, the entire system might be dimensioned differently to save money both in the installation phase and during operation. By moving part of the cooling capacity to the colder night time, overall energy consumption can be reduced, since the work done by the compressor to obtain a certain evaporation temperature is dependent on the pressure difference, which in turn depends on the temperature surrounding the condenser. In contrast, shifting loads according to fluctuations in electricity prices actually make the system consume more energy. Thus, the profitability rests upon the extra heat loss during periods when the extra coldness is stored in the system is at least counterbalanced by the difference in electricity price.

It is evident from the discussion above that the potential in load shifting depends to a great extent on both the thermal capacity and the differences in electricity prices and outdoor temperatures. However, the rate of change of these parameters in comparison

with the time constants of the cold-room temperatures also plays an important role.

3.3. Simulation

In this section we present the conditions used for simulating a realistic scenario with the supermarket refrigeration system in a setting where predictions of electricity prices as well as outdoor temperatures exist. We use the economic MPC controller described in Section 2. Results of the simulations are presented and discussed.

3.3.1. Scenario

We have chosen a supermarket refrigeration system with three units attached. This roughly corresponds in size to 1/10 of one of the supermarkets we have been monitoring and the capacity of the system has been scaled accordingly. The three units are very different. The shelving unit is usually used for smaller items like sliced meat and does not hold a very large mass of foodstuff. The heat load is relatively high due to the large vertical opening to the surroundings. The chest display case holds larger amounts of e.g. minced meat and due to the horizontal opening, which also has a glass cover, the heat load is rather low. The frost room with insulated walls on all sides has the lowest heat load and the mass of frozen meat contained is large. For the frost room, an extra compressor is added, lowering the evaporation temperature to a sufficiently lower level than the evaporation temperature in the cooling units. All three units have different temperature demands, namely [2; 4]°C for the shelving unit, [1; 5]°C for the chest display case and [−25; −15]°C for the frost room. The models were validated with supermarkets in operation in Denmark, January 2011. Electricity prices were downloaded from NordPool's hourly el-spot price for a period of one month. There is a clear trend in these data for each 24-h period. Therefore, for each hour of the day, the average has been found and this 24-h signal was used for the electricity price.

Temperature readings from the Danish Meteorological Institute covering the same period were obtained. It has been found that by low pass filtering and detrending these data, the intra-day variations can be closely approximated by a sinusoid with a 24-h period and a phase shift such that it peaks a couple of hours after noon. The amplitude for this period has been chosen at 3 °C. In addition we have measured the temperature inside the stores. This temperature is allowed to drop by around 2 °C outside opening hours. This effect is included in our simulations.

Simulations are performed over at least 24 h. An issue with MPC is that the long prediction horizons tend to make the problems computationally hard. However, due to the slow dynamics of the refrigeration system, we have chosen a sampling time of 32 min. Thus a prediction horizon of 16 h is implemented with just $N = 30$ samples.

3.3.2. Results

Fig. 2 shows the simulated refrigeration system using the predicted outdoor temperature and electricity price to optimize the cost. As elaborated in Hovgaard et al. [4,41] the cost function is non-convex in the control variables, although a unique global minimum exists within the feasible region. Therefore, we have chosen the nonlinear optimization tool ACADO [22] to solve the repeated problems in our MPC. ACADO implements an SQP algorithm for optimizing the nonlinear cost function while being straightforward to implement.

The amplitude of the electricity price has been multiplied by four to better illustrate the effect and to reflect a scenario with variable taxes instead of the flat-rate fees seen today. This is further discussed below. In this case the cost savings amount to 32%. If the original
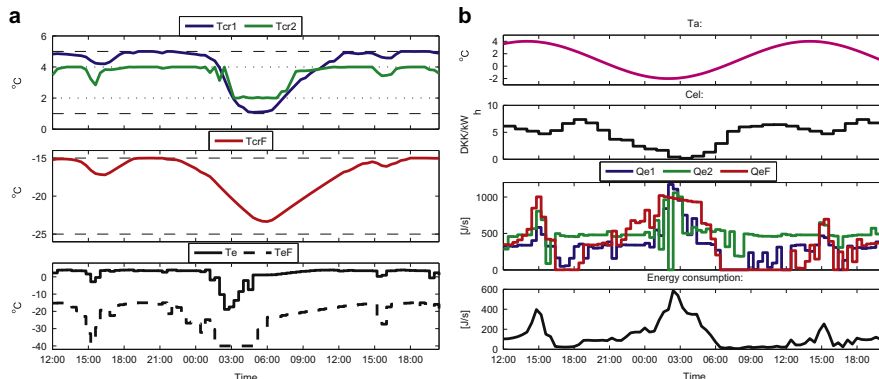
Fig. 2. Simulation showing how variations in outdoor temperature and electricity prices are exploited by utilization of thermal storage. (a) Cold-room and evaporation temperatures. (b) Disturbances, cooling powers and energy consumption.

electricity price is used, less change in cold-room temperatures can be observed and the cost savings amount to 9% in this case. With three-quarters of the electricity price paid in Denmark today being flat-rate taxes and fees, saving 9% on the spot price corresponds to 2.25% of the entire electricity bill. If we are only exploiting the variations in outdoor temperature, the economic MPC control scheme saves around 2% of the energy consumption.

From the results illustrated in Fig. 2 we can conclude that the proposed economic MPC scheme has a positive effect on the costs related to operating the supermarket. Variations in outdoor temperature are utilized to minimize power consumption, whereas exploiting variations in electricity prices tends to increase overall power consumption but at a lower cost. In Fig. 2 the amplitude of the electricity price has been multiplied by four to illustrate the increase in effect gained by the power management. Today the dominant part of the price paid for electricity consists of taxes and connection fees, which are all paid as flat-rate charges per MW h. This blurs the price signals from the market to the users and reduces the incentives to react to such signals. Hence, the simulation shown with four-times amplitude of the el-spot price is an attempt to model a situation where the taxes and other fees are charged as a percentage of the actual el-spot price. This would result in a magnification instead of a smoothing of the market signals.

Obviously flexibility is drastically reduced if the system is running near its maximum capacity just to keep the temperatures below the maximum limits on a hot summer day. It is not possible to increase consumption, whether it be for storing coldness or for down regulation, due to the maximum capacity; nor is it possible to decrease consumption, since this would violate the temperature demands in the cold rooms. This situation leads to a trade-off between saving by dimensioning a smaller system when peak loads can be reduced, and savings related to boosting energy into the system when it is cheap to do so.

4. Flexible power consumption

In order to ensure a sustainable physical balance in the electricity system, there is a need for regulating power and various types of spare capacity. Spare capacity is production capacity or consumption made available in advance to the TSO by parties

responsible for maintaining balance in the system, in return for an availability payment. Various types of spare capacity exist. These types of capacity differ in activating velocity, amount and demands for the upholding period.

With the enablement of flexible consumption in refrigeration systems we are ready to consider other incentives for load shifting than those already mentioned in Section 3. In this section we formulate a framework in which the supermarkets can participate in the primary reserve (the capacity with fastest activation and shortest upholding periods).

4.1. Up-regulating power as primary reserve

Up-regulating power is increased production or reduced consumption. Each player participates with a power amount (MW) specified on an hourly basis and is paid for making the power available to the grid (Danish Kroner (Currency)/MW), regardless of the actual activation. Activation is automatic and linearly frequency-dependent in the range ±200 mHz. Activation is maintained for up to 15 min (typically 2–3 min) and must be fully restored after 15 min. Even though the activated power (MW) might be large, the delivered energy (MW h) is usually small amounts, so a possible change in spot price during the activation will have almost no effect on the economy of the system.

Assumption 1. Since the ambient temperature is generally much higher than the cold-room temperature, the small change in temperature during an activation does not change the load, $\dot{Q}_{load} = UA(T_{amb} - T_{cr})$, much. Hence, by assuming that $\dot{Q}_{load} = UA(T_{amb} - T_{cr,start})$ is constant over the activation period we are somewhat conservative in the calculations.

Assumption 2. In steady state $\dot{Q}_e = \dot{Q}_{load}$ (this might be more of a fact than an assumption, but we exploit the relation in the equations below).

Assumption 3. An activation period of maximum 15 min is relatively short compared to the rate of change in the disturbances (outdoor temperature T_a and electricity spot prices C_{el}). Thus, the cost of the energy required to reestablish the reserve following an activation is approximately the same as the amount saved during the activation.

The amount of power available for up-regulation is described by:

$$\dot{Q}_{\text{reg}\div} = \dot{Q}_e - \dot{Q}_{15\div} \tag{7}$$

where $\dot{Q}_{\text{reg}\div}$ is the cooling capacity that can be released as up-regulating power and $\dot{Q}_{15\div}$ is the cooling need in order to make T_{cr} stay below $T_{\text{cr,max}}$ for 15 min. During an activation the temperature in the cold room is:

$$m \cdot Cp \frac{dT_{\text{cr}}}{dt} = \dot{Q}_{\text{load}} - \dot{Q}_{15\div} = \dot{Q}_{\text{reg}\div} \tag{8}$$

Therefore,

$$m \cdot Cp \int_{T_{\text{cr}}}^{T_{\text{cr,max}}} dT_{\text{cr}} = \int_{0}^{900s} \dot{Q}_{\text{reg}\div} \, dt \Leftrightarrow \tag{9}$$

$$\dot{Q}_{\text{reg}\div} = (T_{\text{cr,max}} - T_{\text{cr}}) \frac{m \cdot Cp}{900s} \tag{10}$$

For up-regulating power there is a potential decrease in heat loss from the system if the reserve is activated. By assuming almost linear cold-room temperature curves within the range we are considering for regulating power reserves, the reduced energy loss during an entire period of activation and the subsequent re-establishment can be averaged by

$$\dot{Q}_{\text{loss}\div} = P_\div \cdot \alpha_\div \cdot UA \cdot (T_{\text{cr,max}} - T_{\text{cr}}) \tag{11}$$

where UA is the overall heat transfer coefficient from the cold room to surroundings and $P_\div$ is the probability of being activated (samples where the system is activated as up-regulating power or is re-establishing after an up-regulation versus the total number of samples). We also introduce a new decision variable $\alpha_\div \in [0; 1]$, which is the amount of available up-regulating power that is actually offered to the grid. Since power cannot be extracted from the stored coldness, we have to introduce a constraint such that the offered up-regulating power is never larger than the actual power consumption at any point of time.

$$\alpha_\div \cdot \dot{Q}_{\text{reg}\div} \leq \dot{Q}_e \tag{12}$$

A cost function including the up-regulating power can then be formulated as:

$$\min_{\mathbf{Q_e}, \alpha_\div} \sum_{k=0}^{N} (C_{\text{el}_k} W_k (\dot{Q}_{e,k} - \dot{Q}_{\text{loss}\div,k}, T_{a,k})$$
$$- C_{\text{upreg}_k} W_k (\alpha_\div \cdot \dot{Q}_{\text{reg}\div,k}, T_{a,k})) \tag{13}$$

where C_{upreg} is the disposal payment for up-regulating reserves.

4.2. Down-regulating power as primary reserve

Down-regulating power is reduced production or increased consumption. The rules of participation are equal to those described for up-regulating power. Assumptions 1–3 are still in effect, however Assumption 3 is the opposite; namely that the cost of extra energy used during an activation equals the amount that can be saved following the activation.

The system can participate with down-regulating power as given by:

$$\dot{Q}_{\text{reg}+} = \dot{Q}_{15+} - \dot{Q}_e \tag{14}$$

where $\dot{Q}_{\text{reg}+}$ is the extra cooling capacity that can be used as down-regulating power and $\dot{Q}_{15+}$ is the cooling capacity that makes T_{cr} go to $T_{\text{cr,min}}$ in 15 min. Performing the same calculations as in Eqs. (8) and (9) yields the following:

During an activation the temperature in the cold room is:

$$m \cdot Cp \frac{dT_{\text{cr}}}{dt} = \dot{Q}_{\text{load}} - \dot{Q}_{15+} = -\dot{Q}_{\text{reg}+} \tag{15}$$

Therefore,

$$m \cdot Cp \int_{T_{\text{cr}}}^{T_{\text{cr,min}}} dT_{\text{cr}} = \int_{0}^{900s} -\dot{Q}_{\text{reg}+} \, dt \Leftrightarrow \tag{16}$$

$$\dot{Q}_{\text{reg}+} = (T_{\text{cr}} - T_{\text{cr,min}}) \frac{m \cdot Cp}{900s} \tag{17}$$

As with up-regulating power, an activation of the reserve changes the heat loss from the system. This is not accounted for in the calculations above. Whereas the original cost function covers the extra heat loss caused by maintaining up-regulating reserves (a decrease in cold-room temperature and thereby increase in heat loss in time periods with no activation) there is no extra cost, in terms of heat loss, related to maintaining down-regulating reserves. This cost only comes into play when activation occurs. Again, we assume almost linear temperature curves within the range of interest and the energy loss during an entire period of activation and subsequent re-establishment can be averaged by

$$\dot{Q}_{\text{loss}+} = P_+ \cdot \alpha_+ \cdot UA \cdot (T_{\text{cr}} - T_{\text{cr,min}}) \tag{18}$$

where P_+ is the probability of being activated. A new decision variable, $\alpha_+ \in [0; 1]$, is again introduced describing the share of available down-regulating power that is actually offered to the grid. A cost function including the down-regulating power can then be formulated as:

$$\min_{\mathbf{Q_e}, \alpha_+} \sum_{k=0}^{N} (C_{\text{el}_k} W_k ((\dot{Q}_{e,k} - \dot{Q}_{\text{loss}+,k}), T_{a,k})$$
$$- C_{\text{downreg}_k} W_k (\alpha_+ \cdot \dot{Q}_{\text{reg}+,k}, T_{a,k})) \tag{19}$$

where C_{downreg} is the disposal payment for down-regulating reserves.

The amount of down-regulating power offered must be bounded such that the sum of current cooling capacity and that offered for down-regulation does not exceed the maximum capacity of the system. Thus, even on a hot summer day the following has to be fulfilled:

$$\alpha_+ \cdot \dot{Q}_{\text{reg}+} + \dot{Q}_e \leq \dot{Q}_{\text{max}} \tag{20}$$

4.3. Cost function

We are now able to formulate a cost function including the effects of regulating power:

$$\min_{\mathbf{\dot{Q}_e}, \mathbf{T_e}, \alpha_+, \alpha_+} \sum_{k=0}^{N} [C_{\text{el}_k} W_k ((\dot{Q}_{e,k} - \dot{Q}_{\text{loss}\div,k} + \dot{Q}_{\text{loss}+,k}), (\cdot))$$
$$- C_{\text{upreg}_k} W_k (\alpha_{\div,k} \dot{Q}_{\text{reg}\div,k}, (\cdot))$$
$$- C_{\text{downreg}_k} W_k (\alpha_{+,k} \cdot \dot{Q}_{\text{reg}+,k} (\cdot))]$$
$$\text{s.t.}$$
$$(\dot{\mathbf{Q}}_e, \mathbf{T_e}) \in \varOmega$$
$$\alpha_\div \cdot \dot{Q}_{\text{reg}\div} \leq \dot{Q}_e$$
$$\alpha_+ \cdot \dot{Q}_{\text{reg}+} + \dot{Q}_e \leq \dot{Q}_{\text{max}} \tag{21}$$

where '$(\cdot)$' indicates the remaining parameters from Eq. (1a).

4.4. Simulation

In the following we present simulations similar to the one illustrated in Section 3.3, but with the addition of regulating power and availability payments. The supermarket refrigeration system from Section 3 is used with predictions of electricity prices, regulating power prices and outdoor temperatures. Again the economic MPC controller described in Section 2 is used but with the cost function described in Section 4.3.

4.4.1. Scenario

The same scenario as in Section 3.3.1 is employed with the addition of the availability payment for regulating power from NordPool. As with the hourly el-spot price, the average for each 24-h period over one month was found.

4.4.2. Results

In Fig. 3 the effect of participating in the power balancing market is simulated for a selected scenario of availability payments. In this simulation the outdoor temperature is assumed constant in order to illustrate the effect of availability payments for regulation power versus the electricity spot price as clearly as possible. This simulation reveals an additional saving of up to 70% compared to the case where only the electricity spot price is used for optimization (approximately 30% for up-regulation only).

Therefore, participating in the balancing power market seems to be very beneficial for both the power system and the supermarkets, if we consider the simulation in Fig. 3. At least at the time of the year/day where extra capacity is available and the availability payment is sufficiently high. The availability payments are observed to vary more from day to day than the spot prices, so, the simulation presented in this paper is just for a selected scenario. However a large potential saving has been found, meaning that there is room for deviations from the simulated scenario without ruining the business case of participating with regulating power. Furthermore, it is estimated from the simulations that a supermarket can offer at least 20% of its capacity as regulating power (except on the peak-load days of the year). Currently, the peak demand in Denmark for primary reserves is around 60 MW. With an average supermarket offering about 20% of its capacity, approximately 75% of the total needs for primary reserves could be provided by supermarkets. A single

supermarket is not able to participate with sufficient capacities to place bids on the balancing market, however, an aggregation of e.g. chains of shops would be an obvious solution. With an increasing penetration of intermittent wind energy, the value of regulating reserves is expected to increase [42]. Thus, not only the need for regulating power, but also the incentives to participate in the regulating power market increase.

5. Economic MPC with probabilistic constraints

As already pointed out, the optimal solution to a deterministic optimization problem (e.g. a linear program as in Hovgaard et al. [18]) is not always optimal, nor feasible, in the stochastic case. Therefore we describe means to handle the uncertainties in both forecasts and in the models of the system. We use assumptions of the uncertainty belonging to certain distribution functions and define the confidence level (probability) that the constraints should hold with. The probabilistic constraints are then reformulated as their deterministic counterparts.

First we define the system model in Finite Impulse Response (FIR) form:

$$y_k = b_k + \sum_{i=0}^{k} H_i u_{k-i}, \quad H_i = \begin{cases} D, & \text{for } i = 0 \\ CA^{i-1}B, & \text{for } i > 0 \end{cases} \quad (22)$$

where b_k is a bias term. This form is very handy for formulating the constraints as probability constraints, as we will see in the sequel. This fact comes from the form of the model where the uncertain elements (impulse response coefficients) are multiplied with the decision variable.

The deterministic optimization problem:

$$\min \sum_{k=0}^{N} c_k' u_k \quad (23a)$$

s.t.

$$u_{\min} \leq u_k \leq u_{\max} \quad (23b)$$
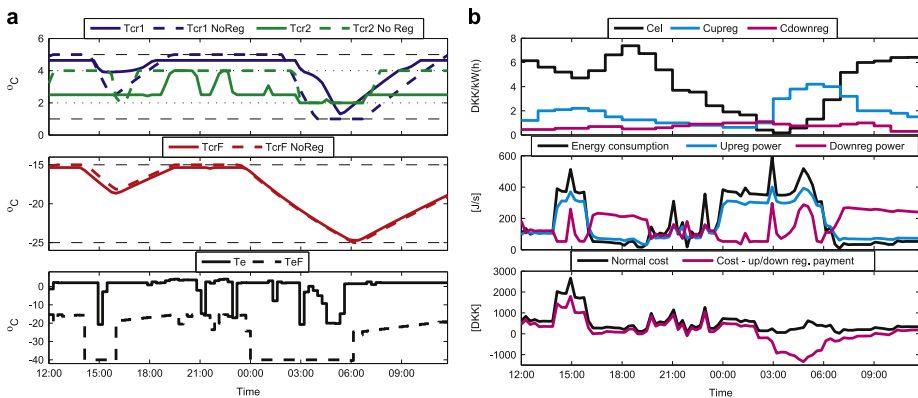
$$y_k \geq r_k \quad (23c)$$

Fig. 3. Simulation showing how the flexible consumption is utilized for offering regulating power to the balancing market. The cold-room temperatures for an optimization utilizing only the electricity spot price over the same period are shown to illustrate the difference. (a) Cold-room and evaporation temperatures. (b) Prices, consumptions and costs.

$$y_k = b_k + \sum_{i=1}^{k} H_i u_{k-i} + \sum_{i=1}^{k} H_{D,i} d_{k-i} \tag{23d}$$

is then reformulated into the stochastic counterpart defined as (boldface variables are uncertain):

$$\min E\left\{ \sum_{k=0}^{N} \mathbf{c}_\mathbf{k}' u_k \right\} \tag{24a}$$

s.t.

$$u_{\min} \le u_k \le u_{\max} \tag{24b}$$

$$\text{Prob}\{\mathbf{y_k} \ge \mathbf{r_k}\} \ge 1 - \alpha, \ \alpha \in [0;1] \tag{24c}$$

$$\mathbf{y_k} = b_k + \sum_{i=1}^{k} \mathbf{H_i} u_{k-i} + \sum_{i=1}^{k} \mathbf{H_{D,i}} \mathbf{d_{k-i}} \tag{24d}$$

where **r** is a reference trajectory, **d** a disturbance, $1 - \alpha$ the confidence level for the constraint, and:

1) $\mathbf{c_k} \sim N\left(\bar{c}_k, \sigma_c^2\right)$, 2) $\mathbf{r_k} \sim N\left(\bar{r}_k, \sigma_r^2\right)$,

3) $\mathbf{H_i} \sim N\left(\overline{H}_i, \Sigma_H^2\right)$, 4) $\mathbf{H_{D,i}} \sim N\left(\overline{H}_{D,i}, \Sigma_H^2\right)$,

5) $\mathbf{d_k} \sim N\left(\bar{d}_k, \sigma_d^2\right)$ $\tag{25}$

1) and 2) in Eq. (25) are forecast uncertainties, 3) and 4) describe model uncertainties while 5) is uncertainty in the disturbances. The uncertain FIR coefficients in the model can be seen as the result of an estimation and identification process involving measurement noise and experimental uncertainty.

5.1. Forecast uncertainty

The description in 1) is uncertainty in the predicted price, $\mathbf{c_k}$. Since we are minimizing the expected value of the objective function we use the certainty equivalent description and substitute $\bar{c}_k$ with c_k.

The uncertainty described by 2) is related to the predicted reference, $\mathbf{r_k}$. The probability constraint is reformulated as a deterministic constraint:

$$\text{Prob}\{Y \ge \mathbf{R}\} \ge 1 - \alpha \tag{26a}$$

$$\frac{\mathbf{R} - \overline{R}}{\sigma_r} \sim N(0,1) \Rightarrow \Phi(\frac{Y - \overline{R}}{\sigma_r}) \ge 1 - \alpha \tag{26b}$$

$\Phi(x)$ is the cumulative distribution function (CDF) of a zero mean unit variance Gaussian random variable x

$$Y \ge \overline{R} + \sigma_r \Phi^{-1}(1 - \alpha) \tag{27}$$

Therefore, a security margin is added to $\mathbf{r_k}$, resulting in a back-off from the optimal (in the deterministic case) boundary. This strategy is closely related to the affine feedback methods described, e.g. in Oldewurtel et al. [29] and Skaf and Boyd [43].

5.2. Model and disturbance uncertainty

The uncertainty descriptions in 3) and 4) from Eq. (25) are model uncertainties and 5) is uncertainty in the predicted disturbance. These all lead to stochastic programming which is described

in this section. We formulate the system using the FIR description in Eqs. (22)–(25):

$$\mathbf{Y} = [\mathbf{C} \ \ \Gamma] \begin{bmatrix} U_{\text{past}} \\ U \end{bmatrix} + [\mathbf{C_D} \ \ \Gamma_\mathbf{D}] \begin{bmatrix} \mathbf{D_{past}} \\ \mathbf{D} \end{bmatrix} \tag{28}$$

and the optimization problem as:

$$\min_U \phi = E\left\{ \sum_{k=0}^{N-1} \mathbf{c_{u,k}} u_k \right\} \tag{29a}$$

s.t.

$$\mathbf{y_k} = [\mathbf{C_k} \ \ \Gamma_\mathbf{k}] \begin{bmatrix} U_{\text{past}} \\ u_k \end{bmatrix} + [\mathbf{C_{D,k}} \ \ \Gamma_{\mathbf{D,k}}] \begin{bmatrix} \mathbf{D_{past}} \\ \mathbf{d_k} \end{bmatrix} \tag{29b}$$

$$\text{Prob}\{\mathbf{y_k} \ge r_k\} \ge 1 - \alpha, \quad k = 1,2,...,N \tag{29c}$$

where $\mathbf{C_k}$ and $\Gamma_\mathbf{k}$ are rows from the corresponding matrices in Eq. (26) and subscript "past" indicates the previous signals corresponding to the number of coefficients in the FIR model.

$$\begin{bmatrix} \Gamma_{N \times N} & | & C_{N \times (n-1)} \end{bmatrix} =$$

$$\begin{bmatrix} H_1 & 0 & \cdots & \cdots & \cdots & 0 \\ \vdots & \ddots & \ddots & & & \vdots \\ H_n & \ddots & \ddots & \ddots & & \vdots \\ 0 & \ddots & \ddots & \ddots & \ddots & \vdots \\ \vdots & \ddots & \ddots & \ddots & \ddots & 0 \\ 0 & \cdots & 0 & H_n & \cdots & H_1 \end{bmatrix} \begin{bmatrix} H_n & \cdots & \cdots & H_2 \\ 0 & \ddots & & \vdots \\ \vdots & & & \vdots \\ 0 & \cdots & 0 & H_n \\ 0 & \cdots & \cdots & 0 \\ 0 & \cdots & \cdots & 0 \end{bmatrix} \tag{30a}$$

$$U_{\text{past}} = \begin{bmatrix} u_{-(n-1)} \\ \vdots \\ u_{-1} \end{bmatrix}, \quad U = \begin{bmatrix} u_1 \\ \vdots \\ u_N \end{bmatrix} \tag{30b}$$

The statistical properties of the resulting output $\mathbf{y_k}$ can be described as:

$$\mathbf{Y_U} \sim N(\overline{Y}_U, \Sigma_{Y_U}), \quad \mathbf{Y_D} \sim N(\overline{Y}_D, \Sigma_{Y_D}) \tag{31a}$$

$$\mathbf{Y} = \mathbf{Y_U} + \mathbf{Y_D}, \quad \mathbf{Y} \sim N(\overline{Y}_U + \overline{Y}_D, \Sigma_{Y_U} + \Sigma_{Y_D}) \tag{31b}$$

where:

$$\overline{Y}_{U,k} = [\overline{C}_k \ \ \overline{\Gamma}_k] \begin{bmatrix} U_{\text{past}} \\ U \end{bmatrix} \tag{32a}$$

$$\Sigma_{Y_U,k} = [U_{\text{past}} \ \ U] \begin{bmatrix} \Sigma_{C,k} & 0 \\ 0 & \Sigma_{\Gamma,k} \end{bmatrix} \begin{bmatrix} U_{\text{past}} \\ U \end{bmatrix} \tag{32b}$$

The product of the two normally distributed variables coming from the model uncertainties and the uncertain disturbance, respectively, can be described by an approximate normal distribution with the following properties [44]:

$$\overline{Y}_{D,k} \approx [\overline{C}_{D,k} \ \ \overline{\Gamma}_{D,k}] \begin{bmatrix} \overline{D}_{\text{past}} \\ \overline{D} \end{bmatrix} \tag{33a}$$

$$\Sigma_{Y_D,k} \approx [\overline{D}_{\text{past}} \ \ \overline{D}] \begin{bmatrix} \Sigma_{C_D,k} & 0 \\ 0 & \Sigma_{\Gamma_D,k} \end{bmatrix} \begin{bmatrix} \overline{D}_{\text{past}} \\ \overline{D} \end{bmatrix} +$$
$$[\overline{C}_{D,k} \ \ \overline{\Gamma}_{D,k}] \Sigma_D \begin{bmatrix} \overline{C}_{D,k} \\ \overline{\Gamma}_{D,k} \end{bmatrix} \tag{33b}$$

Hence, using that $(\mathbf{y_k} - \bar{y}_k)/\Sigma_{y,k}^{1/2} \sim N(0,1)$, the probabilistic constraint, $\text{Prob}\{\mathbf{y_k} \ge r_k\} \ge 1 - \alpha$ can be reformulated as a deterministic counterpart:

$$\text{Prob}\{\mathbf{y_k} \geq r_k\} \geq 1 - \alpha \tag{34a}$$

$$\text{Prob}\left\{\frac{y_k - \bar{y}_k}{\sqrt{\Sigma_{y,k}}} \geq \frac{r_k - \bar{y}_k}{\sqrt{\Sigma_{y,k}}}\right\} \geq 1 - \alpha \tag{34b}$$

$$\frac{y_k - \bar{y}_k}{\sqrt{\Sigma_{y,k}}} \sim N(0, 1) \tag{34c}$$

$$1 - \Phi\left(\frac{r_k - \bar{y}_k}{\sqrt{\Sigma_{y,k}}}\right) \geq 1 - \alpha \tag{34d}$$

$$\Phi^{-1}(\alpha) \left\| \Sigma_*^{1/2} \begin{bmatrix} *^{\text{past}} \\ * \end{bmatrix} \right\|_2 + \bar{y}_k \geq r_k \tag{34e}$$

where the '*' indicates that the norm is taken of the vector formed by all the quadratic terms described in Eqs. (32a) and (33b). Hence, in a MIMO (multiple-input/multiple-output) case, where $\mathbf{y_k}$ is the sum of two independent outputs, the vector in the norm would simply contain an element from each of the outputs. This is easily realized by the property $\sqrt{a^2 + b^2 + c^2} = \|[a \ \ b \ \ c]_2\|$. The constraint in Eq. (34e) has the form of a second-order cone and the solution to the optimization problem constrained by Eq. (34e) can be computed using SOCP as in Boyd et al. [30] and Lobo et al. [31].

In summary, uncertain model descriptions alone or in combination with uncertain disturbances lead to second-order cone constraints, while an uncertain reference just adds a margin to the boundary. These two cases can of course be easily combined.

5.3. Simple power management scenario

The case study used in this section includes two controllable power generators and one power consumer. The power consumer is a cold room for which we provide a simple model. This case study is identical to the one presented in Hovgaard et al. [18] to illustrate the properties and potential of economic MPC in managing the power production and consumption in a distributed energy system. The novelty in this simulation is the inclusion of a scenario with uncertainties in both models and forecasts and the means to handle such as described in the previous sections. We use the economic MPC implementation with probabilistic constraints formulated as an SOCP to calculate the cost-optimal control in presence of uncertainties with known probability distribution functions.

5.3.1. Controllable power generators

In Edlund et al. [45] simple models for power generators are provided. In this paper we adopt these models:

$$\phi_i = \sum_{k \in \mathcal{T}} c_i' u_{i,k} \tag{35a}$$

$$Y_i(s) = G_i(s)U_i(s), \quad G_i(s) = \frac{1}{(\tau_i s + 1)^3} \tag{35b}$$

$$u_{\min,i} \leq u_{i,k} \leq u_{\max,i} \tag{35c}$$

$$\Delta u_{\min,i} \leq \Delta u_{i,k} \leq \Delta u_{\max,i} \tag{35d}$$

to model two conventional power generators. u_i is the power set-point for the ith generator. Eq. (35a) represents the costs of producing power from a given power generator. Power generator 1 is cheap and slow, $(c_1, \tau_1, u_{\min,1}, u_{\max,1}, \Delta u_{\min,1}, \Delta u_{\max,1}) = (1, 20, 0, 15, -1, 1)$. Power generator 2 is expensive and fast, $(c_2, \tau_2, u_{\min,2}, u_{\max,2}, \Delta u_{\min,2}, \Delta u_{\max,2}) = (2, 10, 0, 15, -3, 3)$. The model in Eq. (31)

describes the closed-loop system with internal controllers and is therefore quite simple without the lower level complexity of the generators. The model structure has been validated against experimental data at DONG Energy, Denmark.

5.3.2. Simple cold room

The energy balance for the cold room is already defined in Eq. (2). T_{cr} is the temperature in the cold room which must be kept within certain bounds, $T_{cr,\min} \leq T_{cr} \leq T_{cr,\max}$. T_e is the evaporation temperature of the refrigerant. This can be controlled by the compressor work and must satisfy $T_{cr} \geq T_e$. T_{amb} is the ambient temperature. The energy consumed by the refrigeration system is work performed by the compressors: $W_C = \eta Q_e$. η is the coefficient of performance. In this work η is assumed to be constant. Consequently

$$W_C(s) = \frac{a - bs}{\tau s + 1} T_e(s) + \frac{\alpha K_d}{\tau s + 1} T_{amb}(s) \tag{36a}$$

$$T_{cr}(s) = \frac{K_u}{\tau s + 1} T_e(s) + \frac{K_d}{\tau s + 1} T_{amb}(s) \tag{36b}$$

The parameters are

$$K_u = \frac{(UA)_{cr-e}}{(UA)_{cr-e} + (UA)_{amb-cr}} \tag{37a}$$

$$K_d = \frac{(UA)_{amb-cr}}{(UA)_{cr-e} + (UA)_{amb-cr}} \tag{37b}$$

$$\tau = \frac{mc_p}{(UA)_{cr-e} + (UA)_{amb-cr}} \tag{37c}$$

$$(\alpha, a, b) = (\eta(UA)_{cr-e}, \alpha(K_u - 1), \alpha \tau) \tag{37d}$$

The constraints are

$$T_{cr,\min} \leq T_{cr} \leq T_{cr,\max} \tag{38a}$$

$$0 \leq T_{cr} - T_e \leq \infty \tag{38b}$$

$$T_{e,\min} \leq T_e \leq T_{e,\max} \tag{38c}$$

Eq. (36) is a simplified, linear description of the energy consumption. It does not capture the real world as well as the cost function described in Eq. (5), however, the resulting dynamics are well suited for illustrating the conceptual case here, since the refrigeration system can be modeled in a form compatible with the economic MPC as a linear program.

5.3.3. Supply and demand

The production by the power generators, $y_{1,k} + y_{2,k}$, must exceed the demand for power by the cooling house and the other consumers

$$y_{1,k} + y_{2,k} \geq y_{3,k} + r_k, \quad k \in \mathcal{T} \tag{39}$$

We model wind farms as instantaneously changing systems and include the effect of their power production in the exogenous net power demand signal, r_k. This is seen in the case study in Fig. 5.

5.3.4. Uncertainty

In our scenario the models of power plants and refrigeration systems are not perfectly known and an uncertain FIR as in Eqs. (22)–(25) is used for the system models. The temperature surrounding the cold room (T_{amb}) is stochastic, as is the reference
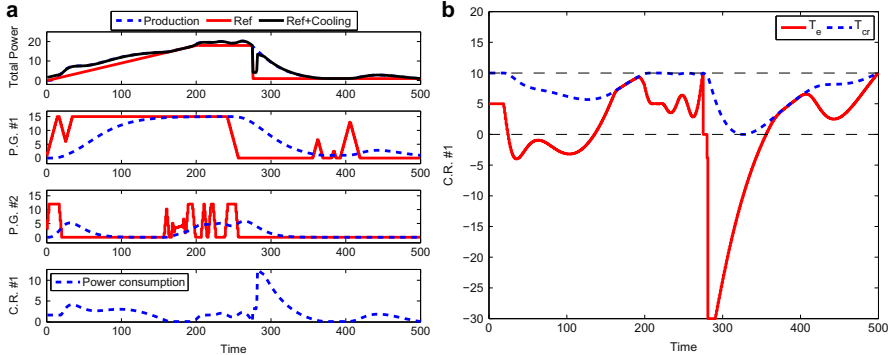
Fig. 4. Simulation of deterministic Power Management scenario. (a) Power productions/consumption. P.G. #1 and #2 show the power productions from the two power plants (dotted blue) and their power set-points (solid red). C.R. #1 is power consumption in the cold room and "Total Power" shows total power production (dotted blue) versus the reference consumption (with (solid black) and without (solid red) the consumption for refrigeration included). (b) Temperature in the cold-room T_{cr} and the control signal for the refrigeration system T_e. $T_{cr,min}$ and $T_{cr,max}$ are shown with dotted black. (For interpretation of the references to color in this figure legend, the reader is referred to the web version of this article.)

(**r**). The latter is caused by the predictions of both non-controllable consumption and non-controllable production being uncertain. We have already seen how the price (c) can be assumed as deterministic without changing the solution.

5.3.5. Results

In Hovgaard et al. [18] we have demonstrated the significant savings gained by including controllable consumers in the setup. A simulation from this study is repeated in Fig. 4. It is seen how the excess power produced after the sudden drop in demand is absorbed by the refrigeration system. Thereby, the temperature is pulled down to the lower limit and energy is stored such that the power demand for refrigeration is lowered afterwards. In this section, we will mainly consider the improved ability to handle

uncertainties without unnecessary high costs or severe violation of constraints. The simulations can be compared to those in Fig. 4.

Using YALMIP [46] we have simulated the scenario. The constraints on the cold-room temperature and on balancing supply and demand are formulated as probability constraints and implemented with SOCP as described previously in this section. A simulation scenario is provided in Fig. 5. The figure shows how the refrigeration system is utilized to balance the power demand such that extra power is used when it is freely available and less is used at other times. This is further elaborated in Hovgaard et al. [18]. But more important for the work presented here are the confidence intervals shown as shaded areas around each of the trajectories. The solid lines are the expected outcomes, while the shaded areas are created by 10,000 simulations with random instances of the noise
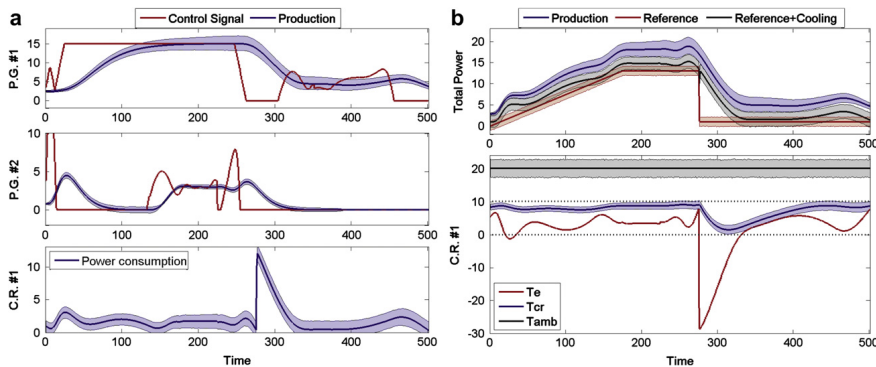
Fig. 5. Simulation of Power Management scenario with uncertainty. $\alpha = 0.5$, $H_i \sim N(\overline{H}_i, 0.0055^2)$, $r_k \sim N(\overline{r}_k, 0.7071^2)$, $T_{amb} \sim N(\overline{T}_{amb}, 1.7321^2)$. The shaded bands show the 95% confidence interval from 10,000 random instances. (a) Power productions/consumption. P.G. #1 and #2 show the power productions from the two power plants (blue) and their power set-points (red). C.R. #1 is power consumption in the cold room. (b) "Total Power" shows total power production (blue) versus the reference consumption (with (black) and without (red) refrigeration). C.R. #1 shows the temperature in the cold-room T_{cr} and the control signal T_e, ($T_{cr,min}$, $T_{cr,max}$) and outdoor temperature, T_{amb}, are shown with dotted and solid black, respectively. (For interpretation of the references to color in this figure legend, the reader is referred to the web version of this article.)

descriptions. The 95% percentile was used both in the SOCP formulation and for plotting the shaded areas. It is easily seen how the amount of back-off from the boundaries is just enough to account for the 95% confidence interval of the uncertainty descriptions for the system. This is particularly clear in Fig. 5(b), where the total production is above the total consumption, T_{cr} stays within the boundaries specified and $T_e \leq T_{cr}$ is satisfied; all with 95% probability. The behavior is similar to what is observed in the deterministic case in Fig. 4, although room is made allowing for the uncertainties.

Regarding the uncertainty of the predictions of outdoor temperature and power demand in a closed-loop scenario, a variance that increases over the prediction horizon could be chosen such that the short-term predictions are more certain than those at the end of the horizon. Furthermore, the disturbances could be measured at each time step, minimizing the uncertainty in the vector of past disturbances to the level related to doing the measurement.

6. Future work

In this paper, we have separated the analysis of the actual potential gained by shifting loads according to outdoor temperatures and prices, and by offering flexible consumption, from the presentation of means to handle uncertainties. The simulations regarding potential savings use realistic data as well as the very realistic, but non-convex, description of energy consumption, whereas we formulate a simplified linear program for the simulations with uncertainty. Future work includes the addition of uncertainty in the more realistic scenarios by reformulating or separating the non-convex cost function, as e.g. in Hovgaard et al. [4], such that it fits into the form of the SOCP formulations that we have presented. Another motivation for simplifying or separating the cost function is to ease the optimization. The very generic optimization tools tested in the simulations shown here are simple to use for prototyping but are not fast enough for real-time implementation in industrial hardware. This fact calls for a simplified optimization problem and/or tailored algorithms.

7. Conclusions

A power management scheme for a supermarket refrigeration system has been presented in this paper. We have described an economic MPC control policy and demonstrated how it can reduce the operational costs of the system. Models, parameters and other quantities used have been verified and are to scale with realistic scenarios in Denmark. For the realistic formulation of energy consumption, we end up with a non-convex cost function. Nevertheless a unique minimum exists within the feasible region of this function. Using a nonlinear MPC solver we illustrated that significant savings of up to 9—32% can be achieved by utilizing thermal storage capacities together with predictions of varying loads and energy prices. With a novel formulation of the cost function we have revealed a potential for using the flexibility in power demand gained to participate in the balancing power market, with remarkable cost reductions of up to 70% as the result.

We have also presented a novel formulation, including uncertainties from both system models and forecasts in the framework of probabilistic constraints. This allows an economic MPC based on linear programming to evolve to a stochastic economic MPC that can be implemented as a convex SOCP. This was demonstrated in a small conceptual case study and our future work will include the fusion of these techniques with the realistic cost function.

The results are especially valuable for proving the potential of the concept and for benchmarking future algorithms that might include computational simplifications and/or implementation of the robustifying means in the economic MPC formulation.

References

[1] Finn P, Fitzpatrick C, Connolly D, Leahy M, Relihan L. Facilitation of renewable electricity using price based appliance control in Irelands electricity market. Energy 2011;36(5). ISSN: 0360-5442:2952—60. doi:10.1016/j.energy.2011.02. 038.

[2] Energinet.dk. Potential and opportunities for flexible electricity consumption with special focus on individual heat pumps (in Danish). Tech. Rep.. Denmark: Energinet.dk, The Danish TSO owned by the Danish Climate and Energy Ministry; 2011. http://www.energinet.dk/SiteCollectionDocuments/Danske% 20dokumenter/El/Potentiale%20og%20muligheder%20for%20fleksibelt% 20elforbrug%20med%20særligt%20fokus%20på%20individuelle% 20varmepumper.pdf.

[3] Larsen LFS, Thybo C, Rasmussen H. Potential energy savings optimizing the daily operation of refrigeration systems. In: Proceedings of European control conference, Kos, Greece; 2007. p. 4759—64.

[4] Hovgaard TG, Larsen LFS, Skovrup MJ, Jørgensen JB. Power consumption in refrigeration systems — modeling for optimization. In: Fourth international symposium on advanced control of industrial processes, 2011; 2011. p. 234—9.

[5] Andersson SL, Elofsson AK, Galus MD, Göransson L, Karlsson S, Johnsson F, et al. Plug-in hybrid electric vehicles as regulating power providers: case studies of Sweden and Germany. Energy Policy 2010;38(6). ISSN: 0301-4215: 2751—62.

[6] Han S, Han S, Sezaki K. Development of an optimal vehicle-to-grid aggregator for frequency regulation. IEEE Transactions on Smart Grid 2010;1(1):65—72. doi:10.1109/TSG.2010.2045163. ISSN 1949-3053.

[7] Saele H, Grande OS. Demand response from household customers: experiences from a pilot study in Norway. IEEE Transactions on Smart Grid 2011; 2(1):90—7. doi:10.1109/TSG.2010.2104165. ISSN 1949-3053.

[8] Molina-Garcia A, Kessler M, Fuentes JA, Gomez-Lazaro E. Probabilistic characterization of thermostatically controlled loads to model the impact of demand response programs. IEEE Transactions on Power Systems 2011;26(1): 241—51. doi:10.1109/TPWRS.2010.2047659. ISSN 0885-8950.

[9] Kirschen DS. Demand-side view of electricity markets. IEEE Transactions on Power Systems 2003;18(2). ISSN: 0885-8950:520—7.

[10] Pina A, Silva C, Ferrao P. The impact of demand side management strategies in the penetration of renewable electricity. Energy 2012;41(1): 128—97.

[11] Qin SJ, Badgwell TA. A survey of industrial model predictive control technology. Control Engineering Practice 2003;11(7):733—64.

[12] Sarabia D, Capraro F, Larsen LFS, de Prada C. Hybrid NMPC of supermarket display cases. Control Engineering Practice 2008;17(4). ISSN: 09670661:428—41.

[13] Edlund K, Bendtsen JD, Jørgensen JB. Hierarchical model-based predictive control of a power plant portfolio. Control Engineering Practice 2011;19: 1126—36.

[14] Blarke MB, Dotzauer E. Intermittency-friendly and high-efficiency cogeneration: operational optimisation of cogeneration with compression heat pump, flue gas heat recovery, and intermediate cold storage. Energy 2011;36(12). ISSN: 0360-5442:6867—78. doi:10.1016/j.energy.2011.10.008.

[15] Rawlings JB, Amrit R. Optimizing process economic performance using model predictive control, nonlinear model predictive control: towards new challenging applications; 2009. p. 119—38.

[16] Diehl M, Amrit R, Rawlings J. A Lyapunov function for economic optimizing model predictive control. IEEE Transactions on Automatic Control 2011;56(3). ISSN: 0018-9286:703—7. doi:10.1109/TAC.2010.2101291.

[17] Angeli D, Amrit R, Rawlings JB. On average performance and stability of economic model predictive control. IEEE Transactions on Automatic Control, in press.

[18] Hovgaard TG, Edlund K, Jørgensen JB. The potential of economic MPC for power management. In: 49th IEEE conference on decision and control, 2010; 2010. p. 7533—8.

[19] Van Harmelen GL. The virtual power station targeting residential, industrial and commercial controllable loads. In: IFAC conference on technology transfer in developing countries — automation in infrastructure creation (DECOM-TT 2000). Proceedings volume from IFAC conference; 2001. p. 45—8.

[20] Bush R, Wolf G. Utilities load shift with thermal storage. Transmission & Distribution World 2009;12. ISSN: 10870849.

[21] Oldewurtel F, Parisio A, Jones CN, Morari M, Gyalistras D, Gwerder M, et al. Energy efficient building climate control using stochastic model predictive control and weather predictions. In: Proceedings of American control conference, 2010; 2010. p. 5100—5.

[22] B. Houska, H. Ferreau, M. Diehl, ACADO toolkit—an open source framework for automatic control and dynamic optimization, Optimal Control Applications and Methods ISSN 1099-1514.

[23] Faria P, Vale Z. Demand response in electrical energy supply: an optimal real time pricing approach. Energy 2011;36(8). ISSN: 0360-5442:5374—84. doi:10. 1016/j.energy.2011.06.049.

[24] Hovgaard TG, Larsen LFS, Jørgensen JB. Robust economic MPC for a power management scenario with uncertainties. In: 50th IEEE conference on decision and control and European control conference;2011. p. 1515—1520.

[25] Bemporad A, Morari M. Robust model predictive control: a survey. Robustness in Identification and Control; 1999:207—26.

[26] Couchman PD, Cannon M, Kouvaritakis B. Stochastic MPC with inequality stability constraints. Automatica 2006;42(12):2169—74.

[27] Lee JH, Cooley BL. Optimal feedback control strategies for state-space systems with stochastic parameters. IEEE Transactions on Automatic Control 1998; 43(10):1469.

[28] Van Hessem DH, Scherer CW, Bosgra O. LMI-based closed-loop economic optimization of stochastic process operation under state and input constraints. In: IEEE conference on decision and control, 2001, vol. 5; 2001. p. 4228—33.

[29] Oldewurtel F, Jones CN, Morari M. A tractable approximation of chance constrained stochastic MPC based on affine disturbance feedback. In: 47th IEEE conference on decision and control, 2008; 2008. p. 4731—6.

[30] Boyd S, Crusius C, Hansson A. Control applications of nonlinear convex programming. Journal of Process Control 1998;8(5—6):313—24.

[31] Lobo MS, Vandenberghe L, Boyd S, Lebret H. Applications of second-order cone programming* 1. Linear Algebra and Its Applications 1998;284(1—3):193—228.

[32] Schwarm AT, Nikolaou M. Chance-constrained model predictive control. AIChE Journal 1999;45(8):1743—52.

[33] Li P, Wendt M, Wozny G. A probabilistically constrained model predictive controller. Automatica 2002;38(7):1171—6.

[34] Kassmann DE, Badgwell TA, Hawkins RB. Robust steady-state target calculation for model predictive control. AIChE Journal 2000;46(5):1007—24.

[35] Shin M, Primbs JA. A fast algorithm for stochastic model predictive control with probabilistic constraints. In: American control conference, 2010; 2010. 5489—94.

[36] Carrion M, Philpott A, Conejo A, Arroyo J. A stochastic programming approach to electric energy procurement for large consumers. IEEE Transactions on Power Systems 2007;22(2):744—54. ISSN 0885-8950.

[37] Parvania M, Fotuhi-Firuzabad M. Demand response scheduling by stochastic SCUC. IEEE Transactions on Smart Grid 2010;1(1):89—98. ISSN 1949-3053.

[38] Shayesteh E, Yousefi A, Moghaddam MP. A probabilistic risk-based approach for spinning reserve provision using day-ahead demand response program.

Energy 2010;35(5). ISSN: 0360-5442:1908—15. doi:10.1016/j.energy.2010.01.001.

[39] Partovi F, Nikzad M, Mozafari B, Ranjbar AM. A stochastic security approach to energy and spinning reserve scheduling considering demand response program. Energy 2011;36(5). ISSN: 0360-5442:3130—7. doi:10.1016/j.energy.2011.03.002.

[40] Skovrup M. Thermodynamic and thermophysical properties of refrigerants — software package in borland delphi. Tech. Rep.. Kgs. Lyngby, Denmark: Department of Energy Engineering, Technical University of Denmark; 2000. http://www.ipu.dk/IPU-Teknologiudvikling/Koele—og-energiteknik/Downloads/CoolPack.aspx.

[41] Hovgaard TG, Larsen LFS, Jørgensen JB. Flexible and cost efficient power consumption using economic MPC — a supermarket refrigeration benchmark. In: 50th IEEE conference on decision and control and European control conference;2011. p. 848—854.

[42] Meyn S, Negrete-Pincetic M, Wang G, Kowli A, Shafieepoorfard E. The value of volatile resources in electricity markets. In: 49th IEEE conference on decision and control, 2010; 2010. p. 1029—36.

[43] Skaf J, Boyd SP. Design of affine controllers via convex optimization. IEEE Transactions on Automatic Control 2010;55(11):2476—87. ISSN 0018-9286.

[44] Ware R, Lad F. Approximating the distribution for sums of products of normal variables. Tech. Rep.. New Zealand: Department of Mathematics and Statistics, University of Canterbury; 2010. http://www.math.canterbury.ac.nz/php/research/abstracts/abstract(2003-15).php.

[45] Edlund K, Mølbak T, Bendtsen JD. Simple models for model-based portfolio load balancing controller synthesis. In: IFAC symposium on power plants and power systems control; 2009.

[46] Löfberg J. Modeling and solving uncertain optimization problems in YALMIP. In: IFAC world congress, 2008; 2008.

Optimal Energy Consumption in Refrigeration Systems - Modelling and Non-Convex Optimisation

Optimal Energy Consumption in Refrigeration Systems - Modelling and Non-Convex Optimisation

Tobias Gybel Hovgaard,[1,2,3]* Lars F. S. Larsen,[1,2] Morten J. Skovrup[4]
and John Bagterp Jørgensen[3]

1. Danfoss A/S, Nordborgvej 81, DK-6430 Nordborg, Denmark

2. Vestas Technology R&D, Hedeager 42, DK-8200 Aarhus N, Denmark

3. DTU Informatics, Technical University of Denmark, Richard Petersens Plads, Building 321, DK-2800 Kgs, Lyngby, Denmark

4. IPU Technology Development, Building 403, DK-2800 Kgs, Lyngby, Denmark

Supermarket refrigeration consumes substantial amounts of energy. However, due to the thermal capacity of the refrigerated goods, parts of the cooling capacity delivered can be shifted in time without deteriorating the food quality. In this study, we develop a realistic model for the energy consumption in super market refrigeration systems. This model is used in a Nonlinear Model Predictive Controller (NMPC) to minimise the energy used by operation of a supermarket refrigeration system. The model is non-convex and we develop a computational efficient algorithm tailored to this problem that is somewhat more efficient than general purpose optimisation algorithms for NMPC and still near to optimal. Since the non-convex cost function has multiple extrema, standard methods for optimisation cannot be directly applied. A qualitative analysis of the system's constraints is presented and a unique minimum within the feasible region is identified. Following that finding we propose a tailored minimisation procedure that utilises the nature of the feasible region such that the minimisation can be separated into two linear programs; one for each of the control variables. These subproblems are simple to solve but some iterations might have to be performed in order to comply with the maximum capacity constraint. Finally, a nonlinear solver is used for a small example without separating the optimisation problem, and the results are compared to the outcome of our proposed minimisation procedure for the same conceptual example. The tailored approach is somewhat faster than the general optimisation method and the solutions obtained are almost identical.

Keywords: modelling and simulation, energy efficiency, optimisation, model predictive control, thermodynamics

INTRODUCTION

Supermarket refrigeration and refrigeration systems in general have been modelled for both analysis and control in several previous publications. These are both concerned with the overall system (Larsen, 2005; Larsen et al., 2007a,b; Hovgaard et al., 2010a) and the complex thermodynamics of the individual parts such as evaporators and condensers (Willatzen et al., 1998; Rasmussen and Larsen, 2009). However, the focus in this study is on describing the power consumption of supermarket refrigeration systems in a form that enables us to use optimisation methods like Model Predictive Control (MPC) (see e.g. Maciejowski, 2002; Rawlings and Mayne, 2009) to minimise the total cost of the system. This is not a completely new idea. In Larsen (2005) and Sarabia et al. (2008) MPC is applied to refriger-

ation systems and in Larsen et al. (2007b) optimisation is applied in order to utilise the daily variations to minimise power consumption. However, the models used in such papers tend to be rather simple in their description of, for example, the work done in the compressor in order to make the models fit into standard forms suitable for optimisation and MPC. In the latter only one decision variable is used in the objective function and the power

consumption is modelled by a quadratic approximation. This has not been found accurate enough for more than a conceptual study of the potential gained by shifting the load and furthermore, this formulation is limited to a 1-to-1 (compressor to cold room) system. In Larsen (2005) and Sarabia et al. (2008) the objective is not energy optimisation and the controllers does not manipulate the compressors. Hence, power consumption cannot be reduced directly. In addition, the dependency on the surrounding temperature is left out. Thus, a contribution from the current work is a model with an abstraction level such that sufficient simplicity can be obtained but with significantly improved accuracy with respect to energy consumption. This is obtained by disregarding the complex dynamics inside, for example, the evaporator, assuming that inner control loops are in operation for superheat control, etc., and focusing only on the stored energy content in the system together with the fully accurate description of power consumption. The other major contribution of this study is a new minimisation approach for the specific problem in question that overcomes nonlinearities and non-convexity in the cost function. The optimality of the optimisation scheme we present in this study rests upon the assumption that a unique minimum of the objective function exists within the feasible region. Thus, one has to perform an analysis of the specific problem as we do in Power Consumption Section, for example, by graphical interpretation of the objective function and the constraints. To the best of our knowledge there is no general method for checking for the existence of several minima.

Our motivation for the model described in this study is the desire to utilise economic optimising MPC for refrigeration systems in order to reduce energy costs related to operating the system and to enable the refrigeration system to be a flexible power consumer. Different goals can be achieved by applying, for example, economic MPC strategies for shifting the load of supermarket refrigeration systems. Energy consumption can be minimised by shifting loads to periods with lower outdoor temperatures, equipment can be dimensioned smaller or operated at more efficient levels by reducing peak loads, cost of power can be reduced by utilising varying electricity prices and by participation in Smart Grid and regulating power schemes. All these benefits can reward the system for its flexibility while delivering crucial services to a power grid with increasing amounts of fluctuating, renewable energy sources. Smart Grids are the intelligent electrical infrastructure required to significantly increase the amount of green energy. To obtain more electricity from intermittent energy sources, such as solar and wind, we must not only control the production of electricity but also the consumption of electricity in an efficient, agile and probably proactive manner. In Hovgaard et al. (2010b) we demonstrated the potential of Economic MPC for an example portfolio with two power plants and one large cold room. This study revealed significant possibilities for saving power and for better utilisation of green energy. However, the models used for the cold room were much simplified, and only worked for this conceptual case, revealing the need for improved modelling to simulate realistic scenarios.

Traditionally, MPC is designed using objective functions which penalise deviations from a given set-point. MPC based on optimising economic objectives has only recently emerged as a general methodology with efficient numerical implementations and provable stability properties (Rawlings et al., 2008; Diehl et al., 2010; Edlund et al., 2009; Rawlings and Amrit, 2009). The main purpose of controlling a refrigeration system is usually not to track a certain cold room temperature exactly, but merely to keep it within specified bounds at the lowest possible cost.

Thus, economic MPC is an appealing strategy, and this study presents a suitable objective function which is directly related to the power consumption and which has properties such that it can be optimised in an Economic MPC scheme. Furthermore, a minimisation procedure for minimising the resulting non-convex objective function is proposed.

The remaining parts of this paper are organized as follows. Modelling the Refrigeration System Section models the dynamics of a refrigeration system from an appropriate abstraction level and presents the constraints of the system. Power Consumption Section presents the functions for estimating the power consumption along with linearisation of the nonlinear terms. The constraints are compared to the power consumption and the possibility for minimising the function uniquely is discussed. A procedure for minimisation of the power consumption is suggested in Minimisation Procedure Section. We give conclusions in Conclusion Section.

MODELLING THE REFRIGERATION SYSTEM

A supermarket refrigeration system is most often based on a vapor compression cycle where a refrigerant is circulated in a closed loop consisting of a compressor, an expansion valve and two heat exchangers, an evaporator in the cold storage room and a condenser/gas cooler located in the surroundings. When the refrigerant evaporates, it absorbs heat from the cold reservoir which is rejected to the hot reservoir by condensation. In order to keep the refrigeration cycle flowing with the heat transfers as described here, the evaporation temperature (T_e) has to be lower than the temperature in the cold reservoir (T_{CR}) and the condensation temperature has to be higher than the temperature at the hot reservoir (T_a). By inserting a compressor between the evaporator and the condenser, the pressure, and thereby also the saturation temperature, of the refrigerant is increased such that the necessary temperature differences are achieved. Thus, low-pressure refrigerant (P_e) from the outlet of the evaporator is compressed to a high pressure (P_c) at the inlet to the condenser. The expansion valve at the inlet to the evaporator maintains the pressure difference ($P_c > P_e$). The setup is sketched in Figure 1 with one cold storage room connected to the system. In most supermarket refrigeration systems several cold storage rooms, for example, display cases, are connected to a common compressor rack and condensing unit. Hence, all the individual display cases, which might have to satisfy different demands to temperatures, often see the same evaporation temperature. However, each unit has its own inlet valve for individual temperature control.

The detailed dynamics inside each display case are nonlinear and require several dynamic variables to be modelled for a full description. Furthermore, the inlet valve in many systems can only be on or off, rather than continuously controlled, which leads to switched dynamics. However, from a higher abstraction level considering only the long-term average of the temperature in the stored goods, all these complicated dynamics can be neglected by assuming that inner control loops controlling the inlet valve are already established. This is a reasonable assumption if we consider a typical control strategy for most Danfoss refrigeration systems today, since it relies on precisely such an inner temperature controller which opens and closes the inlet valve according to defined hysteresis boundaries on the temperature in the cold room. A superheat controller measures temperature and pressure at the outlet of the evaporator and makes sure that the liquid–gas front in the evaporator keeps a certain distance to the outlet.
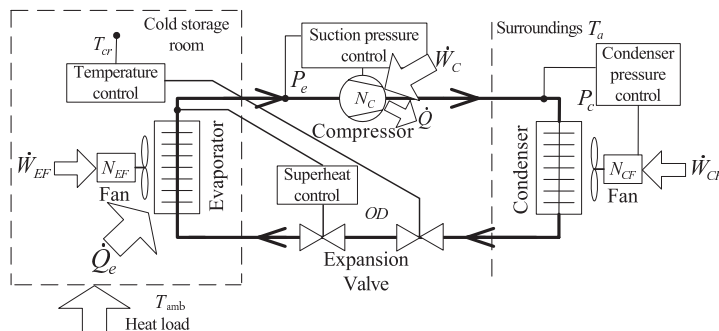
Figure 1. Schematic layout of basic refrigeration system.

The condensing pressure is normally controlled by a fan blowing air across the condenser. According to Jakobsen and Skovrup (2001), the optimal condensing temperature ($T_c^* = T_{sat}(P_c^*)$) can be computed quite accurately as:

$$T_c^* = T_a + \Delta T \tag{1}$$

where ΔT is a constant.

From Figure 1 we note that energy is consumed to drive the compressor rack, the fans at the condensation unit and a fan circulating the air in the cold room through the evaporator. Therefore, total energy consumption is given by:

$$\dot{W} = \dot{W}_C + \dot{W}_{CF} + \dot{W}_{EF} \tag{2}$$

where $\dot{W}$ denotes power consumption and the subscripts indicate the individual components; compressor (C), condenser fan (CF) and evaporator fan (EF). As stated in Larsen et al. (2007b) and also illustrated in Figure 2 the power consumed by the compressor is by far the largest and this will be the scope of further modelling in this work.

The temperature dependence on the condensing pressure is also seen from Figure 2. The figure illustrates the fact that it requires less energy to decrease the condensation pressure when the ambi-

ent temperature is low. Hence, the work done in the compressor can be drastically reduced if the major part of the cooling load can be shifted to colder periods of the day.

Simple Cold Room

In this section, we formulate sufficient dynamics for optimising power consumption in a refrigeration system. It is assumed that the mass of the refrigerated goods acts as a low pass filter with respect to the temperature such that the switching in the inlet valve can be neglected. By doing this, the cooling capacity applied to the cold room ($\dot{Q}_e$) can be considered as a continuous manipulable variable. Additionally, the evaporation temperature (T_e) is considered continuously controllable. In practice a local suction pressure controller acts on the compressors in order to keep T_e as desired. The dynamics of this inner control loop, and those of the temperature control loop at the inlet valve, are much faster than the change of temperature in the goods. Therefore, it is reasonable to assume that if we ask for a certain T_e or $\dot{Q}_e$, then, from the system's point of view, it is achieved (almost) immediately. The controllable inputs are bounded by constraints on, for example, maximum compressor capacity, and these limitations will also be considered. The output of the system is the cold room temperature (T_{cr}) and the purpose of controlling the refrigeration system
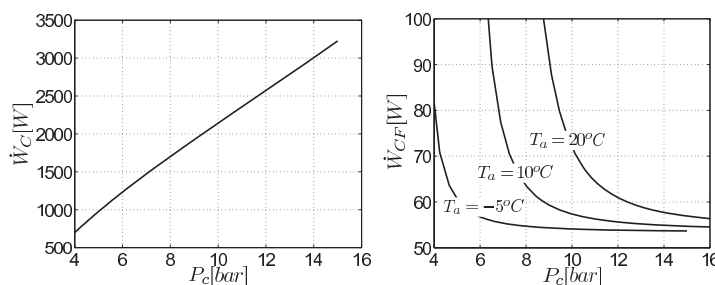

Figure 2. Power consumption in the compressor and the condenser fan at varying condensing pressures. $P_e = 2$ bar and $T_{cr} = 10°C$.

is to keep this temperature within certain bounds and to do so as cheaply as possible with respect to energy consumption and costs.

The temperature in the cold room can be described by a simple energy balance:

$$mc_p \frac{dT_{cr}}{dt} = \dot{Q}_{load} - \dot{Q}_e \tag{3}$$

with

$$\dot{Q}_{load} = (UA)_{amb-cr}(T_{amb} - T_{cr}) \tag{4a}$$

$$\dot{Q}_e = (UA)_{cr-e}(T_{cr} - T_e) \tag{4b}$$

where UA is the heat transfer coefficient and m and c_p are the mass and the overall heat capacity of the refrigerated goods, respectively. T_{amb} is the temperature of the ambient air which puts the heat load on the refrigeration system.

In order to get the equations in the right form for the optimisation algorithms we insert (4a) in (3), while leaving $\dot{Q}_e$ as a direct input.

$$T_{cr}(s) = \frac{K_u}{\tau s + 1}\dot{Q}_e(s) + \frac{K_d}{\tau s + 1}T_{amb}(s) \tag{5}$$

$$K_u = -\frac{1}{(UA)_{amb-cr}}, \quad K_d = 1, \quad \tau = \frac{mc_p}{(UA)_{amb-cr}} \tag{6}$$

The different variables of the system are limited by the following constraints:

$$T_{cr,\,min} \leq T_{cr} \leq T_{cr,\,max} \tag{7a}$$

$$0 \leq T_{cr} - T_e \leq \infty \tag{7b}$$

$$0 \leq \dot{Q}_e \leq (UA)_{cr-e,\,max}(T_{cr} - T_e) \tag{7c}$$

We define the sets Ω and Υ as all $\dot{Q}_e$ and T_e respectively, that satisfy the system dynamics (5) and the constraints given in (7).

Multi-Zone Refrigeration

So far we have only presented a formulation with one cold storage room connected to the system. Most systems, however, contain several cold rooms that vary mutually in size, temperature demands and loads. By expanding $\dot{Q}_e$, T_{cr} and T_{amb} from the models described in the previous section to the vector case where $(T_e, \dot{Q}_{e,i})$, $T_{cr,i}$ and $T_{amb,i}$ are inputs, output and disturbance respectively for the ith cold room, the same equations still hold.

POWER CONSUMPTION

The work done in the compressor is by far the most dominant for the refrigeration system. Therefore, we will focus solely on the energy consumption in the compressor in the rest of this study. This can be expressed by the mass flow of refrigerant (m_{ref}) and the change in energy content of the refrigerant over the compressor. Energy content is described by the enthalpy of the refrigerant at the inlet and at the outlet of the compressor (h_{ic} and h_{oc}, respectively). The power used by the compressor is:

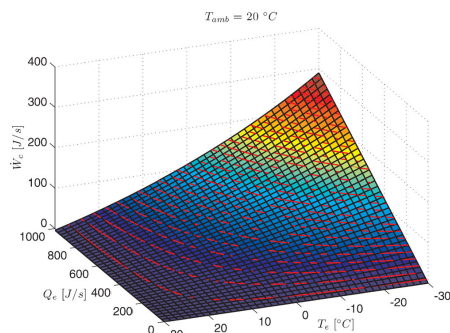$$\dot{W}_c = \frac{m_{ref}(h_{oc}(T_e, P_c) - h_{ic}(T_e))}{\eta_{is}(P_c/P_e)} \tag{8}$$

Figure 3. Power consumption in the compressor for varying $\dot{Q}_e$ and T_e and fixed condensation pressure. Contours for $\dot{W}_c$ are shown in red. Refrigerant R134a is used. [Color figure can be seen in the online version of this article, available at http://onlinelibrary.wiley.com/journal/10.1002/(ISSN)1939-019X]

where the enthalpies depend on the evaporation temperature and the condensing pressure as stated. Actually they also depend on the superheat (ΔT_{SH}) and the heat loss in the compressor. We assume that these parameters are constant. This is a fair assumption for most systems. The isentropic efficiency (η_{is}) is a compressor-dependent function of the ratio P_C/PE. In the normal range of operation it was found that the addition of this function did not change the shape of (8) significantly and it is therefore omitted in the rest of this study. For future improvements and for a wider range of operation isentropic efficiency might need to be considered.

The mass flow can be determined as the ratio between cooling capacity and change of enthalpy over the evaporator:

$$m_{ref} = \frac{\dot{Q}_e}{h_{oe}(T_e) - h_{ie}(P_c)} \tag{9}$$

Furthermore, we note that $h_{oe} = h_{ic}$. All the enthalpies given here are functions of T_e, P_c or both and are nonlinear refrigerant-dependent functions that can be calculated, for example, by the software package 'RefEqns' (Skovrup, 2000). We calculate the surface shown in Figure 3 using the description from (8) to (9) and 'RefEqns' for the enthalpy calculations in a scenario with fixed condensation pressure and with varying $\dot{Q}_e$ and T_e. In the figure, the entire region is shown without paying attention to the constraints from (7).

From the above and Figure 3, it is evident that the power consumption in a vapor compression refrigeration system is not a convex function in the control variables. The bi-linearity in the decision variables $\dot{Q}_e$ and T_e causing this non-convexity is clearly seen in (12) which is a combination of (8)–(11). Furthermore, constraints could be thought of in a way that could cause the system to have several minima. This is a highly unwanted situation in online optimisation systems and special care has to be taken when choosing the optimisation method. The nature of the constraints will be carefully studied in this scope.

Linearised Model

Our purpose of modelling the power consumption is to use the expression in a minimisation framework. Therefore, we simplify

the expression of $\dot{W}_c$ by finding a linear approximation to the function. By using 'RefEqns' for a specific refrigerant, the two enthalpy differences for instance can be expressed as in:

$$h_{oe} - h_{ie} \approx \alpha_1 \times P_c + \beta_1 \qquad (10a)$$

$$h_{oc} - h_{ic} \approx \alpha_{21} \times T_e + \alpha_{22} \times P_c + \beta_2 \qquad (10b)$$

Doing the above linear approximation for the refrigerant R134a yields the following constants:

$$\alpha_1 = -9.51 \times 10^3 \qquad (11a)$$

$$\beta_1 = 219.38 \times 10^3 \qquad (11b)$$

$$\alpha_{21} = -800 \qquad (11c)$$

$$\alpha_{22} = 4.94 \times 10^3 \qquad (11d)$$

$$\beta_2 = -10.10 \times 10^3 \qquad (11e)$$

Figure 4a shows the same surface as seen in Figure 3 but using the linearised expressions for the enthalpy differences instead of the exact values. The linearisation leads to an error which is plotted in Figure 4b. From the surface in Figure 4a it seems that the linearisation has preserved the basic shape and features of the function for work done in the compressor. From the error plot, it is noted that the error is most severe at the extrema of T_e, where it amounts to approximately 10% of the range for $\dot{W}_c$. This could have been improved by making the enthalpy difference over the evaporator (Equation 10a) dependent on T_e. However, since the enthalpy difference over the evaporator appears in the denominator of the function describing the power consumption, it is highly undesirable to make it dependent on one of the control variables.

For the case with multiple cold rooms in the system, (9) has to be replaced by the sum of the mass flows from the individual subsystems (i.e. $\sum_i m_{ref,i}$).

By assuming ideal inner control loops, the model developed in this study avoids considering the complicated nonlinear dynamics in the refrigeration system. In combination with the accurate model of the power used by the compressor, this yields the simplest possible model which is still sufficiently accurate for minimising the energy needed for operation of a refrigeration system.

Figure 5. Illustration of the feasible solution area. The arrows indicate from which side of the lines the area is constrained. [Color figure can be seen in the online version of this article, available at http://onlinelibrary.wiley.com/journal/10.1002/(ISSN)1939-019X]

Constraints

The system is constrained by several factors. A list of constraints in both inputs and outputs of the system was given in (7). In this section these will be related to the surface describing the power consumption in the compressor in order to give a good understanding of the actual set of feasible solutions.

Figure 5 illustrates how the constraints limit the two control variables ($\dot{Q}_e$ and T_e) and a description is given in the following. The upper and lower bounds on the cold room temperature pose limitations on the cooling capacity, $\dot{Q}_e$. For a constant ambient temperature it is seen from (4a) that the heat transfer from the surroundings to the cold room depends on the cold room temperature. Since this heat transfer has to be balanced by a heat transfer to the refrigerant ($\dot{Q}_e$) for the derivative in (3) to be zero, the lower limit of T_{cr} clearly puts an upper limit on $\dot{Q}_e$ and vice versa. The evaporation temperature is limited from above by the actual cold room temperature to assure that the heat flow from cold room to refrigerant in the evaporator is positive. Figure 5 shows $-T_e$ on the x-axis, which is then bounded from below. Actually, the evaporation temperature is also bounded by the condensing temperature
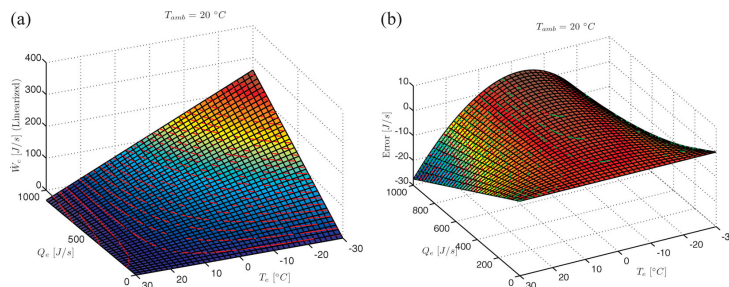

Figure 4. Power consumption in the compressor for the same scenario as in Figure 3 but with linearised enthalpies as given in (10). (a) Power consumption with linearised enthalpies. (b) Errors by linearisation. [Color figure can be seen in the online version of this article, available at http://onlinelibrary.wiley.com/journal/10.1002/(ISSN)1939-019X]

$(T_c \geq T_e)$, however, the limit from T_{cr} is more conservative. The last constraint (7c) limits the cooling capacity (Q_e) as a function of T_e. It is readily seen that this dependence is linearly proportional with $-T_e$.

All the constraints mentioned above are plotted on top of the surface from Figure 4a as an example with fixed P_c and T_{cr} to provide a feeling of the nature of these constraints and of the feasible area. In addition, one of the contours (thin red lines) is highlighted to indicate the effect of a constraint stemming from a limitation of the maximum possible work provided by the compressor.

From Figure 5 it can be observed that the structure of the constraints is such that only one minimum of the power consumption exists in the feasible region. This means that it is possible to minimise the function uniquely even though it is not convex. It is also noted that if the constraint from (7c) had a negative slope, such that it could be tangent to one of the contour curves of the power consumption, then two minima of the function would have existed.

MINIMISATION PROCEDURE

In order to optimise the power consumption over the horizon where parameters such as energy prices and outdoor temperature can be predicted (N time steps), a cost function related to energy costs can be constructed based on the discussion in the previous sections. The entire problem can be described as:

$$\min_{T_e \in \Upsilon, \, \dot{Q}_e \in \Omega} \sum_{k=1}^{N} c_{el,k} \times \dot{Q}_e \times \frac{\alpha_{21} \times T_e + \alpha_{22} \times P_c + \beta_2}{\alpha_1 \times P_c + \beta_1} \qquad (12)$$

where c_{el} is the electricity cost and the rest of the equation comes from the combination of (8) and (9) using the linearisation from (10).

Recalling the shape of the cost function and the constraints from Figure 5, it can be realised that the minimum of (12) can be obtained by fixing T_e to any feasible value while minimising over $\dot{Q}_e$ and subsequently minimising over T_e using the values for Q_e that were found in the first minimisation. This procedure will be described in further details in the following.

We assume that we have available a prediction of the electricity prices and the outdoor temperature that governs the condensing pressure for the next N time steps (the prediction and control horizon). Furthermore, a feasible evaporation temperature can be chosen. The first step is then to solve (13) for $\dot{Q}_e$, where $\dot{Q}_e$ in this case is a vector that contains the cooling capacity for each of the p cold rooms connected to the system for each of the N time steps.

$$\min_{Q_e \in \Omega} \sum_{k=1}^{N} c_{el,k} \times \sum_{i=1}^{p} \dot{Q}_{e_k} \times \frac{\alpha_{21} \times T_e + \alpha_{22} \times P_{c_k} + \beta_2}{\alpha_1 \times P_{c_k} + \beta_1} \qquad (13)$$

Equation (13) can be solved as the linear program (LP)

$$\min_{\dot{Q}_e^* \in \Omega} C^T \dot{Q}_e \qquad (14)$$

where:

$$C^T = [c_{el,1} \Delta h_1 \times 1_p, \ldots, c_{el,N} \Delta h_N \times 1_p]$$
$$p : \text{\# of cold rooms} \qquad (15a)$$
$$1_p : \text{A p-length vector of ones}([1_1, 1_2, \ldots, 1_p])$$

$$\dot{Q}_e = \left[[\dot{Q}_{e_{1,1}}, \dot{Q}_{e_{2,1}}, \ldots, \dot{Q}_{e_{p,1}}], \, [\dot{Q}_{e_{1,2}}, \dot{Q}_{e_{2,2}}, \ldots, \dot{Q}_{e_{p,2}}], \ldots, \right.$$
$$\left. \times \, [\dot{Q}_{e_{1,N}}, \dot{Q}_{e_{2,N}}, \ldots, \dot{Q}_{e_{p,N}}] \right]^T \qquad (15b)$$

$$\Delta h_k = \frac{\alpha_{21} \times T_e + \alpha_{22} \times P_{c_k} + \beta_2}{\alpha_1 \times P_{c_k} + \beta_1} \qquad (15c)$$

The size of C^T is $(1 \times (p \times N))$ and the size of $\dot{Q}_e$ is $((p \times N) \times 1)$. Next, we need to solve the minimisation given in (16) to find the optimal T_e. As before, P_c is a constant vector in time and $\dot{Q}_e^*$ is the optimal cooling capacity found as the solution to (14).

$$\min_{T_e^* \in \Upsilon} \sum_{k=1}^{N} c_{el,k} \times \dot{Q}_{e_k}^* \times \frac{\alpha_{21} \times T_{e_k} + \alpha_{22} \times P_{c_k} + \beta_2}{\alpha_1 \times P_{c_k} + \beta_1} \qquad (16)$$

The fraction can be rewritten such that the expression in (16) yields:

$$\min_{T_e^* \in \Upsilon} \sum_{k=1}^{N} c_{el,k} \times \dot{Q}_{e_k}^* \left(\frac{\alpha_{21}}{\alpha_1 \times P_{c_k} + \beta_1} T_{e_k} + \frac{\alpha_{22} \times P_{c_k} + \beta_2}{\alpha_1 \times P_{c_k} + \beta_1} \right) \qquad (17)$$

The last term is constant with respect to T_e and can be omitted in the optimisation problem. This optimisation problem can be formulated as a LP

$$\min_{T_e^* \in \Upsilon} C^T T_e \qquad (18)$$

where:

$$C^T = [h_1 \times c_{el,1} \times \dot{Q}_{e, \, \text{sum}_1}^*, \ldots, h_N \times c_{el,N} \times \dot{Q}_{e, \, \text{sum}_N}^*] \qquad (19a)$$

$$\dot{Q}_{e, \, \text{sum}} = \begin{bmatrix} [1_p]_1 & 0 & \cdots & 0 \\ 0 & [1_p]_2 & \cdots & 0 \\ \vdots & \vdots & \ddots & \vdots \\ 0 & 0 & \cdots & [1_p]_N \end{bmatrix} \dot{Q}_e^* \qquad (19b)$$

$$T_e = [T_{e_1}, T_{e_2}, \ldots, T_{e_N}] \qquad (19c)$$

$$h_k = \left(\frac{\alpha_{21}}{\alpha_1 \times P_{c_k} + \beta_1} \right) \qquad (19d)$$

The matrix multiplied by $\dot{Q}_{e_k}^*$ in (19b) is $(N \times (N \times p))$. $\dot{Q}_{e, \, \text{sum}}$ and C are both of size $(N \times 1)$.

When optimal values for both $\dot{Q}_e^*$ and T_e^* over the prediction horizon have been computed, it must be checked whether the evaporation temperature violates the constraint on maximum compressor work at any time. If it does, it must be limited to the extremum that can be achieved and the minimisation in (13) must be repeated. This procedure may have to be applied for some iterations before all capacity violations are handled well. Figure 6 shows a simulation result using the models and optimisation procedure presented in this study. For the simulations, the following parameter values have been used: $K_u = 1.111$, $K_D = 1$, $\tau = 111.11$, $T_{cr} \in [0 : 10]$. The control and prediction horizon is $N = 250$ and the sample time is $T_s = 1$.

When formulating the economic MPC, we make use of the turnpike theorems as described by McKenzie (1976) and Rawlings and Amrit (2009). By choosing a sufficiently long control and prediction horizon, N, the turnpike theorems guarantee nominal stability of the closed-loop system. From Figure 6, it is observed
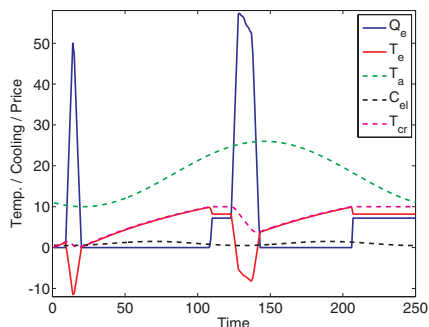
Figure 6. Simulation using economic MPC with the proposed separated optimisation procedure for the presented refrigeration system. [Color figure can be seen in the online version of this article, available at http://onlinelibrary.wiley.com/journal/10.1002/(ISSN)1939-019X]
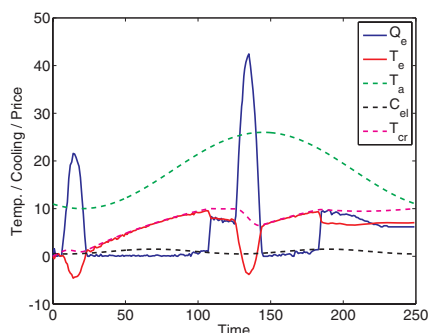

Figure 7. Simulation using economic MPC with nonlinear optimisation tool for the presented refrigeration system. [Color figure can be seen in the online version of this article, available at http://onlinelibrary.wiley.com/journal/10.1002/(ISSN)1939-019X]

how the load is shifted such that the entire temperature range (0–10°C) is utilised in order to benefit from the variations in outdoor temperature and electricity price. Furthermore, the peak around time step 135 has been limited due to a chosen maximum compressor capacity. Six iterations where needed with the given scenario.

Summary: Procedure for Minimising Power Consumption

- Predict condensing temperature/pressure (P_c) and electricity prices (c_{el}).
- Find feasible guess on T_e.
- $\min_{\dot{Q}_e \in \Omega} \sum c_{el} \times \dot{Q}_e \times \frac{\alpha_{21} \times T_e + \alpha_{22} \times P_c + \beta_2}{\alpha_1 \times P_c + \beta_1}$, with fixed P_c, c_{el} and T_e to find $\dot{Q}_e^*$.
- $\min_{T_e \in \Upsilon} \sum c_{el} \times \dot{Q}_e^* \times \frac{\alpha_{21} \times T_e + \alpha_{22} \times P_c + \beta_2}{\alpha_1 \times P_c + \beta_1}$ with fixed P_c, c_{el} and $\dot{Q}_e^*$ from the above minimisation to find T_e^*.
- Check if T_e^* is feasible, otherwise set T_e^* according to the maximum compressor work and repeat the minimisation over $\dot{Q}_e$ with $T_e = T_e^*$ fixed.
- Implement T_e^* and $\dot{Q}_e^*$.

This procedure boils down to solving a series of LPs for which well-established and efficient solvers exist. The method we have chosen for solving the LPs uses condensing (state elimination) and the computational demands scale cubically with the control and prediction horizon, N. Each of the LPs are simple with one dynamical state per cold room. Due to the separation of the problems, only one extra LP has to be solved per iteration for each extra cold room added. If state elimination is not applied, the LP can be solved using Riccati iterations and scales linearly with the control and prediction horizon, N.

Nonlinear Optimisation

In this section, we solve the scenario from Figure 6 using the nonlinear optimisation toolbox ACADO (Houska et al., 2010). The resulting plot is seen in Figure 7.

As illustrated in the figures, our proposed optimisation method yields very similar results when comparing to the solution we got from solving the complete problem in one go with a nonlinear solver. The overall trajectories are very similar but still some dif-

ferences can be noted, especially due to the different nature of the two algorithms. The total cost savings in the two cases amount to approx. 11 % for the separated optimisation and approx. 12% when the entire problem is solved with the nonlinear solver. Thus, we can conclude that our proposed minimisation method only finds a suboptimal solution, though it seems very close to what we can find with other and much more computationally expensive solvers. The advantage of the suboptimal tailored optimisation algorithm over ACADO is that it is much faster and can be implemented on industrial hardware. ACADO used several minutes for solution of the problem while the tailored suboptimal algorithm used less than a second.

Hovgaard et al. (2011, 2012) use the cost function presented in this study together with the nonlinear optimisation tool to simulate realistic scenarios for a three-unit supermarket and real electricity price data. This study showed how the system can gain around 10% in savings by optimisation of its own costs and much more if it is enabled to participate with flexible power consumption for which it is economically rewarded.

CONCLUSION

In this study, we have presented a model of supermarket refrigeration systems with special focus on the power consumption in the compressor which we have formulated in a novel way. The contribution of this model is its ability to work with economic optimising MPC while maintaining a realistic and accurate description of the power consumption. This makes it possible to use the model for power management schemes in which the load on the refrigeration system can be shed in order to minimise the cost of power for operating the system. Furthermore, flexible power consumption is enabled. Difficulties regarding non-convexity of the objective function were described along with a new minimisation procedure that is capable of finding a unique minimum inside the feasible region. This was done by separating the optimisation problem in the two control variables and solving a LP for each of them. Since violation of the constraint of maximum capacity in the compressor can only be checked when both control variables are found there may be a need for iterating between the two subproblems until a feasible solution is found. We have compared the solution from the proposed minimisation

method with a nonlinear optimisation tool using a simple example scenario. The trajectories and costs computed by the two algorithms are very similar. The proposed tailored algorithm is very fast but suboptimal. However, empirical evidence from simulation scenarios suggests that its solution is very close to the optimal solution. For the proposed method to be applicable the problem in question must be analysed in order to ensure the existence of a unique minimum within the feasible region. The model developed in this study can also be used with other optimisation algorithms. Investigation of such algorithms to the model is part of our future work.

REFERENCES

Diehl, M., R. Amrit and J. B. Rawlings, ''A Lyapunov Function for Economic Optimising Model Predictive Control,'' IEEE Trans. Automatic Control **56**(3), 703–707 (2010).

Edlund, K., L. E. Sokoler and J. B. Jørgensen, ''A Primal-Dual Interior-Point Linear Programming Algorithm for MPC,'' In: Joint 48th IEEE Conference on Decision and Control and 28th Chinese Control Conference. IEEE (2009), pp. 351–356.

Houska, B., H. Ferreau and M. Diehl, ''ACADO Toolkit—An Open Source Framework for Automatic Control and Dynamic Optimisation,'' Optimal Control Appl. Methods **32**(3), 298–312 (2010).

Hovgaard, T. G., M. Blanke, H. Niemann and R. Izadi-Zamanbadi, ''Active Sensor Configuration Validation for Refrigeration Systems,'' In: American Control Conference (ACC) (2010a), pp. 3604–3610.

Hovgaard, T. G., K. Edlund and J. B. Jørgensen, ''The Potential of Economic MPC for Power Management,'' In: 49th IEEE Conference on Decision and Control (2010b), pp. 7533–7538.

Hovgaard, T. G., L. F. Larsen, K. Edlund and J. B. Jrgensen, ''Model Predictive Control Technologies for Efficient and Flexible Power Consumption in Refrigeration Systems,'' Energy. Available at: dx.doi.org/10.1016/j.energy.2011.12.007 (2012).

Hovgaard, T. G., L. F. S. Larsen and J. B. Jørgensen, ''Flexible and Cost Efficient Power Consumption Using Economic MPC—A Supermarket Refrigeration Benchmark,'' In: 50th IEEE Conference on Decision and Control and European Control Conference (2011), pp. 848–854.

Jakobsen, A. and M. J. Skovrup, ''Forslag Til Energioptimal Styring af Kondenseringstryk (in Danish),'' Tech. Rep. MEK Tech. Univ. Denmark (2001).

Larsen, L. F. S., ''Model Based Control of Refrigeration Systems,'' Ph.D. Thesis, Aalborg University, Department of Control Engineering (2005).

Larsen, L. F. S., R. Izadi-Zamanabadi and R. Wisniewski, ''Supermarket Refrigeration System—Benchmark for Hybrid System Control,'' Proc. European Control Conference (2007a), pp. 113–120.

Larsen, L. F. S., C. Thybo and H. Rasmussen, ''Potential Energy Savings Optimising the Daily Operation of Refrigeration Systems,'' Proc. European Control Conference, Kos, Greece (2007b), pp. 4759–4764.

Maciejowski, J. M., ''Predictive Control: With Constraints,'' Pearson Educ. (2002).

McKenzie, L., ''Turnpike Theory,'' Econometrica **44**, 841–865 (1976).

Rasmussen, H. and L. F. S. Larsen, ''Nonlinear Superheat and Capacity Control of a Refrigeration Plant,'' 17th Mediterranean Conference on Control and Automation (2009), pp. 1072–1077.

Rawlings, J. and R. Amrit, ''Optimising process economic performance using model predictive control,'' in ''Nonlinear Model Predictive Control. Vol. 384 of Lecture Notes in Control and Information Sciences,'' L. Magni, D. Raimondo and F. Allgower, Eds., Springer, Berlin/Heidelberg (2009), pp. 119–138.

Rawlings, J. B., D. Bonne, J. B. Jørgensen, A. N. Venkat and S. B. Jørgensen, ''Unreachable Setpoints in Model Predictive Control,'' IEEE Trans. Automatic Control **53**(9), 2209–2215 (2008).

Rawlings, J. B. and D. Q. Mayne, ''Model Predictive Control: Theory and Design,'' Nob Hill Publishing, Madison, WI (2009).

Sarabia, D., F. Capraro, L. F. S. Larsen and C. de Prada, ''Hybrid NMPC of Supermarket Display Cases,'' Control Eng. Pract. **17**(4), 428–441 (2008).

Skovrup, M., ''Thermodynamic and Thermophysical Properties of Refrigerants—Software Package in Borland Delphi,'' Tech. Rep. Dep. Energy Eng. Tech. Univ. Denmark (2000).

Willatzen, M., N. Pettit and L. Ploug-Sørensen, ''A General Dynamic Simulation Model for Evaporators and Condensers in Refrigeration. Part I: Moving-Boundary Formulation of Two-Phase Flows with Heat Exchange,'' Int. J. Refrigerat. **21**(5), 398–403 (1998).

P A P E R C

Nonconvex Model Predictive Control for Commercial Refrigeration

Taylor & Francis
Taylor & Francis Group

Nonconvex model predictive control for commercial refrigeration

Tobias Gybel Hovgaard[ab]*, Stephen Boyd[c], Lars F.S. Larsen[a] and John Bagterp Jørgensen[b]

[a]Vestas Technology R&D, DK-8200 Aarhus N, Denmark; [b]DTU Informatics, Technical University of Denmark, DK-2800 Lyngby, Denmark; [c]Information Systems Laboratory, Department of Electrical Engineering, Stanford University, 94305 Stanford, USA

We consider the control of a commercial multi-zone refrigeration system, consisting of several cooling units that share a common compressor, and is used to cool multiple areas or rooms. In each time period we choose cooling capacity to each unit and a common evaporation temperature. The goal is to minimise the total energy cost, using real-time electricity prices, while obeying temperature constraints on the zones. We propose a variation on model predictive control to achieve this goal. When the right variables are used, the dynamics of the system are linear, and the constraints are convex. The cost function, however, is nonconvex due to the temperature dependence of thermodynamic efficiency. To handle this nonconvexity we propose a sequential convex optimisation method, which typically converges in fewer than 5 or so iterations. We employ a fast convex quadratic programming solver to carry out the iterations, which is more than fast enough to run in real time. We demonstrate our method on a realistic model, with a full year simulation and 15-minute time periods, using historical electricity prices and weather data, as well as random variations in thermal load. These simulations show substantial cost savings, on the order of 30%, compared to a standard thermostat-based control system. Perhaps more important, we see that the method exhibits sophisticated response to real-time variations in electricity prices. This demand response is critical to help balance real-time uncertainties in generation capacity associated with large penetration of intermittent renewable energy sources in a future smart grid.

Keywords: energy management; optimisation methods; predictive control; nonlinear control systems; smart grids

1. Introduction

To obtain an increasing amount of electricity from intermittent energy sources such as solar and wind, we must not only control the production of electricity, but also the consumption, in an efficient, flexible and proactive manner. In, e.g. Finn, Fitzpatrick, Connolly, Leahy, and Relihan (2011), facilitation of wind generated electricity by price optimised thermal storage was described. In contrast to the current centralised power generation system, the electricity grid will be a network of many independent power generators. The smart grid will be the future intelligent electricity grid that incorporates all these. The Danish transmission system operator has the following definition of smart grids which we adopt in this work: 'Intelligent electrical systems that can integrate the behaviour and actions of all connected users—those who produce, those who consume and those who do both—to provide a sustainable, economical and reliable electricity supply efficiently' (Energinet.dk 2011). Different means of utilising demand response in a smart grid setting have been investigated in an increasing number of publications, e.g. Andersson et al. (2010), Han, Han, and

Sezaki (2010), Saele and Grande (2011) and Molina-Garcia, Kessler, Fuentes, and Gomez-Lazaro (2011), for plug-in electric vehicles and heat pumps. Kirschen (2003) investigated demand response and price elasticity and Pina, Silva, and Ferrão (2012) analysed different demand side management strategies.

In Denmark around 4500 supermarkets consume more than 550,000 MWh annually. This corresponds roughly to 2% of the entire electricity consumption in the country. Refrigerated goods constitute a large capacity in which energy can be stored in the form of 'coldness'. The thermostat (hysteresis) control policy most commonly used today does not exploit this and a large potential for energy and cost reductions exists. Preliminary investigations have been carried out in Larsen, Thybo, and Rasmussen (2007) and Hovgaard, Edlund, and Jørgensen (2010).

We propose an economic optimising model predictive controller, economic Model Prodictive Control (MPC), to address this for a commercial refrigeration system. Predictive control – also known as receding horizon control – for constrained systems has emerged during the past 30 years as one of the most successful

---

*Corresponding author. Email: togho@vestas.com

methodologies to control industrial processes (Qin and Badgwell 2003) and is increasingly being considered to control both refrigeration and power systems (Sarabia, Capraro, Larsen, and de Prada 2008; Blarke and Dotzauer 2011; Edlund, Bendtsen, and Jørgensen 2011). MPC based on optimising economic objectives has only recently emerged as a general methodology with efficient numerical implementations and provable stability properties (Rawlings and Amrit 2009; Angeli, Amrit, and Rawlings 2012; Diehl, Amrit, and Rawlings 2011) and is now considered for smart grid related problems too (Halvgaard, Poulsen, Madsen, and Jørgensen 2012; Hindi, Greene, and Laventall 2012). We have previously demonstrated the capability of economic MPC in, e.g. Hovgaard et al. (2010), Hovgaard, Larsen, and Jørgensen (2011a) and Hovgaard, Larsen, Edlund, and Jørgensen (2012a) to minimise the total cost of energy for a commercial refrigeration system while enabling it to participate in demand response schemes. Economic MPC has the ability to choose the optimal cooling strategy from predictions of the disturbances such as load, efficiency and price of electricity. This is achieved by utilising the thermal capacity to shift the consumption in time, while keeping the temperatures within certain bounds. We choose these bounds so that they have no consequences for food quality and safety. Van Harmelen (2001), Bush and Wolf (2009) and Oldewurtel et al. (2010) also described the use of load-shifting capabilities to reduce total energy consumption. For other reviews of the use of thermal storage and for the importance of MPC in demand response schemes see, e.g. Camacho, Samad, Garcia-Sanz, and Hiskens (2011) and Arteconi, Hewitt, and Polonara (2012).

An underlying challenge in applying MPC to vapour compression refrigeration systems is that the classical thermodynamics models are quite complex, and include many nonlinearities, such as temperature-dependent efficiencies. One approach, called nonlinear MPC (NMPC), is to accept the optimisation problem to be solved as nonlinear and nonconvex, and use generic nonlinear optimisation methods, such as sequential quadratic programming (SQP) (Boggs and Tolle 1995). This is the approach taken in Hovgaard et al. (2012a), which used ACADO (Houska, Ferreau, and Diehl 2010), a generic nonlinear optimal control code, to solve the optimisation problems. NMPC is widely used in the chemical process industry (see, e.g. Biegler 2009) but in general it requires special attention to ensure (local) convergence, and the computational complexity can be prohibitively high.

Our method differs from NMPC in the following ways. First, our formulation (choice of variables) results in an optimisation problem with linear constraints, but

an objective function that is nonconvex. Instead of a generic SQP (or other) method, we use a sequential convex programming (SCP) method, in which the objective is approximated by a convex function in each iteration; the equality and inequality constraints, which are convex, are preserved, giving us the speed and reliability of solvers for convex optimisation (Boyd and Vandenberghe 2004). Our method, like SQP, involves the solution of a sequence of (convex) quadratic programs (QPs), but differs very much in how the QPs are formed. In SQP, an approximation to the Lagrangian of the problem is used; the linearisation required in each step can end up dominating the computation (Dinh, Savorgnan, and Diehl 2011). In our SCP method, the convexification step needed in each iteration is quite straightforward. Unlike SQP, our method does not exhibit terminal quadratic convergence, but since our method converges in practice in just a handful of iterations, this does not seem to be an issue, at least in this application. We use the tool CVXGEN (Mattingley and Boyd 2012) to generate fast custom solvers for the QPs that arise in our method, achieving solution times measured in milliseconds.

We describe the method in detail, and report careful numerical simulations on a realistic supermarket refrigeration system. For prediction of outdoor temperatures and real-time electricity prices we build models using three years of historical data. With 15-minute sample time and a prediction horizon of 48 steps CVXGEN transforms the original optimisation problem into a standard form QP with 573 variables and 1248 constraints, which can be solved by the custom solver in a couple of milliseconds. This extreme speed allows us to carry out a simulation for a full year with 15-minute increments in around 4 min on a single-core processor. The results are quite interesting. Immediately we see cost savings on the order of 30%. We see that MPC does pre-cooling, i.e. cools to a lower than normal temperature (without leaving the acceptable temperature range) to reduce cooling needed at times with higher electricity prices. By scatter plotting electricity price and energy consumption, we show that our MPC controller exhibits a sophisticated form of demand response to prices, reducing consumption when the prices are high and pre-cooling when prices are low, while maintaining temperatures within the required range.

1.1 Prior work

Leducq, Guilpart, and Trystram (2006) used NMPC with an iterative routine to optimise the coefficient of performance (COP) for a refrigeration plant while maintaining a fixed cooling capacity. Since the focus

was not on load-shifting, a quadratic cost function was used to track the cooling capacity. As the cooling capacity was not a decision variable the problem became convex in the cost function. Still due to the computational burden, the prediction horizon was limited to 3–4 sample periods. Elliott and Rasmussen (2008) controlled a multi-evaporator refrigeration system with MPC that tracked energy efficient set-points. By optimising only over the cooling capacity from each evaporator and using a PI controller based on the most loaded unit for controlling the evaporation temperature, the optimisation problem rendered convex and linear. But this strategy completely disregarded these two variables' interdependency on the system efficiency. As we will see in this study, the multi-variate problem has to be taken into account. A sequential NMPC approach was also used in Sonntag, Devanathan, and Engell (2008) to minimise the compressor switching. Even though computational complexity is not reported directly, the authors state that 'the approach does not yield satisfactory results for larger systems due to the combinatorial growth of the search space'.

Predictive control and optimisation for energy cost reductions in vapour compression cycles have been investigated for building temperature regulation too. Ma, Qin, Salsbury, and Xu (2012) considered time-of-use pricing in that context. The problem was formulated as a linear program (LP) but no specific details were given on how the power consumption was approximated. Oldewurtel et al. (2010), Ma, Kelman, Daly, and Borrelli (2012a) and Ma et al. (2012b) all used weather predictions to optimise the energy efficiency. In the first one, the cost reduced to a linear function while stochastic disturbances were handled by affine disturbance feedback. In the latter two, power consumption was implemented as a 5-D lookup and a move-blocking strategy was used to reduce computational burden. An average computational time of 20 min was reported.

SQP is a well-known method used for NMPC and, e.g. Ma and Borrelli (2012) applied a tailored SQP algorithm to building temperature regulation. However, the energy consumption model was a static function of the load on the air-side and again the control decisions' influence on the COP was lost. 10–13 seconds' computation times on a 3 GHz dual-core processor were reported. In Oldewurtel et al. (2012), the studies from Oldewurtel et al. (2010) were extended and a sequential LP algorithm was used to deal with a bilinear cost. No computational times were reported in this study.

The need for computationally efficient optimisation in MPC applied to systems with either fast sampling or limited computational resources are considered in an increasing number of publications. In Diehl et al. (2002), a direct multiple shooting method was presented, capable of solving an NMPC problem with 42 differential states and 122 algebraic states over 20 control intervals in 10 s and in Wang and Boyd (2010) a quadratic MPC problem with 12 states, 3 controls and a horizon of 30 intervals was solved in 5 ms using warm-starting. Another approach to real-time MPC is the explicit methods as reported in, e.g. Zeilinger, Jones, and Morari (2008), where the technique was used in combination with online optimisation for solving QPs under restrictions on the computational time. Grancharova, Johansen, and Tøndel (2007) gives an extension to explicit NMPC. However, it was reported that it is troublesome to ensure stability if the problem is nonconvex, and in addition, the explicit methods are not suitable for larger problems due to extremely large state spaces. Approaches to parallel implementation of MPC algorithms for real-time execution were shown in, e.g. Jerez, Constantinides, Kerrigan, and Ling (2011), where a problem with 32 states, 16 inputs and 10 control intervals was solved in 344 ms on an FPGA. For further reviews of numerical methods for solution of real-time optimal control problems in NMPC see, e.g. Diehl, Ferreau, and Haverbeke (2009).

Embedded convex optimisation applications have recently become more available to non-experts by the introduction of the automatic code generator CVXGEN (Mattingley and Boyd 2012). Remarkable speed-ups achieved using tailored QP-solvers exported from CVXGEN have been reported in, e.g. Kraning, Wang, Akuiyibo, and Boyd (2011) and Mattingley, Wang, and Boyd (2011). In a recent report (O'Donoghue, Stathopoulos, and Boyd (2012), a splitting technique to a generic linear-convex optimal control problem is introduced and computation times faster than what is obtained by CVXGEN are reported. This suggests that our method could speed up even further.

1.2 Outline

In Section 2, we describe the dynamic models used for the commercial multi-zone refrigeration system. We define variables and constraints and briefly describe the control policy most commonly used in commercial refrigeration today. In Section 3, we establish an MPC controller for the system and give details on the proposed iterative optimisation scheme. We describe the method for obtaining a convex approximate objective function and how to solve this using CVXGEN. We demonstrate the method by simulation of a case study for which we describe the scenario,
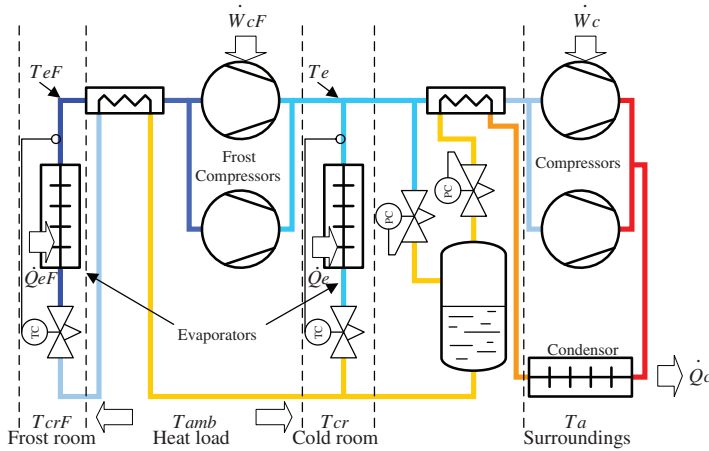
T.G. Hovgaard et al.

Figure 1. Schematic layout of basic refrigeration system.

along with very simple predictors in Section 4. Following this, the results of the numerical examples appear. We simulate the system for a full year and report on computation time, convergence, cost savings and demand response behaviour. In Section 5, we give concluding remarks.

2. Commercial refrigeration

In this section, we describe the dynamic model of a commercial multi-zone refrigeration system. Such systems can include supermarkets, warehouses or air-conditioning. We describe the thermodynamics, the constraints of the system and the function reflecting the economic cost of operating the plant.

2.1 Model

The model describes a system with multiple cold rooms in which a certain temperature for the stored foodstuff has to be maintained. We describe the temperature dynamics and the energy cost of the system using SI units throughout: energy flows and power consumption are in Watts, temperatures are in degrees centigrade, pressures are in Pascal, enthalpies are in Joules/kg and instantaneous electricity prices are in EUR/W. This fixes the units of all quantities used.

The refrigeration system considered utilises a vapour compression cycle in which a refrigerant circulates in a closed loop consisting of a compressor, an expansion valve and two heat exchangers, an evaporator in the cold storage room, as well as a

condenser/gas cooler located in the surroundings. When the refrigerant evaporates, it absorbs heat from the cold reservoir which is rejected to the hot reservoir. To sustain these heat transfers, the evaporation temperature $T_e(t)$ (given by the pressure $P_e(t)$) has to be lower than the temperature in the cold reservoir $T_{air}(t)$ and the condensation temperature has to be higher than the temperature at the hot reservoir $T_a(t)$. Low pressure refrigerant, with the pressure $P_e(t)$, from the outlet of the evaporator is compressed in the compressors to a high pressure $P_c(t)$ at the inlet to the condenser to increase the saturation temperature. In these expressions t denotes time. To lighten notation, we will drop the time argument (t) in time-dependent functions in the sequel.

The setup is shown in Figure 1, with one cold storage room and one frost room connected to the system. Usually, several cold storage rooms, e.g. display cases, connect to a common compressor rack and condensing unit. Because of this, the individual display cases see the same evaporation temperature, but each unit has its own inlet valve for individual temperature control.

2.2 Temperature dynamics

We use a first principles model and describe the dynamics in the cold room by simple energy balances. The temperature of the foodstuff is denoted by $T_{food}(t)$ and satisfies the differential equation,

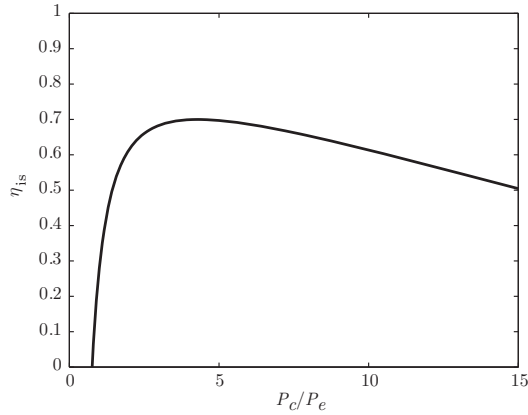$$m_{food}c_{p,food}\frac{dT_{food}}{dt} = \dot{Q}_{food-air}, \tag{1}$$

Figure 2. Isentropic efficiency of the compressor as a function of the pressure ratio P_c/P_e.

where $\dot{Q}_{food-air}(t)$ is the energy flow from the air in the cold room to the foodstuff, m_{food} is the (assumed constant) mass of food and $c_{p,food}$ is the constant specific heat capacity of the food. The temperature of the air in the cold room $T_{air}(t)$ satisfies the differential equation,

$$m_{air}c_{p,air}\frac{dT_{air}}{dt} = \dot{Q}_{load} - \dot{Q}_{food-air} - \dot{Q}_e, \quad (2)$$

where $\dot{Q}_e(t)$ is the applied cooling capacity (energy absorbed in the evaporator), $\dot{Q}_{load}(t)$ is heat load from the surroundings to the air, m_{air} is the constant mass of air and $c_{p,air}$ is the constant specific heat capacity of the air. We describe the heat flows using Newton's law of cooling,

$$\dot{Q}_{food-air} = k_{food-air}(T_{air} - T_{food}),$$

$$\dot{Q}_{load} = k_{amb-cr}(T_{amb} - T_{air}) + \dot{Q}_{dist},$$

$$\dot{Q}_e = k_{evap}(T_{air} - T_e),$$

where k is the constant overall heat transfer coefficient between two media, $T_{amb}(t)$ is the temperature of the ambient air which puts the heat load on the refrigeration system and $\dot{Q}_{dist}(t)$ is a disturbance to the load (e.g. an injection of heat into the cold room).

2.3 Energy cost

The energy used by the compressor, denoted $\dot{W}_c(t)$, dominates the power consumption in the system. It can be expressed by the mass flow of refrigerant $m_{ref}(t)$ and

the change in energy content. We describe energy content by the enthalpy of the refrigerant at the inlet and at the outlet of the compressor ($h_{ic}(t)$ and $h_{oc}(t)$, respectively). These enthalpies are refrigerant-dependent functions of T_e and P_c (or equivalently, outdoor temperature T_a) as denoted in (3). They are computed using, e.g. the software package REFEQNS (Skovrup 2000), which models the thermodynamical properties of different refrigerants. We describe $\dot{W}_c$ as

$$\dot{W}_c = \frac{m_{ref}(h_{oc}(T_e, P_c) - h_{ic}(T_e))}{\eta_{is}(P_c/P_e)(1 - \eta_{heat})}, \quad (3)$$

where the isentropic efficiency $\eta_{is}(t)$ is a function mapping the pressure ratio over the compressor into compression efficiency and η_{heat} is a constant heat loss (in per cent) from the compressor. The mass flow is determined as the ratio between cooling capacity and change of enthalpy over the evaporator ($h_{oe}(t) - h_{ie}(t)$):

$$m_{ref} = \frac{\dot{Q}_e}{h_{oe}(T_e) - h_{ie}(P_c)}.$$

The efficiency function η_{is} can be found in several ways. We used data from first principles thermodynamic calculations to fit a model of the form

$$\eta_{is}(\alpha) = c_1 + c_2\alpha + c_3\alpha^{1.5} + c_4\alpha^3 + c_5\alpha^{-1.5},$$

where $c_1, \ldots, c_5$ are constant parameters. We found this approximation to be accurate within 1%. Figure 2 shows η_{is} versus the pressure ratio $\alpha = P_c/P_e$.

Another compressor sits between the frost evaporator and the suction side of the other compressors, as seen in Figure 1. This compressor decreases the evaporation temperature for the frost part of the

system to a lower level. We can describe the work in the frost compressor by identical equations but the pressure at its outlet is determined by the evaporation temperature for the cooling part. The mass flow through the frost compressor adds to the flow through the cooling compressors. We use the subscript *F* to denote variables related to the frost part.

We describe the instantaneous energy cost of operating the system by multiplying power consumption by the real-time electricity price $p_{el}(t)$. The energy cost C over the period $[T_0, T_{final}]$ is

$$C = \int_{T_0}^{T_{final}} p_{el}(\dot{W}_c + \dot{W}_{cF}) dt. \tag{4}$$

For later reference we express (4) using the coefficients of performance, COP, ($\eta_{COP}(t)$ and $\eta_{COP,F}(t)$ respectively),

$$C = \int_{T_0}^{T_{final}} p_{el}\left(\frac{1}{\eta_{COP}}\dot{Q}_e + \frac{1}{\eta_{COP,F}}\dot{Q}_{eF}\right) dt.$$

$\eta_{COP}(t)$ and $\eta_{COP,F}(t)$ are complicated functions of the outdoor temperature and of the controllable variables $\dot{Q}_e$ and T_e. For any given values of these variables we can, however, compute the coefficients of performance using the steps outlined in Algorithm 1.

Algorithm 1: Calculating the COP for a three-unit system

Require:

1. Initial values: T_e and $\{\dot{Q}_{e,i}\}_{i=1}^{3}$.
2. Prediction of outdoor temperature T_a.

Compute:

1. Pressure in gas cooler P_c.
2. Enthalpy into evaporator h_{ie} as a function of P_c.
3. Enthalpy out from evaporators $h_{oe,i}$ as a function of T_e and $\dot{Q}_{e,i}$.
4. Enthalpy into compressor h_{ic} using mass and energy balances to combine $h_{oe,i}$'s.
5. Enthalpy out of compressor h_{oc} as a function of h_{ic}, T_e, and P_c.
6. η_{is} as a function of T_e and P_c.
7. COP as $\eta_{is}(1 - \eta_{heat})(h_{oei} - h_{ie})/(h_{oc} - h_{ic})$.

2.4 Control

2.4.1 Manipulated variables

Our controller manipulates the cooling capacity in each zone and the evaporation temperatures T_e and

T_{eF}. The latter two are common for the entire refrigeration part and the entire frost part, respectively. In practice, this is achieved by setting the set-points for inner control loops which operate with a high sample rate (compared to our control). This fast local control system allows us to ignore the complex and highly nonlinear behaviour in the gas–liquid mixture in the evaporator.

2.4.2 Measured variables

The controller bases its decisions on measurements of air and food temperatures in each unit, on the known current outdoor temperature and electricity price, and on the predicted future values of the latter two. The heat disturbances are unknown.

2.5 Constraints

We would like the food temperatures to satisfy the inequalities

$$T_{food,min} \leq T_{food} \leq T_{food,max}, \tag{5}$$

where $T_{food,min}$ and $T_{food,max}$ are a given allowable range given for each of the individual units. With randomly occurring load disturbances, it is not possible to guarantee that the temperatures are always in this range. So in lieu of imposing the constraints, we encode (5) as a set of soft constraints, i.e. as a term added to the cost function,

$$V = \int_{T_0}^{T_{final}} \rho_{soft,max}(T_{food} - T_{food,max})_+$$
$$+ \rho_{soft,min}(T_{food,min} - T_{food})_+ dt,$$

where $(a)_+ = \max\{a, 0\}$. This objective term penalises violations of the temperature range constraints. We choose the positive constants $\rho_{soft,max}$ and $\rho_{soft,min}$ so that violations are very infrequent in closed-loop operation. This formulation ensures a feasible problem even in the presence of uncertain loads. In a stochastic formulation, such as the one presented in Hovgaard, Larsen, and Jørgensen (2011b), probabilistic constraints guarantee a feasible problem.

In addition, two constraints that cannot be violated are given by the nature of the system,

$$0 \leq \dot{Q}_e \leq k_{evap,max}(T_{air} - T_e), \tag{6}$$

$$0 \leq \dot{W}_c \leq \dot{W}_{c,max}, \tag{7}$$

where $k_{evap,max}$ is the constant overall heat transfer coefficient from the refrigerant to the air when the evaporator is completely full and $\dot{W}_{c,max}$ is the constant limit on maximum energy consumption in

the compressors. We define the set Ω as all $(\dot{Q}_e, T_e)$ that satisfy the system dynamics (1)–(2) and the constraints (6)–(7).

2.6 Thermostat control

Today, most display cases and cold rooms are controlled by a thermostat. This means that maximum cooling is applied when the cold room temperature reaches an upper limit and shut off when the lower limit is reached. The advantage of this control policy is that it is simple and robust. The disadvantages, however, include: a high operating cost since the controller is completely unaware of system efficiency and electricity prices, no capability of demand response and no specific handling of disturbances. All of these are addressed in our proposed method by intelligently exploiting the thermal capacity in the refrigerated mass.

3. Method

Figure 3 outlines the overall structure of the proposed method and in the following sections we describe the details of the controller.

3.1 Economic MPC controller

The refrigeration system is influenced by a number of disturbances which we can predict (with some uncertainty) over a time horizon into the future. The controller must obey certain constraints, while minimising the cost of operation. Economic MPC addresses all these concerns. Whereas the cost function in MPC traditionally penalises a deviation from a set-point, the proposed economic MPC directly reflects the actual costs of operating the plant. This formulation is tractable for refrigeration systems, where we are interested in keeping the outputs (cold room temperatures) within certain ranges, while minimising the cost of doing so.
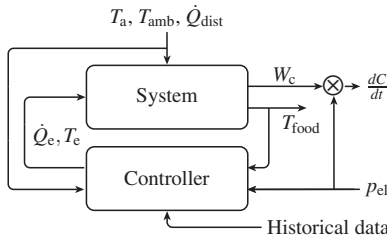

Figure 3. Block diagram of the MPC controller.

Like in traditional MPC, we implement the controller in a receding horizon manner, where an optimisation problem over N time steps (the control and prediction horizon) is solved at each step. The result is an optimal input sequence for the entire horizon, out of which only the first step is implemented. The controller aims at minimising the electricity cost of operation. This cost relates to the energy consumption but we do not aim specifically at minimising this, nor do we focus on tracking certain temperatures in the cold rooms. The optimisation problem is thus formulated as

$$
\begin{aligned}
&\text{minimise } C + V, \\
&\text{subject to } (\dot{\mathbf{Q}}_e, \mathbf{T}_e) \in \Omega, \\
&\qquad T_{\text{food}}^{T_{\text{final}}} = (T_{\text{food, min}} + T_{\text{food, max}})/2,
\end{aligned} \tag{8}
$$

where the variables are $\dot{Q}_e$ and T_e (both functions of time). The feasible set Ω imposes the system dynamics and constraints, and is defined by (1)–(2) and (6)–(7). We add a terminal constraint that the final food temperature $T_{\text{food}}^{T_{\text{final}}}$ must be at the midpoint of the allowable range of temperatures.

Instead of (8) we solve a discretised version with N steps over the time interval $[T_0, T_{\text{final}}]$,

$$
\dot{\mathbf{Q}}_e = \{\dot{Q}_e^k\}_{k=0}^{N-1}, \quad \mathbf{T}_e = \{T_e^k\}_{k=0}^{N-1}. \tag{9}
$$

The MPC feedback law is the first move in (9).

The controller uses the initial state as well as predictions of the real-time electricity cost, the outdoor temperature and the injected heat loads for the time interval. The predictions could come from any source, including national weather service, market or balance responsible parties on the power grid, etc. In this article we use very simple implementations of predictors that we describe in Section 4.4.

3.2 SCP method

The feasible set Ω, the terminal constraint and the cost function term V are all convex. Unfortunately, as C is nonconvex in the controllable variables $\dot{Q}_e$ and T_e, the problem in (8) is not convex.

Instead of using a generic nonlinear optimisation tool, we choose to solve the optimisation problem iteratively using convex programming, replacing the nonconvex cost function C with a convex approximation,

$$
\hat{C}^i = \int_{T_0}^{T_{\text{final}}} p_{\text{el}} \left(\frac{1}{\hat{\eta}_{\text{COP}}^i} \dot{Q}_e + \frac{1}{\hat{\eta}_{\text{COP, F}}^i} \dot{Q}_{eF} \right) dt, \tag{10}
$$

where $\hat{\eta}_{\text{COP}}^i$ and $\hat{\eta}_{\text{COP, F}}^i$ are calculated for the ith iteration as in Algorithm 1 using $\dot{Q}_e^{i-1}$ and T_e^{i-1} found

in the previous iteration. Thus in each iteration we solve a convex optimisation problem, which can be done very reliably and extremely quickly. Our approximation in each step is simple and natural: we use the COP calculated for the last iteration trajectory.

While our proposed method gives no theoretical guarantee on the performance, we must remember that the optimisation problem is nothing but a heuristic for computing a good control and that the quality of closed-loop control with MPC is generally good without solving each problem accurately. Indeed, we have found that very early termination of this SCP method, well before convergence, still yields very good quality closed-loop control.

Algorithm 2 outlines the method. In the algorithm, φ_{prox} and φ_{roc} are regularisation terms which we describe in Section 3.3.

Algorithm 2: Iterative optimisation with nonconvex objective

Initialise
  $\dot{Q}_e^0$, T_e^0, and $i = 1$.
Compute
  $\hat{\eta}_{\text{COP}}^i$ and $\hat{\eta}_{\text{COP,F}}^i$, as functions of $\{\dot{Q}_e, T_e\}^{i-1}$ and T_a.
Solve
  minimise $\hat{C}^i + V + \varphi_{\text{prox}} + \varphi_{\text{roc}}$,
  subject to $(\dot{Q}_e^i, T_e^i) \in \Omega$,
          $T_{\text{food}}^{T_{\text{final}}, i} = (T_{\text{food,min}} + T_{\text{food,max}})/2$,
Update
  $\dot{Q}_e^i$, T_e^i, and $i = i + 1$
Repeat until convergence.

In Hovgaard, Larsen, Skovrup, and Jørgensen (2012c), we concluded that a unique minimum of the power consumption function exists within the feasible region. This assures that an iterative approach will converge to the intended extremum point.

3.3 Regularisation

We use two different types of regularisation in the optimisation problem. To avoid oscillations from iteration to iteration we add proximal regularisation of the form

$$\varphi_{\text{prox}} = \rho_{\text{prox}} \sum_{k=0}^{N-1} \|\dot{Q}_e^k - \dot{Q}_e^{k,\text{prev}}\|_2^2, \tag{11}$$

where the superscript 'prev' indicates that it is the solution from the previous iteration and ρ_{prox} is a constant weight chosen to damp large steps in each iteration. Smaller steps will of course increase the

number of iterations required for the SCP method to converge, but, since we warm-start the algorithm from the solution in the previous time step, the difference is negligible.

Without proximal regularisation oscillatory behaviour can occur due to the nature of the thermodynamics in the refrigeration system: in one iteration of the sequential optimisation, greater amounts of cooling capacity are applied to time steps where the efficiency of the system is high. Doing this causes the mass flow of refrigerant, the pressure difference over the compressor, or both to increase, and thereby lowers the efficiency. If this effect is sufficiently powerful, the COP calculated in the following iteration might be completely different and the optimisation will try to reduce cooling at those time steps and the outcome will differ greatly from the previous. Proximal regularisation eliminates this oscillatory behaviour.

Finally, we add a quadratic penalty on the rate-of-change of $\dot{Q}_e$,

$$\varphi_{\text{roc}} = \rho_{\text{roc}} \sum_{k=1}^{N-1} \|\dot{Q}_e^k - \dot{Q}_e^{k-1}\|_2^2. \tag{12}$$

This regularisation term serves two purposes: it improves the convergence of the sequential programming method, and also discourages rapid changes or switches in compressor levels, which helps reduce wear and tear of the compressor.

Adding (11) and (12) to the linear objective formed by $\hat{C} + V$ results in a QP which we must solve once in each iteration. Due to the special structure of the MPC problem this QP is sparse; see, e.g. Jørgensen, Rawlings, and Jørgensen (2004), Jørgensen (2005) and Wang and Boyd (2010).

3.4 Non-homogeneous sampling

To benefit from the variations in outdoor temperature and electricity prices we want to have an effective prediction horizon of at least 12 h. Since the tail of the control sequence calculated in open loop is typically not identical to the optimal closed-loop sequence, we choose a sufficiently long prediction and control horizon of 24 h.

Speed of computation is a major concern in this work and we want to limit the size of the QPs that we solve in each iteration. A sampling time of 15 min directly gives 96 steps to be computed for the 24-hour prediction horizon. One way of reducing the problem size is non-homogeneous sampling over the prediction horizon, exploiting that accuracy becomes less important towards the end of the open-loop sequence. Hence, we are using a prediction horizon augmented of three sequences with increasing sample time.

4. Case study

By simulation of realistic case studies we have verified the functionality and performance of the proposed MPC controller. In this section, we describe the scenarios used and present the outcomes of the simulations.

4.1 Scenario

Data from supermarkets actually in operation in Denmark have been collected. From these data, typical parameters such as time constants, heat loads, temperature ranges, capacities and normal control policies have been estimated for three very different units; a milk cold room, a vertical shelving display case and a frost storage room. These units differ widely in load, mass of goods and temperature demands. The cooling capacity is controlled individually for each unit and we index these variables as $\{\dot{Q}_{e,i}\}_{i=1}^{3}$. The refrigeration system that we monitored uses CO_2 as refrigerant. CO_2 is getting increasingly popular for supermarket refrigeration since it is non-poisonous and non-flammable and since several governments put restrictions on the usage of conventional HFC refrigerants. We use calculations of the power consumption capable of handling both sub- and super-critical operation of the CO_2 system. Table 1 gives the key parameters for the system. In Hovgaard, Larsen, Skovrup, and Jørgensen (2012b), we demonstrated how to estimate the parameters and design an observer for the food temperatures in the refrigeration system. We convert the system in Section 2.1 to the discrete-time equivalent using these parameters. Since inner control loops are in place we have found that a sampling time of 15 min for the MPC controller is appropriate.

We model a contribution from the uncertain load by a 40% increase in the normal heat load. The increase occurs at random instances in 25% of the 15-minute periods. To account for this, back-offs from the temperature limits are introduced. We adjust these such that violations of the limits occur only 0.5–1% of the time. Less than 0.1° is often sufficient.

The temperature in the frost room (which has the slowest dynamics) increases from $T_{\text{food,min}}$ to $T_{\text{food,max}}$ in approximately 11.5 h if no cooling is applied. This supports the need for a horizon of at least 12 h as mentioned in Section 3.

4.2 Algorithm details

We use a prediction horizon of 24 h, with non-homogeneous sampling. The first 6-hour interval is sampled every 15 min, followed by the second 6-hour interval sampled every 30 min, and the last 12-hour interval is sampled every hour. This gives us a total of 48 values to describe the 24-hour period.

For regularisation of the optimisation problems the best behaviour was observed with parameters in the order of $\rho_{\text{prox}} = 0.08$ and $\rho_{\text{roc}} = 0.06$; however, the method seems to be quite robust to changes in these values. With these values of the regularisation parameters, the SCP method typically converged in 5 or so steps. We found that early termination, after only 2 steps, still resulted in quite good closed-loop control performance.

Recent advances in convex optimisation allow for convex QPs to be solved at millisecond and microsecond time scales. We use CVXGEN (Mattingley and Boyd 2012) to generate a custom embedded solver for ultra-fast computation of each convex QP in the sequential approach. CVXGEN transformed the original optimisation problem into a standard form QP with 573 variables and 1248 constraints. In CVXGEN, we specify and exploit the sparsity of the special problem structure.

4.3 Temperatures and prices

As outdoor temperatures and electricity prices affect the efficiency and the cost, respectively, of operating

Table 1. Key parameters for the refrigeration system used in the case study scenario.

Unit 1: Milk cooler		
$m_{\text{food}}c_{\text{p,food}}$	550.0	kJ/K
$m_{\text{air}}c_{\text{p,air}}$	80.0	kJ/K
$k_{\text{amb}-\text{cr}}$	8.0	W/K
$k_{\text{food}-\text{air}}$	45.0	W/K
$k_{\text{evap,max}}$	135.0	W/K
$T_{\text{food,min}}$	1.0	°C
$T_{\text{food,max}}$	4.0	°C
Unit 2: Vertical display		
$m_{\text{food}}c_{\text{p,food}}$	395	kJ/K
$m_{\text{air}}c_{\text{p,air}}$	100.0	kJ/K
$k_{\text{amb}-\text{cr}}$	11.0	W/K
$k_{\text{food}-\text{air}}$	80.0	W/K
$k_{\text{evap,max}}$	170.0	W/K
$T_{\text{food,min}}$	2.0	°C
$T_{\text{food,max}}$	3.0	°C
Unit 3: Frost room		
$m_{\text{food}}c_{\text{p,food}}$	775	kJ/K
$m_{\text{air}}c_{\text{p,air}}$	50.0	kJ/K
$k_{\text{amb}-\text{cr}}$	2.3	W/K
$k_{\text{food}-\text{air}}$	19.0	W/K
$k_{\text{evap,max}}$	88.0	W/K
$T_{\text{food,min}}$	−22.0	°C
$T_{\text{food,max}}$	−18.0	°C
Common		
T_{amb}	20.0	°C
$T_{\text{e,min}}$	−12.0	°C
$T_{\text{eF,min}}$	−35.0	°C
Compressor heat loss (η_{heat})	15	%

T.G. Hovgaard et al.

the system, they are important factors in the MPC formulation. In our scenario, we use temperature measurements from a meteorological station in the Danish city Sorø sampled every 30 min, along with hourly electricity spot prices downloaded from the Nordic electricity market, Nordpool. We simulate the scenario with data covering an entire calendar year and use three years of data for training the predictors.

4.4 Predictors

A prerequisite to solve the problem in (8) is to have available predictions of the outdoor temperatures and the electricity prices for the chosen prediction horizon. Only past values of such parameters can be available to the controller and in the present work we incorporate predictors that can provide a sufficiently good estimate of the disturbances using a series of past measurements. We use historical data to train these predictors.

In the literature, predictors are suggested for different purposes and with different levels of complexity. In Galanis and Anadranistakis (2002) a Kalman filter approach is taken to correct temperature forecasts and in Leephakpreeda (2012) a grey prediction model is used for outdoor temperatures as well. Mohsenian-Rad and Leon-Garcia (2010) used a correlation-based analysis to find coefficients for a polynomial estimator of real-time electricity prices. In this work, we use predictors that are simple to find from historical data and require extremely little computational effort in the real-time closed-loop implementation. Predictions of both electricity prices and outdoor temperatures are computed in the same manner which we describe here.

We use the historical training data set to construct typical days that describe the mean daily variation for each month in the year. If, e.g. price is sampled every hour we get 24 data points for each one of the 12 months. We compute a smooth baseline covering all 365 days in a year using linear interpolation of two adjacent months.

For the entire historical data set we calculate the residual (difference between baseline and historical data) and compute a residual predictor by solving the convex optimisation problem

$$\text{minimise } \sum_{k=1}^{K} \left\| [R_{k-n}, \ldots, R_k] X - [R_{k+1}, \ldots, R_{k+N}] \right\|_2^2$$
$$+ \lambda \|X\|_1, \tag{13}$$

for X, where K is the number of data points in the training data set, n is the number of past data points used for prediction, N is the number of future data

points that we want to predict, X is the $n+1 \times N$ predictor matrix and R are the residuals. The ℓ_1-regularisation on the predictor, with positive parameter λ, yields a sparse predictor matrix (Boyd and Vandenberghe 2004). By cross-validation with the test data set we choose λ to minimise the validation error.

Now, we can compute the predictions online in each time increment by first predicting the N future residuals from the n past residuals (n past measurements subtracted the baseline) and adding these to the baseline of the corresponding time window.

Algorithm 3 summarises this procedure. After experimenting with the data, we chose to use two days of past data for predicting the outdoor temperature (residual) and seven days for the price prediction. (We use an entire week for the latter since the price pattern is different from weekdays to weekends.)

Algorithm 3: Computing predictors from historical data

Off-line:
1. $D = $ historical data set.
2. Compute typical day for each month by averaging over D.
3. Compute yearly baseline (b) by linear interpolation.
4. Compute residual $R = D - b$.
5. Compute X by (13).

On-line:
1. $R_{past} = $ past measurements $- b$.
2. Predict residual as: $R_{past}^T X$.
3. Compute prediction as: predicted residual $+$ baseline.

For both outdoor temperatures and electricity prices the training sets are defined from 1 January 2007 until 31 December 2009 and the simulation/test set covers the entire year of 2010. Figure 4 shows the mean absolute prediction error for outdoor temperatures and for electricity prices over the prediction horizon. The temperature data cover a range from $-11°C$ to $30°C$ with an average of $6.3°C$, and the price data cover a range from -20 EUR/MWh to 100 EUR/MWh, with an average of 46 EUR/MWh. For the baselines the mean absolute errors are $2.5°C$ and 13.2 EUR/MWh for temperature and price, respectively.

We show an example with baseline, predicted values and real measurements for a randomly chosen point of time in Figure 5. Figure 6 shows histograms for the prediction errors of the outdoor temperatures at 1, 4, 12 and 24 h into the future and Figure 7 gives the same for electricity prices.
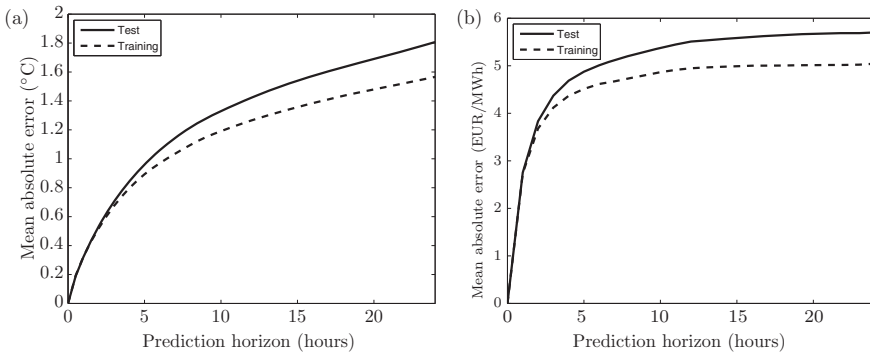
Figure 4. Mean absolute value of prediction errors for (a) outdoor temperature and (b) electricity spot price with training set covering 2007–2009 and test set covering 2010. Prediction horizon is 24 h.
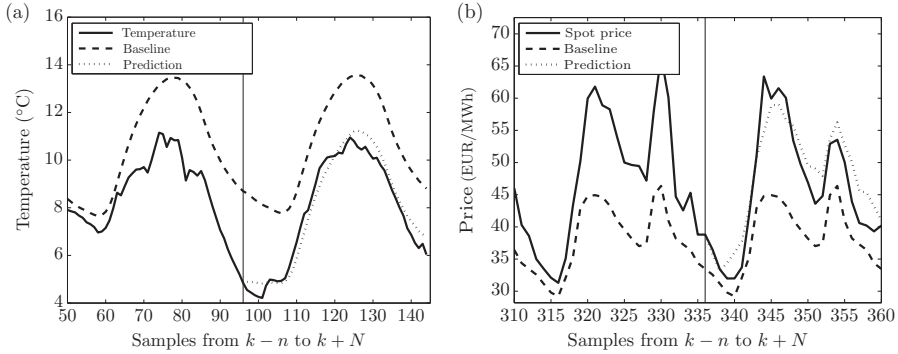
Figure 5. Measurements, baseline and prediction for a randomly chosen point of time, k: (a) outdoor temperature and (b) electricity price. The vertical line indicates k and everything to the left of that point are past measurements used for prediction while the predictions are shown to the right of the line.

For the unknown disturbance in the heat load we use a very simple predictor, namely the expected mean value of the random heat injection.

4.5 Computation times

We have simulated the proposed method with the case study described in the previous sections. The optimisation problems solve in the order of a handful of milliseconds per MPC step which is more than fast enough for real-time implementation. A full year simulates in less than 4 min on a 2.8 GHz Intel Core i7, excluding the time needed outside the optimisation routine for predictors, etc. The same problem with a generic solver such as ACADO takes around 4 min per MPC step on the same processor. For implementation in embedded industrial hardware, a rough estimate of the computation time is around 1000 times of what we have observed here. This is still way below 10 s per time step which certainly allows for real-time implementation.

4.6 Convergence

When cold started the proposed method generally converges in 10–20 iterations. In MPC, however, the open-loop trajectory from the previous run of the optimiser, shifted one time-step, is an excellent guess on the next outcome and is well-suited for warm-starting the algorithm. Using this warm start

Figure 6. Prediction error histograms for outdoor temperature covering 2010: (a) 1 h ahead, (b) 4 h ahead, (c) 12 h ahead and (d) 24 h ahead.

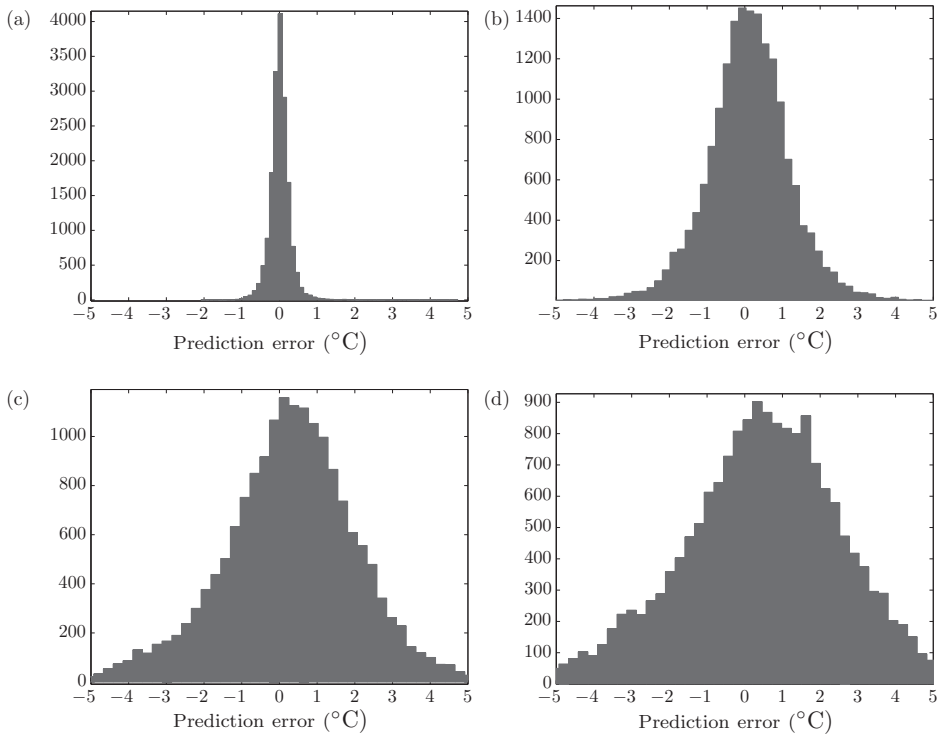initialisation, the method generally converges in less than 5 iterations. In addition, we find that early termination after, e.g. 2–3 iterations, generally gives good results, degrading the overall performance by less than 1%.

4.7 Savings

To benchmark the savings gained by introducing the proposed MPC controller, we have performed a simulation for the same system and conditions but using the conventional thermostat control policy. As in real systems the air temperature surrounding the foodstuff in each unit is the variable used in the thermostat. We have defined upper and lower bounds for switching on and off, such that the interval corresponds to what is normally observed in real operation. Besides, we determine the upper bound such that cooling quality is maintained at a minimal cost,

i.e. such that the food temperatures only violate the upper allowable limit in 0.5–1% of the time (to be comparable with the MPC control). Figure 8 shows a segment of the simulated system with thermostat control versus the proposed MPC controller. We show the trajectory for one unit only and we observe how the food temperature is pulled down by the MPC controller at times with low electricity prices, meaning that pre-cooling is applied. At such times the instantaneous cost of operating the system might be higher than if the conventional thermostat is used, as can be seen in the figure. But this is, however, more than compensated by the savings when the electricity prices go up.

In Figures 9–10, resulting temperature distributions for selected units are shown for both control by thermostat and by MPC. While both control policies tend to keep the temperatures close to the upper limit most of the time, we observe how the MPC controller makes use of the entire range for storing coldness.
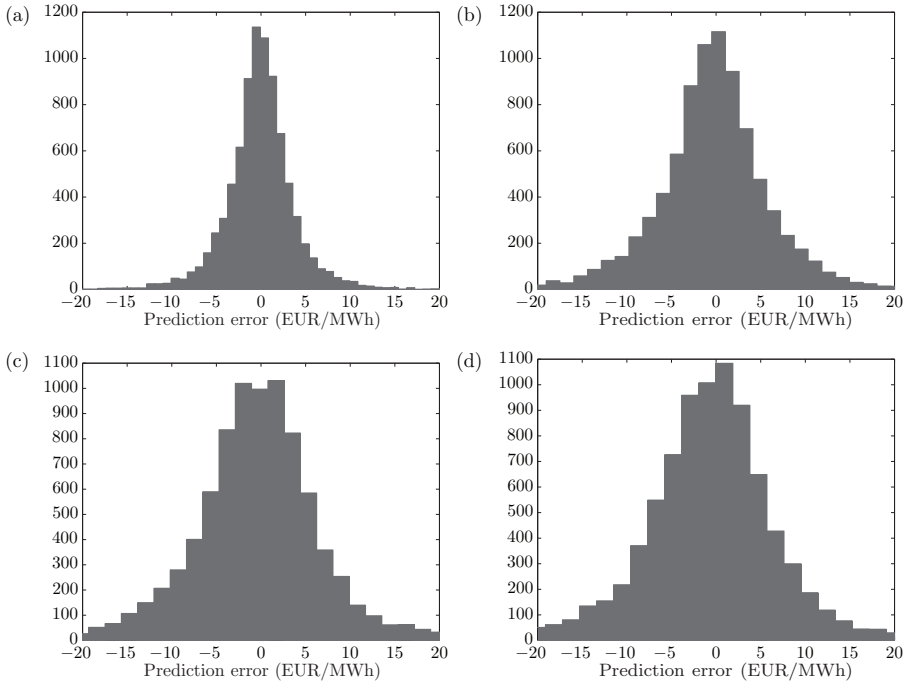
Figure 7. Prediction error histograms for electricity price covering 2010: (a) 1 h ahead, (b) 4 h ahead, (c) 12 h ahead and (d) 24 h ahead.

A unit with larger thermal mass (Figure 9) is utilised to a greater extent than a unit which has less storage capacity (Figure 10).

We observe savings on the order of 40–50% for the simulations covering a full year (2010). However, a part of this comes from the ability to increase the evaporation temperature, and thereby the efficiency, significantly at times where there is almost no cooling demand. In an actual refrigeration system more units are expected and the chance of instances where all of them have an imperceptible cooling demand at the same time decreases. In addition, the most loaded unit might not even be able to participate with flexibility and will thus maintain its cooling demand at all times. A more realistic savings estimate is in the order of 30%.

Adding the uncertain heat load injections and the appropriate back-offs from the temperature limits, as described in Section 4, increases the overall cost by approximately 10%.

Figure 11 compares the cost-per-period distribution for the system controlled by thermostat and by

MPC, respectively. In particular, we observe how a majority of the savings come from avoiding the most expensive instances, e.g. above 0.006 EUR/period, when we use the MPC control policy.

4.8 Demand response

Figure 12 shows the total cooling energy applied to all three units plotted as a function of the electricity price at the time of use. We have selected one month to limit the number of data-points but the picture is almost identical for the entire year of simulation. We observe no correlation between energy consumption and electricity prices when the thermostat controls the refrigeration system while we see a clear tendency to apply more cooling at times with low prices, and vice versa, if we employ the proposed MPC scheme. A linear fit is made using a Huber function regression. The slope is around −50 W/(EUR/MWh) for the MPC controlled system as opposed to 0 for the thermostat which clearly illustrates the demand response behaviour of
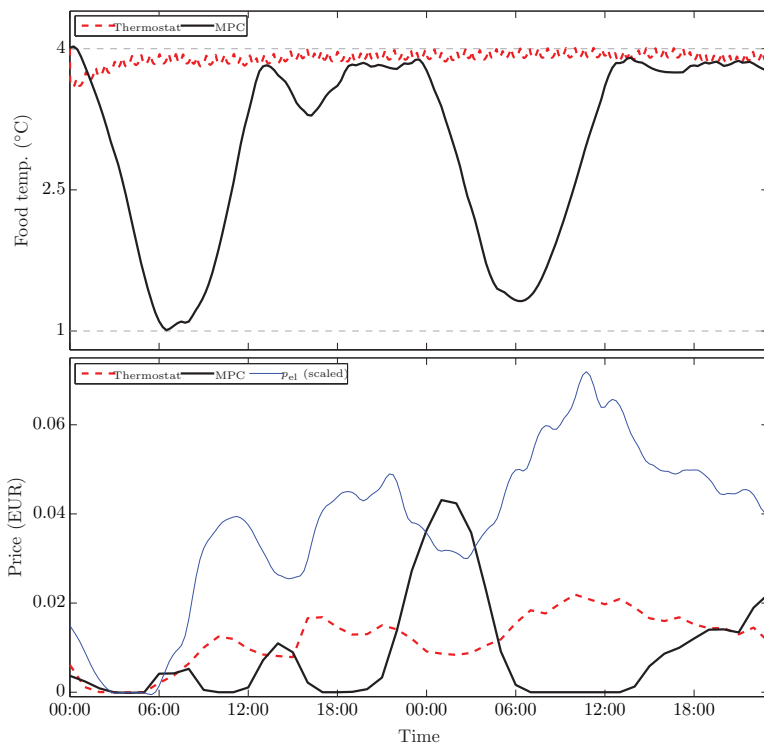
Figure 8. Selected trajectory for food temperature and hourly cost of energy for the refrigeration system controlled by thermostat vs. the proposed MPC controller. In addition, the spot price is plotted for comparison (scaled to fit the range of the other variables).
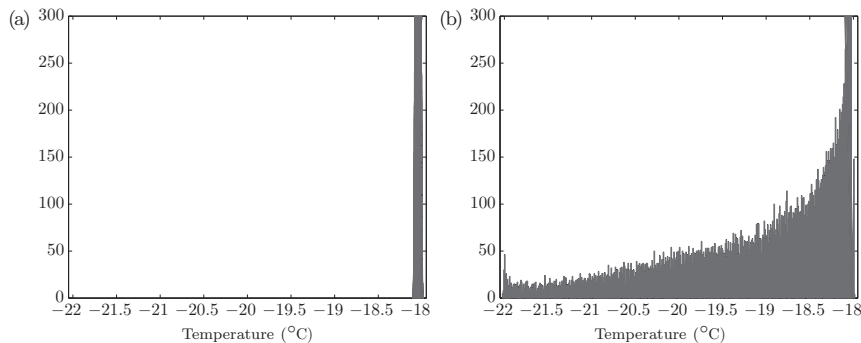
Figure 9. Temperature distribution for selected unit: (a) control by thermostat and (b) control by MPC. Simulation over the full year 2010.
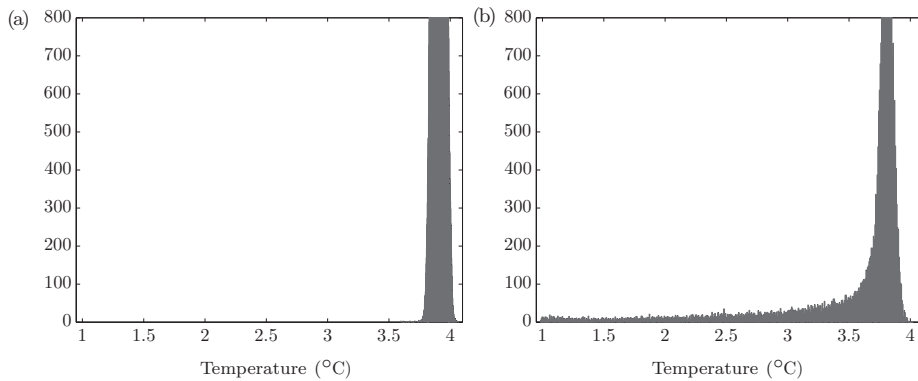
Figure 10. Temperature distribution for selected unit: (a) control by thermostat and (b) control by MPC. Simulation over the full year 2010.
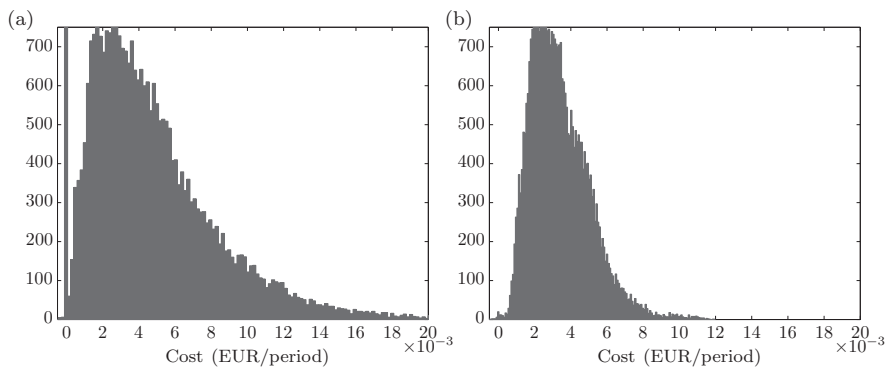
Figure 11. Distribution of cost-per-period: (a) control by thermostat and (b) control by MPC. Simulation over the full year 2010.
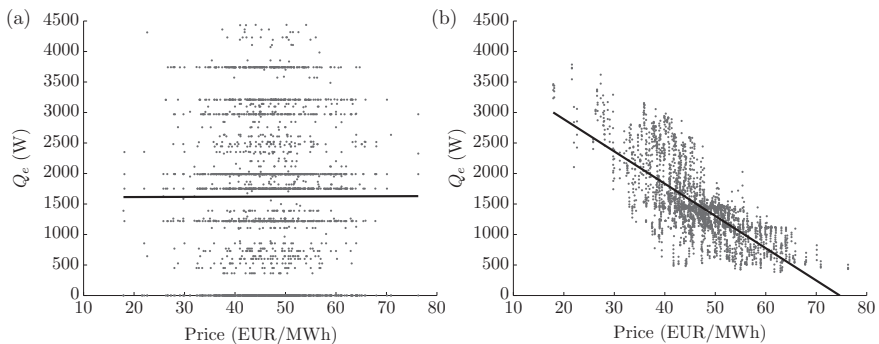
Figure 12. Illustration of demand response in systems controlled by (a) thermostat, the solid line is a linear fit with almost zero slope vs. (b) MPC, the solid line is a linear fit with a slope of $-53\,\mathrm{W}/(\mathrm{EUR}/\mathrm{MWh})$. The data-points are from simulation of July 2010.

the system. We should remember that the spot price used here is just an example and not a prerequisite of our method. In a smart grid the price signal could be artificially made by the balance responsible party to promote demand response.

4.9 Perfect predictions

By again simulating over the full year of 2010, but this time with a prescient setting assuming knowledge of the exact future conditions instead of using their predictions, we are able to compare the performance of the simple predictors and give a rough judgement on how much the method relies on the availability of accurate predictions. We have observed that the extra savings gained by having the full information available are in the order of 1–2%. This justifies the use of simple predictors.

4.10 Plant perturbations

By re-running the simulations using the exact same controller but with reasonable perturbations in the plant parameters we observed that the proposed controller is quite robust. With perturbations of up to at least 20–30% in parameters such as mass of the refrigerated foodstuff and the heat transfer coefficients we see that essentially no changes appear in the closed-loop dynamics and behaviours, like what we reported for the nominal system in Figures 9–12.

5. Conclusion

In this article, we have presented an MPC controller for a commercial multi-zone refrigeration system. We have based our method on convex optimisation, solved iteratively to treat a nonconvex cost function. By employing a fast convex quadratic programming solver to carry out the iterations, the method is more than fast enough to run in real time. Simulation on a realistic scenario reveal significant savings as well as convincing demand response capabilities suitable for implementation with smart grid schemes.

Acknowledgements

References

Andersson, S.L., Elofsson, A.K., Galus, M.D., Göransson, L., Karlsson, S., Johnsson, F., and Andersson, G. (2010), 'Plug-in Hybrid Electric Vehicles as Regulating Power Providers: Case Studies of Sweden and Germany', *Energy Policy*, 38, 2751–2762.

Angeli, D., Amrit, R., and Rawlings, J. (2012), 'On Average Performance and Stability of Economic Model Predictive Control', *IEEE Transactions on Automatic Control*, 57(7), 1615–1626.

Arteconi, A., Hewitt, N.J., and Polonara, F. (2012), 'State of the Art of Thermal Storage for Demand-side Management', *Applied Energy*, 93, 371–389.

Biegler, L. (2009), 'Efficient Nonlinear Programming Algorithms for Chemical Process Control and Operations', in *System Modeling and Optimization*, IFIP Advances in Information and Communication Technology (Vol. 312), eds. A. Korytowski, K. Malanowski, W. Mitkowski, and M. Szymkat, Boston: Springer, pp. 21–35.

Blarke, M.B., and Dotzauer, E. (2011), 'Intermittency-friendly and High-efficiency Cogeneration: Operational Optimisation of Cogeneration with Compression Heat Pump, Flue Gas Heat Recovery, and Intermediate Cold Storage', *Energy*, 36, 6867–6878.

Boggs, P.T., and Tolle, J.W. (1995), 'Sequential Quadratic Programming', *Acta Numerica*, 4, 1–51.

Boyd, S., and Vandenberghe, L. (2004), *Convex Optimization*, Cambridge University Press, New York.

Bush, R., and Wolf, G. (2009), 'Utilities Load Shift with Thermal Storage', *Transmission & Distribution World*, 12.

Camacho, E.F., Samad, T., Garcia-Sanz, M., and Hiskens, I. (2011), 'Control for Renewable Energy and Smart Grids', in *The Impact of Control Technology, Control Systems Society*, eds. T. Samad, and A.M. Annaswamy, IEEE Control Systems Society, pp. 69–88.

Diehl, M., Amrit, R., and Rawlings, J.B. (2011), 'A Lyapunov Function for Economic Optimizing Model Predictive Control', *IEEE Transactions on Automatic Control*, 56, 703–707.

Diehl, M., Bock, H.G., Schlo, J.P., Findeisen, R., Nagy, Z., and Allgöwer, F. (2002), 'Real-time Optimisation and Nonlinear Model Predictive Control of Processes Governed by Differential Algebraic Equations', *Journal of Process Control*, 12, 577–585.

Diehl, M., Ferreau, H., and Haverbeke, N. (2009), 'Efficient Numerical Methods for Nonlinear MPC and Moving Horizon Estimation', in *Nonlinear Model Predictive Control*. Lecture Notes in Control and Information Sciences (Vol. 384), eds. L. Magni, D. Raimondo, and F. Allgöwer, Berlin/Heidelberg: Springer, pp. 391–417.

Dinh, Q.T., Savorgnan, C., and Diehl, M. (2011), 'Real-time Sequential Convex Programming for Nonlinear Model Predictive Control and Application to a Hydro-power Plant', in *Proceedings of the 50th IEEE Conference on Decision and Control and European Control Conference (CDC-ECC)*, pp. 5905–5910.

Edlund, K., Bendtsen, J.D., and Jørgensen, J.B. (2011), 'Hierarchical Model-based Predictive Control of a Power Plant Portfolio', *Control Engineering Practice*, 19, 1126–1136.

Elliott, M.S., and Rasmussen, B.P. (2008), 'Model-based Predictive Control of a Multi-evaporator Vapor Compression Cooling Cycle', in *Proceedings of the American Control Conference*, pp. 1463–1468.

Energinet.dk, (2011), 'Potential and Opportunities for Flexible Electricity Consumption with Special Focus on Individual Heat Pumps (in Danish),' Technical Report, Energinet.dk, The Danish TSO owned by the Danish Climate and Energy Ministry, Denmark.

Finn, P., Fitzpatrick, C., Connolly, D., Leahy, M., and Relihan, L. (2011), 'Facilitation of Renewable Electricity using Price Based Appliance Control in Irelands Electricity Market', *Energy*, 36, 2952–2960.

Galanis, G., and Anadranistakis, M. (2002), 'A One-dimensional Kalman Filter for the Correction of Near Surface Temperature Forecasts', *Meteorological Applications*, 9, 437–441.

Grancharova, A., Johansen, T., and Tøndel, P. (2007), 'Computational Aspects of Approximate Explicit Nonlinear Model Predictive Control', in *Asssessmsnt and Future Directions of Nonlinear Model Predictive Control*, Lecture Notes in Control and Information Sciences (Vol. 358), eds. R. Findeisen, F. Allgöwer, and L. Biegler, Berlin/Heidelberg: Springer, pp. 181–192.

Halvgaard, R., Poulsen, N.K., Madsen, H., and Jørgensen, J.B. (2012), 'Economic Model Predictive Control for Building Climate Control in a Smart Grid', in *2012 IEEE PES Innovative Smart Grid Technologies (ISGT)*, pp. 1–6.

Han, S., Han, S., and Sezaki, K. (2010), 'Development of an Optimal Vehicle-to-grid Aggregator for Frequency Regulation', *IEEE Transactions on Smart Grid*, 1, 65–72.

Hindi, H., Greene, D., and Laventall, C. (2012), 'Coordinating Regulation and Demand Response in Electric Power Grids: Direct and Price-based Tracking using Multirate Economic Model Predictive Control', in *Control and Optimization Methods for Electric Smart Grids*, Power Electronics and Power Systems (Vol. 3), eds. A. Chakrabortty, and M.D. Ilic, US: Springer New York, pp. 111–131.

Houska, B., Ferreau, H., and Diehl, M. (2010), 'ACADO Toolkit–An Open Source Framework for Automatic Control and Dynamic Optimization', *Optimal Control Applications and Methods*, 32(3), 298–312.

Hovgaard, T.G., Edlund, K., and Jørgensen, J.B. (2010), 'The Potential of Economic MPC for Power Management', in *Proceedings of the 49th IEEE Conference on Decision and Control, 2010*, pp. 7533–7538.

Hovgaard, T.G., Larsen, L.F.S., Edlund, K., and Jørgensen, J.B. (2012a), 'Model Predictive Control Technologies for Efficient and Flexible Power Consumption in Refrigeration Systems', *Energy*, 44, 105–116.

Hovgaard, T.G., Larsen, L.F.S., and Jørgensen, J.B. (2011a), 'Flexible and Cost Efficient Power Consumption using Economic MPC – A Supermarket Refrigeration Benchmark', in *Proceedings of the 50th IEEE Conference on Decision and Control and European Control Conference*, pp. 848–854.

Hovgaard, T.G., Larsen, L.F.S., and Jørgensen, J.B. (2011b), 'Robust Economic MPC for a Power Management Scenario with Uncertainties', in *Proceedings of the 50th IEEE Conference on Decision and Control and European Control Conference*, pp. 1515–1520.

Hovgaard, T.G., Larsen, L.F.S., Skovrup, M.J., and Jørgensen, J.B. (2012b), 'Analyzing Control Challenges for Thermal Energy Storage in Foodstuffs', in *Proceedings of the IEEE International Conference on Control Applications (CCA) part of the IEEE Multi-Conference on Systems and Control (MSC)*, pp. 956–961.

Hovgaard, T.G., Larsen, L.F.S., Skovrup, M.J., and Jørgensen, J.B. (2012c), 'Optimal Energy Consumption in Refrigeration Systems – Modelling and Non-convex Optimisation', *The Canadian Journal of Chemical Engineering*, 90(6), 1426–1433.

Jerez, J.L., Constantinides, G.A., Kerrigan, E.C., and Ling, K.V. (2011), 'Parallel MPC for Real-time FPGA-based Implementation', in *Proceedings of the 18th IFAC World Congress*, 1338–1343.

Jørgensen, J.B. (2005), 'Moving Horizon Estimation and Control', Ph.D. thesis, Department of Chemical Engineering, Technical University of Denmark.

Jørgensen, J.B., Rawlings, J.B., and Jørgensen, S.B. (2004), 'Numerical Methods for Large-scale Moving Horizon Estimation and Control', in *Proceedings of the International Symposium on Dynamics and Control Process Systems (DYCOPS)*, 895–900.

Kirschen, D.S. (2003), 'Demand-side View of Electricity Markets', *IEEE Transactions on Power Systems*, 18, 520–527.

Kraning, M., Wang, Y., Akuiyibo, E., and Boyd, S. (2011), 'Operation and Configuration of a Storage Portfolio via Convex Optimization', in *Proceedings of the 18th IFAC World Congress*, , 10487–10492.

Larsen, L.F.S., Thybo, C., and Rasmussen, H. (2007), 'Potential Energy Savings Optimizing the Daily Operation of Refrigeration Systems', in *Proceedings of the European Control Conference*, Kos, Greece, pp. 4759–4764.

Leducq, D., Guilpart, J., and Trystram, G. (2006), 'Nonlinear Predictive Control of a Vapour Compression Cycle', *International Journal of Refrigeration*, 29, 761–772.

Leephakpreeda, T. (2012), 'Implementation of Adaptive Indoor Comfort Temperature Control via Embedded System for Air-conditioning Unit', *Journal of Mechanical Science and Technology*, 26, 259–268.

Ma, J., Qin, J., Salsbury, T., and Xu, P. (2012), 'Demand Reduction in Building Energy Systems Based on Economic Model Predictive Control', *Chemical Engineering Science*, 67, 92–100.

Ma, Y., and Borrelli, F. (2012), 'Fast Stochastic Predictive Control for Building Temperature Regulation', in *Proceedings of the American Control Conference (ACC), 2012*, pp. 3075–3080.

Ma, Y., Borrelli, F., Hencey, B., Coffey, B., Bengea, S., and Haves, P. (2012a), 'Model Predictive Control for the Operation of Building Cooling Systems', *IEEE Transactions on Control Systems Technology*, 20, 796–803.

Ma, Y., Kelman, A., Daly, A., and Borrelli, F. (2012b), 'Predictive Control for Energy Efficient Buildings with Thermal Storage: Modeling, Stimulation, and Experiments', *IEEE Control Systems*, 32, 44–64.

Mattingley, J., and Boyd, S. (2012), 'CVXGEN: A Code Generator for Embedded Convex Optimisation', *Optimization and Engineering*, 13, 1–27.

Mattingley, J., Wang, Y., and Boyd, S. (2011), 'Receding Horizon Control', *IEEE Control Systems Magazine*, 31, 52–65.

Mohsenian-Rad, A.H., and Leon-Garcia, A. (2010), 'Optimal Residential Load Control with Price Prediction in Real-time Electricity Pricing Environments', *IEEE Transactions on Smart Grid*, 1, 120–133.

Molina-Garcia, A., Kessler, M., Fuentes, J.A., and Gomez-Lazaro, E. (2011), 'Probabilistic Characterization of Thermostatically Controlled Loads to Model the Impact of Demand Response Programs', *IEEE Transactions on Power Systems*, 26, 241–251.

O'Donoghue, B., Stathopoulos, G., and Boyd, S. (2012), 'A Splitting Method for Optimal Control, http://www.stanford.edu/˜boyd/papers/oper_splt_ctrl.html

Oldewurtel, F., Parisio, A., Jones, C.N., Gyalistras, D., Gwerder, M., Stauch, V., Lehmann, B., and Morari, M. (2012), 'Use of Model Predictive Control and Weather Forecasts for Energy Efficient Building Climate Control', *Energy and Buildings*, 45, 15–27.

Oldewurtel, F., Parisio, A., Jones, C., Morari, M., Gyalistras, D., Gwerder, M., Stauch, V., Lehmann, B., and Wirth, K. (2010), 'Energy Efficient Building Climate Control using Stochastic Model Predictive Control and Weather Predictions', in *Proceedings of the American Control Conference (ACC)*, pp. 5100–5105.

Pina, A., Silva, C., and Ferrão, P. (2012), 'The Impact of Demand Side Management Strategies in the Penetration of Renewable Electricity', *Energy*, 41, 128–137.

Qin, S.J., and Badgwell, T.A. (2003), 'A Survey of Industrial Model Predictive Control Technology', *Control engineering practice*, 11, 733–764.

Rawlings, J.B., and Amrit, R. (2009), 'Optimizing Process Economic Performance using Model Predictive Control', *Nonlinear Model Predictive Control: Towards New Challenging Applications*, 119–138.

Saele, H., and Grande, O.S. (2011), 'Demand Response from Household Customers: Experiences from a Pilot Study in Norway', *IEEE Transactions on Smart Grid*, 2, 90–97.

Sarabia, D., Capraro, F., Larsen, L.F.S., and de Prada, C. (2008), 'Hybrid NMPC of Supermarket Display Cases', *Control Engineering Practice*, 17, 428–441.

Skovrup, M.J. (2000), 'Thermodynamic and Thermophysical Properties of Refrigerants – Software Package in Borland Delphi', Technical Report, Department of Energy Engineering, Technical University of Denmark, Kgs. Lyngby, Denmark.

Sonntag, C., Devanathan, A., and Engell, S. (2008), 'Hybrid NMPC of a Supermarket Refrigeration System using Sequential Optimization', in *Proceedings of 17th IFAC World Congress*, pp. 13901–13906.

Van Harmelen, G.L. (2001), 'The Virtual Power Station Targeting Residential, Industrial and Commercial Controllable Loads', in *Proceedings of IFAC Conference on Technology Transfer in Developing Countries – Automation in Infrastructure Creation (DECOM-TT 2000)*, pp. 45–48.

Wang, Y., and Boyd, S. (2010), 'Fast Model Predictive Control using Online Optimization', *IEEE Transactions on Control Systems Technology*, 18, 267–278.

Zeilinger, M.N., Jones, C.N., and Morari, M. (2008), 'Real-time Suboptimal Model Predictive Control using a Combination of Explicit MPC and Online Optimisation', in *Proceedings of the 47th IEEE Conference on Decision and Control (CDC)*, pp. 4718–4723.

Model predictive control for wind power gradients

RESEARCH ARTICLE

Model predictive control for wind power gradients

Tobias Gybel Hovgaard[1,3], Stephen Boyd[2] and John Bagterp Jørgensen[3]

[1]Vestas Technology R&D, Denmark. [2]Information Systems Laboratory, Department of Electrical Engineering, Stanford University, USA. [3]DTU Compute, Department of Applied Mathematics and Computer Science, Technical University of Denmark.

ABSTRACT

We consider the operation of a wind turbine and a connected local battery or other electrical storage device, taking into account varying wind speed, with the goal of maximizing the total energy generated while respecting limits on the time derivative (gradient) of power delivered to the grid. We use the turbine inertia as an additional energy storage device, by varying its speed over time, and coordinate the flows of energy to achieve the goal. The control variables are turbine pitch, generator torque, and charge/discharge rates for the storage device, each of which can be varied over given ranges. The system dynamics are quite nonlinear, and the constraints and objectives are not convex functions of the control inputs, so the resulting optimal control problem is difficult to solve globally. In this paper, we show that by a novel change of variables, which focuses on power flows, we can transform the problem to one with linear dynamics and convex constraints. Thus, the problem can be globally solved, using robust, fast solvers tailored for embedded control applications. We implement the optimal control problem in a receding horizon manner and provide extensive closed-loop tests with real wind data and modern wind forecasting methods. The simulation results using real wind data demonstrate the ability to reject the disturbances from fast changes in wind speed, ensuring certain power gradients, with an insignificant loss in energy production. Copyright © 2013 John Wiley & Sons, Ltd.

KEYWORDS

wind power ramps, electrical grid integration, disturbance rejection, model predictive control, convex optimization, wind power control, energy storage, power output optimization

Correspondence

Tobias Gybel Hovgaard, Vestas Technology R&D, Hedeager 42, DK-8200 Aarhus N, Denmark.

E-mail: togho@vestas.com

Received March 22, 2013

1. INTRODUCTION

Today, wind power is the most important renewable energy source. For the years to come, many countries have set goals for further reduction of CO_2 emission, increased utilization of renewable energy, and phase out of fossil fuels. In Denmark one of the means to achieve this is to increase the share of wind power to 50% of electricity consumption by 2020 (in 2012 this number was 30%) and to fully cover the energy supply by renewable energies in general by 2050 [1]. Installing this massive amount of wind turbine capacity introduces several challenges to reliable operation of power systems due to the fluctuating nature of wind power. Thus, modern wind power plants (WPP) are interfaced with power electronic converters that are required and designed to fulfill grid codes (see, *e.g.*[2, 3]).

The Grid Code (GC) is a technical document setting out the rules, responsibilities and procedures governing the operation, maintenance and development of the power system. It is a public document periodically updated with new requirements and it differs from operator to operator. Countries with large amounts of wind power have issued dedicated GCs for its connection to transmission and distribution levels, focused mainly on power controllability, power quality and fault ride-through capability [4, 5]. In general, wind power plants at transmission level shall act as close as possible to conventional power plants, providing a wide range of power output control based on transmission system operator (TSO) instructions. For instance, Denmark, Ireland and Britain establish some of the most demanding requirements regarding active power control [6]. One of the regulation functions required is a power gradient constraint that limits the maximum rate-of-change of non-commanded variations in the power output from the WPP to the grid. The reason for such grid codes

is that if large WPPs are allowed to produce power as the wind blows, other units on the grid must compensate for the power fluctuations. This can lead to very high power prices as well as stand in the way for phasing out the conventional power sources. As of today, this constraint is softened if the power production in the WPP drops due to the lack of wind. This is merely out of necessity and the GCs are expected to tighten further regarding this requirement. Ensuring slow power gradients reduces the risk of instability on the grid, allows the TSO time for counteracting the change, and improves the predictability of power output, enabling the WPP owner to put less conservative bids on the power market. In Europe, the ENTSO-E Network Codes for all types of Generators [7], published in June 2012, aims to establish a coherent set of non-discriminatory requirements applicable to all types of generators.

Energy storage addresses the major problems of wind power and joining energy storage with WPPs to smooth variations and improve the power quality is not a new idea. In, *e.g.*, [8, 9, 10, 11] the benefits, economics, and challenges of using different means of storage, *i.e.*, batteries, hydrogen, flywheels etc., in combination with wind power are investigated. [12] uses a Lithium-iron-phosphate battery to achieve power forecast improvement and output power gradient reduction. However, the additional cost of batteries or other energy storages is usually the showstopper, at least as the market is today. In our previous works, we have shown how thermal capacity, *e.g.*, in supermarket refrigeration, can be utilized for flexible power consumption [13, 14]. It is very likely that such techniques (where the capacity is a bi-product of fulfilling another need) can play a major role instead of adding expensive technologies which have storage as their sole purpose. In the rest of this paper, we consider energy storage in general without distinguishing actual storage from flexible power consumption.

Traditionally, the rotor speed of modern wind turbines is controlled such that it tracks the tip-speed ratio (TSR = angular rotor speed × rotor radius / wind speed) that extracts the maximum amount of power from the wind and is below the maximum allowed rotor speed. However, due to the inertia of the rotating masses in the turbine, there is a potential for improving the quality of the power output by actively letting the rotor speed deviate from the optimal setting. This might of course come at a cost of slightly reduced power output. In, *e.g.*, [15, 16] turbine inertia is used for frequency response and power oscillation damping. In these papers, the goal is to enable the wind turbines to offer ancillary services to the grid, whereas in this paper, we focus on maximizing the power output while observing strict grid codes. In addition, a vast amount of work exists that address power optimization, fatigue load reduction and pitch control for individual turbines in the more traditional sense, *e.g.*, [17, 18, 19, 20, 21]. Some of these take optimization and model predictive control approaches to solve the problems and many rely on a known operating point (*e.g.*, local wind speed and power set-point) for deriving linearized models. Other works consider the control of large wind farms where the power extracted by upwind turbines reduces the power that is available from the wind and increases the turbulence intensity in the wake reaching other turbines (see, *e.g.*, [22, 23, 24, 25, 26]).

The key contributions in this paper are: 1) A convex reformulation of the wind turbine model to a convex problem, 2) a fast solution algorithm for this problem, and 3) demonstration of the application by simulation using real wind speed data. We demonstrate how model predictive control (MPC) using forecasts of the wind speed can ensure very low power gradients (*e.g.*, less than 3% of the rated power per minute) to effectively limit the ramping up or down of power production even when such power ramps would be caused by sudden lack of wind speed. We do this with a central energy storage added to the WPP and show how we can utilize the inertia in the individual turbines to further improve this and minimize the extra storage capacity needed. In [27], we present a sequential convex programming approach to solve the optimal control problem for the same wind turbine problem as in this paper. The main novelties in this paper are the convex reformulation, the fast algorithm, and the demonstrations with real wind data, as mentioned above. During the last 30 years, MPC for constrained systems has emerged as one of the most successful methodologies for control of industrial processes [28, 29, 30]. Traditionally, MPC is designed using objective functions penalizing deviations from a given set-point. MPC based on economic performance functions that directly address minimization of the operational costs is an emerging methodology known as economic optimizing MPC [31, 32, 33, 34, 35]. The potential usefulness of Economic MPC has been demonstrated for a number of smart energy systems in, *e.g.*, [14, 36, 37]. Economic MPC addresses the concerns of controlling a system influenced by a number of disturbances which we can predict (with some uncertainty) over a time horizon into the future, obeying certain constraints, while minimizing the cost (or maximizing the profit) of operation. MPC is applied to wind turbine control in, *e.g.*, [38, 39] and in particular with focus on convex optimization in [40, 41]. [42, 43] consider convex optimization for a network of electrical devices, such as generators, fixed loads, deferrable loads, and storage devices. [44, 45, 46, 47] describe methods for improving the speed of MPC, using online optimization. These custom methods exploit the particular structure of the MPC. Embedded convex optimization applications have recently become more available to non-experts by the introduction of the automatic code generator CVXGEN [48]. Remarkable speed-ups achieved using tailored QP-solvers exported from CVXGEN have been reported in, *e.g.*, [42, 49] and in this paper, we use the same type of custom, embedded solvers. In a recent paper [50] a splitting technique to a generic linear-convex optimal control problem is introduced and computation times faster than what is obtained by CVXGEN are reported.

T. G. Hovgaard et al.   MPC for Wind Power Gradients

1.1. Outline

In §2, we introduce the dynamic model for a wind turbine along with the constraints from both physical/mechanical limitations and the constraints we impose in order to fulfill certain requirements to the operation. We specify and explain the individual terms in the composite objective function for the optimal control problem in §2.2. In §3, we show how the optimal control problem can be formulated as a convex optimal control problem, *i.e.*, one with linear dynamics convex constraints, and a concave objective functional (to be maximized). We provide a novel change of variables and justify the necessary approximations. §4 gives a numerical simulation of the open-loop optimization for a constructed scenario and we evaluate the performance of our proposed method. Finally, in §5, we propose an economic MPC based on the convex optimal control formulation and demonstrate the capability in closed-loop on three different scenarios with real wind measurement series and their corresponding forecasts using modern wind predictors. We give concluding remarks in §6.

2. SYSTEM MODEL

2.1. Dynamics and constraints

We model the turbine, transmission, and generator as a single rotational system, with generator speed $\omega_g(t)$ in rad/s, and rotor speed $\omega_r(t) = \omega_g(t)/N$ in rad/s, where N is the gear ratio of the transmission. We let J_g and J_r denote the inertias of the generator and rotor, respectively, and we let $J = J_g + J_r/N^2$ denote the equivalent inertia at the generator shaft. Neglecting losses, the dynamics is given by

$$J\dot{\omega}_g(t) = T_r(t)/N - T_g(t), \tag{1}$$

where $T_g(t)$ is the generator (back) torque and $T_r(t)$ is the rotor torque from the wind, in Nm. The generator speed and torque must lie within given bounds:

$$\omega_{g,\min} \le \omega_g(t) \le \omega_{g,\max},$$

$$0 \le T_g(t) \le T_{g,\max}.$$

The rotor torque $T_r(t)$ is a function of rotor speed $\omega_r(t)$, wind speed $v(t)$ (in m/s), and the blade pitch angle, denoted $\beta(t)$ (by convention in degrees), which must satisfy

$$\beta_{\min} \le \beta(t) \le \beta_{\max}.$$

The mechanical power extracted from the wind, denoted P_w, is

$$P_w(t) = \omega_r(t)T_r(t) = \frac{1}{2}\rho A C_P(v(t), \omega_r(t), \beta(t))v(t)^3,$$

where ρ is the air density, A is the swept rotor area, and C_P is the coefficient of power, which is a function of wind speed, rotor speed, and blade pitch, typically given by a lookup table, found from aerodynamic simulations or tests. We write this in the form

$$T_r(t) = \Phi(v(t), \omega_r(t), \beta(t))v(t)^3/\omega_r(t),$$

where we combine several terms into one function

$$\Phi(v(t), \omega_r(t), \beta(t)) = (1/2)\rho A C_P(v(t), \omega_r(t), \beta(t)).$$

The generator produces power $P_g(t)$, given by

$$P_g(t) = \eta_g T_g(t)\omega_g(t),$$

where $\eta_g \in [0, 1]$ is the generator efficiency. This power is constrained by

$$P_{\min} \le P_g(t) \le P_{\text{rated}},$$

where P_{rated} is the rated power of the generator.

Let $Q(t)$ denote the state-of-charge of the energy storage device, in J. With a small charge and discharge loss, the dynamics of $Q(t)$ is

$$\dot{Q}(t) = P_{\text{chg}}(t) - \eta_{\text{loss}}\left|P_{\text{chg}}(t)\right|, \tag{2}$$

where $P_{\text{chg}}(t)$ is the charge rate, in W. (Negative $P_{\text{chg}}(t)$ means discharging.) $\eta_{\text{loss}} \in [0, 1]$ is the loss in per cent. Charge rate and state-of-charge are limited by

$$P_{\text{chg,min}} \le P_{\text{chg}}(t) \le P_{\text{g}}(t),$$

and

$$0 \le Q(t) \le Q_{\text{max}}.$$

Finally, the power supplied to the grid is

$$P_{\text{grid}}(t) = P_{\text{g}}(t) - P_{\text{chg}}(t).$$

2.2. Optimization

We assume that the limits on quantities, data such as N and J, the function Φ (and therefore the functions $\omega_{\text{r}}^{\star}$ and $\beta_{\text{r}}^{\star}$), are known, along with the initial rotor speed and state of charge. We assume that the wind speed $v(t)$ is known (or estimated) over the time interval $0 \le t \le T$. Our goal is to choose the blade pitch $\beta(t)$, generator torque $T_{\text{g}}(t)$, and charge rate $P_{\text{chg}}(t)$, over the time interval $0 \le t \le T$, subject to all the constraints described above.

We have several objectives to consider. The first is the total energy E over the period,

$$E = \int_0^T P_{\text{grid}}(t)\, dt,$$

which we want to maximize. The second is a penalty (which we wish to minimize) for violating a target maximum value of power rate of change, G (in W/s):

$$R_{\text{pen}} = \int_0^T (|\dot{P}_{\text{grid}}(t)| - G)_+\, dt,$$

where $(b)_+ = \max(b, 0)$. The third objective, which we want to minimize, is a measure of variation of delivered power over time:

$$R_{\text{var}} = \int_0^T \dot{P}_{\text{grid}}(t)^2\, dt.$$

The forth objective is a penalty (which we will minimize) on rotational speeds above the rated speed $\omega_{\text{g,rated}}$:

$$R_{\text{speed}} = \int_0^T (\omega_{\text{g}}(t) - \omega_{\text{g,rated}})_+\, dt,$$

so over-speed is limited when it is not needed for storing kinetic energy. Finally, the fifth objective is to reduce the generator torque by increasing rotational speed to the rated speed when more power is available in the wind than what the generator is able to extract. This is achieved by maximizing

$$R_\Phi = \int_0^T \Phi(v(t), \omega_{\text{r}}(t), \beta(t))\, dt.$$

We handle these objectives by maximizing the composite objective

$$E - \lambda R_{\text{pen}} - \mu R_{\text{var}} - \rho R_{\text{speed}} + \gamma R_\Phi,$$

where λ, μ, ρ, and γ are positive constants that determine the tradeoffs among the objectives. We are to choose $\beta(t)$, $T_{\text{g}}(t)$, and $P_{\text{chg}}(t)$ to maximize the composite objective, subject to the constraints given above, and the final charge constraint $Q(T) = Q(0)$, which says that the net energy from the storage device over the period is zero.

This is a classical continuous-time optimal control problem, with nonlinear dynamics and nonlinear objective functional.

3. CONVEX FORMULATION

In this section, we show how the optimal control problem described above can be formulated as a convex optimal control problem, *i.e.*, one with linear dynamics, convex constraints, and a concave objective functional (to be maximized). This implies that the problem can be solved globally, with great efficiency and also great reliability [51].

The trick is to work with power flows and energies, treating $\beta(t)$ and $T_{\text{g}}(t)$ as variables derived from the powers. In our formulation we choose the quantities

$$P_{\text{g}}(t), \quad P_{\text{grid}}(t), \quad P_{\text{chg}}(t), \quad P_{\text{w}}(t), \quad Q(t), \quad K(t),$$

Model predictive control for wind power gradients 163

T. G. Hovgaard et al. MPC for Wind Power Gradients

over the time interval $0 \leq t \leq T$, where $K(t) = (J/2)\omega_g(t)^2$ is the kinetic energy stored in the rotational motion and $P_w(t) = T_r(t)\omega_r(t)$ is the power extracted from the wind. Note that the rotor speed can be expressed in terms of the kinetic energy as

$$\omega_r(t) = (1/N)\sqrt{(2/J)K(t)}$$

(which shows how we reconstruct it from the variables above).

The objective E is a linear function of the variables, hence concave. The minimization objectives R_{pen} and R_{var} are convex functions of the variables, and R_{speed} translates directly to:

$$R_{speed} = \int_0^T (K(t) - (J/2)\omega_{g,rated}^2)_+ \, dt,$$

which is a convex function of K. So the over all objective $E - \lambda R_{pen} - \mu R_{var} - \rho R_{speed} + \gamma R_\Phi$, which is to be maximized, is concave if R_Φ is concave. We will come back to this shortly.

Many of the constraints are immediately convex. For example, limits on the quantities above are simple linear inequality constraints. The charge state dynamics, $\dot{Q}(t) = P_{chg}(t) - \eta_{loss}|P_{chg}(t)|$, is a linear differential equation. We now turn to the other constraints, and show how they can be expressed as convex constraints on the variables listed above.

We can express the dynamics in terms of the kinetic energy as

$$\dot{K}(t) = J\omega_g(t)\dot{\omega}_g(t) = \omega_g(t)\left(\frac{T_r(t)}{N} - T_g(t)\right) = P_w(t) - P_g(t)/\eta_g,$$

which is a linear differential equation relating K, P_w, and $P_g(t)$. The limits on rotor speed can be expressed as limits on kinetic energy, as

$$(J/2)\omega_{g,min}^2 \leq K(t) \leq (J/2)\omega_{g,max}^2.$$

These are simple linear (convex) inequalities.

The generator torque is

$$T_g(t) = \frac{P_g(t)}{\eta_g\sqrt{(2/J)K(t)}}$$

(which shows how we can reconstruct it from the variables above), so the generator torque constraints translate into

$$0 \leq P_g(t) \leq \eta_g\sqrt{(2/J)K(t)}T_{g,max},$$

which is a convex constraint on $P_g(t)$ and $K(t)$, since $\sqrt{(2/J)K(t)}$ is a concave function of $K(t)$.

Finally, we explain how to reconstruct the blade pitch $\beta(t)$ from the variables listed above. We define the available wind power, as a function of wind speed and kinetic energy,

$$P_{av}(v, K) = \max_{\beta_{min} \leq \beta \leq \beta_{max}} \Phi(v, (1/N)\sqrt{(2/J)K}, \beta)v^3.$$

This function is readily found (or tabulated in lookup table form) from Φ. By definition, we have

$$P_w(t) \leq P_{av}(v(t), K(t)), \tag{3}$$

which states that the extracted wind power cannot exceed the maximum available power.

Now we use a property of the function Φ: As β varies over its range, the extracted power varies from 0 to P_{av}. In other words, by blade pitch control, we can vary the extracted power from 0 up to the maximum available power. We disregard the effects of dynamic inflow of the wind during fast pitching events, described in, *e.g.*, [52, 53, 54]. In these papers, the transient time of the dynamic inflow is observed to be in the range of 8-20 s. Thus, with a sample rate of 10 s, such effects are not relevant to this study. We define the function $\Psi(v, K, P_w)$ as the value of β that gives the extracted power P_w. (This is how we will extract the blade pitch angle from the variables above.)

Now finally we turn to convexity of the constraint (3) and concavity of the objective term R_Φ. The latter readily translates into

$$R_\Phi = \int_0^T P_{av}(v(t), K(t)) \, dt.$$

What is needed to satisfy both is that, for each wind speed v, P_{av} is a concave function of K. Amazingly, this is the case with realistic coefficient of power models. (This is discussed below in §3.1.)
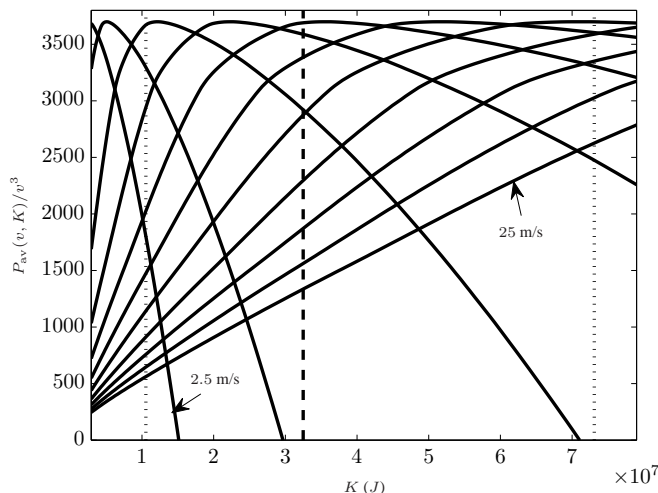
Figure 1. $P_{av}(v, K)$ normalized by v^3 plotted for a number of different wind speeds evenly distributed between 2.5m/s and 25m/s. The dotted vertical lines show the minimum and maximum speeds and the dashed vertical line is the rated speed.

3.1. Concavity of the available power function

The concavity of the available power $P_{av}(v, K)$ is not a mathematical fact. However, as we illustrate in Figure 1, the available power is nearly a concave function of K for each wind speed. Consequently, we can approximate each of these with a concave function which is very accurate. Let, $\hat{P}_{av, v_i}(K)$ be the approximation of $P_{av}(v, K)$ (concave of K) at the wind speed v_i. We fit piecewise linear (PWL) functions to express this as

$$\hat{P}_{av, v_i}(K(t)) = \min \{a_1 K(t) + b_1, \ldots, a_k K(t) + b_k\} \, v^3,$$

with k affine functions (see, *e.g.*, [55]). We compute $\hat{P}_{av, v_i}(K)$ for a number of discrete values v_i of the wind speed.

For any given wind speed, we find the concave approximation $\hat{P}_{av}(v, K)$ of the available power $P_{av}(v, K)$ by linear interpolation of the two neighboring functions $\hat{P}_{av, v_i}(K)$, *e.g.*,

$$\hat{P}_{av}(v(t), K(t)) = (1 - \Theta)\hat{P}_{av, v_1}(K(t)) + \Theta\hat{P}_{av, v_2}(K(t)),$$

with $\Theta = \frac{v(t) - v_1}{v_2 - v_1}$. $\hat{P}_{av}(v, K)$ is a concave function of K as it is the linear interpolation of concave functions.

We validate the approximation by showing the error in $\hat{P}_{av}(v, K)$ vs. $P_{av}(v, K)$ for the valid range of v and K. We test with much smaller steps in v than what we have used for the PWL functions. See Figure 2. Our simple interpolated PWL fit has maximum error of a few percent, and typical error well under one percent.

4. NUMERICAL SIMULATION

We provide careful numerical simulations using the parameters for the NREL 5MW wind turbine model. The model is openly available and is described in detail in, *e.g.*, [56, 57]. For this turbine, the rated power is $P_{rated} = 5$ MW which is reached at wind speeds above 11.4 m/s. The turbine cuts in at 3 m/s and out at 25 m/s. In this and in the following section, we present simulation results as normalized values using the per unit (pu) system throughout. We define this in Table I. We solve the optimal control problem for a single turbine using our convex formulation:

$$
\begin{aligned}
\text{maximize} \quad & E - \lambda R_{pen} - \mu R_{var} - \rho R_{speed} + \gamma R_{\Phi}, \\
\text{subject to} \quad & \text{constraints and dynamics given in §3,}
\end{aligned}
\tag{4}
$$

where the variables are P_g, P_{grid}, P_{chg}, P_w, Q, and K (all functions of time). The optimization uses an initial state of the dynamic variables $K(t)$ and $Q(t)$ as well as known wind speeds for the interval. Instead of (4) we solve a discretized version with N_p steps over the time interval $[0, T]$ using the sample time T_s.
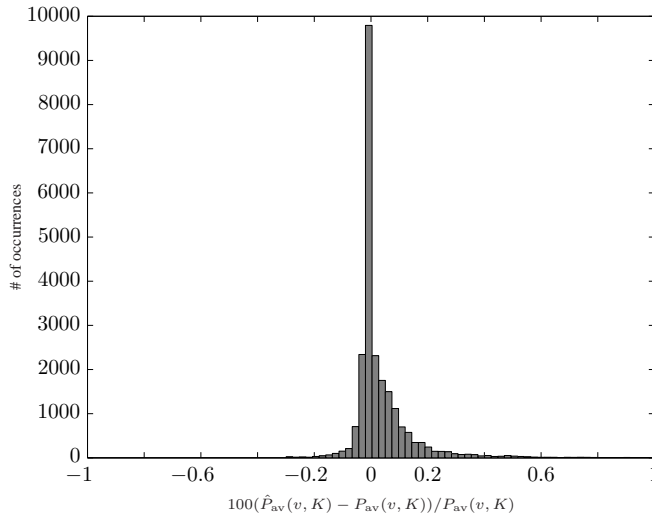
Figure 2. $\hat{P}_{av}(v, K)$ error in percentage.

QUANTITY	FACTOR	INTERPRETATION
Power P	$1/P_{rated}$	1 pu = rated turbine power
Kinetic energy K	$1/K_{rated}$	1 pu = kinetic energy at rated speed
Storage capacity Q	$1/P_{rated}$	1 pu = energy produced by the turbine at rated power in 1 s
Speed ω_g	$1/\omega_{g,rated}$	1 pu = rated generator speed

Table I. Nomenclature for the pu system.

λ	$1 \cdot 10^2$	
μ	$1 \cdot 10^{-5}$	
ρ	$1 \cdot 10^{-2}$	
γ	$1 \cdot 10^{-2}$	
N_p	200	
T_s	10	s
η_{loss}	2	%
G	2.5	kW/s

Table II. Parameters for numerical simulation.

In addition to the parameters given by the model, we must choose values for the introduced dimensionless tuning parameters, for the target maximum value of power rate of change, for the charge/discharge loss, the sample time and the length of the interval. We let the maximum power gradient G be rather tight by allowing only a rate of change less than 3% of the maximum rated power per minute. We choose λ sufficiently high to enforce this maximum power gradient whenever possible. We want μ, ρ, and γ to be as small as possible and we adjust these by trial and error to give the desired behavior, *i.e.*, infrequent violation of the power gradient constraint, little variation in the power output, and limited use of overspeed. The method seems to be quite robust to changes in these values as the performance is merely dependent on the mutual relative size of the parameters. In this study we use a charge/discharge loss which is almost neglectable but still sufficient to avoid excessive charging and discharging over the interval. Table II gives the values used in the simulation. To put the kinetic energy in the rotational motion into play we allow over-speed up to 150% of the rated speed. The objective term R_{speed} keeps the turbine from over-speed when running in steady-state operation. The maximum storage capacity is varied in order to produce the trade-off plot in Figure 4. We formulate and solve this problem using CVX [58, 59].
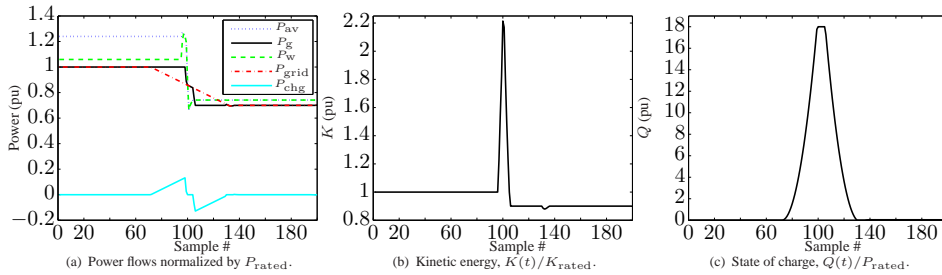
(a) Power flows normalized by P_{rated}.

(b) Kinetic energy, $K(t)/K_{rated}$.

(c) State of charge, $Q(t)/P_{rated}$.

Figure 3. Test of power gradient satisfaction. We use pu as the unit for all quantities and let the wind speed drop from 12 m/s to 10 m/s linearly from sample 99 to 101.
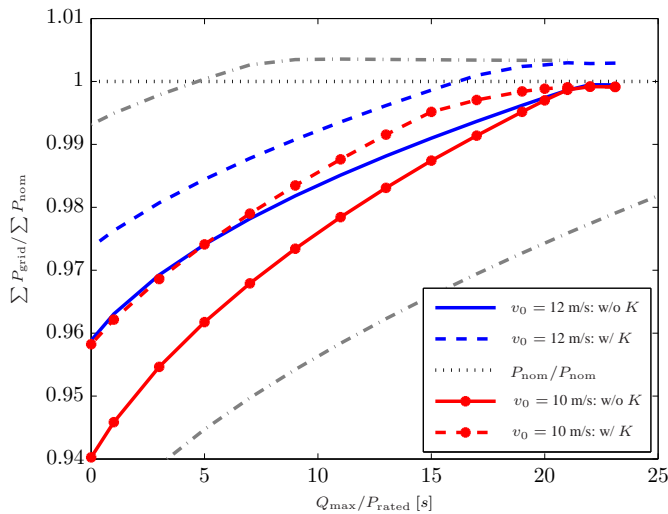
Figure 4. Energy delivered to the grid for varying storage capacity. We show two cases with a power drop of 0.3 pu over 20 s starting from v_0 above rated speed and below rated speed, respectively. We show this with and without kinetic energy storage K. The two grey dash-dot lines illustrate the dependency on the enforced power gradient as the upper curve comes from doubling the allowed gradient (loosening the constraint) while the lower curve is the result of allowing only half the power gradient (tightening the constraint). Both curves correspond to the $v_0 = 12$ m/s: w/ K curve (dashed blue). The lower curve reaches 1 at a storage level of approx. 40 pu.

Figure 3 shows the output from the optimizer for a selected scenario where the wind speed drops from 12 m/s to 10 m/s over a period of 20 s (2 samples). This equals a drop in available power (given in per unit (pu), *i.e.*, normalized by P_{rated}) from around 1.2 pu to 0.7 pu. Q_{max} is 18 pu in this case. The difference between P_w and P_g that is noted in the figure in steady operation is due to the generator efficiency.

Figure 4 shows the accumulated power delivered to the grid over the interval as a function of available storage capacity. We demonstrate a drop in available power of 0.3 pu over 20 s for two different cases. One where the initial wind speed contains more power than P_{rated} and one where the available power is below P_{rated} for the entire interval. The figure shows both cases with and without the use of rotor inertia as additional energy storage. From Figure 4 we see how the active use of rotor inertia as energy storage can reduce the needed extra storage capacity by up to 30% without reducing the power output (when the initial wind speed is above rated). When no extra storage is available the power output can be increased around 2% in both cases by use of kinetic energy storage.

Model predictive control for wind power gradients   167

T. G. Hovgaard et al.   MPC for Wind Power Gradients

SCENARIO #	1	b	2	2b	3	3b	
Mean wind, $\bar{v}$	8.03	-	9.92/8.26	-	13.96/11.19	-	m/s
Max wind, $\max(v)$	9.88	-	12.31/9.47	-	15.59/13.18	-	m/s
Nominal vs. MPC, ΔP_{grid}	0.57	4.79	0.42	10.75	-0.93	2.97	%
Accumulated charge/discharge loss	0.21	-	0.23	-	0.04	-	%
Max storage, $Q_{\max}$	15.34	-	50	-	31.86	-	pu
Mean storage, $\bar{Q}$	5.45	-	16.60	-	8.31	-	pu
Max speed $\frac{\max(w_{\mathrm{g}})}{w_{\mathrm{g,rated}}}$	0.95	0.95	1.43	1.00	1.36	1.00	pu
Mean speed $\frac{\bar{w}_{\mathrm{g}}}{w_{\mathrm{g,rated}}}$	0.77	0.79	0.89	0.83	0.99	0.95	pu
Gradient violation time	1.05	21.15	1.54	28.04	1.27	14.41	%

Table III. Selected figures from the three closed-loop simulations. For scenario 2 and 3, the wind speed is given separately for the intervals before and after the drop in mean wind speed. To compare the performance of the controllers, ΔP_{grid} gives the difference in total delivered energy to the grid in per cent $100 \frac{\sum P_{\mathrm{grid,nominal}} - \sum P_{\mathrm{grid,MPC}}}{\sum P_{\mathrm{grid,nominal}}}$. For each scenario, the column denoted with 'b' provides the lost energy and the amount of power gradient violations for the same scenario but without the extra storage and overspeed capabilities.

5. MODEL PREDICTIVE CONTROL

In this section, we show simulations with real wind data series measured at the Danish wind turbine test site Høvsøre in 2004. The controller bases its decisions on a prediction of future wind speeds. We use the predictions generated in [60, 61] by modern continuous time formulations of the predictors together with spline basis expansions. The predictors use upstream wind speed information from other turbines or measurements located several hundred meters in front of the turbine. For the simulations in this section, we implement an economic optimizing model predictive controller to address the closed-loop control of a single wind turbine. Like in traditional MPC, we implement the controller in a receding horizon manner, where an optimization problem over N time steps (the control and prediction horizon) is solved at each step. The result is an optimal input sequence for the entire horizon, out of which only the first step is implemented. Our controller repeatedly solves the optimal control problem in (4). Consequently, the aim is to maximize the power delivered to the grid while obeying the strict requirements to power gradient constraints. This objective function relates to maximizing the profit within the limits of mechanical as well as regulated constraints, and we do not focus on tracking certain set-points as tend to be the trend in standard MPC.

We use the parameters for the optimal control problem given in Table II and present three different wind scenarios. Each scenario contains a number of 10-second averages of measured wind speed and their corresponding predictions. Scenario 1 covers 86 minutes with a quite constant mean wind speed while both scenario 2 and 3 show examples of significant drops in mean wind speed. Scenario 2 and 3 cover 215 minutes and 175 minutes, respectively. Figures 5–7 illustrate the wind scenario (measurement and prediction), the wind speed prediction error, power delivered to the grid, and the distribution of power gradients for each of the three scenarios. In each case, we compare our controller to the nominal controller in the full Simulink model for the NREL 5MW wind turbine [56, 57]. This turbine delivers all the power it produces directly to the grid and the pitch and generator torque control is based on gain-scheduled PI controllers that track optimal set-points given as look-up tables. This approach is standard in controlling wind turbines today. In addition to the figures, Table III provides a summary of interesting results from the simulations.

In all three scenarios, we note how the heavy fluctuations in power delivered to the grid almost disappear with our MPC controller. We see a much smoother power signal which is supported by the histograms that clearly show how the rate of change of the power (with a few exceptions) is limited to the $\pm 3\%$/minute range that we allow in the problem formulation. For scenario 1 and 2 the total amount of energy delivered to the grid is reduced by 0.57% and 0.42%, respectively. This reduction is due to a total accumulated charge/discharge loss of around 0.2% and some periods with suboptimal operation since we change the rotor speed. Note that this lost energy production should be seen in relation to the much higher losses incurred when no storage is available (columns denoted 'b' in Table III), as the power gradient is regarded as a strictly enforced grid code. In scenario 3, the wind speed is above the rated speed most of the time and our MPC controller increases the amount of energy delivered to the grid in this case. This increase comes from the improved power coefficient during overspeed. Table III provide further results regarding maximum and mean utilization of external storage capacity, maximum and mean rotor speed, etc.

6. CONCLUSION

In this paper, we have presented an approach to power gradient reduction for fulfilling future, tighter grid codes and for improving the quality of power delivered to the grid from wind power plants. We utilize turbine inertia as a resource of distributed energy storage, limited by the rotational speed, in addition to a central storage unit which is associated with an extra cost. We have demonstrated that by a novel change of variables we can transform the quite nonlinear system dynamics to a model with linear dynamics and convex constraints. Thus, the problem can be solved for its global optimum using very efficient and reliable algorithms. Simulations on realistic models reveal a significant ability to reject the disturbances from fast changes in wind speed, ensuring certain power gradients, while keeping the amount of produced power very close to nominal.

ACKNOWLEDGEMENTS

REFERENCES

1. Danish Ministry of Climate E, Building. Energy policy report 2012. `http://www.ens.dk/en-US/policy/danish-climate-and-energy-policy/Sider/danish-climate-and-energy-policy.aspx` 2012.

2. Morren J, Pierik J, de Haan SWH. Inertial response of variable speed wind turbines. *Electric Power Systems Research* 2006; **76**(11):980–987.

3. Conroy JF, Watson R. Frequency Response Capability of Full Converter Wind Turbine Generators in Comparison to Conventional Generation. *IEEE Transactions on Power Systems* 2008; **23**(2):649–656.

4. Iov F, Hansen A, Sørensen P, Cutululis N. A survey of interconnection requirements for wind power. *Proc. of the Nordic wind power conference (NWPC)*, Risø National Laboratory, 2007.

5. Singh B, Singh S. Wind Power Interconnection into the Power System: A Review of Grid Code Requirements. *The Electricity Journal* 2009; **22**(5):54–63.

6. Eltra/Elkraft/Energinetdk. Regulation TF 3.2.5, Wind turbines connected to grids with voltages above 100 kV — Technical regulation for the properties and the regulation of wind turbines. `https://selvbetjening.preprod.energinet.dk/NR/rdonlyres/E4E7A0BA-884F-4E63-A2F0-98EB5BD8D4B4/0/WindTurbinesConnectedtoGridswithVoltageabove100kV.pdf` 2004.

7. ENTSO-E. Network code for requirements for grid connection applicable to all generators. `https://www.entsoe.eu/fileadmin/user_upload/_library/consultations/Network_Code_RfG/120626_final_Network_Code_on_Requirements_for_Grid_Connection_applicable_to_all_Generators.pdf` 2012.

8. Korpås M, Holen AT. Operation planning of hydrogen storage connected to wind power operating in a power market. *IEEE Transactions on Energy Conversion* 2006; **21**(3):742–749.

9. Black M, Strbac G. Value of Bulk Energy Storage for Managing Wind Power Fluctuations. *IEEE Transactions on Energy Conversion* 2007; **22**(1):197–205.

10. Stroe DI, Stan AI, Diosi R, Teodorescu R, Andreasen SJ. Short term energy storage for grid support in wind power applications. *Proc. of the 13th International Conference on Optimization of Electrical and Electronic Equipment (OPTIM)*, 2012; 1012–1021.

11. Budischak C, Sewell DA, Thomson H, Mach L, Veron DE, Kempton W. Cost-Minimized Combinations of Wind Power, Solar Power and Electrochemical Storage, Powering the Grid up to 99.9% of the Time. *Journal of Power Sources* 2013; **225**:60–74.

12. Swierczynski M, Teodorescu R, Rodriguez P. Lifetime investigations of a lithium iron phosphate (LFP) battery system connected to a wind turbine for forecast improvement and output power gradient reduction. *Proc. of the 15th Battcon Stationary Battery Conference and Trade Show*, 2011; 20.1–20.8.

13. Hovgaard TG, Larsen LFS, Edlund K, Jørgensen JB. Model predictive control technologies for efficient and flexible power consumption in refrigeration systems. *Energy* 2012; **44**(1):105 – 116.

Model predictive control for wind power gradients 169

T. G. Hovgaard et al.   MPC for Wind Power Gradients

14. Hovgaard TG, Larsen LFS, Jørgensen JB, Boyd S. Nonconvex model predictive control for commercial refrigeration. *International Journal of Control* 2012; :In PressURL http://www.stanford.edu/~boyd/papers/noncvx_mpc_refr.html.

15. Knuppel T, Nielsen JN, Jensen KH, Dixon A, Østergaard J. Power oscillation damping controller for wind power plant utilizing wind turbine inertia as energy storage. *Proc. of the IEEE Power and Energy Society General Meeting*, 2011; 1–8.

16. Tarnowski GC. Coordinated Frequency Control of Wind Turbines in Power Systems with High Wind Power Penetration. PhD Thesis, Technical University of Denmark 2012.

17. Hau E. *Wind turbines: fundamentals, technologies, application, economics*. Springer Verlag, 2006.

18. Hammerum K, Brath P, Poulsen NK. A fatigue approach to wind turbine control. *Journal of Physics: Conference Series* 2007; **75**.

19. Dang DQ, Wu S, Wang Y, Cai W. Model Predictive Control for maximum power capture of variable speed wind turbines. *International Power Electronics Conference*, 2010; 274–279.

20. Henriksen LC, Poulsen NK, Hansen MH. Nonlinear Model Predictive Control of a Simplified Wind Turbine. *Proc. of the 18th IFAC World Congress*, 2011; 551–556.

21. Adegas FD, Stoustrup J, Odgaard PF. Repetitive model predictive approach to individual pitch control of wind turbines. *Proc. of the IEEE Conference on Decision and Control*, 2011; 3664–3670.

22. Hansen AD, Sørensen P, Iov F, Blaabjerg F. Centralised power control of wind farm with doubly fed induction generators. *Renewable Energy* 2006; **31**(7):935–951.

23. Spudic V, Jelavic M, Baotic M. Wind turbine power references in coordinated control of wind farms. *AUTOMATIKA* 2011; **52**(2):82–94.

24. Madjidian D, Rantzer A. A Stationary Turbine Interaction Model for Control of Wind Farms. *Proc. of the 18th IFAC World Congress*, 2011; 4921–4926.

25. Soleimanzadeh M, Wisniewski R, Kanev S. An optimization framework for load and power distribution in wind farms. *Journal of Wind Engineering and Industrial Aerodynamics* 2012; .

26. Hovgaard TG, Larsen LFS, Jørgensen JB, Boyd S. Sequential Convex Programming for Power Set-point Optimization in a Wind Farm using Black-box Models, Simple Turbine Interactions, and Integer Variables. *Proc. of the 10th European Workshop on Advanced Control and Diagnosis (ACD)*, 2012; 1–8.

27. Hovgaard TG, Larsen LFS, Jørgensen JB, Boyd S. MPC for Wind Power Gradients Utilizing Forecasts, Rotor Inertia, and Central Energy Storage. *Proc. of the European Control Conference*, 2013; 4071–4076.

28. Garcia CE, Prett DM, Morari M. Model predictive control: theory and practice-a survey. *Automatica* 1989; **25**(3):335–348.

29. Bemporad A, Morari M. Robust model predictive control: A survey. *Robustness in Identification and Control* 1999; :207–226.

30. Qin SJ, Badgwell TA. A survey of industrial model predictive control technology. *Control engineering practice* 2003; **11**(7):733–764.

31. Rawlings JB, Amrit R. Optimizing Process Economic Performance Using Model Predictive Control. *Nonlinear Model Predictive Control: Towards New Challenging Applications* 2009; :119–138.

32. Diehl M, Amrit R, Rawlings JB. A Lyapunov Function for Economic Optimizing Model Predictive Control. *Automatic Control, IEEE Transactions on* 2011; **56**(3):703–707.

33. Angeli D, Amrit R, Rawlings J. On average performance and stability of Economic Model Predictive Control. *Automatic Control, IEEE Transactions on* 2012; **57**(7):1615–1626.

34. Rawlings JB, Angeli D, Bates C. Fundamentals of economic model predictive control. *Proc. of the 51th IEEE Conference on Decision and Control*, 2012; 3851–3861.

35. Grüne L. Economic receding horizon control without terminal constraints. *Automatica* 2013; **49**(3):725–734.

36. Halvgaard R, Poulsen NK, Madsen H, Jørgensen JB. Economic Model Predictive Control for building climate control in a Smart Grid. *Innovative Smart Grid Technologies (ISGT), 2012 IEEE PES*, 2012; 1–6.

37. Oldewurtel F, Parisio A, Jones CN, Gyalistras D, Gwerder M, Stauch V, Lehmann B, Morari M. Use of model predictive control and weather forecasts for energy efficient building climate control. *Energy and Buildings* 2012; **45**(0):15–27.

38. Mirzaei M, Poulsen NK, Niemann HH. Robust Model Predictive Control of a Wind Turbine. *Proc. of the 2012 American Control Conference*, 2012; 4393–4398.

39. Henriksen LC, Hansen MH, Poulsen NK. Wind turbine control with constraint handling: a model predictive control approach. *I E T Control Theory and Applications* 2012; **6**(11):1722–1734.

40. Biegel B, Juelsgaard M, Kraning M, Boyd S, Stoustrup J. Wind turbine pitch optimization. *IEEE International Conference on Control Applications (CCA)*, 2011; 1327–1334.

41. Soltani M, Wisniewski R, Brath P, Boyd S. Load reduction of wind turbines using receding horizon control. *IEEE International Conference on Control Applications (CCA)* , 2011; 852–857.

42. Kraning M, Wang Y, Akuiyibo E, Boyd S. Operation and Configuration of a Storage Portfolio via Convex Optimization. *Proc. of the 18th IFAC World Congress*, 2011; 10 487–10 492.
43. Kraning M, Chu E, Lavaei J, Boyd S. Dynamic Network Energy Management via Proximal Message Passing. *Foundations and Trends in Optimization* 2013; **1**(2):70–122. URL http://www.stanford.edu/~boyd/papers/msg_pass_dyn.html.
44. Rao CV, Wright SJ, Rawlings JB. Application of interior-point methods to model predictive control. *Journal of optimization theory and applications* 1998; **99**(3):723–757.
45. Jørgensen JB. Moving Horizon Estimation and Control. PhD Thesis, Department of Chemical Engineering, Technical University of Denmark 2005.
46. Wang Y, Boyd S. Fast Model Predictive Control Using Online Optimization. *IEEE Transactions on Control Systems Technology* 2010; **18**(2):267–278.
47. Jørgensen JB, Frison G, Gade-Nielsen NF, Dammann B. Numerical methods for solution of the extended linear quadratic control problem. *Proc. of the 4th IFAC Nonlinear Model Predictive Control Conference*, 2012; 187–193.
48. Mattingley J, Boyd S. CVXGEN: a code generator for embedded convex optimization. *Optimization and Engineering* 2012; **13**:1–27.
49. Mattingley J, W Y, Boyd S. Receding Horizon Control. *IEEE Control Systems Magazine* 2011; **31**(3):52–65.
50. O'Donoghue B, Stathopoulos G, Boyd S. A Splitting Method for Optimal Control. *IEEE Transactions on Control Systems Technology* 2013; :In PressURL http://www.stanford.edu/~boyd/papers/oper_splt_ctrl.html.
51. Boyd S, Vandenberghe L. *Convex Optimization*. Cambridge University Press, 2004.
52. Øye, S. Tjæreborg Wind Turbine. *AFM notat*, Department of fluid mechanics, DTU, Denmark., 1991.
53. Øye, S. Fast pitch step experiments in a wind tunnel and comparison with computational methods. *Proc. of the 1996 European Union Wind Energy Conference*, 1996; 741–744.
54. Knudsen, T and Bak, T. Simple model for describing and estimating wind turbine dynamic inflow. *Proc. of the American Control Conference (ACC)*, 2013; 640–646.
55. Magnani A, Boyd S. Convex piecewise-linear fitting. *Optimization and Engineering* 2009; **10**(1):1–17.
56. Jonkman JM, Butterfield S, Musial W, Scott G. *Definition of a 5-MW reference wind turbine for offshore system development*. National Renewable Energy Laboratory, 2009.
57. Grunnet JD, Soltani M, Knudsen T, Kragelund MN, Bak T. Aeolus Toolbox for Dynamics Wind Farm Model, Simulation and Control. *Proc. of the European Wind Energy Conference and Exhibition, EWEC*, 2010.
58. CVX Research I. CVX: Matlab Software for Disciplined Convex Programming, version 2.0 beta. http://cvxr.com/cvx 2012.
59. Grant M, Boyd S. Graph implementations for nonsmooth convex programs. *Recent Advances in Learning and Control*, V Blondel and S Boyd and H Kimura (ed.). Lecture Notes in Control and Information Sciences, Springer-Verlag Limited, 2008; 95–110.
60. Nielsen HA, Madsen H, Sørensen P. Ultra-short term wind speed forecasting. *Proc. of the European Wind Energy Conference & Exhibition, London*, 2004.
61. Nielsen HA, Madsen H. Forecasting wind speeds on the minute time-scale using up-stream information. *Technical Report*, Technical University of Denmark, Informatics and Mathematical Modelling 2004.

(a) Measured wind speed (dashed red) and predicted wind speed (solid black).

(b) Wind speed prediction error in per cent

(c) Nominal controller: P_{grid} (solid black), max P_{av} (dotted green), and $\Delta P_{\mathrm{grid}}/\mathrm{sample}$ (dashed red).

(d) Nominal controller: Power gradient in per cent of rated power per minute.

(e) MPC controller: P_{grid} (solid black), max P_{av} (dotted green), and $\Delta P_{\mathrm{grid}}/\mathrm{sample}$ (dashed red).

(f) MPC controller: Power gradient in per cent of rated power per minute.
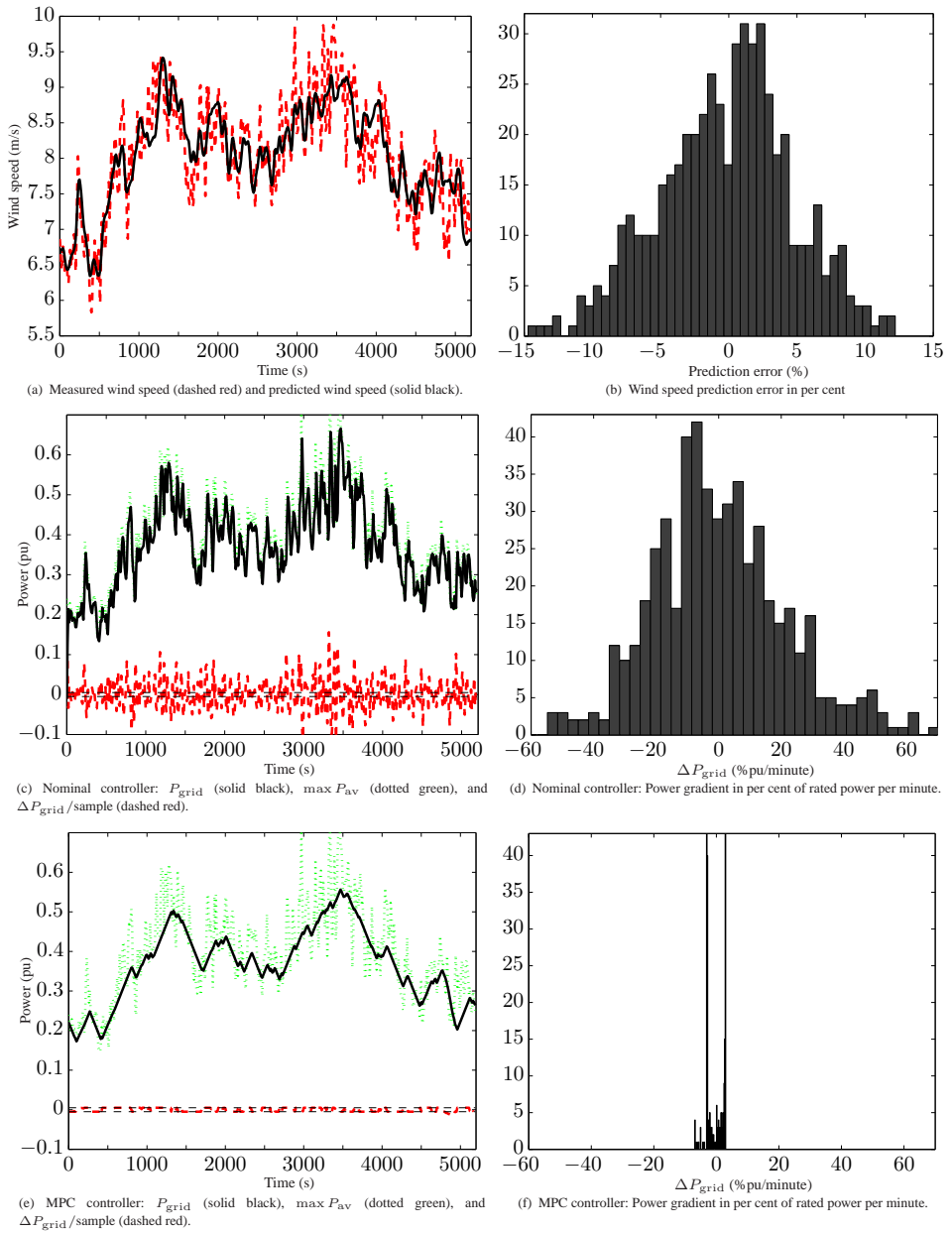
Figure 5. Closed-loop simulation of MPC controller with wind scenario 1.

(a) Measured wind speed (dashed red) and predicted wind speed (solid black).

(b) Wind speed prediction error in per cent

(c) Nominal controller: P_{grid} (solid black), $\max P_{av}$ (dotted green), and ΔP_{grid}/sample (dashed red).

(d) Nominal controller: Power gradient in per cent of rated power per minute.

(e) MPC controller: P_{grid} (solid black), $\max P_{av}$ (dotted green), and ΔP_{grid}/sample (dashed red).

(f) MPC controller: Power gradient in per cent of rated power per minute.

Figure 6. Closed-loop simulation of MPC controller with wind scenario 2.

Model predictive control for wind power gradients   173

T. G. Hovgaard et al.   MPC for Wind Power Gradients

(a) Measured wind speed (dashed red) and predicted wind speed (solid black).

(b) Wind speed prediction error in per cent

(c) Nominal controller: P_{grid} (solid black), max P_{av} (dotted green), and ΔP_{grid}/sample (dashed red).

(d) Nominal controller: Power gradient in per cent of rated power per minute.

(e) MPC controller: P_{grid} (solid black), max P_{av} (dotted green), and ΔP_{grid}/sample (dashed red).

(f) MPC controller: Power gradient in per cent of rated power per minute.

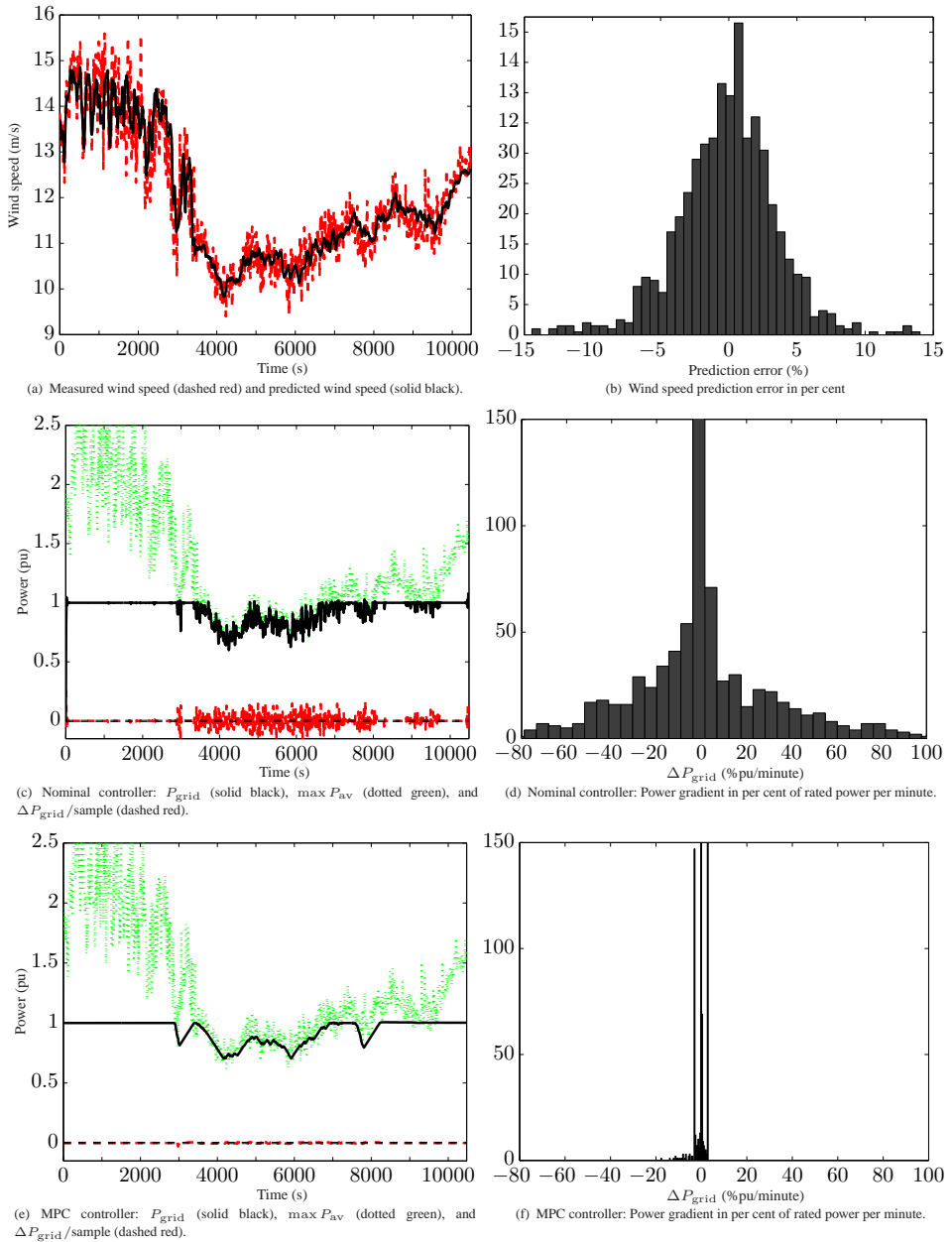**Figure 7.** Closed-loop simulation of MPC controller with wind scenario 3.

The Potential of Economic MPC for Power Management

The Potential of Economic MPC for Power Management

Tobias Gybel Hovgaard, Kristian Edlund, John Bagterp Jørgensen

Abstract— Economic Model Predictive Control is a receding horizon controller that minimizes an economic objective function rather than a weighted least squares objective function as in Model Predictive Control (MPC). We use Economic MPC to operate a portfolio of power generators and consumers such that the cost of producing the required power is minimized. The power generators are controllable power generators such as combined heat and power generators (CHP), coal and gas fired power generators, as well as a significant share of uncontrollable power generators such as parks of wind turbines. In addition, some of the power consumers are controllable. In this paper, the controllable power consumers are exemplified by large cold rooms or aggregations of super markets with refrigeration systems. We formulate the Economic MPC as a linear program. By simulation, we demonstrate the performance of Economic MPC for a small conceptual example.

I. Introduction

The United States' and Europe's development for future intelligent electricity grid is called GridWise and SmartGrid, respectively. GridWise and SmartGrid are intended to be the smart electrical infrastructure required to increase the amount of green energy (solar and wind) significantly. To obtain an increasing amount of electricity from intermittent energy sources such as solar and wind, we must not only control the production of electricity but also the consumption of electricity in an efficient, agile and proactive manner. In contrast to the current rather centralized power generation system, the future electricity grid is going to be a network of a very large number of independent power generators. To address such problems there has been an increasing interest in hierarchical and distributed control [1].

In this paper we introduce Economic MPC to control a number of independent dynamic systems that must collaborate to minimize the overall cost in satisfying the cooling demand for some goods. Power producing companies must minimize the cost of producing enough power to meet the market demand and respect their contracts with transmission system operators. Minimizing the cost of operation and providing supply security, becomes increasingly difficult as a larger share of intermittent stochastic power generating sources such as solar and wind are introduced in the power system. To balance demand and supply of electricity in a flexible and cost efficient manner, we consider using large power consumers such as cold rooms to adjust the power

T.G. Hovgaard is with Danfoss A/S, Nordborgvej 81, DK-6430 Nordborg, Denmark tgh@danfoss.com

K. Edlund is with DONG Energy A/S, Kraftværksvej 53, DK-7000 Fredericia, Denmark kried@dongenergy.dk

J.B. Jørgensen is with DTU Informatics, Technical University of Denmark, Richard Petersens Plads, Building 321, DK-2800 Kgs. Lyngby, Denmark jbj@imm.dtu.dk

demand profile to the power supply. Due to the large thermal capacity of cold rooms, they can to some degree shift the consumption of electricity to periods of the day at which there is a surplus production capacity. The thermal capacity in the refrigerated goods can be utilized to store "coldness" such that the refrigeration system can cool extra when the energy is free (i.e. there is an over production from the generators). Thereby a lower than normally required cooling capacity can be applied later, for a period of time when the energy prices are above zero again. The demands to the temperature in the cold room are not violated at any time since the same total cooling capacity is applied though shifted in a more optimal way. We exploit that the dynamics of the temperature in the cold room are rather slow while the power consumption can be changed rapidly. This, of course, imposes a constraint on the time constant of the temperature in the cold room. If e.g. no goods are loaded into the cold room the dynamics will be must faster reducing the positive effects gained from load shifting.

Our control strategy is an economic optimizing model predictive controller, Economic MPC. Model Predictive Control (MPC) for constrained systems has emerged during the last 30 years as the most successful methodology for control of industrial processes [2]–[4]. MPC is increasingly being considered for refrigeration systems [5]–[7] and for power production plants [8], [9]. Traditionally, MPC is designed using objective functions penalizing deviations from a given set-point. MPC based on optimizing economic objectives has only recently emerged as a general methodology with efficient numerical implementations and provable stability properties [10]–[13]. The idea of utilizing load shifting capabilities to reduce total energy consumption is slowly gaining acceptance (see [14], [15]). However in this paper it is assumed that both power plants and refrigeration systems are owned by the same stakeholder since we are trying to optimize the combined operation.

This paper is organized as follows. Section II introduces Economic MPC. Section III describes the models used for our case study, and the results are provided in Section IV. We give conclusions in Section V.

II. Economic MPC for Linear Systems

In this section we describe the Economic Model Predictive Controller (MPC) for linear systems. The Economic MPC minimizes an economic cost directly as opposed to minimizing the deviation from a set-point in some norm. We consider continuous variables only and the resulting optimal control problem is formulated as a linear program. The solution of this program is implemented on the system in a receding

horizon manner. The Economic MPC is implemented for a linear distributed system with independent dynamics that must collaborate to meet a common goal.

A. Centralized System

The linear system in continuous time may be represented as

$$Y(s) = G_{yu}(s)U(s) + G_{yd}(s)D(s) \tag{1a}$$

$$Z(s) = G_{zu}(s)U(s) + G_{zd}(s)D(s) \tag{1b}$$

in which the transfer functions are multi-input-multi-output. $U \in \mathbb{C}^{n_u}$ is the manipulable variables, $D \in \mathbb{C}^{n_d}$ is known disturbances, $Y \in \mathbb{C}^{n_y}$ is the outputs associated with a cost, and $Z \in \mathbb{C}^{n_z}$ is the outputs associated with output constraints. G_{yu}, G_{yd}, G_{zu}, and G_{zd} are transfer function matrices of compatible size. Using a zero-order-hold discretization of the inputs, $u(t)$ and $d(t)$, that are related to $U(s)$ and $D(s)$, (1) may be represented as the discrete-time state space model

$$x_{k+1} = Ax_k + Bu_k + Ed_k \tag{2a}$$

$$y_k = Cx_k + Du_k + Fd_k \tag{2b}$$

$$z_k = C_z x_k + D_z u_k + F_z d_k \tag{2c}$$

Using this linear model we may formulate the Economic MPC as the linear program

$$\min_{\{x,u,y,z\}} \quad \phi = \sum_{k \in \mathcal{T}} c_y' y_k + c_u' u_k \tag{3a}$$

$$s.t. \quad x_{k+1} = Ax_k + Bu_k + Ed_k \quad k \in \mathcal{T} \tag{3b}$$

$$y_k = Cx_k + Du_k + Fd_k \quad k \in \mathcal{T} \tag{3c}$$

$$z_k = C_z x_k + D_z u_k + F_z d_k \quad k \in \mathcal{T} \tag{3d}$$

$$u_{\min} \le u_k \le u_{\max} \quad k \in \mathcal{T} \tag{3e}$$

$$\Delta u_{\min} \le \Delta u_k \le \Delta u_{\max} \quad k \in \mathcal{T} \tag{3f}$$

$$z_{\min} \le z_k \le z_{\max} \quad k \in \mathcal{T} \tag{3g}$$

with $\mathcal{T} \in \{0, 1, \ldots, N\}$. The cost of the Economic MPC is a linear function of the manipulable inputs, u_k, and the outputs, y_k. Typically, the cost is only dependent on the manipulable inputs, u_k, and $c_y = 0$. The manipulable inputs, u_k, are constrained by the input constraints (3e) and (3f). (3e) is a bound constraint on the inputs while (3f) is a constraint on the rate of movement ($\Delta u_k = u_k - u_{k-1}$). The outputs, z_k, are limited by the output constraints (3g). We assume that the Economic MPC (3) is feasible, i.e. that the initial state, x_0, and the disturbances, $\{d_k\}_{k=0}^N$, are such that the feasible manipulable variables, $\{u_k\}_{k=0}^N$, can bring the system to satisfy the output constraints (3g). If this is not the case, the output constraints must be formulated as soft constraints with a large penalty associated with violating the output limits, $z_{\min}$ and $z_{\max}$.

By state elimination, the Economic MPC (3) may be expressed as the linear program

$$\min_x \quad \psi = c'x \tag{4a}$$

$$s.t. \quad Ax \ge b \tag{4b}$$

and algorithms for linear programs (4) may be used for computing the solution of the Economic MPC.

B. Distributed Independent System

In this paper, we consider a distributed independent system

$$Y_i(s) = G_{yu,i}(s)U_i(s) + G_{yd,i}(s)D_i(s) \quad i \in \mathcal{P} \tag{5a}$$

$$Z_i(s) = G_{zu,i}(s)U_i(s) + G_{zd,i}(s)D_i(s) \quad i \in \mathcal{P} \tag{5b}$$

with $i \in \mathcal{P} = \{1, 2, \ldots, P\}$ being an index referring to each plant. The dynamically independent plants must collaborate to meet a common objective i.e. satisfy the market demand for the goods they produce. This representation may be related to (1) by $Y = [Y_1; Y_2; \ldots; Y_P]$, $Z = [Z_1; Z_2; \ldots; Z_P]$, $U = [U_1; U_2; \ldots; U_P]$, $D = [D_1; D_2; \ldots; D_P]$, $G_{yu}(s) = \text{diag}\{G_{yu,1}(s), G_{yu,2}(s), \ldots, G_{yu,P}(s)\}$, $G_{yd}(s) = \text{diag}\{G_{yd,1}(s), G_{yd,2}(s), \ldots, G_{yd,P}(s)\}$, $G_{zu}(s) = \text{diag}\{G_{zu,1}(s), G_{zu,2}(s), \ldots, G_{zu,P}(s)\}$, and $G_{zd}(s) = \text{diag}\{G_{zd,1}(s), G_{zd,2}(s), \ldots, G_{zd,P}(s)\}$. The representation (5) is useful because it may be used in Dantzig-Wolfe solution procedures for systems with a large number of plants, P [9], [16]. The set of plants, $\mathcal{P}$, consists of controllable producers (e.g. conventional power plants), $\mathcal{S}_C$, non-controllable producers (e.g. farms of wind turbines), $\mathcal{S}_{NC}$, and controllable consumers (e.g. large industrial facilities or cooling houses as in this paper), $\mathcal{D}$. We denote the producing plants by $\mathcal{S} = \mathcal{S}_C \cup \mathcal{S}_{NC}$.

The plants must collaborate such that the supply of goods exceed the demand of goods at all times

$$\sum_{i \in \mathcal{S}} y_{i,k} \ge \sum_{i \in \mathcal{D}} y_{i,k} + r_k \quad k \in \mathcal{T} \tag{6}$$

r_k is the demand from non-controllable consumers at time $k \in \mathcal{T}$.

The optimal control problem defining the Economic MPC for (5) may be stated as the block-angular linear program:

$$\min_{\{x,u,y,z\}} \quad \phi = \sum_{i \in \mathcal{S}} \left(\sum_k c_{u,i}' u_{i,k} + c_{y,i}' y_{i,k} \right) \tag{7a}$$

$$s.t. \quad \sum_{i \in \mathcal{S}} y_{i,k} - \sum_{i \in \mathcal{D}} y_{i,k} \ge r_k \tag{7b}$$

$$x_{i,k+1} = A_i x_{i,k} + B_i u_{i,k} + E_i d_{i,k} \tag{7c}$$

$$y_{i,k} = C_i x_{i,k} + D_i u_{i,k} + F_i d_{i,k} \tag{7d}$$

$$z_{i,k} = C_{z,i} x_{i,k} + D_{z,i} u_{i,k} + F_{z,i} d_{i,k} \tag{7e}$$

$$u_{\min,i} \le u_{i,k} \le u_{\max,i} \tag{7f}$$

$$\Delta u_{\min,i} \le \Delta u_{i,k} \le \Delta u_{\max,i} \tag{7g}$$

$$z_{\min,i} \le z_{i,k} \le z_{\max,i} \tag{7h}$$

with $i \in \mathcal{P}$ and $k \in \mathcal{T}$. The objective function (7a) says that the total cost of production from all the power plants in the time horizon considered must be minimal. (7b) couples the independent plants by requiring that the supply exceeds the demand. (7c)-(7e) is a discrete-time state space realization of (5). (7f) and (7g) constitute the input constraints. The output constraints are represented by (7h).

The supply-demand constraint (7b) and the output constraints (7h) may not be feasible for every disturbance and initial state scenario. In such situations (7) may be modified to a feasible linear program by representing (7b) and (7h) as soft constraints with large constraint violation penalties.

The Economic MPC (7) may be expressed as the block-angular linear program

$$\min_{\{x_i\}_{i \in \mathcal{P}}} \quad \psi = \sum_{i \in \mathcal{P}} c_i' x_i \tag{8a}$$

$$s.t. \quad \sum_{i \in \mathcal{P}} A_i x_i \geq b \tag{8b}$$

$$B_i x_i \geq d_i \quad i \in \mathcal{P} \tag{8c}$$

which may be solved efficiently using Dantzig-Wolfe decomposition. (8) is an instance of a linear program (4) with

$$x = \begin{bmatrix} x_1 \\ x_2 \\ \vdots \\ x_P \end{bmatrix} \quad c = \begin{bmatrix} c_1 \\ c_2 \\ \vdots \\ c_P \end{bmatrix} \quad A = \begin{bmatrix} A_1 & A_2 & \dots & A_P \\ B_1 & & & \\ & B_2 & & \\ & & \ddots & \\ & & & B_P \end{bmatrix} \quad b = \begin{bmatrix} b \\ d_1 \\ d_2 \\ \vdots \\ d_P \end{bmatrix}$$

C. Linear Programs and Control

The optimum of a linear program is an extreme point as illustrated in Fig. 1. This property of linear programs leads to either dead-beat or idle control when linear programs are used for solving model predictive control problems with an ℓ_1-penalty [17]. For Economic MPC the fact that the optimum is an extreme point implies that even small perturbations in the data or the disturbances may change the optimal solution dramatically. In practice, to handle this situation one often backs off a bit from the boundaries of the feasible region to leave some room for robustness. For the purpose of revealing the potential of Economic optimizing MPC for the combined control of both energy producing and consuming plants, we will use the Economic MPC in its basic form as described above.
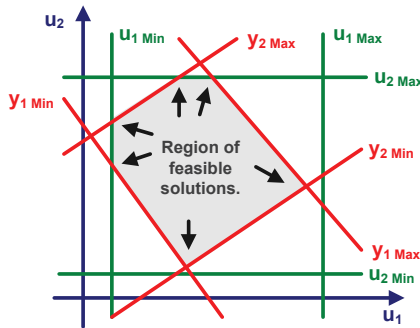

Fig. 1. Example of LP with two inputs and two outputs. Boundaries of the feasible region are illustrated with green for input constraints and red for output constraints. The arrows indicate possible optimal solutions which are always found at one of the vertexes depending on the objective function.

III. MODELS FOR A POWER SYSTEM

The case study used in this paper includes two controllable power generators and one power consumer. The power consumer is a cold room for which we provide a simple model. This case study is used to illustrate the properties and potential of Economic MPC in managing the power production and consumption in a distributed energy system. Compared to the studies in [8], [9], [16], the novelty in this paper is inclusion of a controllable power consumer to shed the power load.

A. Controllable Power Generators

[18] provides simple models for power generators. In this paper we used the models of the form

$$\phi_i = \sum_{k \in \mathcal{T}} c_i' u_{i,k} \tag{9a}$$

$$Y_i(s) = G_i(s) U_i(s) \qquad G_i(s) = \frac{1}{(\tau_i s + 1)^3} \tag{9b}$$

$$u_{\min,i} \leq u_{i,k} \leq u_{\max,i} \tag{9c}$$

$$\Delta u_{\min,i} \leq \Delta u_{i,k} \leq \Delta u_{\max,i} \tag{9d}$$

to model two conventional power generators where u_i is the power set-point for the i-th generator. (9a) represents the costs of producing power from a given power generator. Power generator 1 is cheap and slow, $(c_1, \tau_1, u_{\min,1}, u_{\max,1}, \Delta u_{\min,1}, \Delta u_{\max,1}) = (1, 20, 0, 15, -1, 1)$. Power generator 2 is expensive and fast, $(c_2, \tau_2, u_{\min,2}, u_{\max,2}, \Delta u_{\min,2}, \Delta u_{\max,2}) = (2, 10, 0, 12, -3, 3)$. The model in Eq. (9) describes the closed-loop system with internal controllers and is therefore quite simple without the lower level complexity of the generators. The model has been validated versus experimental data at DONG Energy, Denmark.

B. Simple Cold Room

The energy balance for the cold room is

$$mc_p \frac{dT_{cr}}{dt} = Q_{load} - Q_e \tag{10}$$

with

$$Q_{load} = (UA)_{amb-cr}(T_{amb} - T_{cr}) \tag{11a}$$

$$Q_e = (UA)_{cr-e}(T_{cr} - T_e) \tag{11b}$$

T_{cr} is the temperature in the cold room which must be kept within certain bounds, $T_{cr,\min} \leq T_{cr} \leq T_{cr,\max}$. T_e is the evaporation temperature of the refrigerant. It can be controlled by the compressor work and must satisfy $T_{cr} \geq T_e$. T_{amb} is the ambient temperature. UA is the heat transfer coefficient. m and c_p are the mass and the overall heat capacity of the refrigerated goods, respectively. The energy consumed by the refrigeration system is work performed by the compressors: $W_C = \eta Q_e$. η is the coefficient of performance. In this work η is assumed to be constant and

independent of the temperatures. Consequently

$$W_C(s) = \frac{a - bs}{\tau s + 1} T_e(s) + \frac{\alpha K_d}{\tau s + 1} T_{amb}(s) \qquad (12a)$$

$$T_{cr}(s) = \frac{K_u}{\tau s + 1} T_e(s) + \frac{K_d}{\tau s + 1} T_{amb}(s) \qquad (12b)$$

with $Y_3 = W_C$, $Z_3 = [T_{cr}; T_{cr} - T_e]$, $U_3 = T_e$, $D_3 = T_{amb}$. The parameters are

$$K_u = \frac{(UA)_{cr-e}}{(UA)_{cr-e} + (UA)_{amb-cr}} \qquad (13a)$$

$$K_d = \frac{(UA)_{amb-cr}}{(UA)_{cr-e} + (UA)_{amb-cr}} \qquad (13b)$$

$$\tau = \frac{mc_p}{(UA)_{cr-e} + (UA)_{amb-cr}} \qquad (13c)$$

$$\alpha = \eta(UA)_{cr-e} \qquad (13d)$$

$$a = \alpha(K_u - 1) \qquad (13e)$$

$$b = \alpha\tau \qquad (13f)$$

and the constraints are

$$T_{cr,min} \leq T_{cr} \leq T_{cr,max} \qquad (14a)$$

$$0 \leq T_{cr} - T_e \leq \infty \qquad (14b)$$

In addition to these constraints, we enforce the evaporation temperature (T_e) to be between specified limits and to respect some rate of change constraints. Therefore, the cooling system can be modeled in a form compatible with the Economic MPC for linear systems.

The model here is quite simplified, especially the assumption for (12). However the resulting dynamics are well suited for illustrating the conceptual case in this paper.

C. Supply and Demand

The production by the power generators, $y_{1,k} + y_{2,k}$, must exceed the demand for power by the cooling house and the other consumers

$$y_{1,k} + y_{2,k} \geq y_{3,k} + r_k \quad k \in \mathcal{T} \qquad (15)$$

We model farms of wind turbines as instantaneously changing systems and include the effect of their power production in the exogenous net power demand signal, r_k.

IV. RESULTS

The Economic Optimizing MPC as described above has been implemented in Matlab and simulations are presented in this section. Fig. 2 visualizes a simulation. In this scenario, the power demand from all other consumers than the cold room increases slowly, then stays at a steady state and eventually drops significantly. This sudden drop could for instance be seen as an increase in wind speed that changes the demand to the power generators drastically. The ambient temperature is assumed to be constant in this scenario.

If the cold room was a non-controllable load from the power producers' point of view but of course still had to consume as little power as possible then, intuitively, the evaporation temperature T_e would stabilize at a level sufficient for keeping the temperature T_{cr} just below

the upper constraint. Thus, with a constant load on the refrigeration system the power demand W_C that should be added to the reference r would simply be a constant over the entire scenario. Among other things, the result is that a great amount of surplus electricity is produced after the sudden drop in demand. However, when the cold room is considered a controllable consumer it is able to absorb the majority of this otherwise redundant energy, as seen in Fig. 2. This causes the temperature in the cold room to decrease from the upper constraint to the lowest feasible level. Due to the thermal capacity in the refrigerated goods the "pre-cooling" applied when the power is "free" makes it possible to entirely shut down the cooling and thereby limit power consumption at a time where the production cost has increased. Other positive effects can be noticed. A slight pre-cooling occurs up to time= 160 such that the refrigeration system can be shut off just before the power demand reaches its maximum, thereby limiting the overshoot in the production. Also at time= 275 it is seen how the power consumed by the refrigeration system momentarily goes to zero allowing the decrease in the slow power generator to be initiated earlier without causing an underproduction.

As mentioned the potential savings depend on the time constant and the temperature limits of the cold room and thereby its ability to store coldness. Fig. 3 is the result of running a series of simulations on both a system with the cold room made controllable by the power producer and one where it is non-controllable. The simulations are performed for a range of mc_p, i.e. different amounts of goods in the cold room but identical loads on the system, and the savings for each pair of simulations are calculated in percentages and plotted. As expected larger time constants entails larger savings. Furthermore the savings tend to go asymptotically towards some maximum value. The maximum is clearly dependent on the chosen scenario since the amount of "free" power available sets an upper limit on the potential savings.

Another possibility for utilizing the combined control scheme for controllable power producers and controllable consumers lies in the daily variations. For instance the outdoor temperature is usually higher, causing a higher load on the refrigeration system, during the day than it is at nighttime. Also power demands are known to vary over the day, e.g. due to industries and domestic users shutting down most of their consumption at night while the wind turbines are still producing roughly the same amount of energy. The potential savings by controlling some of the loads in a scenario with varying outdoor temperature and power demands are investigated in the two simulations seen in Fig. 4. In Fig. 4.(a)-(b) it is observed how the behavior of the refrigeration system is as expected when the cold room is non-controllable. When the outdoor temperature is high a lot of cooling has to be applied in order to keep the temperature in the cold room at the maximal limit. Unfortunately this coincides with a time where the demand from all other
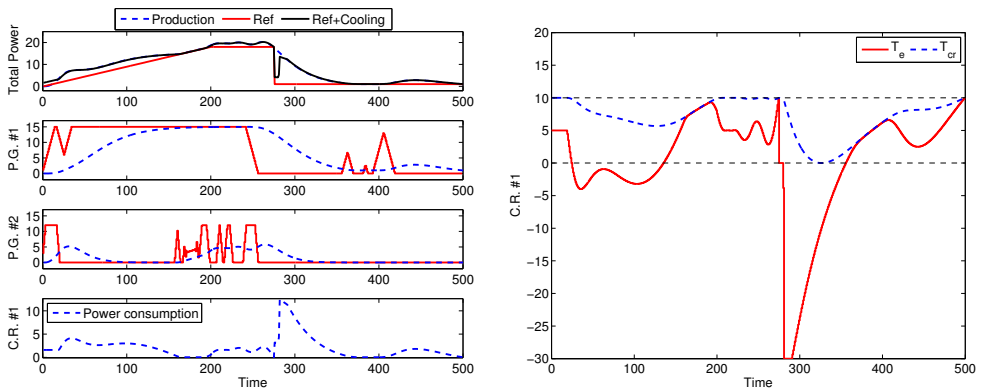
(a) Power productions / consumption. P.G. #1 and 2 show the power productions from the two power plants (dotted blue) and their power setpoints (solid red). C.R. #1 is power consumption in the cold room and "Total Power" shows total power production (dotted blue) versus the reference consumption (with (solid black) and without (solid red) the consumption for refrigeration included.)

(b) Temperature in the cold room T_{cr} and the control signal for the refrigeration system T_e. $T_{cr,min}$ and $T_{cr,max}$ are shown with dotted black.

Fig. 2. Simulation of Power Generation problem

consumers is high too, causing the needed cooling capacity to be rather expensive to deliver. If we instead take a look at Fig. 4.(c)-(d) an evaporation temperature trajectory that would have been hard to come up with by intuition is seen. The system now uses the ability to pre-cool when excess power is available and thereby saves a lot of power by reducing the cooling capacity when the energy is in high demand. The temperature of the cold room is varying between the maximal limit and almost down to the lower constraint. In this particular scenario the savings amount to 17 % for a system with $mc_p = 60$.
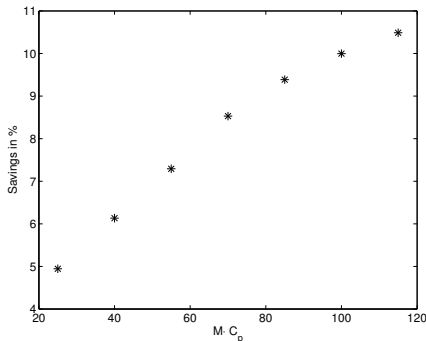

Fig. 3. Savings compared to non-controllable load for different values of mc_p

V. CONCLUSION

We have presented Economic MPC and demonstrated its use on a conceptual example with a portfolio of power producers (power generators) and a power consumer (a cold room). Economic MPC provides the most cost efficient production plan to make supply exceed demand while observing plant limitations. For the conceptual example used in this paper, Economic MPC can utilize the thermal capacity in the cold room such that significant cost savings are obtained. The purpose of this paper was to present the concept of Economic MPC for a set of independent dynamic systems that must be coordinated to minimize a common objective and motivate this type of controllers in energy systems engineering. Future extensions include demonstration of Economic MPC for large scale systems using Dantzig-Wolfe decomposition.

REFERENCES

[1] R. Scattolini, "Architectures for distributed and hierarchical model predictive control," *Journal of Process Control*, pp. 723–731, 2009.
[2] S. J. Qin and T. A. Badgwell, "A survey of industrial model predictive control technology," *Control engineering practice*, vol. 11, no. 7, pp. 733–764, 2003.
[3] J. B. Rawlings and D. Q. Mayne, *Model Predictive Control: Theory and Design*. Nob Hill Publishing, 2009.
[4] J. M. Maciejowski, *Predictive control: with constraints*. Pearson education, 2002.
[5] L. F. S. Larsen, "Model based control of refrigeration systems," Ph.D. dissertation, Aalborg University, Dep. of Control Engineering, 2005.
[6] D. Sarabia, F. Capraro, L. F. S. Larsen, and C. de Prada, "Hybrid nmpc of supermarket display cases," *Control Engineering Practice*, vol. 17, no. 4, pp. 428–441, 2008.
[7] L. F. S. Larsen, T. Geyer, and M. Morari, "Hybrid mpc in supermarket refrigeration system," in *IFAC world congress*, Prague, Czech Republic, 2005.
[8] K. Edlund, J. D. Bendtsen, S. Børresen, and T. Mølbak, "Introducing Model Predictive Control for Improving Power Plant Portfolio Performance," in *Proceedings of the 17th IFAC World Congress*, 2008.

(a) Power productions / consumption. Non-controllable load.

(b) Temperatures. Non-controllable load. $T_{cr,min}$ and $T_{cr,max}$ with dotted black.

(c) Power productions / consumption. Controllable load.

(d) Temperatures. Controllable load. $T_{cr,min}$ and $T_{cr,max}$ with dotted black.
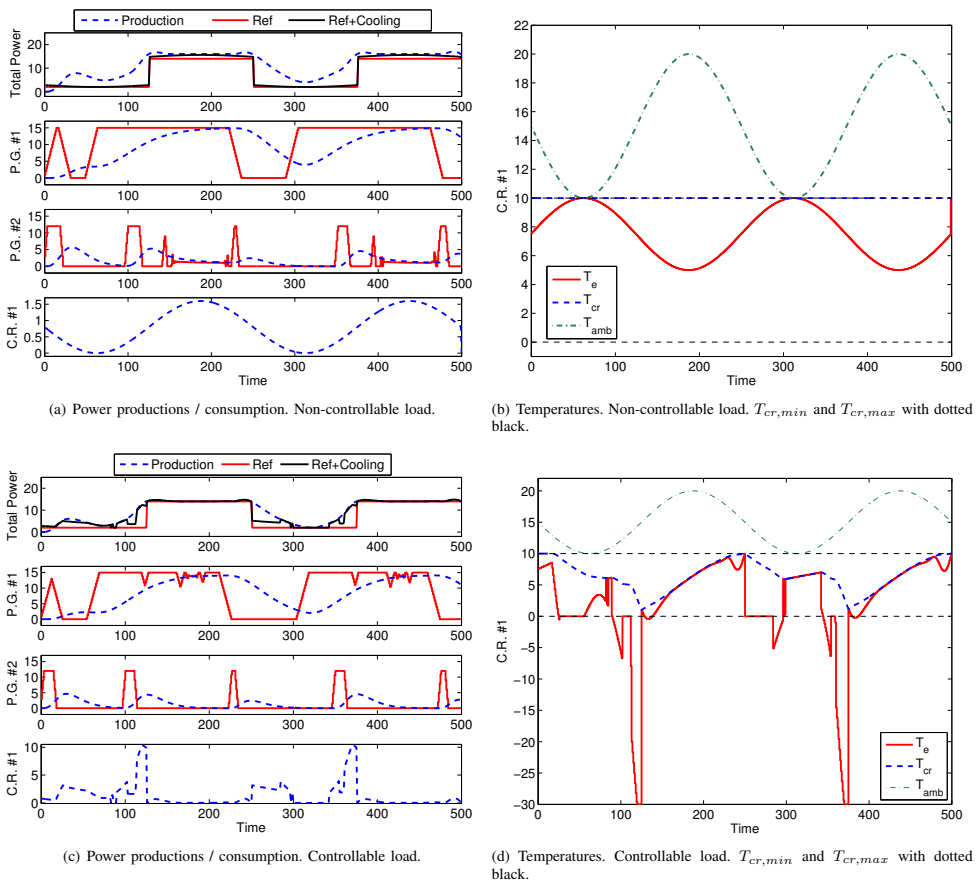
Fig. 4. Simulation of Power Generation problem with varying outdoor temperature and night/day power usage. For Fig. (a) and (c) P.G. #1 and 2 show the power productions from the two power plants (dotted blue) and their power set-points (solid red). C.R. #1 is power consumption in the cold room and "Total Power" shows total power production (dotted blue) versus the reference consumption (with (solid black) and without (solid red) the consumption for refrigeration included. Fig. (b) and (d) show the temperature in the cold room T_{cr} and the control signal for the refrigeration system T_e.

[9] K. Edlund and J. B. Jørgensen, "A dantzig-wolfe MPC algorithm for power plant portfolio control," *International Journal of Control*, p. submitted, 2010.

[10] J. B. Rawlings, D. Bonne, J. B. Jørgensen, A. N. Venkat, and S. B. Jørgensen, "Unreachable setpoints in model predictive control," *IEEE Transactions on Automatic Control*, vol. 53, no. 9, pp. 2209–2215, 2008.

[11] M. Diehl, R. Amrit, and J. B. Rawlings, "A Lyapunov Function for Economic Optimizing Model Predictive Control," *IEEE Transactions on Automatic Control*, 2009.

[12] J. B. Rawlings and R. Amrit, "Optimizing Process Economic Performance Using Model Predictive Control," *Nonlinear Model Predictive Control: Towards New Challenging Applications*, pp. 119–138, 2009.

[13] K. Edlund, L. E. Sokoler, and J. B. Jørgensen, "A primal-dual interior-point linear programming algorithm for MPC," in *Joint 48th IEEE Conference on Decision and Control and 28th Chinese Control Conference*. Shanghai, P.R. China, December 16-18, 2009: IEEE,

2009, pp. 351–356.

[14] G. L. van Harmelen, "The virtual power station targeting residential, industrial and commercial controllable loads," *Proceedings of the IFAC Conference on Technology Transfer in Developing Countries*, pp. 45–48, 2001.

[15] R. Bush and G. Wolf, "Utilities load shift with thermal storage." *Transmission & Distribution World*, p. 12, 2009.

[16] K. Edlund, J. D. Bendtsen, and J. B. Jørgensen, "Hierarchical model-based predictive control of a power plant portfolio," *Control Engineering Practice*, p. submitted, 2010.

[17] C. V. Rao and J. B. Rawlings, "Linear programming and model predictive control," *Journal of Process Control*, vol. 10, no. 2-3, pp. 283–289, 2000.

[18] K. Edlund, T. Mølbak, and J. D. Bendtsen, "Simple models for model-based portfolio load balancing controller synthesis," in *IFAC Symposium on Power Plants and Power Systems Control*. Tampera, Finland: IEEE, 2009.

Economic MPC for Power Management in the Smart Grid

Economic MPC for Power Management in the SmartGrid

Tobias Gybel Hovgaard[a,c], Kristian Edlund[b], John Bagterp Jørgensen[c]

[a]Danfoss Refrigeration and A/C Controls, Nordborgvej 81, 6430 Nordborg, Denmark
[b]DONG Engergy A/S, Kraftværksvej53, 7000 Fredericia, Denmark
[c]DTU Informatics, Richard Petersens Plads, Building 321, 2800 Lyngby, Denmark

Abstract

To increase the amount of green energy (e.g. solar and wind) significantly a new intelligent electrical infrastructure is needed. We must not only control the production of electricity but also the consumption in an efficient and proactive manner. This future intelligent grid is in Europe known as the SmartGrid. In this paper we demonstrate the use of Economic Model Predictive Control to operate a portfolio of power generators and consumers such that the cost of producing the required power is minimized. With conventional coal and gas fired power generators representing the controllable power production and a significant share of renewable energy, such as parks of wind turbines, representing the uncontrollable power generators we have demonstrated how the addition of controllable consumers, such as large cold rooms or supermarkets with a thermal capacity, can infuse the desired flexibility of the grid for utilization of more green energy and also lower the total cost. We formulate the supply-demand constraint as a probabilistic constraint, thereby robustifying the solution against uncertainties in power demand. We use small conceptual examples for simulations.
Keywords: Predictive Control, Smart Power Applications, Optimization.

1. Introduction

In this paper we extend the results presented in Hovgaard et al. (2010). We have introduced Economic MPC to control a number of independent dynamic systems that must collaborate to minimize the overall cost in satisfying the cooling demand for some goods while meeting market demands for power at all times. A larger share of intermittent stochastic power generating sources such as wind turbines makes it difficult to balance demand and supply of electricity in a flexible and cost efficient manner. To account for this we introduce large power consumers, such as cold rooms, or an aggregation of a number of alike consumers like supermarket systems, with the ability to adjust the power consumption profile to the power supply. Due to the large thermal capacity of cold rooms, their consumption of electricity can, to some degree, be shifted in time to benefit the overall system. The thermal capacity in the refrigerated goods is then utilized to store "coldness" such that the refrigeration system can cool extra when there is an over production of energy and thereby lower its consumption at other times. The temperature is allowed to vary within certain bounds which have no impact on food quality. Van Harmelen (2001), Bush and Wolf (2009) and Oldewurtel et al. (2010) also utilized load shifting capabilities to reduce total energy consumption.

Our control strategy is an economic optimizing model predictive controller, Economic MPC. MPC for constrained systems has emerged during the last 30 years as the most successful methodology for control of industrial processes (Qin and Badgwell, 2003). MPC is increasingly being considered for refrigeration systems (Sarabia et al. (2008) and Larsen et al. (2005)) and for power production plants (Edlund et al., 2008). MPC

based on optimizing economic objectives has only recently emerged as a general methodology (Rawlings et al. (2008) and Diehl et al. (2009)). To put our strategy into a more realistic scenario in which different uncertainties affect the system this paper extends the Economic MPC to provide robust performance in the presence of forecast uncertainties. This is done in a way similar to Oldewurtel et al. (2010) where energy consumption for climate control is minimized under influence of uncertain weather predictions. Several works exist that consider constrained MPC in the presence of uncertainty (Bemporad and Morari, 1999). Boyd et al. (1998) and Lobo et al. (1998) demonstrate that probabilistic linear constraints can be written as second-order cone (SOC) constraints that are convex provided the probability involved is greater than 0.5.

2. Economic MPC for Linear Systems

The Economic MPC minimizes an economic cost directly as opposed to minimizing the deviation from a setpoint in some norm. We consider continuous variables only and the resulting optimal control problem is formulated as a linear program. The solution of this program is implemented on the system in a receding horizon manner.

2.1. Distributed Independent Systems

We consider a distributed independent system in continuous time. The optimal control problem defining the Economic MPC may then be stated as the block-angular linear program:

$$\min_{\{x,u,y,z\}} \phi = \sum_{i \in S_C} \left(\sum_k c'_{u,i} u_{i,k} + c'_{y,i} y_{i,k} \right) \tag{1a}$$

$$s.t. \quad \sum_{i \in S_C} y_{i,k} - \sum_{i \in D} y_{i,k} \geq r_k \tag{1b}$$

$$x_{i,k} = A_i x_{i,k} + B_i u_{i,k} + E_i d_{i,k} \tag{1c}$$

$$y_{i,k} = C_i x_{i,k} + D_i u_{i,k} + F_i d_{i,k} \tag{1d}$$

$$z_{i,k} = C_{z,i} x_{i,k} + D_{z,i} u_{i,k} + F_{z,i} d_{i,k} \tag{1e}$$

$$u_{\min,i} \leq u_{i,k} \leq u_{\max,i}, \quad \Delta u_{\min,i} \leq \Delta u_{i,k} \leq \Delta u_{\max,i} \tag{1f}$$

$$z_{\min,i} \leq z_{i,k} \leq z_{\max,i} \tag{1g}$$

The set of plants, P, consists of controllable producers (e.g. conventional power plants), S_C, non-controllable producers (e.g. farms of wind turbines), S_{NC}, and controllable consumers (e.g. large cooling houses as in this paper), D. The dynamically independent plants must collaborate to meet a common objective i.e. satisfy the market demand for the goods they produce. We model farms of wind turbines as instantaneously changing systems and combine the effect of their power production with the non-controllable consumption in the exogenous net power demand signal r_k. $i \in P$ and $k \in T$. $T \in \{0, 1, \ldots, N\}$. The objective function (1a) says that the total cost of production from all the power plants in the time horizon considered must be minimal. (1b) couples the independent plants by requiring that the supply exceeds the demand. (1c)-(1e) is a discrete time state space realization of the independent system. (1f) constitute the input constraints and a constraint on the rate of movement and (1g) is an output constraint.

2.2. Linear Programs and Control with Uncertainty

The optimum of a linear program is an extreme point as illustrated in Fig. 1. This property of linear programs leads to either dead-beat or idle control when linear

programs are used for solving model predictive control problems with an $l1$-penalty (Rao and Rawlings, 2000). For Economic MPC the fact that the optimum is an extreme point implies that even small perturbations in the data may change the optimal solution dramatically. Exemplified by the power production case, an optimal solution is one where the amount of power produced exactly matches the consumption. However, due to the optimization relying on a prediction of power production from non-controllable producers there is a risk of power shortage if e.g. the estimate of power from non-controllable producers was overstated. Since this situation is very expensive a more desirable solution would
be to produce just enough extra power to leave room for most of the effect from uncertainties. In this work we introduce a confidence interval such that the solution accounts for the amount of uncertainty. The tubes in Fig. 1 illustrates this.
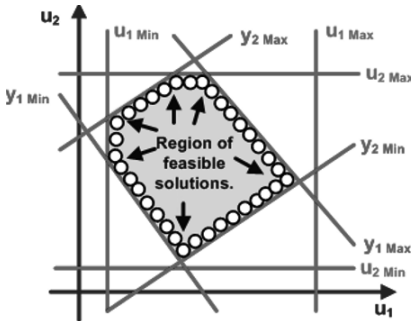

Fig. 1. Example of LP with two inputs and two outputs. Boundaries of the feasible region are illustrated with green for input constraints and red for output constraints. The arrows indicate possible optimal solutions and the circles illustrate the confidence interval around a solution caused by uncertainty.

2.3. Probabilistic Constraints
In the presence of uncertainty we formulate a stochastic optimization problem as:

$$\min\ E\left\{\sum_{k=0}^{N} c'_{u,k}\, u_k\right\} \tag{2a}$$

$$s.t.\quad \Pr ob\left\{\sum_{i\in S_C} y_{i,k} - \sum_{i\in D} y_{i,k} \ge r_k\right\} \ge 1-\alpha,\quad \alpha\in[0;1] \tag{2b}$$

Eq. (2a) is furthermore subject to the constraints in Eq. (1c)-(1h). By assuming that the uncertain variable r_k is distributed as $r_k \approx N(\bar{r}_k, \sigma^2)$ the probability constraint in Eq. (2b) can be reformulated as follows:

$$\Pr ob\{Y \ge R\} \ge 1-\alpha \tag{3a}$$

$$\frac{R-\bar{R}}{\sigma} \approx N(0,1) \Rightarrow \Phi\left(\frac{Y-\bar{R}}{\sigma}\right) \ge 1-\alpha \quad\Rightarrow\quad Y \ge \bar{R} + \sigma\cdot\Phi^{-1}(1-\alpha) \tag{3b}$$

where $\Phi(x)$ is the cumulative distribution function of a zero mean unit variance Gaussian random variable x. The constraint in Eq. (3b) is a deterministic constraint.

3. Simple Power Management Scenario
The case study used in this paper includes two controllable power generators and one power consumer. The power consumer is a cold room for which we provide a simple model.

3.1. Controllable Power Generators
Edlund et al. (2009) provides simple models for power generators. In this paper we use the models of the form:

$$\phi_i = \sum_{k \in T} c'_{u,i} \, u_{i,k} \tag{4a}$$

$$Y_i(s) = G_i(s)U_i(s), \quad G_i(s) = \frac{1}{(\tau_i s + 1)^3} \tag{4b}$$

$$u_{\min,i} \le u_{i,k} \le u_{\max,i}, \quad \Delta u_{\min,i} \le \Delta u_{i,k} \le \Delta u_{\max,i} \tag{4c}$$

where u is power set-point. Generator 1 is cheap and slow while generator 2 is fast and expensive.

3.2. Simple Cold Room

By setting up the energy balances for the cold room we find the following simplified dynamics:

$$W_C(s) = \frac{a - bs}{\tau s + 1} T_e(s) + \frac{\alpha K_d}{\tau s + 1} T_{amb}(s) \tag{5a}$$

$$T_{cr}(s) = \frac{K_u}{\tau s + 1} T_e(s) + \frac{K_d}{\tau s + 1} T_{amb}(s) \tag{5b}$$

T_{cr} is the temperature in the cold room which must be kept within certain bounds, $T_{cr,\min} \le T_{cr} \le T_{cr,\max}$. T_e is the evaporation temperature of the refrigerant. It can be controlled by the compressor work and must satisfy $T_e \le T_{cr}$. T_{amb} is the ambient temperature and W_C is the energy consumed by the system.

4. Results

This section illustrates the results from simulation of our case study on a scenario with a sudden steps in net power demand. Fig. 2 shows an example without utilizing the consumer in the power management problem. Hence the cold room consumes a constant amount of energy that is sufficient for keeping the temperature below the upper limit as this minimizes the energy consumption. In Fig. 3 the cold room is regarded as a controllable consumer. It is seen how the surplus electricity following the drop in demand is absorbed by the refrigeration system resulting in a lower energy consumtion later on.
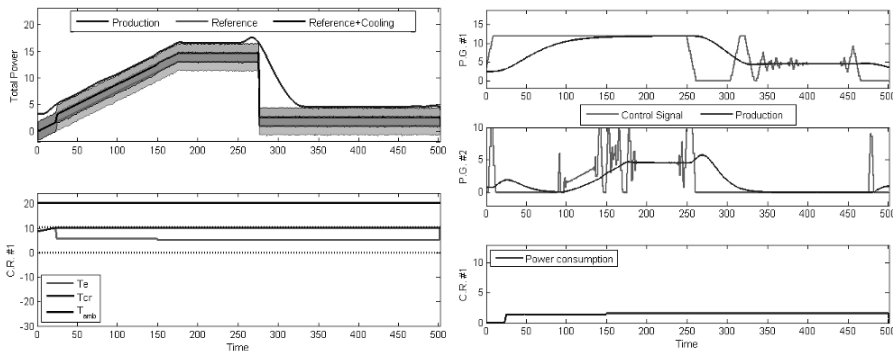

Fig. 2. No collaboration between power producers and consumers.
Left: "Total Power" shows total power production (blue) versus the reference consumption (with (black) and without (red) the refrigeration). C.R. #1 shows the temperature in the cold room T_{cr} and the control signal T_e. ($T_{cr,min}$, $T_{cr,max}$) and outdoor temperature, T_{amb}, are shown with dotted and solid black respectively. Right: Power productions / consumptions. The shaded band show the 99% confidence interval from 10,000 random instances.
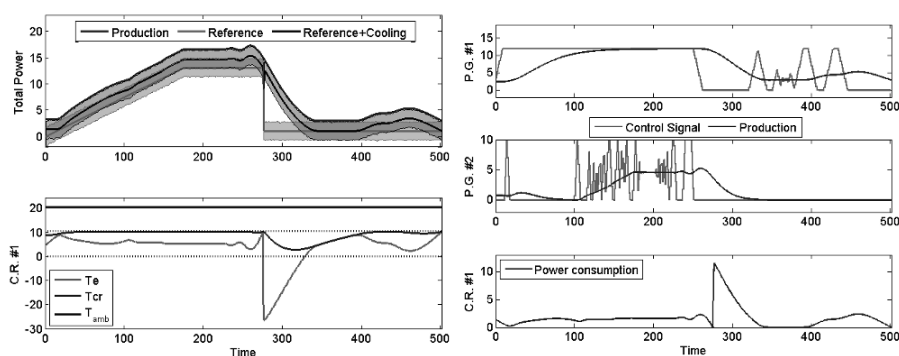
Fig. 3. Collaboration between power producers and consumers.

References

Bemporad, A. and Morari, M. (1999). Robust model predictive control: A survey. Robustness in Identification and Control, 207–226.

Boyd, S., Crusius, C., and Hansson, A. (1998). Control applications of nonlinear convex programming. Journal of Process Control, 8(5-6), 313–324.

Bush, R. and Wolf, G. (2009). Utilities load shift with thermal storage. Transmission & Distribution World, 12.

Diehl, M., Amrit, R., and Rawlings, J.B. (2009). A Lyapunov Function for Economic Optimizing Model Predictive Control. IEEE Transactions on Automatic Control.

Edlund, K., Bendtsen, J.D., Børresen, S., and Mølbak, T. (2008). Introducing Model Predictive Control for Improving Power Plant Portfolio Performance. In Proceedings of the 17th IFAC World Congress. IFAC.

Edlund, K., Mølbak, T., and Bendtsen, J.D. (2009). Simple models for model-based portfolio load balancing controller synthesis. In IFAC Symposium on Power Plants and Power Systems Control 2009. IEEE.

Hovgaard, T.G., Edlund, K., and Jørgensen, J.B. (2010). The Potential of Economic MPC for Power Management. In 49th IEEE Conference on Decision and Control, 2010, accepted.

Larsen, L.F.S., Geyer, T., and Morari, M. (2005). Hybrid mpc in supermarket refrigeration system. In IFAC world congress 2005. Prague, Czech Republic.

Lobo, M.S., Vandenberghe, L., Boyd, S., and Lebret, H. (1998). Applications of second-order cone programming* 1. Linear Algebra and its Applications, 284(1-3), 193–228.

Oldewurtel, F., Parisio, A., Jones, C.N., Morari, M., Gyalistras, D., Gwerder, M., Stauch, V., Lehmann, B., andWirth, K. (2010). Energy Efficient Building Climate Control using Stochastic Model Predictive Control and Weather Predictions. In Proc. of American Control Conference 2010, 5100–5105.

Qin, S.J. and Badgwell, T.A. (2003). A survey of industrial model predictive control technology. Control engineering practice, 11(7), 733–764.

Rao, C.V. and Rawlings, J.B. (2000). Linear programming and model predictive control. Journal of Process Control, 10(2-3), 283–289.

Rawlings, J.B., Bonne, D., Jørgensen, J.B., Venkat, A.N., and Jørgensen, S.B. (2008). Unreachable setpoints in model predictive control. IEEE Transactions on Automatic Control, 53(9), 2209–2215.

Sarabia, D., Capraro, F., Larsen, L.F.S., and de Prada, C. (2008). Hybrid nmpc of supermarket display cases. Control Engineering Practice, 17(4), 428–441.

Van Harmelen, G.L. (2001). The virtual power station targeting residential, industrial and commercial controllable loads. IFAC Conference on Technology Transfer in Developing Countries - Proceedings volume from IFAC Conference, 45–48.

Power Consumption in Refrigeration Systems – Modeling for Optimization

Power Consumption in Refrigeration Systems - Modeling for Optimization

Tobias Gybel Hovgaard, Lars F.S. Larsen, Morten J. Skovrup, John Bagterp Jørgensen

Abstract— **Refrigeration systems consume a substantial amount of energy. Taking for instance supermarket refrigeration systems as an example they can account for up to $50 - 80\%$ of the total energy consumption in the supermarket. Due to the thermal capacity made up by the refrigerated goods in the system there is a possibility for optimizing the power consumption by utilizing load shifting strategies. This paper describes the dynamics and the modeling of a vapor compression refrigeration system needed for sufficiently realistic estimation of the power consumption and its minimization. This leads to a non-convex function with possibly multiple extrema. Such a function can not directly be optimized by standard methods and a qualitative analysis of the system's constraints is presented. The description of power consumption contains nonlinear terms which are approximated by linear functions in the control variables and the error by doing so is investigated. Finally a minimization procedure for the presented problem is suggested.**

I. INTRODUCTION

Supermarket refrigeration and refrigeration systems in general have been modeled for both analysis and control in several preceding publications. These are both concerned with the overall system [1]–[4] and the complex thermodynamics of the individual parts as evaporators and condensers [5], [6]. However the focus in this paper is on describing the power consumption in supermarket refrigeration systems on a form that enables us to use optimization methods like Model Predictive Control (MPC) (see e.g. [7], [8]) for minimizing the total cost of running the system. This is not a completely new idea either. In [1] and [9] MPC is applied to refrigeration systems and in [4] optimization is applied in order to utilize the daily variations to minimize power consumptions. The models used in such papers tend to be rather simple in their description of e.g. the work done in the compressor in order to make them fit into standard forms suitable for optimization and MPC. Thus, the current work focuses on choosing an abstraction level for the model such that sufficient simplicity can be obtained but with significantly improved accuracy with respect to energy consumption.

Our motivation for the model described in this paper is the desire to utilize Economic Optimizing MPC for refrigeration systems in order to cut down on energy

costs related to operating the system and to enable the refrigeration system to be a flexible power consumer. The United States' and Europe's development for future intelligent electricity grid is called GridWise and SmartGrid, respectively. GridWise and SmartGrid are intended to be the smart electrical infrastructure required to increase the amount of green energy (solar and wind) significantly. To obtain an increasing amount of electricity from intermittent energy sources such as solar and wind, we must not only control the production of electricity but also the consumption of electricity in an efficient, agile and probably proactive manner. In [10] we demonstrated the potential of Economic MPC for an example portfolio with two power plants and one large cold room. This study revealed significant possibilities for saving power and for better utilization of green energy. However the models used for the cold room were very simplified and only worked for this conceptual case and the need for improved modeling for simulating realistic scenarios was revealed.

Traditionally, MPC is designed using objective functions penalizing deviations from a given set-point. MPC based on optimizing economic objectives has only recently emerged as a general methodology with efficient numerical implementations and provable stability properties [11]–[14]. The main purpose of controlling a refrigeration system is usually not to track a certain cold room temperature exactly but merely to keep it within specified bounds at the lowest possible cost. Thus, Economic MPC is an appealing strategy and a suitable objective function which is directly related to the power consumption and which has properties such that it can be optimized in an Economic MPC scheme is presented in this paper. Furthermore a minimization procedure for minimizing the resulting non-convex objective function is proposed.

The remaining parts of this paper are organized as follows. Section II models the dynamics of a refrigeration system from an appropriate abstraction level and presents the constraints of the system. Section III presents the functions for estimating the power consumption along with linearization of the nonlinear terms. The constraints are compared to the power consumption and the possibility for minimizing the function uniquely is discussed. A procedure for minimization of the power consumption is suggested in section IV. We give conclusions in Section V.

T.G. Hovgaard and L.F.S. Larsen are with Danfoss A/S, Nordborgvej 81, DK-6430 Nordborg, Denmark {tgh,lars.larsen}@danfoss.com

M.J. Skovrup is with IPU Technology Development, Building 403, DK-2800 Kgs. Lyngby, Denmark mjs@ipu.dk

J.B. Jørgensen is with DTU Informatics, Technical University of Denmark, Richard Petersens Plads, Building 321, DK-2800 Kgs. Lyngby, Denmark jbj@imm.dtu.dk

Fig. 1.   Schematic layout of basic refrigeration system.

Fig. 2.   Power consumption in the compressor and the condenser fan at varying condensing pressure. ($P_e = 2$ bar and $T_{cr} = 10°C$).

II. Modeling the Refrigeration System

Most supermarket refrigeration systems utilize a vapor compression cycle where a refrigerant is circulated in a closed loop consisting of a compressor, an expansion valve and two heat exchangers, an evaporator in the cold storage room and a condenser/gas cooler located in the surroundings. When the refrigerant evaporates it absorbs heat from the cold reservoir which is rejected to the hot reservoir by condensation. In order to keep the refrigeration cycle flowing with the heat transfers as described here, the evaporation temperature (T_e) has to be lower than the temperature in the cold reservoir (T_{cr}) and the condensation temperature has to be higher than the temperature at the hot reservoir (T_a). By inserting a compressor between the evaporator and the condenser the pressure, and thereby also the saturation temperature, of the refrigerant is increased such that the necessary temperature differences are achieved. Thus, low pressure refrigerant (P_e) from the outlet of the evaporator is compressed to a high pressure (P_c) at the inlet to the condenser. The expansion valve at the inlet to the evaporator upholds the pressure difference ($P_c > P_e$). The setup is sketched in Fig. 1 with one cold storage room connected to the system. In most supermarket refrigeration systems several cold storage rooms, e.g. display cases, are connected to a common compressor rack and condensing unit. Hence, all the individual display cases, which might have to satisfy different demands to temperatures, often sees the same evaporation temperature in a typical setup. However each unit has its own inlet valve for individual temperature control.

The dynamics inside each display case are nonlinear and require several dynamic variables to be modeled in order to get at proper fit. Furthermore the inlet valve in many systems can only be on or off rather than continuously controlled which leads to switched dynamics. But from a higher abstraction level considering only the long-term average of the temperature in the stored goods all these complicated dynamics can be neglected by assuming that inner control loops controlling the inlet valve are already established. If we consider a typical control strategy for most Danfoss refrigeration systems today this is a reasonable assumption since it relies on precisely such an inner controller which
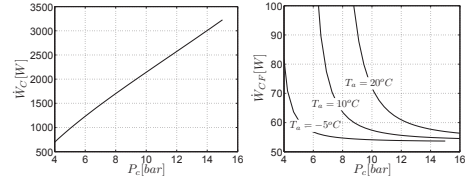
opens and closes the inlet valve according to defined hysteresis boundaries on the temperature in the cold room and a superheat controller which measures temperature and pressure at the outlet of the evaporator and makes sure that the liquid-gas front in the evaporator keeps a certain distance to the outlet.

The condensing pressure is normally controlled by a fan blowing air across the condenser. According to [15] the optimal condensing temperature ($T_c^* = T_{sat}(P_c^*)$) can be computed quite accurately as:

$$T_c^* = T_a + \Delta T \tag{1}$$

where ΔT is a constant.

It is obvious from Fig. 1 that energy is consumed for driving the compressor rack, the fans at the condensation unit and a fan circulating the air in the cold room through the evaporator. Hence, total energy consumption is given by:

$$\dot{W} = \dot{W}_C + \dot{W}_{CF} + \dot{W}_{EF} \tag{2}$$

where $\dot{W}$ denotes power consumption and the subscripts indicates the individual components; compressor (C), condenser fan (CF) and evaporator fan (EF). As it is stated in [4] and also illustrated on Fig. 2 the power consumed by the compressor is by far the largest and this will be the scope of further modeling in this work.

Fig. 2 furthermore illustrates that it requires less energy to decrease the condensation pressure when the ambient temperature is low. Hence the work done in the compressor can be drastically reduced.

A. Simple Cold Room

In the following the sufficient dynamics for optimizing power consumption in a refrigeration system are presented. It is assumed that the mass of the refrigerated goods acts as a low pass filter with respect to the temperature such that the switching in the inlet valve can be neglected. By doing this the cooling capacity applied to the cold room ($\dot{Q}_e$) can be considered as a continuous manipulable variable. Additionally, the evaporation temperature (T_e) is considered continuously controllable. In practice a local suction pressure controller acts on the compressors in order

to keep T_e as desired but since the dynamics of this inner control loop, and those of the temperature control loop at the inlet valve, are typically much faster than the change of temperature in the goods it is reasonable to assume that if we ask for a certain T_e or $\dot{Q}_e$ then, from the system's point of view it is achieved (almost) immediately. The controllable inputs are bounded by constraints on e.g. maximum compressor capacity and these limitations will also be considered. The output of the system is the cold room temperature (T_{cr}) and the purpose of controlling the refrigeration system is to keep this temperature within certain bounds and to do so as cheap as possible with respect to energy consumption and costs.

The temperature in the cold room can be described by setting up a simple energy balance as in Eq. (3).

$$mc_p \frac{dT_{cr}}{dt} = \dot{Q}_{load} - \dot{Q}_e \qquad (3)$$

with

$$\dot{Q}_{load} = (UA)_{amb-cr} \cdot (T_{amb} - T_{cr}) \qquad (4a)$$

$$\dot{Q}_e = (UA)_{cr-e} \cdot (T_{cr} - T_e) \qquad (4b)$$

where UA is the heat transfer coefficient and m and c_p are the mass and the overall heat capacity of the refrigerated goods, respectively. T_{amb} is the temperature of the ambient air which puts the heat load on the refrigeration system.

In order to get the equations on the right form for the optimization algorithms we insert (4a) in (3), while leaving $\dot{Q}_e$ as a direct input. Then the Laplace transform is applied from which we get the following system description:

$$T_{cr}(s) = \frac{K_u}{\tau s + 1} \dot{Q}_e(s) + \frac{K_d}{\tau s + 1} T_{amb}(s) \qquad (5)$$

where the parameters are given as:

$$K_u = -\frac{1}{(UA)_{amb-cr}}, \quad K_d = 1, \quad \tau = \frac{m \cdot c_p}{(UA)_{amb-cr}} \quad (6)$$

The different variables of the system are limited by the following constraints:

$$T_{cr,min} \leq T_{cr} \leq T_{cr,max} \qquad (7a)$$

$$0 \leq T_{cr} - T_e \leq \infty \qquad (7b)$$

$$0 \leq \dot{Q}_e \leq (UA)_{cr-e,max} \cdot (T_{cr} - T_e) \qquad (7c)$$

We define the sets Ω and Υ as all $\dot{Q}_e$ and T_e respectively, that satisfies the system dynamics (Eq. (5)) and the constraints given in Eq. (7).

B. Multi-zone refrigeration

In the section above only one cold storage room was connected to the system. Most systems however, contain several cold rooms that vary mutually in both size, temperature demands and loads. By expanding $\dot{Q}_e$, T_{cr} and T_{amb} from the models described in the previous section to the vector case where $(T_e, \dot{Q}_{e,i})$, $T_{cr,i}$ and $T_{amb,i}$ are inputs, output and disturbance respectively for the ith cold room the same equations still hold.

III. POWER CONSUMPTION

As already mentioned we will consider only the energy consumed in the compressor in the sequel. The work done by the compressor can be expressed by the mass flow of refrigerant (m_{ref}) and the change in energy content of the refrigerant over the compressor. Energy content is described by enthalpy of the refrigerant at the inlet and at the outlet of the compressor (h_{ic} and h_{oc} respectively). Hereby the expression in Eq. (8) is given.

$$\dot{W}_c = \frac{m_{ref} \cdot (h_{oc}(T_e, P_c) - h_{ic}(T_e))}{\eta_{is}(P_c/P_e)} \qquad (8)$$

where the enthalpies depend on the evaporation temperature and the condensing pressure as stated. Actually they also depend on the superheat (ΔT_{SH}) and the heat loss in the compressor but without too much loss of generality we assume these parameters constant. The isentropic efficiency (η_{is}) is a compressor dependent function of the ratio P_c/P_e. In the normal range of operation it was found that the addition of this function did not change the shape of Eq. (8) significantly and it is therefore omitted in the sequel. For future improvements and for a wider range of operation isentropic efficiency might need to be considered.

The mass flow can be determined as the ratio between cooling capacity and change of enthalpy over the evaporator:

$$m_{ref} = \frac{\dot{Q}_e}{h_{oe}(T_e) - h_{ie}(P_c)} \qquad (9)$$

Furthermore we note that $h_{oe} = h_{ic}$. All the enthalpies given here as functions of T_e, P_c or both are non-linear refrigerant dependent functions which can be calculated e.g. by the software package "RefEqns" [16]. Using the description from (8)-(9) and "RefEqns" for the enthalpy calculations in a scenario with fixed condensation pressure and with varying $\dot{Q}_e$ and T_e gives the surface shown in Fig.
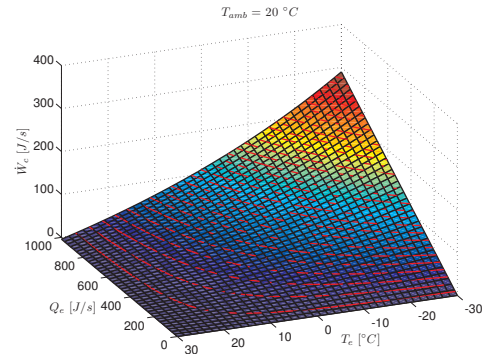

Fig. 3.   Power consumption in the compressor for varying $\dot{Q}_e$ and T_e and fixed condensation pressure. Contours for $\dot{W}_c$ are shown in red. Refrigerant R134a is used.

3. In the figure the entire region is shown without paying attention to the constraints from Eq. (7).

From the above and Fig. 3 it is evident that the power consumption in a vapor compression refrigeration system is not a nice convex function in the control variables. Furthermore constraints could be thought of in a way that could cause the system to have several minima. This is a highly unwanted situation in optimization and special care has to be taken when choosing the optimization method. The nature of the constraints will be carefully studied in this scope.

A. Linearized Model

Since we will use the expression of $\dot{W}_c$ for minimization we will find a linear approximation to the function. By using "RefEqns" for a specific refrigerant the two enthalpy differences can for instance be expressed as in

$$h_{oe} - h_{ie} \approx \alpha_1 \cdot P_c + \beta_1 \quad (10a)$$
$$h_{oc} - h_{ic} \approx \alpha_{21} \cdot T_e + \alpha_{22} \cdot P_c + \beta_2 \quad (10b)$$

Doing the above linear approximation for the refrigerant R134a yields the following constants:

$$\alpha_1 = -9.51 \cdot 10^3 \quad (11a)$$
$$\beta_1 = 219.38 \cdot 10^3 \quad (11b)$$
$$\alpha_{21} = -800 \quad (11c)$$
$$\alpha_{22} = 4.94 \cdot 10^3 \quad (11d)$$
$$\beta_2 = -10.10 \cdot 10^3 \quad (11e)$$

Fig. 4.(a) shows the same surface as seen in Fig. 3 but using the linearized expressions for the enthalpy differences instead of the exact values. The linearization leads to an error which is plotted in Fig. 4.(b). From the surface in Fig. 4.(a) it seems that the linearization has preserved the basic shape and features of the function for work done in the compressor and from the error plot it is noted that the error is most severe at the extrema of T_e where it amounts to approximately 10% of the range for $\dot{W}_c$. This could have been improved by making the enthalpy difference over the evaporator (Eq. (10a)) dependent on T_e. However, since the enthalpy difference over the evaporator appears in the denominator of the function describing the power consumption, it is highly undesired to make it dependent on one of the control variables.

For the case with multiple cold rooms on the system Eq. (9) has to replaced by the sum of the mass flows from the individual subsystems (i.e. $\sum_i m_{ref,i}$).

B. Constraints

A list of constraints on both inputs and outputs of the system were given in Eq. (7). In this section these will be related to the surface describing the power consumption in the compressor in order to give a good understanding of the actual set of feasible solutions.

Fig. 5 illustrates how the constraints limit the two control variables ($\dot{Q}_e$ and T_e) and a description is given in the following. The upper and lower bounds on the cold room temperature poses limitations on the cooling capacity, $\dot{Q}_e$. For a constant ambient temperature it is seen from Eq. (4a) that the heat transfer from the surroundings to the cold room depends on the cold room temperature. Since this heat transfer has to be balanced by a heat transfer to the refrigerant ($\dot{Q}_e$) for the derivative in Eq. (3) to be zero, the lower limit of T_{cr} clearly puts an upper limit on $\dot{Q}_e$ and vice versa. The evaporation temperature is limited from above by the actual cold room temperature to assure that the heat flow from cold room to refrigerant in the evaporator is positive. Fig. 5 shows $-T_e$ on the x-axis which is then bounded from below. Actually the evaporation temperature is also bounded by the condensing temperature ($T_c \geq T_e$) however the limit from T_{cr} is more conservative. The last constraint (Eq. 7c) limits the cooling capacity (Q_e) as a function of T_e. It is readily seen that this dependence is linear proportional with $-T_e$.

All the constraints mentioned above are plotted on top of the surface from Fig. 4.(a) as an example with fixed P_c and T_{cr} to provide a feeling of the nature of these constraints and of the feasible area. In addition one of the contours (thin red lines) is highlighted to indicate the effect of a constraint stemming from a limitation of the maximum possible work provided by the compressor.

From Fig. 5 it can be observed that the structure of the constraints is such that only one minimum of the power consumption can be found. This means that it is possible to minimize the function uniquely even though it is not convex. It is also noted that if the constraint from Eq. (7c) had a negative slope such that it could be tangent to one of the contour curves of the power consumption then two minima of the function would have existed.

IV. MINIMIZATION PROCEDURE

In order to optimize the power consumption over the horizon where parameters such as energy prices and outdoor temperature can be predicted (N time steps) a minimization function can be setup on the basis of the previous sections. The entire problem can be described as in Eq. (12).

$$\min_{T_e \in \Upsilon, \dot{Q}_e \in \Omega} \sum_{k=1}^{N} c_{el,k} \cdot \dot{Q}_e \cdot \frac{\alpha_{21} \cdot T_e + \alpha_{22} \cdot P_c + \beta_2}{\alpha_1 \cdot P_c + \beta_1} \quad (12)$$

where c_{el} is the electricity cost and the rest of the equation comes from the combination of Eq. (8) and (9) using the linearization from (10).

Recalling the shape of the cost function and the constraints from Fig. 5 it can be realized that the minimum of Eq. (12) can be obtained by fixing T_e to any feasible value while minimizing over $\dot{Q}_e$ and subsequently minimize over T_e using the values for Q_e that were found in the first

(a) Power consumption with linearized enthalpies.

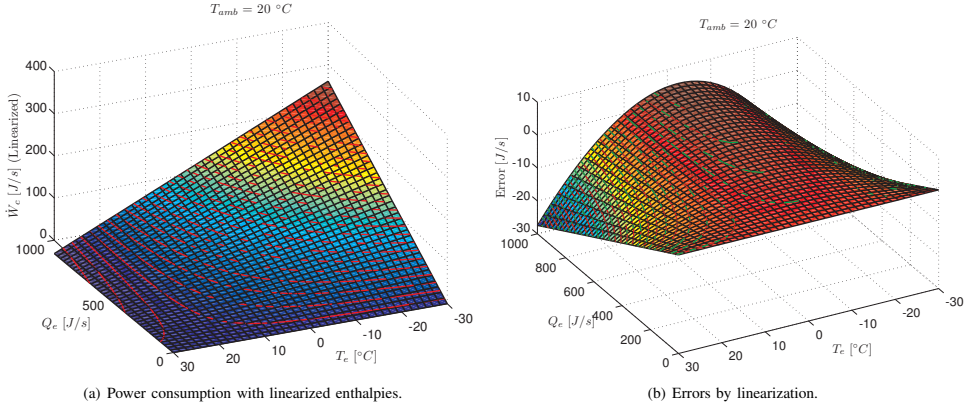

(b) Errors by linearization.

Fig. 4.   Power consumption in the compressor for the same scenario as in Fig. 3 but with linearized enthalpies as given in Eq. (10).
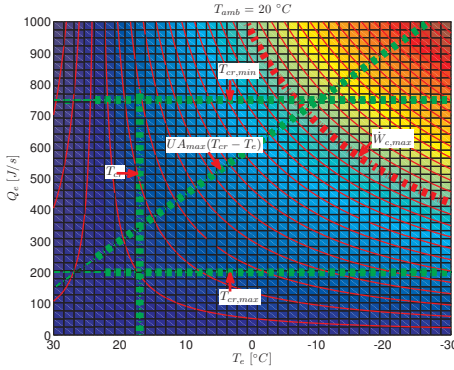

Fig. 5.   Illustration of the feasible solution area. The arrows indicate from which side of the lines the area is constrained.

minimization. This procedure will be described in further details in the following.

We assume that we have available a prediction of the electricity prices and the outdoor temperature that governs the condensing pressure for the next N time steps (the prediction/planning horizon). Furthermore a feasible evaporation temperature can be chosen. The first step is then to solve Eq. (13) for $\dot{Q}_e$ where $\dot{Q}_e$ in this case is a vector that contains the cooling capacity for each of the i cold rooms connected to the system for each of the N time steps.

$$\min_{\dot{Q}_e \in \Omega} \sum_{k=1}^{N} c_{el,k} \cdot \sum_i \dot{Q}_{e_k} \cdot \frac{\alpha_{21} \cdot T_e + \alpha_{22} \cdot P_{c_k} + \beta_2}{\alpha_1 \cdot P_{c_k} + \beta_1} \quad (13)$$

If we call the fraction at the end of the above expression

Δh_k Eq. 13 can be formulated as the linear program:

$$\min_{\dot{Q}_e^* \in \Omega} C^T \dot{Q}_e \quad (14)$$

where:

$$C^T = [c_{el,1} \Delta h_1 \cdot 1_p, \cdots, c_{el,N} \Delta h_N \cdot 1_p] \quad (15a)$$

$\quad p : \#$ of cold rooms

$\quad 1_p$: A p-length vector of ones ($[1_1, 1_2, \cdots, 1_p]$)

$$\dot{Q}_e = \Big[[\dot{Q}_{e_{1,1}}, \dot{Q}_{e_{2,1}}, \cdots, \dot{Q}_{e_{p,1}}], [\dot{Q}_{e_{1,2}}, \dot{Q}_{e_{2,2}}, \cdots, \dot{Q}_{e_{p,2}}],$$
$$\cdots, [\dot{Q}_{e_{1,N}}, \dot{Q}_{e_{2,N}}, \cdots, \dot{Q}_{e_{p,N}}]\Big]^T \quad (15b)$$

Hence, the size of C^T is $(1 \times (p \cdot N))$ and the size of $\dot{Q}_e$ is $((p \cdot N) \times 1)$.

Next, we need to solve the minimization given in Eq. (16) to find the optimal T_e. As before P_c is a constant vector in time and $\dot{Q}_e^*$ is the optimal cooling capacity found as the solution to Eq. (14).

$$\min_{T_e^* \in \Upsilon} \sum_{k=1}^{N} c_{el,k} \cdot \dot{Q}_{e_k}^* \cdot \frac{\alpha_{21} \cdot T_{e_k} + \alpha_{22} \cdot P_{c_k} + \beta_2}{\alpha_1 \cdot P_{c_k} + \beta_1} \quad (16)$$

The fraction can be rewritten such that the expression in (16) yields:

$$\min_{T_e^* \in \Upsilon} \sum_{k=1}^{N} c_{el,k} \cdot \dot{Q}_{e_k}^* \left(\frac{\alpha_{21}}{\alpha_1 \cdot P_{c_k} + \beta_1} T_{e_k} + \frac{\alpha_{22} \cdot P_{c_k} + \beta_2}{\alpha_1 \cdot P_{c_k} + \beta_1} \right) \quad (17)$$

The last term is constant with respect to T_e and can be omitted in the optimization problem. If the other term (that is multiplied with T_e) is called h_k the problem in Eq. (17) can be formulated as a linear program:

$$\min_{T_e^* \in \Upsilon} C^T T_e \quad (18)$$

where:

$$C^T = \left[h_1 \cdot c_{el,1} \cdot \dot{Q}^*_{e,sum_1}, \cdots, h_N \cdot c_{el,N} \cdot \dot{Q}^*_{e,sum_N} \right]$$

$$\dot{Q}_{e,sum} = \begin{bmatrix} [1_p]_1 & 0 & \cdots & 0 \\ 0 & [1_p]_2 & \cdots & 0 \\ \vdots & \vdots & \ddots & \vdots \\ 0 & 0 & \cdots & [1_p]_N \end{bmatrix} \cdot \dot{Q}^* \qquad (19)$$

$$T_e = [T_{e_1}, T_{e_2}, \cdots, T_{e_N}]$$

The matrix multiplied with $\dot{Q}^*_e$ in Eq. (19) is $(N \times (N \cdot p))$. Thus, $\dot{Q}_{e,sum}$ and C are both of size $(N \times 1)$.

When optimal values for both $\dot{Q}^*_e$ and T^*_e over the prediction horizon are found it must be checked whether the evaporation temperature violates the constraint on maximum compressor work at any time. If it does so it must be limited to the extremum that can be achieved and the minimization in Eq. (13) must be repeated. This procedure might have to be applied for some iterations before all capacity violations are handled well. Fig. 6 shows a simulation result using the models and optimization procedure presented in this paper. It is observed how the load is shifted such that the entire temperature range $(0 - 10°C)$ is utilized in order to benefit from the variations in outdoor temperature and electricity price. Furthermore the peak around time step 135 has been limited due to a chosen maximum compressor capacity.

V. Conclusion

In this paper we have presented a new model of supermarket refrigeration systems. The contribution of this model is its ability to work with Economic Optimizing MPC
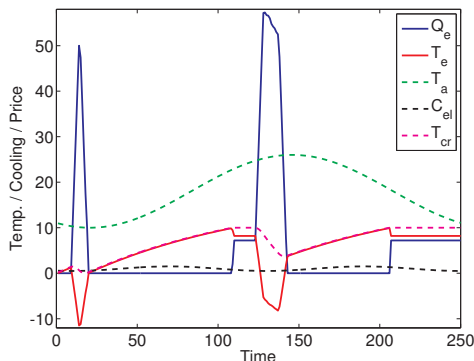

Fig. 6. Simulation using Economic MPC for the presented refrigeration system.

while maintaining a realistic and accurate description of the power consumption. Hereby it is possible to use the model for power management schemes in which the load on the refrigeration system can be shed in order to minimize the cost of power for operating the system. Furthermore flexible power consumption is enabled. Difficulties regarding non-convexity of the objective function were described along with a minimization procedure that overcomes this problem.

References

[1] L. F. S. Larsen, "Model based control of refrigeration systems," Ph.D. dissertation, Aalborg University, Departement of Control Engineering, 2005, ph.D. Thesis.

[2] T. Hovgaard, "Active sensor configuration validation for refrigeration systems," Automation and Control, Technical University of Denmark, Tech. Rep., 2009, master's Thesis. [Online]. Available: http://orbit.dtu.dk

[3] L. Larsen, R. Izadi-Zamanabadi, and R. Wisniewski, "Supermarket refrigeration system - benchmark for hybrid system control." *Proc. European Control Conference*, pp. 113–120., 2007.

[4] L. F. S. Larsen, C. Thybo, and H. Rasmussen, "Potential energy savings optimizing the daily operation of refrigeration systems," *Proc. European Control Conference, Kos, Greece*, pp. pp. 4759–4764., 2007.

[5] H. Rasmussen and L. Larsen, "Nonlinear superheat and capacity control of a refrigeration plant," *2009 17th Mediterranean Conference on Control and Automation*, pp. 1072–1077, 2009.

[6] M. Willatzen, N. Pettit, and L. Ploug-Sørensen, "A general dynamic simulation model for evaporators and condensers in refrigeration. Part I: moving-boundary formulation of two-phase flows with heat exchange," *International Journal of Refrigeration*, vol. 21, no. 5, pp. 398–403, 1998.

[7] J. Maciejowski, *Predictive control: with constraints.* Pearson education, 2002.

[8] J. B. Rawlings and D. Q. Mayne, *Model Predictive Control: Theory and Design.* Nob Hill Publishing, 2009.

[9] D. Sarabia, F. Capraro, L. Larsen, and C. de Prada, "Hybrid nmpc of supermarket display cases," *Control Engineering Practice*, vol. 17, no. 4, pp. 428–441, 2008.

[10] T. Hovgaard, K. Edlund, and J. Jørgensen, "The potential of economic mpc for power management." *Proc. Conference on Decision and Control*, p. accepted, 2010.

[11] J. Rawlings, D. Bonne, J. Jorgensen, A. Venkat, and S. Jorgensen, "Unreachable setpoints in model predictive control," *IEEE Transactions on Automatic Control*, vol. 53, no. 9, pp. 2209–2215, 2008.

[12] M. Diehl, R. Amrit, and J. Rawlings, "A Lyapunov Function for Economic Optimizing Model Predictive Control," *IEEE Transactions on Automatic Control*, 2009.

[13] J. Rawlings and R. Amrit, "Optimizing Process Economic Performance Using Model Predictive Control," *Nonlinear Model Predictive Control: Towards New Challenging Applications*, pp. 119–138, 2009.

[14] K. Edlund, L. E. Sokoler, and J. B. Jørgensen, "A primal-dual interior-point linear programming algorithm for MPC," in *Joint 48th IEEE Conference on Decision and Control and 28th Chinese Control Conference.* Shanghai, P.R. China, December 16-18, 2009: IEEE, 2009, pp. 351–356.

[15] A. Jakobsen and M. Skovrup, "Forslag til energioptimal styring af kondenseringstryk (in danish)," MEK, Technical University of Denmark, Tech. Rep., 2001. [Online]. Available: http://www.et.web.mek.dtu.dk/ESO/Index.htm

[16] M. Skovrup, "Thermodynamic and thermophysical properties of refrigerants - software package in borland delphi." Department of Energy Engineering, Technical University of Denmark, Tech. Rep., 2000. [Online]. Available: http://www.et.web.mek.dtu.dk/WinDali/Files/RefEqns

Robust Economic MPC for a Power Management Scenario with Uncertainties

Robust Economic MPC for a Power Management Scenario with Uncertainties

Tobias Gybel Hovgaard, Lars F. S. Larsen and John Bagterp Jørgensen

Abstract— This paper presents a novel incorporation of probabilistic constraints and Second Order Cone Programming (SOCP) with economic Model Predictive Control (MPC). Hereby the performance of the controller is robustyfied in the presence of both model and forecast uncertainties. Economic MPC is a receding horizon controller that minimizes an economic objective function and we have previously demonstrated its usage to include a refrigeration system as a controllable power consumer with a portfolio of power generators such that total cost is minimized. The main focus for our work is power management of the refrigeration system. Whereas our previous study was entirely deterministic, models of e.g. supermarket refrigeration systems are uncertain, as are forecasts of outdoor temperatures and electricity demand. The linear program we have formulated does not cope with uncertainties and thus it is, liable to drive an optimal solution to an infeasible or very expensive solution. The main contribution of this paper is the Finite Impulse Response (FIR) formulation of the system models, allowing us to describe and handle model uncertainties in the framework of probabilistic constraints. Our new solution using this setup for robustifying the economic MPC is demonstrated by simulation of a small conceptual example. The scenario is primarily chosen to illustrate the effect of our proposed method in that it can be compared with our previous deterministic simulations.

I. Introduction

In [1] we introduced economic MPC to control a number of independent dynamic systems that must collaborate to minimize the overall cost of satisfying the cooling demand for some goods while meeting market demands for power at all times. Our control strategy is an economic optimizing model predictive controller, economic MPC. MPC for constrained systems has emerged during the last 30 years as the most successful methodology for control of industrial processes [2]. MPC is increasingly being considered for refrigeration systems [3], [4] and for power production plants [5]. MPC based on optimizing economic objectives has only recently emerged as a general methodology with efficient numerical implementations and provable stability properties [6]–[8]. Our proposed economic MPC controller has previously been formulated in a deterministic setting and the contribution of this paper is to put our strategy into a more realistic scenario where different uncertainties always affect the system. Thus, this paper provides a novel extension to the economic MPC to provide robust performance in the presence of both forecast and model

uncertainties. This is done in a way similar to [9] where energy consumption for climate control is minimized under influence of uncertain weather predictions but also the ability to handle model uncertainties in the closed-loop MPC is an important issue in this paper.

The Smart Grid is the future intelligent electricity grid and is intended to be the smart electrical infrastructure required to increase the amount of green energy significantly. The Danish transmission system operator (TSO) has the following definition of Smart Grids which we adopt in this work: "Intelligent electrical systems that can integrate the behavior and actions of all connected users - those who produce, those who consume and those who do both - in order to provide a sustainable, economical and reliable electricity supply efficiently" [10]. A larger share of intermittent stochastic power-generating sources such as wind turbines makes it difficult to balance demand and supply of electricity in a flexible and cost-efficient manner. To account for this we previously introduced large power consumers, such as cold rooms, or an aggregation of a number of like consumers such as supermarket systems, with the ability to adjust the power consumption profile to the power supply. Due to the large thermal capacity of cold rooms, their consumption of electricity can, to some degree, be shifted in time to benefit the overall system. The thermal capacity in the refrigerated goods is then utilized to store "coldness" such that the refrigeration system can increase cooling when there is an over production of energy and then lower its consumption at other times. The temperature is allowed to vary within certain bounds, which have no impact on food quality. We exploit that the dynamics of the temperature in the cold room are rather slow while the power consumption can be changed rapidly. [9], [11], [12] also utilized load shifting capabilities to reduce total energy consumption.

Several works exist that consider constrained model predictive control (MPC) in the presence of uncertainty [13]. In many applications distributions can be quantified for uncertainty and if this information is ignored (e.g. by defining worst-case costs and invoking constraints over all uncertainty realizations) it can lead to conservative results, and the need for a stochastic extension to constrained MPC is clear [14]. Taking expected values of the cost provides an obvious way to utilize probabilistic information [15]. However constraints often admit a probabilistic formulation too, e.g. a variable should not exceed a certain bound with a given probability.

T. G. Hovgaard and L. F. S. Larsen are with Danfoss Refrigeration and A/C Controls, DK-6430 Nordborg, Denmark. {tgh,lars.larsen}@danfoss.com
J. B. Jørgensen is with DTU Informatics, Technical University of Denmark, DK-2800 Lyngby, Denmark. jbj@imm.dtu.dk

[16] and [17] considered MPC with probabilistic constraints with the cost based on the expected value of a linear function of the states. In the former the implementation of probabilistic constraints can be conservative due to the use of statistical confidence ellipsoidal approximations, whereas the latter uses affine disturbance feedback. [18] and [19] demonstrate that probabilistic linear constraints can be written as second-order cone (SOC) constraints that are convex provided the probability involved is greater than 0.5. Probabilistic constraints are also introduced in [20] for model uncertainties and in [21] for uncertain disturbances. Both works confine the analysis to open loop optimization whereas [22] uses SOCP methods to calculate steady-state targets for MPC under uncertainty. In [23] a fast algorithm for MPC with probabilistic constraints is presented. For power management scenarios e.g. [24] proposed a risk-constrained stochastic programming for signing day-ahead contracts under uncertain price forecasts and in [25] a stochastic mixed-integer program is proposed for the scheduling of reserves by demand response under forecast uncertainty and random outages of generating units and transmission lines.

This paper is organized as follows. Section II introduces economic MPC and illustrates the problem with linear programming for uncertain systems. In section III we explain the different sources of uncertainty and reformulate both the model and forecast uncertainties to fit into solutions with probabilistic constraints. Section IV describes the models, assumptions and scenarios used for our case study, and the results are provided in section V. We give conclusions in Section VI.

II. Economic MPC for Linear Systems

In this section we describe the economic MPC for linear systems. The Economic MPC minimizes an economic cost directly as opposed to minimizing the deviation from a set-point in some norm. We consider continuous variables only and the resulting optimal control problem is formulated as a linear program. The solution of this program is implemented on the system in a receding horizon manner.

A. Distributed Independent System

In this paper, we consider a distributed independent system represented in continuous time as:

$$Y_i(s) = G_{yu,i}(s)U_i(s) + G_{yd,i}(s)D_i(s) \quad i \in \mathcal{P} \quad (1a)$$

$$Z_i(s) = G_{zu,i}(s)U_i(s) + G_{zd,i}(s)D_i(s) \quad i \in \mathcal{P} \quad (1b)$$

with $i \in \mathcal{P} = \{1, 2, \ldots, P\}$ being an index referring to each plant. $U \in \mathbb{C}^{n_u}$ is the manipulable variables, $D \in \mathbb{C}^{n_d}$ is known disturbances, $Y \in \mathbb{C}^{n_y}$ is the outputs associated with a cost, and $Z \in \mathbb{C}^{n_z}$ is the outputs associated with output constraints. G_{yu}, G_{yd}, G_{zu}, and G_{zd} are transfer function matrices of compatible size.

The set of plants, $\mathcal{P}$, consists of controllable producers (e.g. conventional power plants), $\mathcal{S}_C$, non-controllable producers (e.g. wind farms), $\mathcal{S}_{NC}$, controllable consumers

(e.g. large cooling houses as in this paper), $\mathcal{D}_C$ and non-controllable consumers, $\mathcal{D}_{NC}$. We combine the effect from all non-controllable units in the net power demand signal r. In this signal we model changes in e.g. wind speed as step-like changes. The dynamically independent plants must collaborate to meet a common objective i.e. satisfy the market demand for the goods they produce. The optimal control problem defining the economic MPC for (1) may then be stated as the block-angular linear program:

$$\min_{\{x,u,y,z\}} \quad \phi = \sum_{i \in \mathcal{S}} \left(\sum_k c'_{u,i}u_{i,k} + c'_{y,i}y_{i,k} \right) \quad (2a)$$

$$s.t. \quad \sum_{i \in \mathcal{S}_C} y_{i,k} - \sum_{i \in \mathcal{D}_C} y_{i,k} \geq r_k \quad (2b)$$

$$x_{i,k+1} = A_i x_{i,k} + B_i u_{i,k} + E_i d_{i,k} \quad (2c)$$

$$y_{i,k} = C_i x_{i,k} + D_i u_{i,k} + F_i d_{i,k} \quad (2d)$$

$$z_{i,k} = C_{z,i} x_{i,k} + D_{z,i} u_{i,k} + F_{z,i} d_{i,k} \quad (2e)$$

$$u_{\min,i} \leq u_{i,k} \leq u_{\max,i} \quad (2f)$$

$$\Delta u_{\min,i} \leq \Delta u_{i,k} \leq \Delta u_{\max,i} \quad (2g)$$

$$z_{\min,i} \leq z_{i,k} \leq z_{\max,i} \quad (2h)$$

with $i \in \mathcal{P}$ and $k \in \mathcal{T}$. $\mathcal{T} \in \{0, 1, \ldots, N\}$. The objective function (2a) says that the total cost of production from all the power plants in the time horizon considered must be minimal. (2b) couples the independent plants by requiring that the supply exceeds the demand. This is not a realistic constraint for controlling an entire Smart Grid where supply and demand have to balance at all times. But for the illustration of the effect gained from including controllable consumers, this simplification does not change the solution. (2c)-(2e) are the discrete-time state space realization of (1), (2f) constitutes the input constraints and (2g) is a constraint on the rate of movement ($\Delta u_k = u_k - u_{k-1}$). The output constraints are represented by (2h).

The supply-demand constraint (2b) and the output constraints (2h) may not be feasible for every disturbance and initial state scenario. In such situations (2) may be modified to a feasible linear program by representing (2b) and (2h) as soft constraints with large constraint violation penalties.

(2) can be formulated as an instance of a linear program which may be solved efficiently using Dantzig-Wolfe decomposition [26].

B. Linear Programs and Control with Uncertainty

The optimum of a linear program is an extreme point, as illustrated in Fig. 1. This property of linear programs leads to either dead-beat or idle control when linear programs are used to solve model predictive control problems with an ℓ_1-penalty [27]. For economic MPC the fact that the optimum is an extreme point implies that even small perturbations in the data or the disturbances may change the otherwise optimal solution to an infeasible or very expensive solution. Uncertainties are always present in real systems and the solution we presented in [1] is therefore entirely conceptual. Exemplified by the power production case, an optimal solution is one where the amount of power produced exactly

matches the consumption. However, due to the optimization relying on a prediction of power production from non-controllable producers, there is a risk of power shortage if e.g. the estimate of power from non-controllable producers was overstated. Since this situation is very expensive, a more desirable solution would be to produce just enough extra power to leave room for most of the effect from uncertainties. Another scenario would be the cold room temperature that, in an energy context, optimally aims at the upper limit, causing the foodstuff to be damaged if the surrounding temperature gets higher than predicted or if the real dynamics of the refrigeration system are slightly different than modeled. This has previously been handled by adding a somewhat arbitrary amount of back-off from the calculated optimal point. In this work we want to introduce a confidence interval such that the solution accounts for the amount of uncertainty. The tubes in Fig. 1 illustrate this.

III. ECONOMIC MPC WITH PROBABILISTIC CONSTRAINTS

As pointed out above the optimal solution to a deterministic LP is not always optimal, nor feasible, in the stochastic case. Therefore we describe means to handle the uncertainties in both forecasts and in the models of the system. We are using assumptions of the uncertainty belonging to certain distribution functions and define the confidence level (probability) that the constraints should hold with. The probabilistic constraints are then reformulated as their deterministic counterparts.

First we define the system model in Finite Impulse Response (FIR) form:

$$y_k = b_k + \sum_{i=0}^{k} H_i u_{k-i}, \ H_i = \begin{cases} D & for \ i=0 \\ CA^{i-1}B & for \ i>0 \end{cases} \quad (3)$$
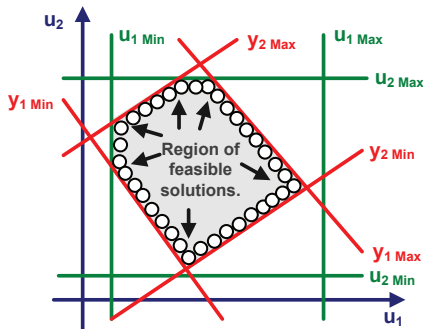

Fig. 1. Example of LP with two inputs and two outputs. Boundaries of the feasible region are illustrated with green for input constraints and red for output constraints. The arrows indicate possible optimal solutions and the circles illustrate the confidence interval around a solution caused by uncertainty.

where b_k is a bias term. Next, the stochastic optimization problem is defined as (boldface variables are uncertain):

$$\min E \left\{ \sum_{k=0}^{N} \mathbf{c_k}' u_k \right\} \quad (4a)$$

$s.t.$

$$u_{min} \leq u_k \leq u_{max} \quad (4b)$$
$$Prob\{\mathbf{y_k} \geq \mathbf{r_k}\} \geq 1 - \alpha, \quad \alpha \in [0;1] \quad (4c)$$
$$\mathbf{y_k} = b_k + \sum_{i=1}^{k} \mathbf{H_i} u_{k-i} + \sum_{i=1}^{k} \mathbf{H_{D,i}} d_{k-i} \quad (4d)$$

where $\mathbf{r}$ is a reference trajectory, $\mathbf{d}$ a disturbance, $1 - \alpha$ the confidence level for the constraint, and:

1) $\mathbf{c_k} \sim N(\bar{c}_k, \sigma_c^2)$ 2) $\mathbf{r_k} \sim N(\bar{r}_k, \sigma_r^2)$
3) $\mathbf{H_i} \sim N(\bar{H}_i, \Sigma_H^2)$ 4) $\mathbf{H_{D,i}} \sim N(\bar{H}_{D,i}, \Sigma_H^2)$ (5)
5) $\mathbf{d_k} \sim N(\bar{d}_k, \sigma_d^2)$

1) and 2) are forecast uncertainties, 3) and 4) describe model uncertainties while 5) is uncertainty in the disturbances.

A. Forecast Uncertainty

1) Uncertainty in price, $\mathbf{c_k}$: Since we are minimizing the expected value of the objective function we use the certainty equivalent description and substitute $\bar{c}_k$ with c_k.

2) Uncertainty in the reference, $\mathbf{r_k}$: The probability constraint is reformulated as a deterministic constraint:

$$Prob\{Y \geq \mathbf{R}\} \geq 1 - \alpha \quad (6a)$$
$$\frac{\mathbf{R} - \bar{R}}{\sigma_r} \sim N(0,1) \Rightarrow \Phi\left(\frac{Y - \bar{R}}{\sigma_r}\right) \geq 1 - \alpha \quad (6b)$$

$\Phi(x)$ is the cumulative distribution function (CDF) of a zero mean unit variance Gaussian random variable x

$$Y \geq \bar{R} + \sigma_r \Phi^{-1}(1 - \alpha) \quad (7)$$

Hence a security margin is added to $\mathbf{r_k}$ resulting in a back-off from the optimal (in the deterministic case) boundary. This strategy is closely related to the affine feedback methods described e.g. in [28] and [17].

B. Model and Disturbance Uncertainty

3), 4) and 5) lead to stochastic programming which is described in this section. We formulate the system using the FIR description in Eq. (3)-(5):

$$\mathbf{Y} = \begin{bmatrix} \mathbf{C} & \mathbf{\Gamma} \end{bmatrix} \begin{bmatrix} U_{past} \\ U \end{bmatrix} + \begin{bmatrix} \mathbf{C_D} & \mathbf{\Gamma_D} \end{bmatrix} \begin{bmatrix} \mathbf{D_{past}} \\ \mathbf{D} \end{bmatrix} \quad (8)$$

and the optimization problem as:

$$\min_U \ \phi = E \left\{ \sum_{k=0}^{N-1} \mathbf{c_{u,k}} u_k \right\} \quad (9a)$$

$s.t.$

$$\mathbf{y_k} = \begin{bmatrix} \mathbf{C_k} & \mathbf{\Gamma_k} \end{bmatrix} \begin{bmatrix} U_{past} \\ u_k \end{bmatrix} + \begin{bmatrix} \mathbf{C_{D,k}} & \mathbf{\Gamma_{D,k}} \end{bmatrix} \begin{bmatrix} \mathbf{D_{past}} \\ \mathbf{d_k} \end{bmatrix} \quad (9b)$$
$$Prob\{\mathbf{y_k} \geq r_k\} \geq 1 - \alpha, \quad k = 1, 2, \cdots, N \quad (9c)$$

where $\mathbf{C_k}$ and $\mathbf{\Gamma_k}$ are rows from the corresponding matrices in Eq. (10) and subscript "past" indicates the previous signals corresponding to the number of coefficients in the FIR model.

$$\begin{bmatrix} \Gamma_{N \times N} & | & C_{N \times (n-1)} \end{bmatrix} =$$

$$\begin{bmatrix} H_1 & 0 & \cdots & \cdots & \cdots & 0 & H_n & \cdots & \cdots & H_2 \\ \vdots & \ddots & \ddots & \ddots & \ddots & \vdots & 0 & \ddots & \ddots & \vdots \\ H_n & \ddots & \ddots & \ddots & \ddots & \vdots & \vdots & \ddots & \ddots & \vdots \\ 0 & \ddots & \ddots & \ddots & \ddots & \vdots & 0 & \cdots & 0 & H_n \\ \vdots & \ddots & \ddots & \ddots & \ddots & 0 & \vdots & \vdots & \vdots & \vdots \\ 0 & \cdots & 0 & H_n & \cdots & H_1 & 0 & \cdots & \cdots & 0 \end{bmatrix} \tag{10a}$$

$$U_{past} = \begin{bmatrix} u_{-(n-1)} \\ \vdots \\ u_{-1} \end{bmatrix}, \quad U = \begin{bmatrix} u_1 \\ \vdots \\ u_N \end{bmatrix} \tag{10b}$$

The statistical properties of the resulting output $\mathbf{y_k}$ can be described as:

$$\mathbf{Y_U} \sim N(\bar{Y}_U, \Sigma_{Y_U}), \quad \mathbf{Y_D} \sim N(\bar{Y}_D, \Sigma_{Y_D}) \tag{11a}$$

$$\mathbf{Y} = \mathbf{Y_U} + \mathbf{Y_D}, \quad \mathbf{Y} \sim N(\bar{Y}_U + \bar{Y}_D, \Sigma_{Y_U} + \Sigma_{Y_D}) \tag{11b}$$

where:

$$\bar{Y}_{U,k} = \begin{bmatrix} \bar{C}_k & \bar{\Gamma}_k \end{bmatrix} \begin{bmatrix} U_{past} \\ U \end{bmatrix} \tag{12a}$$

$$\Sigma_{Y_U,k} = \begin{bmatrix} U_{past} & U \end{bmatrix} \begin{bmatrix} \Sigma_{C,k} & 0 \\ 0 & \Sigma_{\Gamma,k} \end{bmatrix} \begin{bmatrix} U_{past} \\ U \end{bmatrix} \tag{12b}$$

The product of the two normally distributed variables coming from the model uncertainties and the uncertain disturbance respectively can be described by an approximate normal distribution with the following properties [29]:

$$\bar{Y}_{D,k} \approx \begin{bmatrix} \bar{C}_{D,k} & \bar{\Gamma}_{D,k} \end{bmatrix} \begin{bmatrix} \bar{D}_{past} \\ \bar{D} \end{bmatrix} \tag{13a}$$

$$\Sigma_{Y_D,k} \approx \begin{bmatrix} \bar{D}_{past} & \bar{D} \end{bmatrix} \begin{bmatrix} \Sigma_{C_D,k} & 0 \\ 0 & \Sigma_{\Gamma_D,k} \end{bmatrix} \begin{bmatrix} \bar{D}_{past} \\ \bar{D} \end{bmatrix} +$$
$$\begin{bmatrix} \bar{C}_{D,k} & \bar{\Gamma}_{D,k} \end{bmatrix} \Sigma_D \begin{bmatrix} \bar{C}_{D,k} \\ \bar{\Gamma}_{D,k} \end{bmatrix} \tag{13b}$$

Hence, using that $(\mathbf{y_k} - \bar{y}_k)/\Sigma_{y,k}^{1/2} \sim N(0,1)$, the probabilistic constraint can be reformulated as follows:

$$Prob\{\mathbf{y_k} \geq r_k\} \geq 1 - \alpha \tag{14a}$$

$$\Phi^{-1}(\alpha) \left\| \Sigma_*^{1/2} \begin{bmatrix} *_{past} \\ * \end{bmatrix} \right\|_2 + \bar{y}_k \geq r_k \tag{14b}$$

where the '*' indicates that the norm is taken of the vector formed by all the quadratic terms described in Eq. (12b) and (13b). Hence, in a MIMO case where $\mathbf{y_k}$ is the sum of two independent outputs, the vector in the norm would simply contain an element from each of the outputs. This is easily realized by the property $\sqrt{a^2 + b^2 + c^2} = \|[a \ b \ c]\|_2$. The constraint in Eq. (14b) has the form of a second order cone and the solution to the optimization problem constrained by

Eq. (14b) can be computed using SOCP as in [18], [19].

In summary, uncertain model descriptions alone or in combination with uncertain disturbances lead to second order cone constraints, while an uncertain reference just adds a margin to the boundary. These two cases can of course easily be combined.

IV. SIMPLE POWER MANAGEMENT SCENARIO

The case study used in this paper includes two controllable power generators and one power consumer. The power consumer is a cold room for which we provide a simple model. This case study is identical to the one presented in [1] to illustrate the properties and potential of economic MPC in managing the power production and consumption in a distributed energy system. The novelty in this paper is the inclusion of a realistic scenario with uncertainties in both models and forecasts and the means to handle such as described in the previous sections. We use the Economic MPC implementation with probabilistic constraints formulated as an SOCP to calculate the cost-optimal control in presence of uncertainties with known probability distribution functions.

A. Controllable Power Generators

In [30] simple models for power generators are provided. In this paper we adopt these models which are of the form:

$$\phi_i = \sum_{k \in \mathcal{T}} c'_i u_{i,k} \tag{15a}$$

$$Y_i(s) = G_i(s) U_i(s) \qquad G_i(s) = \frac{1}{(\tau_i s + 1)^3} \tag{15b}$$

$$u_{\min,i} \leq u_{i,k} \leq u_{\max,i} \tag{15c}$$

$$\Delta u_{\min,i} \leq \Delta u_{i,k} \leq \Delta u_{\max,i} \tag{15d}$$

to model two conventional power generators where u_i is the power set-point for the i-th generator. (15a) represents the costs of producing power from a given power generator. Power generator 1 is cheap and slow, $(c_1, \tau_1, u_{\min,1}, u_{\max,1}, \Delta u_{\min,1}, \Delta u_{\max,1}) = (1, 20, 0, 15, -1, 1)$. Power generator 2 is expensive and fast, $(c_2, \tau_2, u_{\min,2}, u_{\max,2}, \Delta u_{\min,2}, \Delta u_{\max,2}) = (2, 10, 0, 15, -3, 3)$. The model in Eq. (15) describes the closed-loop system with internal controllers and is therefore quite simple without the lower level complexity of the generators. The model has been validated against experimental data at DONG Energy, Denmark.

B. Simple Cold Room

The energy balance for the cold room is

$$mc_p \frac{dT_{cr}}{dt} = Q_{load} - Q_e \tag{16}$$

with

$$Q_{load} = (UA)_{amb-cr}(T_{amb} - T_{cr}) \tag{17a}$$

$$Q_e = (UA)_{cr-e}(T_{cr} - T_e) \tag{17b}$$

T_{cr} is the temperature in the cold room which must be kept within certain bounds, $T_{cr,\min} \leq T_{cr} \leq T_{cr,\max}$. T_e is the evaporation temperature of the refrigerant. It can be

controlled by the compressor work and must satisfy $T_{cr} \geq T_e$. T_{amb} is the ambient temperature. UA is the heat transfer coefficient. m and c_p are the mass and the overall heat capacity of the refrigerated goods, respectively. The energy consumed by the refrigeration system is work performed by the compressors: $W_C = \eta Q_e$. η is the coefficient of performance. In this work η is assumed to be constant. Consequently

$$W_C(s) = \frac{a - bs}{\tau s + 1} T_e(s) + \frac{\alpha K_d}{\tau s + 1} T_{amb}(s) \qquad (18a)$$

$$T_{cr}(s) = \frac{K_u}{\tau s + 1} T_e(s) + \frac{K_d}{\tau s + 1} T_{amb}(s) \qquad (18b)$$

with $Y_3 = W_C$, $Z_3 = [T_{cr}; T_{cr} - T_e]$, $U_3 = T_e$, $D_3 = T_{amb}$. The constraints are

$$T_{cr,min} \leq T_{cr} \leq T_{cr,max} \qquad (19a)$$

$$0 \leq T_{cr} - T_e \leq \infty \qquad (19b)$$

$$T_{e,min} \leq T_e \leq T_{e,max} \qquad (19c)$$

Thus, the refrigeration system can be modeled in a form compatible with the economic MPC for linear systems. The model here is somewhat simplified, especially the assumption for (18). However the resulting dynamics are well suited for illustrating the conceptual case in this paper.

C. Supply and Demand

The production by the power generators, $y_{1,k} + y_{2,k}$, must exceed the demand for power by the cooling house and the other consumers

$$y_{1,k} + y_{2,k} \geq y_{3,k} + r_k \quad k \in \mathcal{T} \qquad (20)$$

We model wind farms as instantaneously changing systems and include the effect of their power production in the exogenous net power demand signal, r_k. This is seen in the case study in Fig. 2.

D. Uncertainty

In our scenario the models of power plants and refrigeration systems are not perfectly known and an uncertain FIR as in Eq. (3)-(5) is used for the system models. The temperature surrounding the cold room ($\mathbf{T_{amb}}$) is stochastic as is the reference ($\mathbf{r}$). The latter is caused by the predictions of both non-controllable consumption and non-controllable production being uncertain. We have already seen how the price (c) can be assumed as deterministic without changing the solution.

V. RESULTS

In [1] we have demonstrated the significant savings gained by including controllable consumers in the setup. Hence, we will only consider the improved ability to handle uncertainties without unnecessary high costs or severe violation of constraints.

Using Yalmip [31] we have simulated the scenario described in the previous section. The constraints on the cold room temperature and on balancing supply and demand are formulated as probability constraints and implemented with SOCP as described in section III. A simulation scenario is provided in Fig. 2. From the figure it is noted how the refrigeration system is utilized to balance the power demand such that extra power is used when it is freely available and less is used at other times. This is further elaborated on in [1]. But what is more important for the
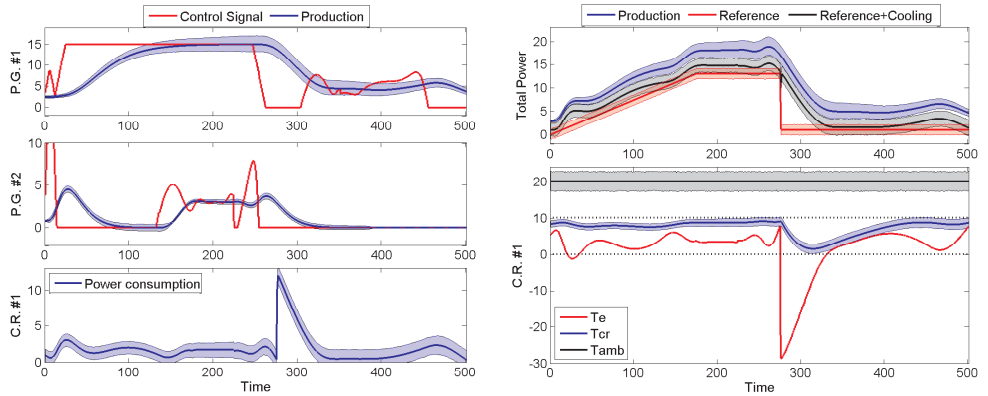
(a) Power productions / consumption. P.G. #1 and 2 show the power productions from the two power plants (blue) and their power set-points (red). C.R. #1 is power consumption in the cold room.

(b) "Total Power" shows total power production (blue) versus the reference consumption (with (black) and without (red) refrigeration. C.R. #1 shows the temperature in the cold room T_{cr} and the control signal T_e. ($T_{cr,min}$, $T_{cr,max}$) and outdoor temperature, T_{amb}, are shown with dotted and solid black respectively.

Fig. 2. Simulation of Power Management scenario. $\alpha = 0.5$, $H_i \sim N(\bar{H}_i, 0.0055^2)$, $r_k \sim N(\bar{r}_k, 0.7071^2)$, $T_{amb} \sim N(\bar{T}_{amb}, 1.7321^2)$. The shaded bands show the 95% confidence interval from 10,000 random instances.

work presented here are the confidence intervals shown as shaded areas around each of the trajectories. The solid lines are the expected outcome, while the shaded areas are created by 10,000 simulations with random instances of the noise descriptions. The 95% percentile was used both in the SOCP formulation and for plotting the shaded areas. It is easily seen how the amount of back-off from the boundaries is just enough to account for the 95% confidence interval of the uncertainty descriptions for the system. This is particular clear in Fig. 2(b), where the total production is above the total consumption, T_{cr} stays within the boundaries specified and $T_e \leq T_{cr}$ is satisfied. All with 95% probability.

Regarding the uncertainty of the predictions of outdoor temperature and power demand in a closed-loop scenario, a variance that increases over the prediction horizon could be chosen such that the short-term predictions are more certain than those at the end of the horizon. Furthermore the disturbances could be measured at each time step, minimizing the uncertainty in the vector of past disturbances to the level related to doing the measurement.

VI. CONCLUSION

In this paper we have extended our analysis of economic MPC for a Power Management scheme in which we included a refrigeration system with thermal storage capabilities as a controllable power consumer in order to minimize the total cost. We have presented a novel formulation including uncertainties from both system models and forecasts in the framework of probabilistic constraints. Thereby our previous economic MPC based on linear programming has evolved into a stochastic economic MPC that can be implemented as a convex SOCP. The concept was demonstrated in a conceptual case as an efficient way to treat uncertainties in the system. Therefore, the proposed economic MPC controller can now be implemented in a realistic scenario with robust performance guarantees.

REFERENCES

[1] T. G. Hovgaard, K. Edlund, and J. B. Jørgensen, "The Potential of Economic MPC for Power Management," in *49th IEEE Conference on Decision and Control, 2010*, 2010, pp. 7533–7538.

[2] S. J. Qin and T. A. Badgwell, "A survey of industrial model predictive control technology," *Control engineering practice*, vol. 11, no. 7, pp. 733–764, 2003.

[3] D. Sarabia, F. Capraro, L. F. S. Larsen, and C. de Prada, "Hybrid nmpc of supermarket display cases," *Control Engineering Practice*, vol. 17, no. 4, pp. 428–441, 2008.

[4] L. F. S. Larsen, T. Geyer, and M. Morari, "Hybrid mpc in supermarket refrigeration system," in *IFAC world congress 2005*, Prague, Czech Republic, 2005.

[5] K. Edlund, J. D. Bendtsen, S. Børresen, and T. Mølbak, "Introducing Model Predictive Control for Improving Power Plant Portfolio Performance," in *Proc. of the 17th IFAC World Congress*, 2008.

[6] J. B. Rawlings, D. Bonne, J. B. Jørgensen, A. N. Venkat, and S. B. Jørgensen, "Unreachable setpoints in model predictive control," *IEEE Transactions on Automatic Control*, vol. 53, no. 9, pp. 2209–2215, 2008.

[7] M. Diehl, R. Amrit, and J. B. Rawlings, "A Lyapunov Function for Economic Optimizing Model Predictive Control," *IEEE Transactions on Automatic Control*, 2009.

[8] J. B. Rawlings and R. Amrit, "Optimizing Process Economic Performance Using Model Predictive Control," *Nonlinear Model Predictive Control: Towards New Challenging Applications*, pp. 119–138, 2009.

[9] F. Oldewurtel, A. Parisio, C. N. Jones, M. Morari, D. Gyalistras, M. Gwerder, V. Stauch, B. Lehmann, and K. Wirth, "Energy Efficient Building Climate Control using Stochastic Model Predictive Control and Weather Predictions," in *Proc. of American Control Conference 2010*, 2010, pp. 5100–5105.

[10] Energinet.dk, "Potential and opportunities for flexible electricity consumption with special focus on individual heat pumps (in Danish)," Energinet.dk, The Danish TSO owned by the Danish Climate and Energy Ministry., Tech. Rep., 2011.

[11] G. L. Van Harmelen, "The virtual power station targeting residential, industrial and commercial controllable loads," *IFAC Conference on Technology Transfer in Developing Countries - Automation in Infrastructure Creation (DECOM-TT 2000) Proceedings volume from IFAC Conference*, pp. 45–48, 2001.

[12] R. Bush and G. Wolf, "Utilities load shift with thermal storage." *Transmission & Distribution World*, p. 12, 2009.

[13] A. Bemporad and M. Morari, "Robust model predictive control: A survey," *Robustness in Identification and Control*, pp. 207–226, 1999.

[14] P. D. Couchman, M. Cannon, and B. Kouvaritakis, "Stochastic MPC with inequality stability constraints," *Automatica*, vol. 42, no. 12, pp. 2169–2174, 2006.

[15] J. H. Lee and B. L. Cooley, "Optimal feedback control strategies for state-space systems with stochastic parameters," *IEEE Transactions on Automatic Control*, vol. 43, no. 10, p. 1469, 1998.

[16] D. H. Van Hessem, C. W. Scherer, and O. Bosgra, "LMI-based closed-loop economic optimization of stochastic process operation under state and input constraints," in *IEEE Conference on Decision and Control 2001*, vol. 5, 2001, pp. 4228–4233.

[17] F. Oldewurtel, C. N. Jones, and M. Morari, "A tractable approximation of chance constrained stochastic MPC based on affine disturbance feedback," in *47th IEEE Conference on Decision and Control, 2008*, 2008, pp. 4731–4736.

[18] S. Boyd, C. Crusius, and A. Hansson, "Control applications of nonlinear convex programming," *Journal of Process Control*, vol. 8, no. 5-6, pp. 313–324, 1998.

[19] M. S. Lobo, L. Vandenberghe, S. Boyd, and H. Lebret, "Applications of second-order cone programming* 1," *Linear Algebra and its Applications*, vol. 284, no. 1-3, pp. 193–228, 1998.

[20] A. T. Schwarm and M. Nikolaou, "Chance-constrained model predictive control," *AIChE Journal*, vol. 45, no. 8, pp. 1743–1752, 1999.

[21] P. Li, M. Wendt, and G. Wozny, "A probabilistically constrained model predictive controller," *Automatica*, vol. 38, no. 7, pp. 1171–1176, 2002.

[22] D. E. Kassmann, T. A. Badgwell, and R. B. Hawkins, "Robust steady-state target calculation for model predictive control," *AIChE Journal*, vol. 46, no. 5, pp. 1007–1024, 2000.

[23] M. Shin and J. A. Primbs, "A fast algorithm for for stochastic model predictive control with probabilistic constraints," in *American Control Conference, 2010*, 2010, pp. 5489–5494.

[24] M. Carrion, A. Philpott, A. Conejo, and J. Arroyo, "A stochastic programming approach to electric energy procurement for large consumers," *IEEE Transactions on Power Systems*, vol. 22, no. 2, pp. 744–754, 2007.

[25] M. Parvania and M. Fotuhi-Firuzabad, "Demand response scheduling by stochastic scuc," *IEEE Transactions on Smart Grid*, vol. 1, no. 1, pp. 89–98, 2010.

[26] K. Edlund, J. D. Bendtsen, and J. B. Jørgensen, "Hierarchical model-based predictive control of a power plant portfolio," *Control Engineering Practice*, p. accepted, 2011.

[27] C. V. Rao and J. B. Rawlings, "Linear programming and model predictive control," *Journal of Process Control*, vol. 10, no. 2-3, pp. 283–289, 2000.

[28] J. Skaf and S. P. Boyd, "Design of affine controllers via convex optimization," *IEEE Transactions on Automatic Control*, vol. 55, no. 11, pp. 2476–2487, 2010.

[29] R. Ware and F. Lad, "Approximating the Distribution for Sums of Products of Normal Variables," Department of Mathematics and Statistics, University of Canterbury, New Zealand, Tech. Rep., 2010.

[30] K. Edlund, T. Mølbak, and J. D. Bendtsen, "Simple models for model-based portfolio load balancing controller synthesis," in *IFAC Symposium on Power Plants and Power Systems Control*, 2009.

[31] J. Löfberg, "Modeling and solving uncertain optimization problems in YALMIP," in *IFAC World Congress 2008*, 2008.

PAPER I

Flexible and Cost Efficient Power Consumption using Economic MPC – A Supermarket Refrigeration Benchmark

Flexible and Cost Efficient Power Consumption using Economic MPC
A Supermarket Refrigeration Benchmark

Tobias Gybel Hovgaard, Lars F. S. Larsen and John Bagterp Jørgensen

Abstract— Supermarket refrigeration consumes substantial amounts of energy. However due to the thermal capacity of the refrigerated goods, parts of the cooling capacity delivered can be shifted in time without deteriorating the food quality. In this paper we introduce a novel economic-optimizing MPC scheme that reduces operating costs by utilizing the thermal storage capabilities. In the study we specifically address advantages coming from daily variations in outdoor temperature and electricity prices but other aspects such as peak load reduction are also considered. An important contribution of this paper is also the formulation of a new cost function for our proposed power management system. This means the refrigeration system is enabled to contribute with ancillary services to the balancing power market. Since significant amounts of regulating power are needed for a higher penetration of intermittent renewable energy sources such as wind turbines, this feature will be in high demand in a future intelligent power grid (Smart Grid). Our perspective is seen from the refrigeration system but, as we demonstrate, the involvement in the balancing market can be economically beneficial for the system itself, while delivering crucial services to the Smart Grid. We simulate the system using models validated against data from real supermarkets as well as weather data and spot and regulating power prices from the Nordic power market.

I. INTRODUCTION

In Denmark around 4500 supermarkets consume more than 550,000 MWh annually. This corresponds roughly to 2% of the entire electricity consumption. The installed cooling capacity equals an electrical wattage ranging from 10 to 200 kW depending on the supermarket size. The refrigerated goods make up a large capacity in which energy can be stored in the form of "coldness". Due to the simple hysteresis control policy most commonly used today, a large unexploited potential for energy and cost reductions exists. Preliminary investigations have been carried out in [1], [2], and in this paper we further analyse this in a realistic setting. Furthermore a novel formulation of the cost function enables the supermarket refrigeration system to benefit from the enablement of flexible power consumption.

To obtain an increasing amount of electricity from intermittent energy sources such as solar and wind, we must not only control the production of electricity but also the consumption of electricity in an efficient, flexible and proactive manner. In contrast to the current rather centralized power generation system, the future electricity grid will be a network of a very large number of independent power generators. The Smart Grid is the future intelligent electricity grid and is intended to be the smart electrical infrastructure required to increase the amount of green energy significantly. The Danish transmission system operator (TSO) has the following definition of Smart Grids which we adopt in this work: "Intelligent electrical systems that can integrate the behavior and actions of all connected users - those who produce, those who consume and those who do both - in order to provide a sustainable, economical and reliable electricity supply efficiently" [3]. In this paper we utilize the flexibility of the refrigeration system to offer ancillary demand response to the power grid as regulating power. Different means of utilizing demand response have been investigated in an increasing number of publications e.g. [4]–[7] for plug-in electrical vehicles and heat pumps and in general concerning price elasticity in [8].

Our proposed control strategy is an economic optimizing model predictive controller, economic MPC. Predictive control for constrained systems has emerged during the last 30 years as one of the most successful methodologies for control of industrial processes [9] and is increasingly being considered to control both refrigeration and power systems [10], [11]. MPC based on optimizing economic objectives has only recently emerged as a general methodology with efficient numerical implementations and provable stability properties [12]–[14]. We have previously introduced economic MPC in [15] to control a power management scheme for large power consumers such as supermarket refrigeration systems. The economic MPC has the ability to adjust the power consumption profile to the power supply. The thermal capacity is utilized to shift the load in time, while keeping the temperatures within certain bounds. These bounds are chosen such that they have no impact on food quality. We exploit the fact that the dynamics of the temperature in the cold room are rather slow, while the power consumption can be changed rapidly. Utilizing load shifting capabilities to reduce total energy consumption has also been described in e.g. [16]–[18]. In the simulations that will be presented in this paper, we use models, parameters and temperatures verified against data logged from real supermarkets, along with electricity prices from the NordPool spot market.

Our cost function is nonlinear in the control variables but instead of doing any simplification we have chosen a nonlinear solver [19] to run the simulations. The proposed

T. G. Hovgaard and L. F. S. Larsen are with Danfoss Refrigeration and A/C Controls, DK-6430 Nordborg, Denmark. {tgh,lars.larsen}@danfoss.com

J. B. Jørgensen is with DTU Informatics, Technical University of Denmark, DK-2800 Lyngby, Denmark. jbj@imm.dtu.dk

nonlinear economic MPC algorithm is not tractable for industrial hardware with limited computational resources. Hence, the contribution of this paper is to illustrate the optimal solution and potential of our approach. The study is therefore suitable for benchmarking future, more appealing algorithms. However it should be kept in mind, that the slow dynamics of the system allow for long sample times and therefore, increased complexity of the controller. Robustifying against uncertainties in predictions and models as in [20] also degrades the cost reductions and the study in this paper is again useful for quantifying this kind of effect.

This paper is organized as follows. Section II describes the physics and models used for the supermarket refrigeration systems as well as the thermal storage capabilities. In section III we formulate the economic MPC controller and in section IV the calculations needed for regulating power are given. The scenario for a realistic simulation and the corresponding results are presented in section V and in section VI we give conclusions.

II. SUPERMARKET REFRIGERATION

The supermarket refrigeration systems we consider utilize a vapor compression cycle where a refrigerant is circulated in a closed loop consisting of a compressor, an expansion valve and two heat exchangers, an evaporator in the cold storage room as well as a condenser/gas cooler located in the surroundings. When the refrigerant evaporates, it absorbs heat from the cold reservoir which is rejected to the hot reservoir. The setup is sketched in Fig. 1 with one cold storage room and one frost room connected to the system. Usually several cold storage rooms, e.g. display cases, are connected to a common compressor rack and condensing unit. Hence, the individual display cases see the same evaporation temperature whereas each unit has its own inlet valve for individual temperature control.

A. Models

The dynamics in the cold room can be described by a simple energy balance:

$$mc_p\frac{dT_{cr}}{dt} = \dot{Q}_{load} - \dot{Q}_e \qquad (1)$$

with

$$\dot{Q}_{load} = (UA)_{amb-cr} \cdot (T_{amb} - T_{cr}) \qquad (2a)$$
$$\dot{Q}_e = (UA)_{cr-e} \cdot (T_{cr} - T_e) \qquad (2b)$$

where UA is the heat transfer coefficient and m and c_p are the mass and the specific heat capacity of the refrigerated goods, respectively. T_{amb} is the temperature of the ambient air which puts the heat load on the refrigeration system. The states and control variables of the system are limited by the following constraints:

$$T_{cr,min} \leq T_{cr} \leq T_{cr,max} \qquad (3a)$$
$$0 \leq T_{cr} - T_e \leq \infty \qquad (3b)$$
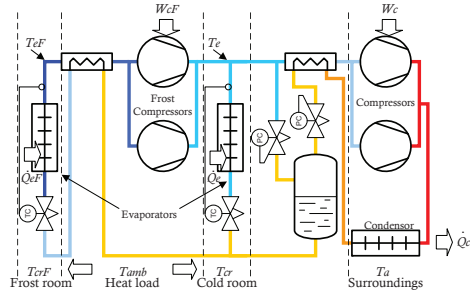$$0 \leq \dot{Q}_e \leq (UA)_{cr-e,max} \cdot (T_{cr} - T_e) \qquad (3c)$$

Fig. 1. Schematic layout of basic refrigeration system.

We define the set Ω as all $(\dot{Q}_e, T_e)$ that satisfy the system dynamics (Eq. (1)) and the constraints given in Eq. (3).

The work done by the compressor dominates the power consumption in the system and can be expressed by the mass flow of refrigerant (m_{ref}) and the change in energy content of the refrigerant. Energy content is described by the enthalpy of the refrigerant at the inlet and at the outlet of the compressor (h_{ic} and h_{oc} respectively). Hereby the expression in Eq. (4) is given.

$$\dot{W}_c = \frac{m_{ref} \cdot (h_{oc}(T_e, P_c) - h_{ic}(T_e))}{\eta_{is}(P_c/P_e)} \qquad (4)$$

where the enthalpies depend on the evaporation temperature and the condensing pressure, as stated. The mass flow can be determined as the ratio between cooling capacity and change of enthalpy over the evaporator:

$$m_{ref} = \frac{\dot{Q}_e}{h_{oe}(T_e) - h_{ie}(P_c)} \qquad (5)$$

All the enthalpies given here as functions of T_e, P_c or both are non-linear refrigerant dependent functions which can be calculated e.g. by the software package "RefEqns" [21]. In the sequel, we adopt the approximation used for $\dot{W}_c$ in [2], where polynomials are fitted for the enthalpy differences and the isentropic efficiency, η_{is}, is assumed constant within the range of operation. When a frost room is included, an extra compressor system is usually added between the frost evaporator and the suction side of the other compressors. This compressor decreases the evaporation temperature for the frost part of the system to a lower level. The work in the frost compressor is similar to what we have already described, but instead of the condensing temperature, the frost compressor sees the evaporation temperature for the cooling part at its outlet. The mass flow through the frost compressor needs to be added to the flow through the compressors from the cooling. We use the subscript F to denote variables related to the frost part.

For the studies in this paper we have collected data from several supermarkets actually in operation in Denmark. From

these data, typical parameters such as time constants, heat loads, temperature ranges and capacities in both individual display cases and for the overall system have been estimated for both horizontal display cases, vertical shelving units and frost rooms. Furthermore the running compressor capacity has been monitored and from the data sheets the relation to energy consumption has been found.

B. Thermal Storage

Today, most display cases and cold rooms in supermarkets are controlled by hysteresis. Thus, maximum cooling is applied when the cold room temperature reaches an upper limit and shut off when the lower limit is reached. This control policy does not exploit the thermal capacity in the refrigerated mass and energy is consumed when it is needed instead of when it is more favorable. Several factors can, however, make it beneficial to shift the load. These include variations in outdoor temperature, fluctuating energy prices, times for restocking and night covers. Obviously several unexploited potentials exist. If peak loads can be predicted, pre-cooling can be applied such that the stored coldness helps reduce the demand at the peak time. Thereby, the entire system might be dimensioned differently, which saves money both in the installation phase and during operation. By moving part of the cooling capacity to the colder night times, overall energy consumption can be reduced since the work done by the compressor to obtain a certain evaporation temperature is dependent on the pressure difference which again depends on the temperature surrounding the condenser. In contrast, shifting loads according to fluctuations in electricity prices actually make the system consume more energy. Thus, the profitability rests upon the extra heat loss during periods when extra coldness is stored in the system is at least counterbalanced by the difference in electricity price.

It is evident from the discussion above that the potential in load shifting in large part depends on both the thermal capacity and the differences in electricity prices and outdoor temperatures. However, the rate of change of these parameters in comparison with the time constants of the cold room temperatures also plays an important role.

III. Economic MPC Setup

A supermarket refrigeration system is influenced by a number of disturbances that can be predicted to some degree of certainty over a time horizon into the future. The controller also has to obey certain constraints for the systems, while minimizing the cost of operation. Thus, we find it reasonable to aim at formulating our controller as an economic optimizing MPC problem. Whereas the cost function in MPC traditionally penalizes a deviation from a set-point, our proposed economic MPC directly reflects the actual costs of operating the plant. This formulation is tractable for refrigeration systems where we are interested in keeping the outputs (cold room temperatures)

within certain ranges, while minimizing the cost of doing so.

Like in traditional MPC, we implement the controller in a receding horizon manner where an optimization problem over N time steps (our control and prediction horizon) is solved at each sample. The result is an optimal input sequence for the entire horizon out of which only the first step is implemented. This procedure is repeated at each sample. The objective function is the cost of operation which in this case is entirely related to electricity consumption. We do not aim specifically at minimizing the energy consumption, nor do we focus on tracking certain temperatures in the cold rooms. The optimization problem is thus formulated as:

$$\min_{(\dot{\mathbf{Q}}_e, \mathbf{T}_e) \in \Omega} \Phi = \sum_{k=0}^{N-1} C_{el,k} W_c(\dot{Q}_{e,k}, T_{e,k}, T_{a,k}, T_{amb,k}) \tag{6a}$$

$$\dot{\mathbf{Q}}_e = \left\{ \dot{Q}_{e,k} \right\}_{k=0}^{N-1} \quad , \quad \mathbf{T}_e = \{T_{e,k}\}_{k=0}^{N-1} \tag{6b}$$

where $W_c(\cdot)$ is the energy consumption as in section II. The MPC feedback law is the first move in Eq. (6b).

Often output constraints are soft in MPC but in this setup constraints on temperatures and capacity are made hard. In reality one could formulate a cost on cold room temperatures outside the allowable range related to the degrading of the food stuff. This cost would then be the cost on slack variables in a soft constraint. However, firstly it is not realistic that an owner of a refrigeration system will damage the food stuff, and secondly, estimating bacteria growth in refrigerated food is, in itself, a complicated study. In a stochastic formulation a feasible problem can be guaranteed using probabilistic constraints.

In the above formulation we assume perfect predictions and therefore we allow the system to go to any extreme point within the feasible region. However in reality both disturbance predictions and models of the systems are subject to uncertainties that are prone to driving the otherwise optimal solution of the economic MPC to a very undesirable solution. For refrigeration systems, such situations could be too high or too low temperatures in the cold room damaging the food stuff; emergency shut down of systems due to maximum capacity being exceeded; penalties for not fulfilling regulating power agreements or unnecessarily high operation costs. Consequently we have formulated a robust economic MPC scheme in [20] using probabilistic constraints and assumed knowledge of the probability density functions for stochastic disturbances and impulse response coefficients of the system models.

IV. Flexible Power Consumption

In order to ensure a sustainable physical balance in the electricity system, there is a need for regulating power and various types of spare capacity. Spare capacity is production capacity or consumption made available in advance to the

TSO by parties responsible for maintaining balance in the syste, in return for an availability payment. Various types of spare capacity exist. These types of capacity differ in activating velocity, amount and demands for the upholding period.

With the enablement of flexible consumption in refrigeration systems we are ready to consider other incentives to load shifting than those already mentioned in section II. In this section we formulate a framework in which the supermarkets can participate in the primary reserve (the capacity with fastest activation and shortest upholding periods).

A. Up regulating power as primary reserve:

Up regulating power is increased production or reduced consumption. Each player participates with a power amount (MW) specified on an hourly basis and is paid for making the power available to the grid (DKK/MW) regardless of the actual activation. Activation is automatic and linearly frequency dependent in the range $\pm 200mHz$. Activation is maintained for up to 15 minutes (typically 2-3 minutes) and must be fully restored after 15 minutes. Even though the activated power (MW) might be large, the delivered energy (MWh) is usually small amounts, so a possible change in spot price during the activation will have almost no effect on the economy.

Assumption 1: Since the ambient temperature is generally much higher than the cold room temperature, the small change in temperature during an activation does not change the load, $\dot{Q}_{load} = UA(T_{amb} - T_{cr})$ much. Hence, by assuming that $\dot{Q}_{load} = UA(T_{amb} - T_{cr,start})$ is constant over the activation period we are almost conservative in the calculations.

Assumption 2: In steady state $\dot{Q}_e = \dot{Q}_{load}$

Assumption 3: An activation period of maximum 15 minutes is relatively short compared to the rate of change in the disturbances (Outdoor temperature T_a and electricity spot prices C_{el}). Thus, the cost of the energy required to reestablish the reserve following an activation is approximately the same as the amount saved during the activation.

The amount of power available for up regulation is described by:

$$\dot{Q}_{reg\div} = \dot{Q}_e - \dot{Q}_{15\div} \qquad (7)$$

where $\dot{Q}_{reg\div}$ is the cooling capacity that can be released as up regulating power and $\dot{Q}_{15\div}$ is the cooling need in order to make T_{cr} stay below Tcr, max for 15 minutes. During an activation the temperature in the cold room is:

$$m \cdot Cp\frac{dT_{cr}}{dt} = \dot{Q}_{load} - \dot{Q}_{15\div} = \dot{Q}_{reg\div} \qquad (8)$$

Therefore:

$$m \cdot Cp\int_{T_{cr}}^{T_{cr,max}} dT_{cr} = \int_0^{900s} \dot{Q}_{reg\div}dt \qquad (9)$$

$$\dot{Q}_{reg\div} = (T_{cr,max} - T_{cr})\frac{m \cdot Cp}{900s} \qquad (10)$$

For up regulating power there is a potential decrease in heat loss from the system if the reserve is activated. By assuming almost linear cold room temperature curves within the range we are considering for regulating power reserves, the reduced energy loss during an entire period of activation and the subsequent re-establishment can be averaged by

$$\dot{Q}_{loss\div} = P_\div \cdot \alpha_\div \cdot UA \cdot (T_{cr,max} - T_{cr}) \qquad (11)$$

where UA is the overall heat transfer coefficient from the cold room to surroundings and $P_\div$ is the probability of being activated (samples where the system is activated as up regulating power or is re-establishing after an up regulation versus the total number of samples). We also introduce a new decision variable $\alpha_\div \in [0;1]$, which is the amount of available up regulating power that is actually offered to the grid. Since power cannot be extracted from the stored coldness we have to introduce a constraint such that the offered up regulating power is never larger than the actual power consumption at any point of time.

$$\alpha_\div \cdot \dot{Q}_{reg\div} \leq \dot{Q}_e \qquad (12)$$

B. Down regulating power as primary reserve:

Down regulating power is reduced production or increased consumption. The rules of participation are equal to those described for up regulating power. The assumptions 1-3 are still in effect, however assumption 3 is the opposite. Namely that the cost of extra energy used during an activation equals the amount that can be saved following the activation.

The system can participate with down regulating power as given by:

$$\dot{Q}_{reg+} = \dot{Q}_{15+} - \dot{Q}_e \qquad (13)$$

where $\dot{Q}_{reg+}$ is the extra cooling capacity that can be used as down regulating power and $\dot{Q}_{15+}$ is the cooling capacity that makes T_{cr} go to Tcr, min in 15 minutes. Performing the same calculations as in Eq. (8)-(9) yields:

$$\dot{Q}_{reg+} = (T_{cr} - T_{cr,min})\frac{m \cdot Cp}{900s} \qquad (14)$$

As with up regulating power, an activation of the reserve changes the heat loss from the system. This is not accounted for in the calculations above. Whereas the original cost function covers the extra heat loss caused by maintaining up regulating reserves (a decrease in cold room temperature and thereby increase in heat loss in time periods with no activation) there is no extra cost, in terms of heat loss, related to maintaining down regulating reserves. This cost only comes into play when activation occurs. Again, we assume almost linear temperature curves within the range of interest and the energy loss during an entire period of activation and subsequent re-establishment can be averaged by

$$\dot{Q}_{loss+} = P_+ \cdot \alpha_+ \cdot UA \cdot (T_{cr} - T_{cr,min}) \qquad (15)$$

where P_+ is the probability of being activated. A new decision variable, $\alpha_+ \in [0;1]$, is again introduced describing

the share of available down regulating power that is actually offered to the grid. The amount of down regulating power offered must be bounded such that the sum of current cooling capacity and that offered for down regulation does not exceed the maximum capacity of the system. Thus, even on a hot summer day the following has to be fulfilled:

$$\alpha_+ \cdot \dot{Q}_{reg+} + \dot{Q}_e \leq \dot{Q}_{max} \qquad (16)$$

C. Cost Function

We are now able to formulate a cost function including the effects of regulating power:

$$\min_{\dot{\mathbf{Q}}_\mathbf{e},\mathbf{T}_\mathbf{e},\alpha_\div,\alpha_+} \sum_{k=0}^{N} \Big[C_{el_k} W_k((\dot{Q}_{e,k} - \dot{Q}_{loss\div,k} + \dot{Q}_{loss+,k}),(\cdot)) $$
$$- C_{upreg_k} W_k(\alpha_{\div,k} \dot{Q}_{reg\div,k},(\cdot)) $$
$$- C_{downreg_k} W_k(\alpha_{+,k} \cdot \dot{Q}_{reg+,k},(\cdot)) \Big] $$
$$s.t. \qquad\qquad\qquad\qquad\qquad\qquad\qquad\qquad (17)$$
$$(\dot{\mathbf{Q}}_\mathbf{e},\mathbf{T}_\mathbf{e}) \in \Omega$$
$$\text{Eq. (12)}$$
$$\text{Eq. (16)}$$

where '$(\cdot)$' indicates the remaining parameters from Eq. (6a).

V. Results

In this section we present the conditions used for simulating a realistic scenario with the supermarket refrigeration system from section II in a setting where predictions of electricity prices, regulating power prices as well as outdoor temperatures exist. We use the economic MPC controller described in section III, and for the regulating power scenarios, the cost function in section IV is employed. Results of the simulations are presented and discussed.

A. Scenario

For the study in this paper we have chosen a supermarket refrigeration system with three units attached. This roughly corresponds in size to between $1/15$ to $1/5$ of one of the supermarkets we have been monitoring and the capacity of the system has been scaled accordingly. The three units are very different. The shelving unit is usually used for smaller items like sliced meat and does not hold a very large mass of food stuff. The heat load is relatively high due to the large vertical opening to the surroundings. The chest display case holds larger amounts of e.g. minced meat and due to the horizontal opening, which also has a glass cover, the heat load is rather low. The frost room with insulated walls on all sides has the lowest heat load and the mass of frozen meat contained is large. For the frost room an extra compressor is added, lowering the evaporation temperature to a sufficiently lower level than the evaporation temperature in the cooling units. All three units have different demands to temperature, namely $[2;4]°$C for the shelving unit, $[1;5]°$C for the chest display case and $[-25;-15]°$C for the frost room. The models were validated

with running supermarkets in Denmark in January 2011. Electricity prices were downloaded from NordPool's hourly el-spot price for a period of one month. There is a clear trend in these data for each 24-hour period. Therefore, for each hour of the day, the average has been found and this 24-hour signal was used for the electricity price. The same was done with the availability payment for regulating power.

Temperature readings from Danish Meteorological Institute covering the same period were obtained. It has been found that by low pass filtering and detrending these data, the intra-day variations can be closely approximated by a sinusoid with a 24-hour period and a phase shift such that it peaks a couple of hours after noon. The amplitude for this period has been chosen to $3°$C.

We divide our simulations into two scenarios. One that illustrates the effect of variations in electricity prices and temperatures, and one that shows how regulating power services can be offered. Simulations are performed over at least 24 hours. An issue with MPC is that the long prediction horizons tend to make the problems computationally hard. However, due to the slow dynamics of the refrigeration system, we have chosen a sampling time of 32 minutes. Thus a prediction horizon of 16 hours is implemented with just $N = 30$ samples.

B. Simulation

Fig. 2 shows the simulated refrigeration system using the predicted outdoor temperature and electricity price to optimize the cost. The amplitude of the electricity price has been multiplied by four to better illustrate the effect and to reflect a scenario with variable taxes instead of the flat rate fees seen today. This is discussed in the next section. In this case the cost savings amount to 32%. If the original electricity price is used, less change in cold room temperatures can be observed and the cost savings amount to 9% in this case. With three quarters of the electricity price paid in Denmark today being flat rate taxes and fees, saving 9% on the spot price corresponds to 2.25% of the entire electricity bill. If we are only exploiting the variations in outdoor temperature, the economic MPC control scheme saves around 2% of the energy consumption.

In Fig. 3 the effect of participating in the power balancing market is simulated for a selected scenario of availability payments. In this simulation the outdoor temperature is assumed constant in order to illustrate the effect of availability payments for regulation power versus the electricity spot price as clearly as possible. This simulation reveals an additional saving of up to 70% compared to the case where only the electricity spot price is used for optimization (approximately 30% for up regulation only).

C. Discussion

From the results illustrated in Fig. 2 we can conclude that the proposed economic MPC scheme has a positive effect

(a) Cold room and evaporation temperatures

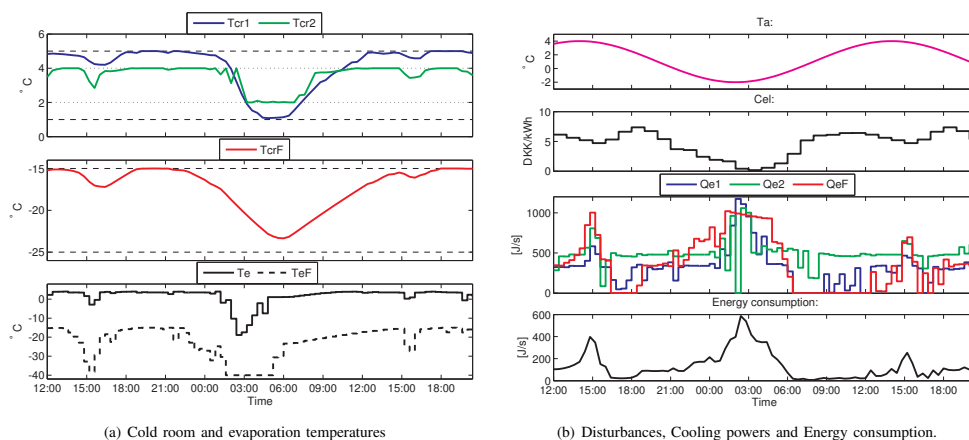(b) Disturbances, Cooling powers and Energy consumption.

Fig. 2. Simulation showing how variations in outdoor temperature and electricity prices are exploited by utilization of thermal storage.

on the costs related to operating the supermarket. Variations in outdoor temperature are utilized to minimize power consumption, whereas exploiting variations in electricity prices tends to increase overall power consumption but at a lower cost. In Fig. 2 the amplitude of the electricity price has been multiplied by four to illustrate the increase in effect gained by the power management. Today the dominant part of the price paid for electricity consists of taxes and connection fees, which are all paid as flat rate charges per MWh. This blurs the price signals from the market to the users and reduces the incentives to react to such signals. Hence, the simulation shown above with four-times amplitude on the el-spot price is an attempt to model a situation where the taxes and other fees are charged as a percentage of the actual el-spot price. This would result in a magnification instead of a smoothing of the market signals.

Obviously the flexibility is drastically reduced if the system is running near its maximum capacity just to keep the temperatures below the maximum limits on a hot summer day. It is not possible to increase consumption, whether it be for storing coldness or for down regulation due to the maximum capacity; nor is it possible to decrease consumption, since this would violate the temperature demands in the cold rooms. This situation leads to a trade-off between saving by dimensioning a smaller system when peak loads can be reduced as described in section II and savings related to flexible consumption and regulating power.

Participating in the balancing power market also seems to be beneficial for both the power system and the supermarkets if we consider the simulation in Fig. 3. At least at the time of the year/day where extra capacity is available and the availability payment is sufficiently high. The availability

payments are observed to vary more from day to day than the spot prices. Hence, the simulation presented in this paper is just for a selected scenario. However a large potential saving has been found, meaning that there is room for deviations from the simulated scenario without ruining the business case of participating with regulating power. Furthermore it is estimated from the simulations that a supermarket can offer at least 20% of its capacity as regulating power (except at the peak load days of the year). Currently the peak demand in Denmark for primary reserves is around 60MW. With an average supermarket offering about 20 percent of its capacity, approximately 75 percent of the total needs for primary reserves could be provided by supermarkets. A single supermarket is not able to participate with sufficient capacities to place bids on the balancing market, however aggregation of e.g. chains of shops would be an obvious solution. With an increasing penetration of intermittent wind energy, the value of regulating reserves is expected to increase [22]. Thus, not only the need for regulating power but also the incentives to participate in the regulating power market increase.

VI. CONCLUSION

We have presented a power management scheme for a supermarket refrigeration system and demonstrated how an economic MPC control policy can reduce operating costs of the system. Models, parameters and other quantities used have been verified and are to scale with realistic scenarios in Denmark. Using a nonlinear MPC solver for our problem we illustrated that significant savings of up to 9-32% can be achieved by utilizing thermal storage capacities together with predictions of varying loads and energy prices. A novel formulation of the cost function flexibilities in the power consumption also revealed a potential for participating in the

(a) Cold room and evaporation temperatures   (b) Prices, consumptions and costs.
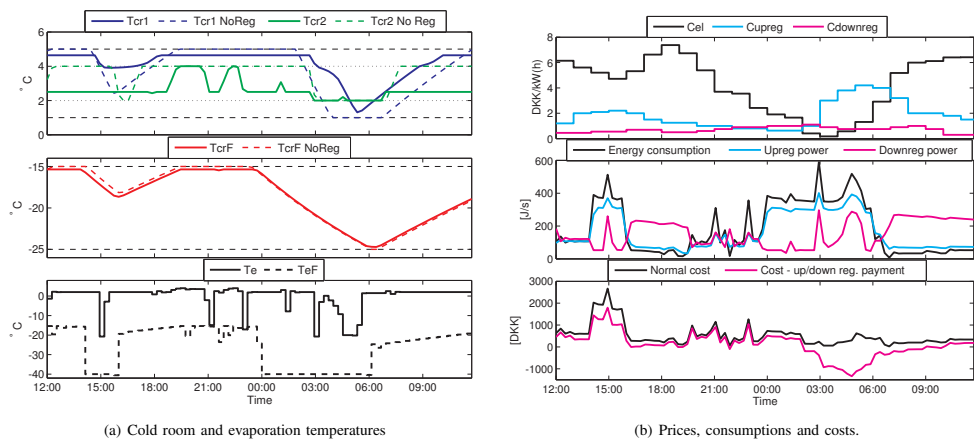
Fig. 3. Simulation showing how the flexible consumption is utilized for offering regulating power to the balancing market. The cold room temperatures for an optimization utilizing only the electricity spot price over the same period are shown to illustrate the difference.

balancing power market with remarkable cost reductions of up to 70% as the result. The results are especially valuable for proving the concept and the new cost function in a realistic setting, but they are also useful for benchmarking future algorithms that might include computational simplifications and/or implementation of robustifying means in the economic MPC formulation.

REFERENCES

[1] L. F. S. Larsen, C. Thybo, and H. Rasmussen, "Potential energy savings optimizing the daily operation of refrigeration systems," *Proc. European Control Conference, Kos, Greece*, pp. 4759–4764., 2007.

[2] T. G. Hovgaard, L. F. S. Larsen, M. J. Skovrup, and J. B. Jørgensen, "Power Consumption in Refrigeration Systems - Modeling for Optimization," in *4th International Symposium on Advanced Control of Industrial Processes, 2011*, 2011, pp. 234–239.

[3] Energinet.dk, "Potential and opportunities for flexible electricity consumption with special focus on individual heat pumps (in Danish)," Energinet.dk, The Danish TSO owned by the Danish Climate and Energy Ministry., Tech. Rep., 2011.

[4] S. L. Andersson, A. K. Elofsson, M. D. Galus, L. Göransson, S. Karlsson, F. Johnsson, and G. Andersson, "Plug-in hybrid electric vehicles as regulating power providers: Case studies of Sweden and Germany," *Energy policy*, vol. 38, no. 6, pp. 2751–2762, 2010.

[5] H. Saele and O. S. Grande, "Demand response from household customers: Experiences from a pilot study in norway," *IEEE Transactions on Smart Grid*, vol. 2, no. 1, pp. 90–97, 2011.

[6] S. Han, S. Han, and K. Sezaki, "Development of an optimal vehicle-to-grid aggregator for frequency regulation," *IEEE Transactions on Smart Grid*, vol. 1, no. 1, pp. 65–72, 2010.

[7] A. Molina-Garcia, M. Kessler, J. A. Fuentes, and E. Gomez-Lazaro, "Probabilistic characterization of thermostatically controlled loads to model the impact of demand response programs," *IEEE Transactions on Power Systems*, vol. 26, no. 1, pp. 241–251, 2011.

[8] D. S. Kirschen, "Demand-side view of electricity markets," *Power Systems, IEEE Transactions on*, vol. 18, no. 2, pp. 520–527, 2003.

[9] S. J. Qin and T. A. Badgwell, "A survey of industrial model predictive control technology," *Control engineering practice*, vol. 11, no. 7, pp. 733–764, 2003.

[10] D. Sarabia, F. Capraro, L. F. S. Larsen, and C. de Prada, "Hybrid nmpc of supermarket display cases," *Control Engineering Practice*, vol. 17, no. 4, pp. 428–441, 2008.

[11] K. Edlund, J. D. Bendtsen, and J. B. Jørgensen, "Hierarchical model-based predictive control of a power plant portfolio," *Control Engineering Practice*, p. accepted, 2011.

[12] D. Angeli, R. Amrit, and J. B. Rawlings, "On average performance and stability of economic model predictive control," *IEEE Transactions on Automatic Control*, p. accepted, 2011.

[13] M. Diehl, R. Amrit, and J. B. Rawlings, "A Lyapunov Function for Economic Optimizing Model Predictive Control," *IEEE Transactions on Automatic Control*, 2009.

[14] J. B. Rawlings and R. Amrit, "Optimizing Process Economic Performance Using Model Predictive Control," *Nonlinear Model Predictive Control: Towards New Challenging Applications*, pp. 119–138, 2009.

[15] T. G. Hovgaard, K. Edlund, and J. B. Jørgensen, "The Potential of Economic MPC for Power Management," in *49th IEEE Conference on Decision and Control, 2010*, 2010, pp. 7533–7538.

[16] G. L. Van Harmelen, "The virtual power station targeting residential, industrial and commercial controllable loads," *IFAC Conference on Technology Transfer in Developing Countries - Automation in Infrastructure Creation (DECOM-TT 2000) Proceedings volume from IFAC Conference*, pp. 45–48, 2001.

[17] R. Bush and G. Wolf, "Utilities load shift with thermal storage." *Transmission & Distribution World*, p. 12, 2009.

[18] F. Oldewurtel, A. Parisio, C. N. Jones, M. Morari, D. Gyalistras, M. Gwerder, V. Stauch, B. Lehmann, and K. Wirth, "Energy Efficient Building Climate Control using Stochastic Model Predictive Control and Weather Predictions," in *Proc. of American Control Conference 2010*, 2010, pp. 5100–5105.

[19] B. Houska, H. Ferreau, and M. Diehl, "ACADO Toolkit–An Open Source Framework for Automatic Control and Dynamic Optimization," *Optimal Control Applications and Methods*, 2010.

[20] T. G. Hovgaard, L. F. S. Larsen, and J. B. Jørgensen, "Robust Economic MPC for a Power Management Scenario with Uncertainties," in *50th IEEE Conference on Decision and Control, 2011*, 2011, p. accepted.

[21] M. J. Skovrup, "Thermodynamic and thermophysical properties of refrigerants - software package in borland delphi." Department of Energy Engineering, Technical University of Denmark, Tech. Rep., 2000.

[22] S. Meyn, M. Negrete-Pincetic, G. Wang, A. Kowli, and E. Shafieepoorfard, "The value of volatile resources in electricity markets," in *49th IEEE Conference on Decision and Control, 2010*, 2010, pp. 1029–1036.

Analyzing Control Challenges for Thermal Energy Storage in Foodstuffs

Analyzing Control Challenges for Thermal Energy Storage in Foodstuffs

Tobias Gybel Hovgaard, Lars F. S. Larsen, Morten J. Skovrup, and John Bagterp Jørgensen

Abstract— We consider two important challenges that arise when thermal energy is to be stored in foodstuffs. We have previously introduced economic optimizing MPC schemes that both reduce operating costs and offer flexible power consumption in a future Smart Grid. The goal is to utilize the thermal capacity of refrigerated goods in a supermarket to shift the load of the system in time without deteriorating the quality of the foodstuffs. The analyses in this paper go before closing any control loops. In the first part, we introduce and validate a new model with which we can estimate the actual temperatures of refrigerated goods from available air temperature measurements. This is based on data obtained from a dedicated experiment. Since limits are specified for food temperatures, the estimate is essential for full exploitation of the thermal potential. Secondly, the thermal properties, shapes and sizes of different foodstuffs make them behave differently when exposed to changes in air temperature. We present a novel analysis based on Biot and Fourier numbers for the different foodstuffs. This provides a valuable tool for determining how different items can be utilized in load-shifting schemes on different timescales and for estimating maximum energy storage time. The results are shown for a large range of parameters, and with specific calculations for selected foodstuff items.

NOMENCLATURE

$\dot{Q}$	Energy flow (W)		
M	Mass (kg)		
$\dot{m}$	Mass flow ($kg\ (dry\ air)/s$)		
T	Temperature ($°C$)		
ΔT	Temperature difference (K)		
P	Pressure (Pa)		
Cp	Specific heat capacity ($J/(kg \cdot K)$)		
UA	Overall heat transfer coefficient (J/K)		
l_{sh}	Relative length of superheat zone		
I	Enthalpy of humid air ($J/kg\ (dry\ air)$)		
RH	Relative humidity (%)		
x	Absolute humidity ($kg/kg\ (dry\ air)$)		
h	Enthalpy (J/kg)		
Δh_{lg}	Latent heat (J/kg)		
λ	Thermal conductivity ($W/(m \cdot K)$)		
ρ	Density (kg/m^3)		
h_{ext}	Surface heat transfer coefficient ($W/(K \cdot m^2)$)		

Subscripts:

e	Evaporation	c	Condensing
amb	Ambient	air	Dry air
ref	Refrigerant	$infilt$	Infiltration
$sens$	Sensible	lat	Latent
sh	Superheat	$surf$	Surface
ex	Exchanged		

T.G. Hovgaard and L.F.S. Larsen are with Vestas Technology R&D, Hedeager 42, DK-8200 Aarhus N, Denmark {togho, lfsla}@vestas.com

M.J. Skovrup is with IPU Technology Development, Building 403, DK-2800 Kgs. Lyngby, Denmark mjs@ipu.dk

J.B. Jørgensen is with DTU Informatics, Technical University of Denmark, Building 321, DK-2800 Kgs. Lyngby, Denmark jbj@imm.dtu.dk

I. INTRODUCTION

In Denmark, around 4500 supermarkets consume more than 550,000 MWh annually. This corresponds roughly to 2% of the entire electricity consumption in Denmark. The capacity for energy storage in the refrigerated goods is not exploited by the thermostat (hysteresis) control policy used today and a large potential for energy and cost reductions exits. Preliminary investigations have been carried out in [1]–[4]. However, accurate estimation of the temperature behavior and distribution in the refrigerated foodstuffs is needed in order to take such simulation studies closer to the challenges seen in an actual supermarket.

A major challenge when exploiting thermal capacity in refrigerated goods is that the temperature of the goods is not normally measured in a supermarket setting. Only air temperatures at the inlets and outlets of the display case are known. However, quality demands, and therefore also temperature ranges, are specified for the foodstuffs. Since the dynamics of larger food items like milk or ground meat packages are much slower than the dynamics of the surrounding air, a substantial share of the potential in thermal energy storage is lost, if we cannot estimate the actual temperatures of the goods. In this paper, we present a model of the display case that links food temperatures to the measurements available.

Different goals can be achieved by applying, *e.g.*, economic model predictive control (MPC) strategies for shifting the load of supermarket refrigeration systems: Energy consumption can be minimized by shifting loads to periods with lower outdoor temperatures. Equipment can be dimensioned smaller or operated at more efficient levels by reducing peak loads. Expenditure on power can be reduced by utilizing varying electricity prices, and by participation in a Smart Grid, the system can be rewarded for its flexibility while delivering crucial services to a power grid with increasing amounts of fluctuating renewable energy sources. This is further discussed in [2], [3], [5]. As shown in our previous work load shifting strategies can be beneficial on different time scales. Participation in the primary regulating power market is mostly on a 15-minute timescale. Peak avoidance and/or utilization of short term variations in electricity prices might call for load shifts of around 2 hours, while day/night variations of both weather and prices work on a timescale of up to 12 hours. Depending on the timescale, energy storage potential is not directly given by the thermal mass in a
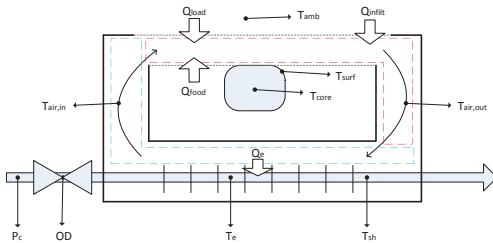
Fig. 1. Refrigerated display case with indications of energy flows, measurements and defined control volumes for air temperatures.
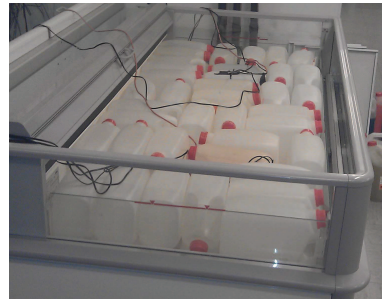

Fig. 2. The experiment setup in the lab.

refrigerated display case. Since only fractions of the stored mass might be affected by the changes in temperature, we introduce the term "active thermal mass". The relevance of applying load shifting strategies on the aforementioned timescales depends on the active thermal mass for a specific item. We analyze this for different types of foodstuffs.

II. SYSTEM DESCRIPTION

The system is a refrigerated display case with a horizontal opening at the top. It is depicted in Fig. 1. Foodstuffs are stacked inside the case where it is kept refrigerated by a "curtain" of cold air flowing between inlets and outlets on either side of the display case. The foodstuffs are hereby separated from the surroundings, and since we disregard any heat transfer by radiation from e.g. light sources in the room, we can assume that heat transfer to/from the foodstuffs only occurs to/from the air curtain. A heat load from the surroundings affects the air curtain both by simple conduction and by infiltration of a degree of ambient air which unavoidably gets mixed into the air stream. The air is circulated by a fan from the air curtain, through a heat exchanger (evaporator) underneath the storage room, and back to the air curtain. In the heat exchanger, heat is removed from the air by evaporation of a refrigerant. The evaporation temperature (T_e) and the opening degree (OD) of an expansion valve at the inlet can be controlled. The superheat temperature is a measure of the distance from the liquid/vapor front to the end of the evaporator, and often an inner loop for superheat control is established. Hence, the set-point of the superheat controller can be considered as a control input instead of the opening degree of the valve.

A. Data set

The data set was collected in the refrigeration lab at Danfoss A/S, Denmark, from a setup using a horizontal 2.5x1.5m supermarket display case. The measured variables (indicated on Fig. 1) are those normally measured in a real supermarket setting; $T_{air,in}$, $T_{air,out}$, T_e, ΔT_{sh}, T_{amb}, OD, and P_c with the addition of two sensors for temperature of the goods; T_{surf} and T_{core}, surface and core temperatures respectively. Canisters filled with ethylenglycol were used to simulate goods instead of actual foodstuffs. A picture

of the setup is seen in Fig. 2. As is the case in most supermarkets, temperature control was done by hysteresis using the temperature of the air flow out of the display case with defined upper and lower limits. Since no foodstuffs could be damaged in this experiment, more variation in the temperature than what is normally possible in a supermarket was allowed. The data were sampled every $T_s = 5$ seconds (which is relatively fast compared to the slow dynamics of the system) and pre-processed with a moving average, low-pass filter. According to the specifications of the sensors, the measurements can have a constant offset of up to $0.5K$.

B. Assumptions

In order to formulate the equations in the next section we need to make some assumptions.

- We define two control volumes for the areas surrounding the measured air temperatures. These areas are shown with blue and red dotted lines on Fig. 1. Within each of these volumes, we assume uniform temperatures.
- We scale the cooling energy in the evaporator according to manufacturer's knowledge of maximal capacity. In this case: $\dot{Q}_{e,max} \approx 0.7kW/m \cdot 1.8m = 1260W$.
- According to [6] the load on a horizontal display case without covers is typically divided so that 75% is due to infiltration of ambient air while the remaining 25% (neglecting radiation) is due to conduction. We adopt this ratio here.
- It is assumed that the relative humidity in the lab environment remains constant at 50%. Furthermore, we assume that the relative humidity is approximately 95% in the air flow after the evaporator since the saturation temperature is normally reached such that water is condensed from the air.
- The inner control loop is much faster than the dynamics we are trying to estimate. Thus, it is neglected in the model of the system.

C. Model

Before we apply a grey-box identification technique, the differential equations governing the system dynamics are established. We have chosen four states, namely $T_{air,in}$, $T_{air,out}$,

T_{surf} and T_{core}, and by setting up the energy balances we get (1)-(4).

$$M_{air,1}Cp_{air}\frac{dT_{air,in}}{dt} = \dot{m}_{air} \cdot (I(T_{air,out},RH_{out}) -$$
$$I(T_{air,in},95\%)) - \dot{Q}_{sens} \qquad (1)$$

$$M_{air,2}Cp_{air}\frac{dT_{air,out}}{dt} = \dot{m}_{air} \cdot (I(T_{air,in},95\%) -$$
$$I(T_{air,out},RH_{out})) +$$
$$\dot{Q}_{load} + \dot{Q}_{infilt} + \dot{Q}_{food} \qquad (2)$$

$$M_{surf}Cp_{food}\frac{dT_{surf}}{dt} = \dot{Q}_{surf-core} - \dot{Q}_{food} \qquad (3)$$

$$M_{core}Cp_{food}\frac{dT_{core}}{dt} = -\dot{Q}_{surf-core} \qquad (4)$$

Some of the energy flows are given by Newton's law of convection:

$$\dot{Q}_{load} = UA_{amb} \cdot (T_{amb} - T_{air,out}) \qquad (5)$$
$$\dot{Q}_{food} = UA_{food} \cdot (T_{surf} - T_{air,out}) \qquad (6)$$
$$\dot{Q}_{surf-core} = UA_{surf-core} \cdot (T_{core} - T_{surf}) \qquad (7)$$

The energy contribution due to infiltration is given by:

$$\dot{Q}_{infilt} = \dot{m}_{ex} \cdot (I(T_{amb},50\%) - I(T_{air,out},95\%)) \qquad (8)$$

For the cooling capacity from the evaporator we have chosen the ε-NTU method which is generally accepted for heat exchanger modeling [7]. Here we assume that the method adopts to humid air.

$$\dot{Q}_e = \dot{Q}_{sens} + \dot{Q}_{lat}$$
$$= \dot{m}_{air}(I(T_{air,out},RH_{out}) - I(T_e,100\%)) \cdot \varepsilon \qquad (9)$$
$$\varepsilon = 1 - \exp(-NTU) \qquad (10)$$
$$NTU = \frac{UA_{evap} \cdot (1 - l_{SH})}{\dot{m}_{air}Cp_{air}} \qquad (11)$$

where $\dot{Q}_{sens}$ is the amount of energy that goes to cooling the air flow, while the energy used for condensing water out of the air is given by:

$$\dot{Q}_{lat} = \dot{m}_{air} \cdot (x_{air,out} - x_{air,in}) \cdot \Delta h_{lg} \qquad (12)$$
$$x_{air,out} = x_{air,in} + \frac{\dot{m}_{ex}}{\dot{m}_{air}} \cdot (x_{amb} - x_{air,in}) \qquad (13)$$

For calculating the relative length of the superheat zone, we adopt the following equations from [8]:

$$l_{SH} = -\ln\left(1 - \frac{T_{SH}}{T_{air,out} - T_e}\right)\frac{\dot{m}_{ref}Cp_{ref}}{UA_{SH}} \qquad (14)$$
$$\dot{m}_{ref} = \dot{m}_{air}\frac{I(T_{air,out},RH_{out}) - I(T_{air,in},95\%)}{h_{out} - h_{in}} \qquad (15)$$
$$h_{out} = HTP(T_{ref,out},T_e), \quad h_{in} = HBub(P_c)$$

where the functions HTP and $HBub$ are nonlinear, refrigerant dependent functions that can be calculated using e.g. the software RefEqns [9]. Additional equations for calculating relative and absolute humidity and enthalpy of humid air are given in [10].

D. Parameters

For the system identification problem based on the equations described in the previous sections, the following parameters are included.

Measured inputs: T_{sh}, T_e, T_{amb}, P_c.

Measured outputs: $T_{air,in}$, $T_{air,out}$, T_{surf}, T_{core}.

Assumed known: $\dot{m}_{air}$, Cp_{air}, Cp_{food}, Cp_{ref}.

where $\dot{m}_{air}$ is derived from knowledge of the maximum evaporator capacity, as will be shown later.

To be estimated:

$$UA_{SH}, \quad UA_{evap}, \quad UA_{amb}, \quad UA_{food}, \quad UA_{surf-core},$$
$$M_{air,1}, \quad M_{air2}, \quad M_{surf}, \quad M_{core}, \quad \dot{m}_{ex},$$
$$offset_1 \quad offset_2 \quad offset_3$$

where UA_{amb} and $\dot{m}_{ex}$ only can be estimated uniquely if the relationship between $\dot{Q}_{load}$ and $\dot{Q}_{infilt}$ is known. The three offsets are used to correct for constant errors in the sensors.

III. SYSTEM IDENTIFICATION

We identify the unknown variables in order to determine the relationship between input/output variables and the food temperatures. The estimation is done in steps for sub-parts of the entire system in order to simplify the calculations and to ensure identifiability.

First, the subsystem consisting of (1)-(2) and the relevant energy equations is considered. This system has the outputs/states $\{T_{air,in}, T_{air,out}\}$ and the inputs $\{T_{sh}, T_e, T_{amb}, P_c, T_{surf}\}$. We use the assumption of maximum cooling capacity and (9) to estimate the mass flow of air circulating in the display case. This results in $\dot{m}_{air} = 0.175kg/s$. The cooling capacity $\dot{Q}_e$ is a non-linear function, so we take a non-linear approach using idnlgrey from the System Identification Toolbox in Matlab [11]. Regarding UA_{amb} and $\dot{m}_{ex}$ we fix e.g. $UA_{amb} = 1$ initially. Then we get an estimate of $\dot{m}_{ex}$ and, with the knowledge about the relationship between $\dot{Q}_{load}$ and $\dot{Q}_{infilt}$, a new guess on UA_{amb} is found. By repeating this a couple of times, values with a good fit and with the correct ratio can be estimated. Next, the system with T_{surf} as the only output/state and the inputs $T_{air,2}$ and T_{core} is estimated in the same manner keeping the already identified parameters fixed. The remaining parameters are found from the system with T_{core} as the only output/state and with T_{surf} as input. The resulting parameters are given in Table I.

In e.g. [12], a finite volume method like the one used for the analysis in section IV is compared to a foodstuff model with only a core and surface layer, and it is found that only a small error occurs for most ranges of the parameters.

A. Analysis and Validation

The parameters are validated qualitatively, and a few observations are easily made. All the estimated offsets are within the $0.5K$ tolerance range specified for the sensors. The masses of surface and core parts of the goods correspond to 40 and 122 liters respectively, which seem realistic for our experiment. The mass of air in the display case ($T_{air,2}$) is,

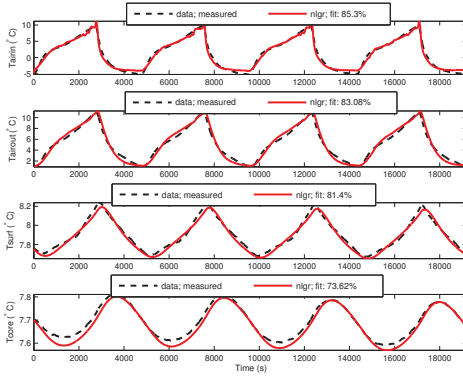|		
$\dot{m}_{air}$	0.175	kg/s
Cp_{air}	1012	$J/(kg \cdot K)$
Cp_{food}	2200	$J/(kg \cdot K)$
Cp_{ref}	1348	$J/(kg \cdot K)$
UA_{SH}	2.94	J/K
UA_{evap}	93.66	J/K
UA_{amb}	10.48	J/K
UA_{food}	14.45	J/K
$UA_{surf-core}$	206.34	J/K
$M_{air,1}$	2.18	kg
$M_{air,2}$	66.10	kg
M_{surf}	45.33	kg
M_{core}	136	kg
$\dot{m}_{ex}$	0.0023	kg/s
$offset_1$	-0.29	K
$offset_2$	0.35	K
$offset_3$	0.14	K

Fig. 3. Comparison of simulated data versus measured data for the test data set. Duration is approximately 5.3 hours.

however, much larger than what can possibly be contained in the display case. But we are aware of several unmodeled effects such as heat capacities in the metal walls. By not including these effects explicitly in the model, the mass of air must account for them, and since the heat capacity and density of metal are much larger than those of air, rather large amounts of air are needed to compensate. The amount of air exchanged with the surroundings is a little less than 2% of the circulated mass flow which also seems reasonable. The sum of the delivered cooling capacity can be compared to the sum of conduction load, infiltration load and exchanged energy with the goods. For the training set, this ratio is 0.96, which is reasonably close to 1.

Fig. 3 shows the identified model versus a validation data set, and it is noted that the identified model captures the dynamics of the system quite well.

IV. ENERGY POTENTIAL IN FOODSTUFFS

We investigate the temperature distribution inside the refrigerated foodstuff by assuming that the foodstuff in question can be compared to a ball that is divided into a finite number of shells. For each shell, the energy balance is formulated by (16)-(18) following the procedure in [12]. $n \in \{1, 2, \dots, N\}$ is the shell number from the center and out, and R is the radius of the ball. The inner shell is shaped like a ball. Hence, for $n = 1$:

$$\rho \cdot V_1 \cdot Cp \cdot \frac{dT_1}{dt} = \frac{\lambda}{\Delta r} \cdot A_1 \cdot (T_2 - T_1) \qquad (16)$$

$$V_1 = \frac{4}{3}\pi \cdot \Delta r^3, \qquad A_1 = 4\pi \cdot \Delta r^2, \qquad \Delta r = \frac{R}{N}$$

For $n \in \{2, \dots, N-1\}$, the shell is shaped like a sphere for which:

$$\rho \cdot V_n \cdot Cp \cdot \frac{dT_n}{dt} = \frac{\lambda}{\Delta r}(A_{n-1} \cdot (T_{n-1} - T_n) + A_n \cdot (T_{n+1} - T_n)) \qquad (17)$$

$$V_n = \frac{4}{3}\pi \cdot \left(\left(\frac{n \cdot R}{N} \right)^3 - \left(\frac{(n-1) \cdot R}{N} \right)^3 \right), \ A_n = 4\pi \cdot \left(\frac{n \cdot R}{N} \right)^2$$

For the outer shell, the boundary condition to the surrounding air applies. Hence:

$$\rho \cdot V_N \cdot Cp \cdot \frac{dT_N}{dt} = \frac{\lambda}{\Delta r} \cdot A_{N-1} \cdot (T_{N-1} - T_N)$$
$$- h_{ext} \cdot A_N \cdot (T_{surf} - T_{air}) \qquad (18)$$

$$T_{surf} = \frac{\frac{\lambda}{0.5 \cdot \Delta r} \cdot T_N + h_{ext} \cdot T_{amb}}{\frac{\lambda}{0.5 \cdot \Delta r} + h_{ext}}$$

Eq. (16)-(18) leads to a dynamic state for each shell in the model. It was found that 10 layers are sufficient for the average size of foodstuff. In addition, we added an extra state, E, integrating the heat flux in and out of the surface layer. By simple frequency analysis of this linear model (from T_{air} to E), it is seen how much energy that can be stored in the specific foodstuff at a specific frequency. We found that the response is very similar to a first order system with a flat DC-gain up to a certain cut-off frequency where it declines for increasing frequencies, until it flattens out at zero gain for very high frequencies. Interpreting this in the context of a layered food model, the DC-gain is the energy stored in an item when its entire mass has taken on the same temperature as the surrounding air, per Kelvin change in air temperature. For higher frequencies, the air temperature changes faster than the inner shell temperature can follow, and the temperature of the item is a function of depth from the surface. Thus, only a fraction of the item's mass is activated for energy storage.

The load-shifting potential is also limited from below on the frequency scale. Even though the entire mass is activated there is a limit to how long the temperature of the outer shell will remain below its upper limit. Therefore, it does not make sense to use the DC-gain as an indicator of the potential on very long timescales. The stored energy will simply disappear from the food item before the time it was

stored for. Using the system from (16)-(18), we can set up the model from T_{air} to T_N (the outer layer that will violate the upper temperature limit first). The 99% rise time of a step response for this system is then used as the upper limit for the time we are able to shift the load for a particular item.

For calculations on a selection of different foodstuffs we have used thermal properties from the data and studies in [13]–[15]. The investigated foodstuffs are: 1-L cow's milk, 500-g of ground beef both refrigerated and frozen, 1-kg frozen solid meat, 50-g of sliced ham, 1-kg frozen vegetables, 2-L fruit juice, a frozen chicken, a fresh egg and 100-L milk tightly packed in a rack.

The solutions to energy storage potential and maximum storage time can be uniquely described by two numbers, the Biot (Bi) number (the ratio of the heat transfer resistances inside and at the surface of a body) and the Fourier (Fo) number (the ratio of the heat conduction rate to the rate of thermal energy storage). These are defined as:

$$Bi = \frac{h \cdot R}{\lambda} \tag{19}$$

$$Fo = \frac{\lambda \cdot t}{\rho \cdot Cp \cdot R^2} \tag{20}$$

In (20) and onwards t is used for the characteristic time which we here use as the load-shifting time, or the time from minimum to peak (half a period) for a sinusoid.

A. Results

By sweeping reasonable ranges for the thermal properties, item sizes and characteristic times, the frequency and rise time analyses mentioned are performed for a range of Biot-Fourier combinations. The energy storage potential for each combination of parameters is found by selecting the magnitude corresponding to the frequency $\omega = \frac{1}{2t} 2\pi rad/s$, where t is the characteristic time. The result is normalized by maximum potential ($\rho \cdot Cp \cdot V$) to get a value between 0 and 1. The rise time is calculated from a step response for each combination of parameters and multiplied by Fo/t in order to be converted to a Fourier number. The result is given in Fig. 4 where the contours are active thermal mass as a fraction of total available thermal mass per degree temperature change in the surrounding air. We also indicate the maximum time period for energy storage in the figure.

In Fig. 4 the locations of the 10 different types of foodstuffs are shown by dotted horizontal lines. For each of the chosen items the Biot number is constant, whereas the Fourier number depends on the time.

For each food item and for each of the three timescales the energy storage potential (ESP) is found by reading the active thermal mass ratio from the plot and multiplying by total energy potential ($\rho \cdot Cp \cdot V$) for that item. The results are shown in Table II sorted by Biot number. The rise times for the outer shell are given in hours in the table. From the results in table II we observe how different foodstuffs are suitable for energy storage on different timescales and how

some items, e.g. a frozen chicken, are not suitable for 12-hour load shifting. This might be a surprising result. Frozen vegetables and fresh eggs can utilize quite large portions of their potential on the two shortest timescales, while milk, fruit juice and refrigerated ground beef seem to be better suited for energy storage on longer timescales. In this study milk is the only item we have considered as both a single item and as a tightly packed number of items. This, of course, can be done for all other types of foodstuffs that are normally packed in a display case by changing the size appropriately. As seen for milk. this drastically extends the period for which the potential can be utilized; however, on the other hand, it severely decreases the fraction of total potential on the shorter timescales.

B. Other Considerations

A few additional factors other than those analyzed in this paper will affect the energy storage potential that can be utilized in load-shifting strategies. One such factor is the duty cycle of the respective display case inlet valve. If the heat load on the display case is almost equal to the maximum available cooling capacity, the average on-time will be high, meaning that there is only a limited freedom for load shifting regardless of the potential in the goods. As the results in the previous section are calculated per mass unit and per degree change in air temperature, the actual potential greatly depends on both the amount of the foodstuff normally kept in a display case, how it is packed and the specific range of allowable temperatures for preserving the food quality. Finally, the rise time as indicator of maximum storage time used in this paper is only valid if the air temperature is changed to the upper limit of allowable temperatures. If, instead, it is changed to the temperature of the surroundings, the rise time should be calculated as a smaller fraction of the step size.

V. CONCLUSIONS

We have established an important relationship between measured variables in a supermarket refrigeration system and the food temperatures that are in play when applying thermal energy storage strategies. This enables a higher degree of utilization of storage potential. In addition, we investigated the thermal properties of different foodstuffs and the link to their temperature distributions. Thereby, we introduced the "active thermal mass", which is an important measure of energy storage potential. Our analysis linked the Biot and Fourier numbers of food items to both "active thermal mass" and maximum energy storage time. The main findings in Fig. 4 show how most food items are appropriate for time shifting within 2 hours, and that a few food items can be used for almost 12-hour load shifts.
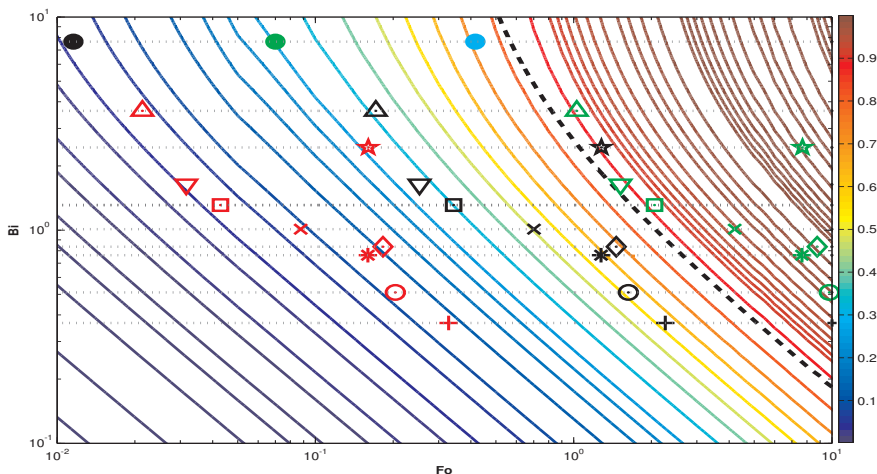
ACKNOWLEDGMENT

Fig. 4.   Energy storage potential versus Biot and Fourier numbers in a double logarithmic scale. The dashed black line indicates the 99% rise time as a Fourier number. Symbols show where different foodstuffs are located in the space as a function of time. Red = 15 min, black = 2 hours, green = 12 hours and cyan = 72 hours. Each horizontal dotted line indicates a selected food item. Refer to Table II, where the types of foodstuffs are shown with their symbols.

TABLE II

ENERGY STORAGE POTENTIAL FOR DIFFERENT FOODSTUFFS, SORTED BY BIOT NUMBER, AT DIFFERENT TIMESCALES. ENERGIES ARE IN J/K.

Symbol	Food item	$\rho \cdot Cp \cdot V$	ESP, 15 min	ESP, 2 hours	ESP, 12 hours	Rise time (h)
$+$	50-g ham	121	11	75	NA	3.8
$\circ$	500-g ground beef, frozen	850	76	486	NA	4.5
$*$	1-kg solid meat, frozen	1,729	167	1,034	NA	4.1
$\diamond$	Fresh egg	183	25	128	NA	3.3
$\times$	Whole chicken, frozen	5,928	414	2.881	NA	6.1
$\square$	500-g ground beef	1,569	79	513	1,397	9.9
$\triangledown$	1-L cow's milk	3,917	157	1,124	3,408	11.1
$\star$	1-kg vegetables, frost	1,494	356	1,267	NA	2.3
$\triangle$	2-L fruit juice	7,710	463	2,544	6,862	9.3
$\bullet$	100-L milk in rack	400,876	4,009	20,044	88,193	96.9

REFERENCES

[1] L. F. S. Larsen, C. Thybo, and H. Rasmussen, "Potential energy savings optimizing the daily operation of refrigeration systems," *Proc. European Control Conference, Kos, Greece*, pp. 4759–4764., 2007.

[2] T. G. Hovgaard, L. F. S. Larsen, and J. B. Jørgensen, "Flexible and Cost Efficient Power Consumption using Economic MPC - A Supermarket Refrigeration Benchmark," in *IEEE Conference on Decision and Control and European Control Conference*, 2011, pp. 848–854.

[3] T. G. Hovgaard, L. F. Larsen, K. Edlund, and J. B. Jørgensen, "Model predictive control technologies for efficient and flexible power consumption in refrigeration systems," *Energy*, 2012.

[4] T. G. Hovgaard, L. F. S. Larsen, M. J. Skovrup, and J. B. Jørgensen, "Optimal energy consumption in refrigeration systems - modelling and non-convex optimisation," *The Canadian Journal of Chemical Engineering*, p. in press, 2012.

[5] T. G. Hovgaard, L. F. S. Larsen, J. B. Jørgensen, and S. Boyd, "Nonconvex model predictive control for commercial refrigeration," http://www.stanford.edu/~boyd/papers/noncvx_mpc_refr.html, 2012.

[6] Y. Ge and S. Tassou, "Performance evaluation and optimal design of supermarket refrigeration systems with supermarket model "supersim", part i: Model description and validation," *International Journal of Refrigeration*, vol. 34, no. 2, pp. 527–539, 2011.

[7] D. P. Dewitt, F. P. Incropera, and T. L. Bergman, *Fundamentals of heat and mass transfer*.   John Wiley & Sons, New York, 1996.

[8] H. Rasmussen and L. F. S. Larsen, "Nonlinear superheat and capacity control of a refrigeration plant," *2009 17th Mediterranean Conference on Control and Automation*, pp. 1072–1077, 2009.

[9] M. Skovrup, "Thermodynamic and thermophysical properties of refrigerants - software package in borland delphi." Department of Energy Engineering, Technical University of Denmark, Tech. Rep., 2000.

[10] P. O. Danig and H. V. Holm, "Humid air." Department of Energy Engineering, Technical University of Denmark, Tech. Rep., 1998.

[11] L. Ljung, *System Identification - Theory for the User*, 2nd ed.   Prentice Hall, 1999.

[12] R. van der Sman, "Simple model for estimating heat and mass transfer in regular-shaped foods," *Journal of Food Engineering*, vol. 60, no. 4, pp. 383–390, 2003.

[13] Y. A. Çengel and A. J. Ghajar, *Heat and Mass Transfer: Fundamentals and Applications*.   McGraw-Hill, 2010.

[14] A. G. Fikiin, K. A. Fikiin, and S. D. Triphonov, "Equivalent thermophysical properties and surface heat transfer coefficient of fruit layers in trays during cooling," *Journal of Food Engineering*, vol. 40, no. 1-2, pp. 7 – 13, 1999.

[15] I. Dincer and O. F. Genceli, "Cooling of spherical products: Part iiheat transfer parameters," *International Journal of Energy Research*, vol. 19, no. 3, pp. 219–225, 1995.

Fast Nonconvex Model Predictive Control for Commercial Refrigeration

Fast Nonconvex Model Predictive Control
for Commercial Refrigeration

Tobias Gybel Hovgard [*,***] **Lars F. S. Larsen** [*]
John Bagterp Jørgensen [**] **Stephen Boyd** [***]

[*] *Vestas Technology R&D, DK-8200 Aarhus N, Denmark (e-mail:*
{togho,lfsla}@vestas.com).
[**] *DTU Informatics, Technical University of Denmark, DK-2800*
Lyngby, Denmark (e-mail: jbj@imm.dtu.dk)
[***] *Information Systems Laboratory, Department of Electrical*
Engineering, Stanford University, USA, (e-mail: boyd@stanford.edu)

Abstract: We consider the control of a commercial multi-zone refrigeration system, consisting of several cooling units that share a common compressor. The goal is to minimize the total energy cost, using real-time electricity prices, while obeying temperature constraints on the zones. We propose a variation on model predictive control to achieve this goal. When the right variables are used, the dynamics of the system are linear, and the constraints are convex. The cost function, however, is nonconvex. To handle this nonconvexity we propose a sequential convex optimization method, which typically converges in fewer than 5 or so iterations. We employ a fast convex quadratic programming solver to carry out the iterations, which is more than fast enough to run in real-time. We demonstrate our method on a realistic model, with a full year simulation, using real historical data. These simulations show substantial cost savings, and reveal how the method exhibits sophisticated response to real-time variations in electricity prices. This demand response is critical to help balance real-time uncertainties associated with large penetration of intermittent renewable energy sources in a future smart grid.

Keywords: Predictive Control, Optimization, Nonlinear Control, Smart Power Applications.

1. INTRODUCTION

To obtain an increasing amount of electricity from intermittent energy sources such as solar and wind, we must not only control the production of electricity, but also the consumption, in an efficient, flexible and proactive manner. The smart grid will be the future intelligent electricity grid that incorporates this. The Danish transmission system operator (TSO) defines it as: "Intelligent electrical systems that can integrate the behavior and actions of all connected users—those who produce, those who consume and those who do both—to provide a sustainable, economical and reliable electricity supply efficiently" (Energinet.dk, 2011).

In Denmark around 4500 supermarkets consume more than 550,000 MWh annually. This corresponds roughly to 2% of the entire electricity consumption in the country. Refrigerated goods constitute a large capacity in which energy can be stored in the form of 'coldness'. As this is not exploited by the thermostat (hysteresis) control policy most commonly used today, we propose an economic optimizing model predictive controller, economic MPC, to address this. MPC based on optimizing economic objectives has only recently emerged as a general methodology with efficient numerical implementations and provable stability properties (Diehl et al., 2011; Angeli et al., 2011) and in, *e.g.*, Hovgaard et al. (2012a) we demonstrated its capability to minimize the total cost of energy for a commercial refrigeration system while enabling it to participate in demand response schemes. The economic MPC has the ability to choose the optimal cooling strategy by utilizing the thermal capacity to shift the consumption in time, while keeping the temperatures within certain bounds.

An underlying challenge in applying MPC to vapor compression refrigeration systems is that the classical thermodynamics models are quite complex, and include many nonlinearities. One approach, called nonlinear MPC (NMPC), is to accept the optimization problem to be solved as nonlinear and nonconvex, and use generic nonlinear optimization methods, such as sequential quadratic programming (SQP) (Boggs and Tolle, 1995). This is the approach taken in Hovgaard et al. (2012a), which used ACADO (Houska et al., 2010), a generic nonlinear optimal control code, to solve the optimization problems. NMPC is widely used in the chemical process industry (see, *e.g.*, Biegler (2009)) but in general it requires special attention to ensure (local) convergence, and the computational complexity can be prohibitively high. Our method differs from NMPC: Instead of a generic SQP (or other) method, we use a a sequential convex programming (SCP) method, in which the objective is approximated by a convex function in each iteration; the convex parts are preserved, giving us the speed and reliability of solvers for convex optimization (Boyd and Vandenberghe, 2004). Our method, like SQP, involves the solution of a sequence of (convex) quadratic programs (QPs), but differs very much in how the QPs are formed. In SQP, an approximation to the Lagrangian

of the problem is used; the linearization required in each step can end up dominating the computation (Dinh et al., 2011). In our SCP method, the convexification step is quite straightforward. We use the tool CVXGEN (Mattingley and Boyd, 2012) to generate fast custom solvers for the QPs that arise in our method, achieving solution times measured in milliseconds.

We show careful numerical simulations on a realistic supermarket refrigeration system using prediction models for outdoor temperatures and real-time electricity prices based on actual data. CVXGEN transforms the original optimization problem into a standard form quadratic program that solves in a couple of milliseconds. This extreme speed allows us to carry out a simulation for a full year with 15-minute increments in around 4 minutes on a single-core processor. The results are quite interesting too. Immediately we see cost savings in the order of 30%. We show that our MPC controller exhibits a sophisticated form of demand response to prices, reducing consumption when the prices are high and pre-cooling when prices are low. Further details and results are provided in Hovgaard et al. (2012b).

Several publications have reported the use of NMPC to control refrigeration systems. See, *e.g.*, Leducq et al. (2006); Elliott and Rasmussen (2008); Sonntag et al. (2008). Predictive control for energy cost reductions in vapor compression cycles have to some extend been investigated for building temperature regulation too. Oldewurtel et al. (2010); Ma et al. (2012b,a) all use weather predictions or time of use pricing to optimize the energy efficiency. However, most of these confine themselves to simple descriptions of the energy consumption, disregarding the interdependency of the control variables and the efficiency. Ma and Borrelli (2012) uses sequential quadratic programming (SQP) to solve this problem. These methods yield long computational times, *e.g.*, starting from 10–13 seconds per step on a 3.00GHz dual-core processor. For general reviews of the use of thermal storage and for the importance of MPC in demand response schemes see, *e.g.*, Camacho et al. (2011); Arteconi et al. (2012). The need for computationally efficient optimization in MPC applied to systems with either fast sampling or limited computational resources is considered in an increasing number of publications such as Diehl et al. (2002); Zeilinger et al. (2008); Diehl et al. (2009); Wang and Boyd (2010). Embedded convex optimization applications have recently become more available to non-experts by the introduction of the automatic code generator CVXGEN (Mattingley and Boyd, 2012).

2. COMMERCIAL REFRIGERATION

In this section we describe the dynamic model of a commercial multi-zone refrigeration system. Such systems can include supermarkets, warehouses, or air-conditioning.

2.1 Model

The model describes a system with multiple cold rooms in which a certain temperature for the stored foodstuff has to be maintained. We describe the temperature dynamics and the energy cost of the system using SI units throughout.

The refrigeration system considered utilizes a vapor compression cycle in which a refrigerant circulates in a closed loop consisting of a compressor, an expansion valve consisting of a compressor, an expansion valve and two heat exchangers, an evaporator in the cold storage room, as well as a condenser/gas cooler located in the surroundings. When the refrigerant evaporates, it absorbs heat from the cold reservoir which is rejected to the hot reservoir. To sustain these heat transfers, the evaporation temperature $T_e(t)$ has to be lower than the temperature in the cold reservoir $T_{air}(t)$ and the condensation temperature has to be higher than the temperature at the hot reservoir $T_a(t)$. Low pressure refrigerant, with the pressure $P_e(t)$, from the outlet of the evaporator is compressed in the compressors to a high pressure $P_c(t)$ at the inlet to the condenser to increase the saturation temperature. In these expressions t denotes time. To lighten notation, we will drop the time argument (t) in time-dependent functions in the sequel. The setup is sketched in Fig. 1, with one cold storage room and one frost room connected to the system. Usually, several cold storage rooms, *e.g.*, display cases, connect to a common compressor rack and condensing unit. Because of this, the individual display cases see the same evaporation temperature; whereas each unit has its own inlet valve for individual temperature control.

2.2 Temperature dynamics

We use a first principles model and describe the dynamics in the cold room by simple energy balances. The temperature of the foodstuff is denoted by $T_{food}(t)$ and satisfies the differential equation,

$$m_{food} c_{p,food} \frac{dT_{food}}{dt} = \dot{Q}_{food-air}, \qquad (1)$$

where $\dot{Q}_{food-air}(t)$ is the energy flow from the air in the cold room to the foodstuff, m_{food} is the (assumed constant) mass of food, and $c_{p,food}$ is the constant specific heat capacity of the food. The temperature of the air in the cold room $T_{air}(t)$ satisfies the differential equation,

$$m_{air} c_{p,air} \frac{dT_{air}}{dt} = \dot{Q}_{load} - \dot{Q}_{food-air} - \dot{Q}_e, \qquad (2)$$

where $\dot{Q}_{food-air}(t)$ is the energy flow from the air to the foodstuff, $\dot{Q}_e(t)$ is the applied cooling capacity (energy absorbed in the evaporator), $\dot{Q}_{load}(t)$ is heat load from the surroundings to the air, m_{air} is the constant mass of air, and $c_{p,air}$ is the constant specific heat capacity of the air. We describe the heat flows using Newton's law of cooling,

$$\dot{Q}_{food-air} = k_{food-air}(T_{air} - T_{food}),$$
$$\dot{Q}_{load} = k_{amb-cr}(T_{amb} - T_{air}) + \dot{Q}_{dist},$$
$$\dot{Q}_e = k_{evap}(T_{air} - T_e),$$

where k is the constant overall heat transfer coefficient between two media, $T_{amb}(t)$ is the temperature of the ambient air which puts the heat load on the refrigeration system, and $\dot{Q}_{dist}(t)$ is a disturbance to the load (*e.g.*, an injection of heat into the cold room).

2.3 Energy cost

The energy used by the compressor, denoted $\dot{W}_c(t)$, dominates the power consumption in the system. It can be
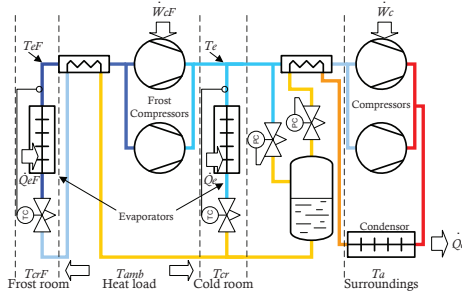
Fig. 1. Schematic layout of basic refrigeration system.

expressed by the mass flow of refrigerant $m_{ref}(t)$ and the change in energy content. We describe energy content by the enthalpy of the refrigerant at the inlet and at the outlet of the compressor ($h_{ic}(t)$ and $h_{oc}(t)$, respectively). These enthalpies are refrigerant-dependent functions of T_e and P_c (or equivalently, outdoor temperature T_a) as denoted in (3). They are computed using, *e.g.*, the software package REFEQNS (Skovrup, 2000), which models the thermodynamical properties of different refrigerants. We describe $\dot{W}_c$ as

$$\dot{W}_c = \frac{m_{ref}\,(h_{oc}(T_e, P_c) - h_{ic}(T_e))}{\eta_{is}(P_c/P_e)(1 - \eta_{heat})}, \tag{3}$$

where the isentropic efficiency $\eta_{is}(t)$ is a function mapping the pressure ratio over the compressor into compression efficiency and η_{heat} is a constant heat loss (in per cent) from the compressor. The mass flow is determined as the ratio between cooling capacity and change of enthalpy over the evaporator ($h_{oe}(t) - h_{ie}(t)$):

$$m_{ref} = \frac{\dot{Q}_e}{h_{oe}(T_e) - h_{ie}(P_c)}.$$

For the efficiency function η_{is} we fitted a polynomial model of the form,

$$\eta_{is}(\alpha) = c_1 + c_2\alpha + c_3\alpha^{1.5} + c_4\alpha^3 + c_5\alpha^{-1.5},$$

where $c_1, \ldots, c_5$ are constant parameters. We found this description to be accurate within 1%.

Another compressor sits between the frost evaporator and the suction side of the other compressors, as seen in Fig. 1. This compressor decreases the evaporation temperature for the frost part of the system to a lower level. We use the subscript F to denote variables related to the frost part.

We describe the instantaneous energy cost of operating the system by multiplying power consumption by the real-time electricity price $p_{el}(t)$. The energy cost C over the period $[T_0, T_{final}]$ is

$$C = \int_{T_0}^{T_{final}} p_{el} \left(\dot{W}_c + \dot{W}_{cF} \right) dt. \tag{4}$$

2.4 Control

Manipulated variables: Our controller manipulates the cooling capacity in each zone and the evaporation temperatures T_e and T_{eF}. The latter two are common for the entire refrigeration part and the entire frost part, respectively. In practice this is achieved by setting the set-points for inner control loops which operate with a high sample rate (compared to our control). This fast local control system allows us to ignore the complex and highly nonlinear behavior in the gas-liquid mixture in the evaporator.

Measured variables: The controller bases its decisions on measurements of air and food temperatures in each unit, on the known current outdoor temperature and electricity price, and on the predicted future values of the latter two. The heat disturbances are unknown.

2.5 Constraints

We would like the food temperatures to satisfy the inequalities

$$T_{food,min} \leq T_{food} \leq T_{food,max}, \tag{5}$$

where $T_{food,min}$ and $T_{food,max}$ are a given allowable range given for each of the individual units. With randomly occurring load disturbances, it is not possible to guarantee that the temperatures are always in this range. So in lieu of imposing the constraints, we encode (5) as a set of soft constraints, *i.e.*, as a term added to the cost function,

$$V = \int_{T_0}^{T_{final}} \rho_{soft,max}(T_{food} - T_{food,max})_+$$
$$+ \rho_{soft,min}(T_{food,min} - T_{food})_+ dt.$$

We choose the positive constants $\rho_{soft,max}$ and $\rho_{soft,min}$ so that violations are very infrequent in closed-loop operation. This formulation ensures a feasible problem even in the presence of uncertain loads. In a stochastic formulation, such as the one presented in Hovgaard et al. (2011), probabilistic constraints guarantee a feasible problem.

In addition, two constraints that cannot be violated are given,

$$0 \leq \dot{Q}_e \leq k_{evap,max}(T_{air} - T_e), \tag{6}$$
$$0 \leq \dot{W}_c \leq \dot{W}_{c,max}, \tag{7}$$

where $k_{evap,max}$ is the constant overall heat transfer coefficient from the refrigerant to the air when the evaporator is completely full and $\dot{W}_{c,max}$ is the constant limit on maximum energy consumption in the compressors. We define the set Ω as all $(\dot{Q}_e, T_e)$ that satisfy the system dynamics (1)–(2) and the constraints (6)–(7).

2.6 Thermostat control

Today, most display cases and cold rooms are controlled by a thermostat. This means that maximum cooling is applied when the cold room temperature reaches an upper limit and shut off when the lower limit is reached. The advantage of this control policy is that it is simple
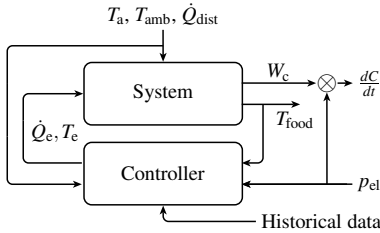
Fig. 2. Block diagram of the MPC controller.

and robust. The disadvantages, however, include: a high operating cost since the controller is completely unaware of system efficiency and electricity prices, no capability of demand response, and no specific handling of disturbances. All of these are addressed in our proposed method by intelligently exploiting the thermal capacity in the refrigerated mass.

3. METHOD

Fig. 2 outlines the overall structure of the proposed method and in the following sections we describe the details of the controller.

3.1 Economic MPC controller

The refrigeration system is influenced by a number of disturbances which we can predict (with some uncertainty) over a time horizon into the future. The controller must obey certain constraints, while minimizing the cost of operation. Economic MPC addresses all these concerns. Whereas the cost function in MPC traditionally penalizes a deviation from a set-point, the proposed economic MPC directly reflects the actual costs of operating the plant. This formulation is tractable for refrigeration systems, where we are interested in keeping the outputs (cold room temperatures) within certain ranges, while minimizing the cost of doing so.

Like in traditional MPC, we implement the controller in a receding horizon manner, where an optimization problem over N time steps (the control and prediction horizon) is solved at each step. The result is an optimal input sequence for the entire horizon, out of which only the first step is implemented. The controller aims at minimizing the electricity cost of operation. This cost relates to the energy consumption but we do not aim specifically at minimizing this, nor do we focus on tracking certain temperatures in the cold rooms. The optimization problem is thus formulated as

$$\begin{aligned} \text{minimize} \quad & C + V, \\ \text{subject to} \quad & (\dot{\mathbf{Q}}_e, \mathbf{T}_e) \in \Omega, \\ & T_{\text{food}}^{T_{\text{final}}} = (T_{\text{food,min}} + T_{\text{food,max}})/2, \end{aligned} \quad (8)$$

where the variables are $\dot{Q}_e$ and T_e (both functions of time). The feasible set Ω imposes the system dynamics and constraints, and is defined by (1)–(2) and (6)–(7). We add a terminal constraint that the final food temperature $T_{\text{food}}^{T_{\text{final}}}$ must be at the midpoint of the allowable range of temperatures.

Instead of (8) we solve a discretized version with N steps over the time interval $[T_0, T_{\text{final}}]$,

$$\dot{\mathbf{Q}}_e = \left\{ \dot{Q}_e^k \right\}_{k=0}^{N-1}, \quad \mathbf{T}_e = \left\{ T_e^k \right\}_{k=0}^{N-1}. \quad (9)$$

The MPC feedback law is the first move in (9). The controller uses the initial state as well as predictions of the real-time electricity cost, the outdoor temperature and the injected heat loads for the time interval.

3.2 Sequential convex programming method

The feasible set Ω, the terminal constraint, and the cost function term V are all convex. Unfortunately, as C is nonconvex in the controllable variables $\dot{Q}_e$ and T_e, the problem in (8) is not convex. Instead of using a generic nonlinear optimization tool, we choose to solve the optimization problem iteratively using convex programming, replacing the nonconvex cost function C with a convex approximation. We express (4) using the coefficients of performance, COP,

$$\hat{C}^i = \int_{T_0}^{T_{\text{final}}} p_{\text{el}} \left(\frac{1}{\hat{\eta}_{\text{COP}}^i} \dot{Q}_e + \frac{1}{\hat{\eta}_{\text{COP,F}}^i} \dot{Q}_{\text{eF}} \right) dt, \quad (10)$$

where the COPs, $\hat{\eta}_{\text{COP}}^i$ and $\hat{\eta}_{\text{COP,F}}^i$, are complicated functions of the outdoor temperature and of the controllable variables $\dot{Q}_e$ and T_e. For any given values of these variables we can, however, compute the COP. Our approximation in each step is simple and natural: We use the COP calculated for the last iteration trajectory. Thus in each iteration we solve a convex optimization problem, which can be done very reliably and extremely quickly.

While our proposed method gives no theoretical guarantee on the performance, we must remember that the optimization problem is nothing but a heuristic for computing a good control and that the quality of closed-loop control with MPC is generally good without solving each problem accurately. Indeed, we have found that very early termination of this sequential convex programming method, well before convergence, still yields very good quality closed-loop control.

Algorithm 1 outlines the method. In the algorithm, φ_{prox} and φ_{roc} are regularization terms which we describe in §3.3.

Algorithm 1 Iterative optimization with nonconvex objective.

Initialize
 $\dot{Q}_e^0$, T_e^0, and $i = 1$.
Compute
 $\hat{\eta}_{\text{COP}}^i$ and $\hat{\eta}_{\text{COP,F}}^i$, as functions of $\{\dot{Q}_e, T_e\}^{i-1}$ and T_a.
Solve
 minimize $\hat{C}^i + V + \varphi_{\text{prox}} + \varphi_{\text{roc}}$,
 subject to $(\dot{Q}_e^i, T_e^i) \in \Omega$,
  $T_{\text{food}}^{T_{\text{final}}, i} = (T_{\text{food,min}} + T_{\text{food,max}})/2$,
Update
 $\dot{Q}_e^i$, T_e^i, and $i = i + 1$
Repeat until convergence.

In Hovgaard et al. (2012c) we concluded that a unique minimum of the power consumption function exists within

the feasible region. This assures that an iterative approach will converge to the intended extremum point.

3.3 Regularization

We use two different types of regularization in the optimization problem. To avoid oscillations from iteration to iteration we add proximal regularization of the form

$$\varphi_{\text{prox}} = \rho_{\text{prox}} \sum_{k=0}^{N-1} \|\dot{Q}_{\text{e}}^k - \dot{Q}_{\text{e}}^{k,\text{prev}}\|_2^2, \tag{11}$$

where the superscript 'prev' indicates that it is the solution from the previous iteration and ρ_{prox} is a constant weight chosen to damp large steps in each iteration. Smaller steps will of course increase the number of iterations required for the sequential convex programming method to converge, but, since we warm-start the algorithm from the solution in the previous time step, the difference is negligible. Without proximal regularization oscillatory behavior can occur due to the nature of the thermodynamics in the refrigeration system. In addition, we add a quadratic penalty on the rate-of-change (roc) of $\dot{Q}_{\text{e}}$,

$$\varphi_{\text{roc}} = \rho_{\text{roc}} \sum_{k=1}^{N-1} \|\dot{Q}_{\text{e}}^k - \dot{Q}_{\text{e}}^{k-1}\|_2^2. \tag{12}$$

This regularization term serves two purposes: it improves the convergence of the sequential programming method, and also discourages rapid changes or switches in compressor levels, which helps reduce wear and tear of the compressor. Adding (11) and (12) to the linear objective formed by $\hat{C} + V$ results in a QP which we must solve once in each iteration. Due to the special structure of the MPC problem this QP is sparse; see, *e.g.*, Jørgensen (2005); Wang and Boyd (2010).

3.4 Non-homogeneous sampling

Speed of computation is a major concern in this work and we want to limit the size of the QPs that we solve in each iteration. A sampling time of 15 minutes directly gives 96 steps to be computed for a 24-hour prediction horizon. By using non-homogeneous sampling over the prediction horizon, exploiting that great accuracy becomes less important towards the end of the open-loop sequence, the number of steps can be reduced.

4. CASE STUDY

By simulation of realistic case studies we have verified the functionality and performance of the proposed MPC controller.

4.1 Scenario

Data from supermarkets actually in operation in Denmark have been collected. From these data, typical parameters such as time constants, heat loads, temperature ranges, capacities, and normal control policies have been estimated for three very different units; a milk cold room, a vertical shelving display case and a frost storage room. These units

differ widely in load, mass of goods, and temperature demands.

We convert the system in §2.1 to the discrete-time equivalent. Since inner control loops are in place we have found that a sampling time of 15 minutes for the MPC controller is appropriate.

We model a contribution from the uncertain load by a 40% increase in the normal heat load. The increase occurs at random instances in 25% of the 15-minute periods. To account for this, back-offs from the temperature limits are introduced. We adjust these such that violations of the limits occur only 0.5–1% of the time. Less than 0.1° is often sufficient.

In our scenario we use temperature measurements from a meteorological station in the Danish city Sorø sampled every 30 minutes, along with hourly electricity spot prices downloaded from the Nordic electricity market, Nordpool. We simulate the scenario with data covering an entire calender year and use three years of data for training the predictors.

4.2 Algorithm details

We use a prediction horizon augmented of three sequences with increasing sample time; a 6-hour interval sampled every 15 minutes, a 6-hour interval sampled every 30 minutes and a 12-hour interval sampled every hour—resulting in 48 steps to be computed.

For regularization of the optimization problems the best behavior was observed with parameters in the order of $\rho_{\text{prox}} = 0.08$ and $\rho_{\text{roc}} = 0.06$; however, the method seems to be quite robust to changes in these values.

Recent advances in convex optimization allow for convex QPs to be solved at millisecond and microsecond timescales. We use CVXGEN to generate a custom embedded solver for ultra fast computation of each convex QP in the sequential approach. CVXGEN transformed the original optimization problem into a standard form QP with 573 variables and 1248 constraints. In CVXGEN we specify and exploit the sparsity of the special problem structure.

4.3 Predictors

A prerequisite to solve the problem in (8) is to have available predictions of the outdoor temperatures and the electricity prices for the chosen prediction horizon, N. Only past values of such parameters can be available to the controller and in the present work we incorporate extremely simple predictors that can provide a sufficiently good estimate of the disturbances using a series of past measurements. We use historical data to train these predictors.

First, we use the historical training data set to create a baseline trajectory. For each month in a year we construct a typical day that describes the mean daily variation. If, *e.g.*, price is sampled every hour we get 24 prices for each of the 12 months. Next we calculate a residual (difference between baseline and historical data) for each one of the 12 baselines. For each of these, residual predictors are computed by

$$\text{minimize} \sum_{k=1}^{K} \|[R_{k-n}, \ldots, R_k]X - [R_{k+1}, \ldots, R_{k+N}]\|_2^2,$$

where K is the number of data points in the training data set, n is the number of past data points used for prediction, N is the number of future data points that we want to predict, X is the $n+1 \times N$ predictor matrix and R are the residuals. We employ an ℓ_1 regularization to avoid numerical instability that could lead to high variance models. Following this, a smoothed baseline is computed using interpolation of two adjacent months. Now, we can compute the predictions by first predicting the residuals of two adjacent months, interpolating these and adding them to the interpolated baseline of the same time window. We have chosen to use two days of past data for predicting the outdoor temperature and seven days for the price prediction. We use an entire week for the latter since the price pattern is different from weekdays to weekends. For both outdoor temperatures and electricity prices the training sets are defined from 1 January 2007 until 31 December 2009 and the simulation/test set covers the entire year of 2010.

For the unknown disturbance in the heat load we use a very simple predictor, namely the expected mean value of the random heat injection.

4.4 Computation times

We have simulated the proposed method with the case study described in the previous sections. The optimization problems solve in the order of a handful of milliseconds per MPC step which is more than fast enough for real-time implementation. A full year simulates in less than 4 minutes on a 2.8GHz Intel Core i7, excluding the time needed outside the optimization routine for predictors etc. The same problem with a generic solver such as ACADO takes around 4 minutes per MPC step on the same processor. For implementation in embedded industrial hardware a rough estimate of the computation time is around 1000 times of what we have observed here. This is still way below 10 seconds per time step which certainly allows for real-time implementation.

4.5 Convergence

When cold-started the proposed method generally converges in 10–20 iterations. In MPC, however, the open-loop trajectory from the previous run of the optimizer, shifted one time-step, is an excellent guess on the next outcome and is well-suited for warm-starting the algorithm. Using this warm start initialization, the method generally converges in fewer than 5 iterations. In addition, we find that early termination after, *e.g.*, 2–3 iterations generally gives good results, degrading the overall performance with less than 1%.

4.6 Savings

To benchmark the savings gained by introducing the proposed MPC controller, we have performed a simulation for the same system and conditions but using the conventional thermostat control policy. As in real systems the air
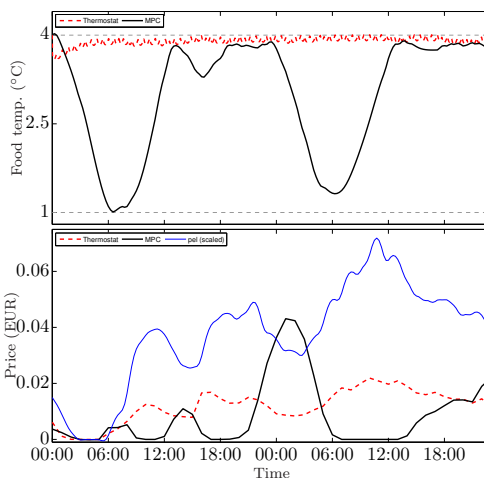

Fig. 3. Selected trajectory for food temperature and hourly cost of energy for control by thermostat vs. the proposed MPC.

temperature surrounding the foodstuff in each unit is the variable used in the thermostat. We have defined upper and lower bounds for switching on and off, such that the interval corresponds to what is normally observed in real operation. Besides, we determine the upper bound such that cooling quality is maintained at a minimal cost, *i.e.*, such that the food temperatures only violate the upper allowable limit in 0.5–1% of the time (to be comparable with the MPC control).

Fig. 3 shows a segment of the simulated system with thermostat control versus the proposed MPC controller. We show the trajectory for one unit only and we observe how the food temperature is pulled down by the MPC controller at times with low electricity prices, meaning that pre-cooling is applied. At such times the instantaneous cost of operating the system might be higher than if the conventional thermostat is used, as can be seen on the figure. But this is, however, more than counteracted by the savings when the electricity prices go up.

In Fig. 4, resulting temperature distributions for a selected unit are shown for both control by thermostat and by MPC. While both control policies tend to keep the temperatures close to the upper limit most of the time, we observe how the MPC controller makes use of the entire range for storing coldness.

We observe savings in the order of 30%. Adding the uncertain heat load injections and the appropriate back-offs from the temperature limits, as described in §4, increases the overall cost by approximately 10%.

4.7 Demand response

Fig. 5 shows the total cooling energy applied to all three units plotted as a function of the electricity price at the time of use. We have selected one month to limit the

Fig. 4. Temperature distribution for selected unit. Simulation over the full year 2010.

(a) Control by thermostat. The solid line is a linear fit with almost zero slope.

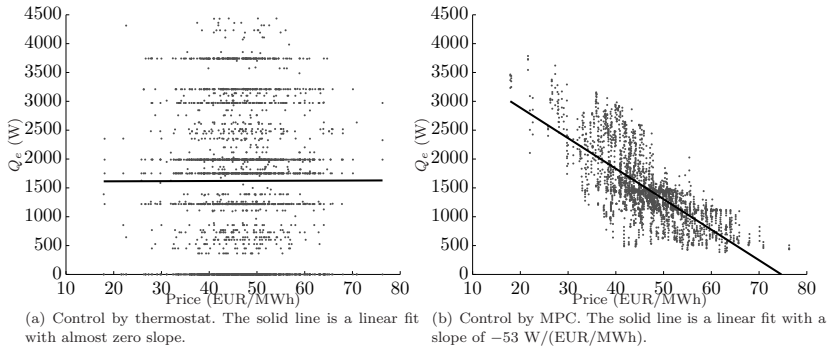(b) Control by MPC. The solid line is a linear fit with a slope of -53 W/(EUR/MWh).
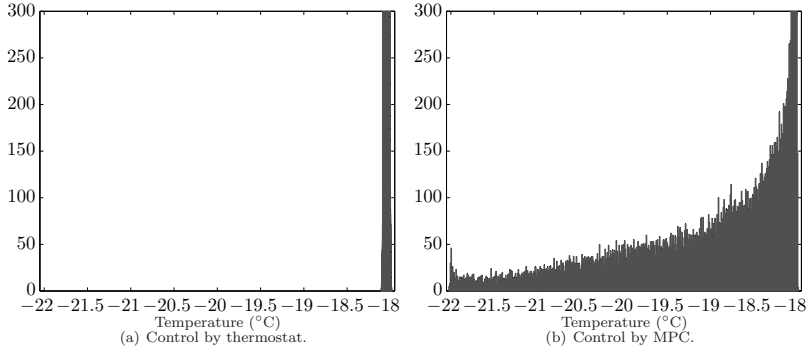
Fig. 5. Illustration of demand response in systems controlled by MPC vs. thermostat control.

number of data-points but the picture is almost identical for the entire year of simulation: We observe no correlation between energy consumption and electricity prices when the thermostat controls the refrigeration system while we see a clear tendency to apply more cooling at times with low prices, and vise versa, if we employ the proposed MPC scheme. A linear fit is made using a Huber function regression. The slope is around -50 W/(EUR/MWh) for the MPC controlled system as opposed to 0 for the thermostat which clearly illustrates the demand response behavior of the system. We should remember that the spot price used here is just an example and not a prerequisite of our method. In a smart grid the price signal could be artificially made by the balance responsible party to promote demand response.

4.8 Plant perturbations

With perturbations of up to at least 20–30% in parameters such as mass of the refrigerated foodstuff and the heat transfer coefficients we see essentially no changes in the closed-loop dynamics.

4.9 Perfect predictions

By again simulating over the full year of 2010, but this time with a prescient setting assuming knowledge of the exact future conditions instead of using their predictions, we are able to compare the performance of the simple predictors and give a rough judgment on how much the method relies on the availability of accurate predictions. We have observed that the extra savings gained by having the full information available are in the order of 1-2%. This justifies the use of simple predictors.

5. CONCLUSION

In this paper we have presented an MPC controller for a commercial multi-zone refrigeration system. We have based our method on convex optimization, solved iteratively to treat a nonconvex cost function. By employing a fast convex quadratic programming solver to carry out the iterations, the method is more than fast enough to run in real-time. Simulation on a realistic scenario reveal significant savings as well as convincing demand response capabilities suitable for implementation with smart grid schemes.

ACKNOWLEDGEMENTS

REFERENCES

Angeli, D., Amrit, R., and Rawlings, J. (2011). On average performance and stability of economic model predictive control. *Automatic Control, IEEE Transactions on*, PP(99), in press.

Arteconi, A., Hewitt, N.J., and Polonara, F. (2012). State of the art of thermal storage for demand-side management. *Applied Energy*, 93(0), 371 – 389.

Biegler, L. (2009). Efficient nonlinear programming algorithms for chemical process control and operations. In A. Korytowski, K. Malanowski, W. Mitkowski, and M. Szymkat (eds.), *System Modeling and Optimization*, volume 312 of *IFIP Advances in Information and Communication Technology*, 21–35. Springer Boston.

Boggs, P.T. and Tolle, J.W. (1995). Sequential quadratic programming. *Acta Numerica*, 4, 1–51.

Boyd, S. and Vandenberghe, L. (2004). *Convex Optimization*. Cambridge University Press.

Camacho, E.F., Samad, T., Garcia-Sanz, M., and Hiskens, I. (2011). Control for renewable energy and smart grids. In T. Samad and A.M. Annaswamy (eds.), *The Impact of Control Technology, Control Systems Society*, 69–88. IEEE Control Systems Society.

Diehl, M., Amrit, R., and Rawlings, J.B. (2011). A lyapunov function for economic optimizing model predictive control. *Automatic Control, IEEE Transactions on*, 56(3), 703 –707.

Diehl, M., Bock, H.G., Schlo, J.P., Findeisen, R., Nagy, Z., and Allgöwer, F. (2002). Real-time optimization and nonlinear model predictive control of processes governed by differential-algebraic equations. *Journal of Process Control*, 12(4), 577–585.

Diehl, M., Ferreau, H., and Haverbeke, N. (2009). Efficient numerical methods for nonlinear MPC and moving horizon estimation. In L. Magni, D. Raimondo, and F. Allgwer (eds.), *Nonlinear Model Predictive Control*, volume 384 of *Lecture Notes in Control and Information Sciences*, 391–417. Springer Berlin / Heidelberg.

Dinh, Q.T., Savorgnan, C., and Diehl, M. (2011). Realtime sequential convex programming for nonlinear model predictive control and application to a hydropower plant. In *Decision and Control and European Control Conference (CDC-ECC), 2011 50th IEEE Conference on*, 5905–5910.

Elliott, M.S. and Rasmussen, B.P. (2008). Model-based predictive control of a multi-evaporator vapor compression cooling cycle. In *American Control Conference, 2008*, 1463 –1468.

Energinet.dk (2011). Potential and opportunities for flexible electricity consumption with special focus on individual heat pumps (in Danish). Technical report, Energinet.dk, The Danish TSO owned by the Danish Climate and Energy Ministry. Denmark.

Houska, B., Ferreau, H., and Diehl, M. (2010). ACADO Toolkit–An Open Source Framework for Automatic Control and Dynamic Optimization. *Optimal Control Applications and Methods*.

Hovgaard, T.G., Larsen, L.F.S., Edlund, K., and Jørgensen, J.B. (2012a). Model predictive control technologies for efficient and flexible power consumption in refrigeration systems. *Energy*, in press.

Hovgaard, T.G., Larsen, L.F.S., and Jørgensen, J.B. (2011). Robust Economic MPC for a Power Management Scenario with Uncertainties. In *50th IEEE Conference on Decision and Control and European Control Conference*, 1515–1520.

Hovgaard, T.G., Larsen, L.F.S., Jørgensen, J.B., and Boyd, S. (2012b). Nonconvex model predictive control for commercial refrigeration. `http://www.stanford.edu/~boyd/papers/noncvx_mpc_refr.html`.

Hovgaard, T.G., Larsen, L.F.S., Skovrup, M.J., and Jørgensen, J.B. (2012c). Optimal energy consumption in refrigeration systems - modelling and non-convex optimisation. *The Canadian Journal of Chemical Engineering*, in press.

Jørgensen, J.B. (2005). *Moving Horizon Estimation and Control*. Ph.D. thesis, Department of Chemical Engineering, Technical University of Denmark.

Leducq, D., Guilpart, J., and Trystram, G. (2006). Nonlinear predictive control of a vapour compression cycle. *International Journal of Refrigeration*, 29(5), 761 – 772.

Ma, J., Qin, J., Salsbury, T., and Xu, P. (2012a). Demand reduction in building energy systems based on economic model predictive control. *Chemical Engineering Science*, 67(1), 92 – 100.

Ma, Y. and Borrelli, F. (2012). Fast stochastic predictive control for building temperature regulation. In *American Control Conference (ACC), 2012*, accepted.

Ma, Y., Borrelli, F., Hencey, B., Coffey, B., Bengea, S., and Haves, P. (2012b). Model predictive control for the operation of building cooling systems. *Control Systems Technology, IEEE Transactions on*, 20(3), 796 –803.

Mattingley, J. and Boyd, S. (2012). CVXGEN: a code generator for embedded convex optimization. *Optimization and Engineering*, 13, 1–27.

Oldewurtel, F., Parisio, A., Jones, C., Morari, M., Gyalistras, D., Gwerder, M., Stauch, V., Lehmann, B., and Wirth, K. (2010). Energy Efficient Building Climate Control using Stochastic Model Predictive Control and Weather Predictions. In *American Control Conference (ACC)*, 5100 – 5105.

Skovrup, M.J. (2000). Thermodynamic and thermophysical properties of refrigerants - software package in borland delphi. Technical report, Department of Energy Engineering, Technical University of Denmark, Kgs. Lyngby, Denmark.

Sonntag, C., Devanathan, A., and Engell, S. (2008). Hybrid NMPC of a supermarket refrigeration system using sequential optimization. In *Proc of 17th IFAC World Congress*, 13901–13906.

Wang, Y. and Boyd, S. (2010). Fast model predictive control using online optimization. *Control Systems Technology, IEEE Transactions on*, 18(2), 267–278.

Zeilinger, M.N., Jones, C.N., and Morari, M. (2008). Real-time suboptimal model predictive control using a combination of explicit MPC and online optimization. In *Proc. of 47th IEEE Conference on Decision and Control (CDC)*, 4718–4723.

Sequential Convex Programming for Power Set-point Optimization in a Wind Farm using Black-box Models, Simple Turbine Interactions, and Integer Variables

Sequential Convex Programming for Power Set-point Optimization in a Wind Farm using Black-box Models, Simple Turbine Interactions, and Integer Variables

Tobias Gybel Hovgard [*,**] **Lars F. S. Larsen** [*]
John Bagterp Jørgensen [**] **Stephen Boyd** [***]

[*] *Vestas Technology R&D, DK-8200 Aarhus N, Denmark (e-mail: {togho,lfsla}@vestas.com).*
[**] *DTU Informatics, Technical University of Denmark, DK-2800 Lyngby, Denmark (e-mail: jbj@imm.dtu.dk)*
[***] *Information Systems Laboratory, Department of Electrical Engineering, Stanford University, USA, (e-mail: boyd@stanford.edu)*

Abstract: We consider the optimization of power set-points to a large number of wind turbines arranged within close vicinity of each other in a wind farm. The goal is to maximize the total electric power extracted from the wind, taking the wake effects that couple the individual turbines in the farm into account. For any mean wind speed, turbulence intensity, and direction we find the optimal static operating points for the wind farm. We propose an iterative optimization scheme to achieve this goal. When the complicated, nonlinear, dynamics of the aerodynamics in the turbines and of the fluid dynamics describing the turbulent wind fields' propagation through the farm are included in a highly detailed black-box model, numerical results for any given values of the parameter sets can easily be evaluated. However, analytic expressions for model representation in the optimization algorithms might be hard to derive and their properties are often not suitable for computationally efficient optimization either. To handle this, we propose a sequential convex optimization method, perturbing the model in each iteration, and demonstrate a typical convergence in fewer than 10 iterations. We derive a coupling matrix from the wind farm model, enabling us to use a very simple linear relationship for describing the turbine interactions. In addition, we allow individual turbines to be turned on or off introducing integer variables into the optimization problem. We solve this within the same framework of iterative convex approximation and compare with mixed-integer optimization tools. We demonstrate the method on a verified model and for various sizes and configurations of the wind farm. For all tested scenarios we observe a distribution of the power set-points which is at least as good as, and in many cases is far superior to, a more naive distribution scheme. We employ a fast convex quadratic programming solver to carry out the iterations in the range of microseconds even for large wind farms.

Keywords: Optimization, Nonlinear Control, Wind Farms, Black-box Models, Integer Programming.

1. INTRODUCTION

Today, wind power is the most important renewable energy source. For the years to come, many countries have set goals for further reduced CO2 emission, increased utilization of renewable energy, and phase out of fossil fuels. In Denmark one of the means to achieve this is to increase the share of wind power to 50% of the electricity consumption by 2020 and to fully cover the energy supply by renewable energy by 2050 (Danish Ministry of Climate and Building, 2012). Installing this massive amount of wind turbines favours the formation of a large number of turbines in wind farms. This is both due to practical considerations but perhaps more importantly, to reduce the cost of wind energy as opposed to production in single wind turbines located far from each other (Johnson and

Thomas, 2009). Extracting maximum power from each wind turbine in a greedy manner does not always result in maximal power output for the entire farm and a wind farm controller is often needed to fully exploit the potential of the installed capacity and to reduce wear and tear of the mechanical structures (Pao and Johnson, 2009). Examples of wind farms in Denmark can have yearly productions around 600 GWh (Horns Rev I) and up to 1600 GWh (Anholt) and typically the power sales price is guaranteed to be at a fixed level for around 10 years of operation—from around 44.25EUR/MWh (Horns Rev I) to around 140.85EUR/MWh (Anholt). With such production levels and power prices, an average change in power output of just 1% changes the yearly revenue by 0.265–2.253 million EUR. Thus, slight improvements in the average extracted

power can have a significant impact on the economics of operating the wind farm.

A vast amount of works exist that address power optimization, fatigue load reduction and pitch control for individual turbines, *e.g.*, Hau (2006); Hammerum et al. (2007); Dang et al. (2010); Henriksen et al. (2011); Adegas et al. (2011). Some of these take optimization and model predictive control approaches to solve the problems and many rely on a known operating point (*e.g.*, local wind speed and power set-point) for deriving linearized models. Other works consider the control of large wind farms where the power extracted by upwind turbines reduces the power that is available from the wind and increases the turbulence intensity in the wake reaching other turbines. Thus, the fluctuations and vibrations of the downwind turbines are greater than upwind turbines and results in more fatigue loads (see, *e.g.*, Hansen et al. (2006); Soleimanzadeh et al. (2011, 2012); Spudic et al. (2011)). As with the single-turbine research, a mean operating point is often assumed for linearization. For farm control a further complication to the models are the aerodynamic interactions in the farm which is still an immature field (Steinbuch et al., 1988; Johnson and Thomas, 2009). A contribution from the present paper is a method to provide the operating points assumed available in many other methods for both local control and farm optimization.

As for the optimization of wind farms like for optimization of other complicated systems in engineering, the modeling is often a very time-consuming task involving cross-disciplinary work. Especially, when analytic expressions that fit into a certain framework (linear, convex, etc.) are desired, it might be a huge challenge to choose the proper simplifications and assumptions for modeling the system. In this paper, we strive to use as little knowledge and as few analytic expressions as possible for formulating the optimization problem. We adopt the wind farm model that was derived in Brand and Wagenaar (2010a) and validated in Brand and Wagenaar (2010b), and use it as a black-box model which for any given values of the parameters can be evaluated rather quickly. By perturbing this model we approximate the derivatives needed. Black-box optimization is only infrequently reported in the literature—see, *e.g.*, Hansen et al. (2010) where different approaches are compared. In Hovgaard et al. (2012a,b) we demonstrated the power of a sequential convex programming (SCP) approach on a model predictive control problem for commercial refrigeration with linear dynamics and constraints but a nonconvex objective. Inspired by this, we apply the same technique to the black-box optimization. Our method, like sequential quadratic programming (SQP) (Boggs and Tolle, 1995), involves the solution of a sequence of (convex) quadratic programs (QPs), but differs very much in how the QPs are formed. In SQP, an approximation to the Lagrangian of the problem is used; the linearization required in each step can end up dominating the computation (Dinh et al., 2011). In our SCP method, the convexification step is quite straightforward as it comes from a few function evaluations of the black-box model. We use the tool CVXGEN (Mattingley and Boyd, 2012) to generate fast custom solvers for the QPs that arise in our method, achieving solution times measured in microseconds.

Due to the mechanical design wind turbines cannot extract power from arbitrarily low wind speeds and they typically turn off around 4–6 m/s. This introduces on/off, or integer, variables into the optimization problem. Reviews of more sophisticated but typically quite computationally demanding algorithms for mixed-integer programming are given in, *e.g.*, Grossmann (2002); Alves and Clímaco (2007). We chose to implement the integer constraint in the framework of sequential optimization using linear approximations. With a heuristic thresholding we find very convincing results for all tested scenarios.

We demonstrate the method with numerical simulations on a number of different wind farm sizes. For large wind farms of up to 50 turbines we observe convergence in fewer than 10 iterations (a handful or so, milliseconds). For all imaginable scenarios that we were able to test, our method performs at least as good as (and in many cases outperforms) a "greedy" optimization where each turbine maximizes its own production. In spite of this, our method gives no guarantee in terms of convergence or optimality.

2. WIND FARMS

In this section we briefly describe the model used for the wind farms in the paper and the features that are extracted from the model a priori to running the optimization.

2.1 Model

The model is a quasi-static wind farm flow model developed in Brand and Wagenaar (2010a). It specifies in real time the wind speed at each turbine in a wind farm plus the tower bending moment, the blade bending moment, the rotor shaft torque and the aerodynamic power of each turbine as a function of "ambient" wind speed, wind direction and turbulence intensity. The farm model has been validated against real measurement data from ECNs Wind turbine Test site Wieringermeer (EWTW) (Brand and Wagenaar, 2010b) and implemented in Matlab in Soleimanzadeh et al. (2011). Fig. 1 illustrates the structure of the model. The wind farm in the examples will consist of turbines using the NREL 5MW model since this is openly available, but, could easily be substituted with any specific turbine model. The turbines are described in detail in, *e.g.*, Grunnet et al. (2010). We choose not to go into detail with the model in this paper and report solely on the features that can be observed from a black-box model by sweeping reasonable ranges of the input parameters.
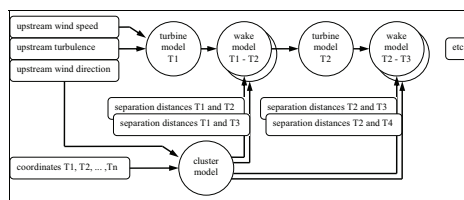

Fig. 1. Block diagram of the wind farm model (Brand and Wagenaar, 2010a).

Sequential Convex Programming for Power Set-point Optimization in a Wind Farm using Black-box Models, Simple Turbine Interactions, and Integer Variables

239

The model has the following basic input/output interface for a farm with n turbines:

$$[P, V, D, \Sigma_{\mathrm{add}}, M_{\mathrm{t}}, M_{\mathrm{b}}, M_{\mathrm{s}}] = f_{\mathrm{farm}}(v_0, \sigma_0, P_{\mathrm{s}}, x, y), \quad (1)$$

where $\{P, V, D, \Sigma_{\mathrm{add}}, M_{\mathrm{t}}, M_{\mathrm{b}}, M_{\mathrm{s}}\}$ are n-length vectors with produced power, local wind speed, wind deficit, added turbulence (velocity standard deviation), bending moment for the tower, bending moment for the blades, and bending moment for the shaft in the drive train. The inputs are ambient wind speed (v_0), ambient turbulence (velocity standard deviation) (σ_0), an n-length vector with power set-points (P_{s}), and two n-length vectors with the coordinates of the turbines (x, y). In addition, we have,

$$[p, d, \sigma_{\mathrm{add}}, m_{\mathrm{t}}, m_{\mathrm{b}}, m_{\mathrm{s}}] = f_{\mathrm{turbine}}(v, \sigma, p_{\mathrm{s}}), \quad (2)$$

for a single turbine using local wind speed, v, and turbulence, σ. We show some example plots sampled from the models in the next sections.

2.2 Constraints

The extracted power, p, must be equal to or less than the available power in the wind, p_{w}, which is a function of the wind speed, v. The turbine is build for a rated power and when the available power in the wind exceeds this level the blades gradually pitch out of the wind to keep the extracted power at the rated level and reduce loads on the turbine. Likewise, the extracted power can only follow the available power curve down to a certain level, P_{min}, due to the mechanical design. Thus,

$$P_{\mathrm{min}} \leq p_i \leq P_{\mathrm{rated}}, \quad (3)$$

$$p_i \leq p_{\mathrm{w},i}(v_i), \quad (4)$$

where i is the index of the turbine in the farm and v_i is the local wind speed at turbine i. This is illustrated in Fig. 2. We observe how the available power goes to 0 at wind speeds above 25 m/s which is for security reasons.

Another important feature of the model is the reduction in wind speed (deficit) when it passes through the rotor of a turbine. Fig. 3 shows how the wind speed is affected when extracting a certain power at a certain wind speed. Added

turbulence in the close vicinity after a turbine rotor can be plotted in the same way as a function of incoming wind speed and extracted power, and we observe a very similar shape.

2.3 Simple Turbine Interaction

We can describe the local wind speed at each turbine as the ambient wind speed minus a linear combination of the deficits (d_i) caused by all other turbines, with the coefficients depending on mutual distance and the relative angle to the wind direction. Likewise, turbulence levels (velocity variance, σ_i^2) at each turbine are the sum of the ambient turbulence (velocity variance, σ_0^2) and a linear combination of the turbulence added by all other turbines. From the black-box model we estimate two coupling matrices, W_{d} and W_{t}, such that,

$$\begin{bmatrix} v_1 \\ v_2 \\ \vdots \\ v_n \end{bmatrix} = v_0 - W_{\mathrm{d}} \begin{bmatrix} d_1 \\ d_2 \\ \vdots \\ d_n \end{bmatrix}, \quad (5)$$

$$\begin{bmatrix} \sigma_1^2 \\ \sigma_2^2 \\ \vdots \\ \sigma_n^2 \end{bmatrix} = \sigma_0^2 + W_{\mathrm{t}} \begin{bmatrix} \sigma_{\mathrm{add},1}^2 \\ \sigma_{\mathrm{add},2}^2 \\ \vdots \\ \sigma_{\mathrm{add},n}^2 \end{bmatrix}. \quad (6)$$

We use an $\mathcal{L}1$-norm sparsifying regularizer to emphasize the strong relations in the couplings and to promote sparse matrices. Fig. 4 shows an estimated W_{d}-matrix example.

2.4 Cost

Our aim is to explicitly address the maximization of total power output from the farm and we do not directly consider loading of the turbines in this work. Thus, for any given wind condition we want to maximize

$$P_{\mathrm{total}} = \sum_{i=1}^{n} p_i,$$
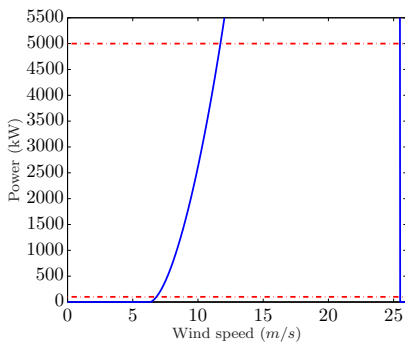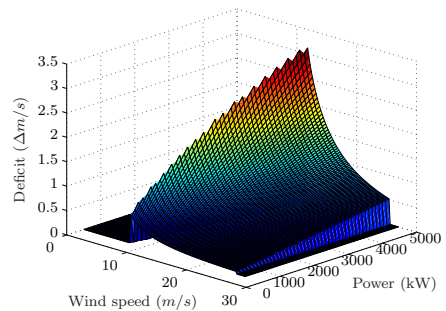
for n turbines in a farm.

Fig. 2. Power as a function of local wind speed for the used turbine model (solid, blue). Red dotted lines indicate maximum (rated) and minimum (due to mechanical design) power levels.

Fig. 3. Wind speed deficit in the close vicinity after a turbine as a function of incoming wind speed and extracted power.
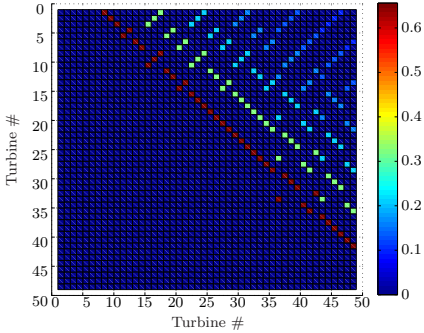
Fig. 4. Example showing the W_{d}-matrix for a 7×7 square wind farm with wind direction parallel to the rows of turbines and mutual distances between the turbines of 3 times the rotor diameter.

2.5 On/off variables

The turbines are not able to produce power from wind speeds below a certain level. However, it might not be optimal on the farm level to downgrade upwind turbines in order to leave enough wind speed to keep all turbines in the row spinning. Turning off one or more of the turbines can be a better solution and we change the constraints in (3) by introducing binary variables, $\{u_i\}_{i=1}^n$.

$$P_{\min} u_i \leq p_i \leq P_{\mathrm{rated}} u_i. \qquad (7)$$

2.6 Loads

Destructive fatigue loads on wind turbines are primarily caused by vibrations due to turbulence in the wind. Under the assumption that the turbines always operate in safe regions, the extreme (instantaneous) loads are avoided and the accumulation of fatigue plays a major role in wearing out the turbines (Frandsen, 2007). To illustrate a sample of the turbine loads from the model, we combine mean wind speed and turbulence standard deviation into one measure, namely, the turbulence intensity, t, defined as the standard deviation of wind speed fluctuations divided by the mean wind speed,

$$t_i = \frac{\sigma_i}{v_i}.$$

Fig. 5 shows the standard deviation of the tower bending moment as a function of turbulence intensity and extracted power. We observe that for increasing turbulence intensity (*i.e.*, higher standard deviation of the fluctuations or lower mean wind speed) and increased power extraction, the standard deviation of the tower bending moment and hence, the vibrations of the structure, become more severe. We also observe the effect of some resonance frequencies in the structure.

2.7 Control

Manipulated variables: Our optimizer manipulates the set-points for extracted power in each individual turbine in
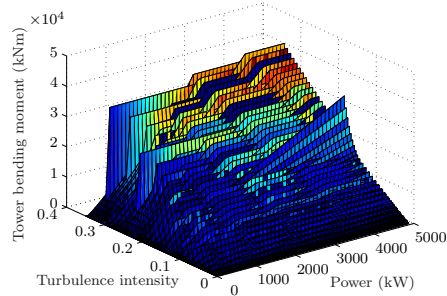

Fig. 5. Standard deviation of the tower bending moment.

the farm. This might have to be done with, *e.g.*, 10-minute intervals for updating the operating points for local controllers on the turbines. By manipulating power set-points, the local wind speeds and turbulence intensities change as a consequence, too.

Measured variables: We assume knowledge of the ambient mean wind speed, mean direction, and the turbulence intensity entering the front row of turbines in the farm. Furthermore, the black-box model in (1) must be validated with the turbines and the specific farm topology in question.

2.8 Greedy Control

We compare the maximized power output using our proposed method to a "greedy" strategy in which each turbine maximizes its own production based on whatever local wind speed there is left from the upwind turbines.

3. METHOD

Our method is based on sequential convex programming where convex approximations are found in each iteration, k, by simple evaluations of the black-box model. We establish the following linear approximations with derivatives estimated by perturbing the model around the operating point found in the previous iteration,

$$
\begin{bmatrix} d_i^k \\ \sigma_i^k \\ p_{\mathrm{w},i}^k \end{bmatrix} = \begin{bmatrix} d_i^{k-1} \\ \sigma_i^{k-1} \\ p_{\mathrm{w},i}^{k-1} \end{bmatrix} + \begin{bmatrix} \dfrac{\Delta d}{\Delta p_{\mathrm{s}}} & \dfrac{\Delta d}{\Delta v} & \dfrac{\Delta d}{\Delta \sigma} \\ \dfrac{\Delta \sigma}{\Delta p_{\mathrm{s}}} & \dfrac{\Delta \sigma}{\Delta v} & \dfrac{\Delta \sigma}{\Delta \sigma} \\ 0 & \dfrac{\Delta p_{\mathrm{w}}}{\Delta v} & \dfrac{\Delta p_{\mathrm{w}}}{\Delta \sigma} \end{bmatrix}_i^{k-1} \begin{bmatrix} p_i^k - p_{\mathrm{s},i}^{k-1} \\ v_i^k - v_i^{k-1} \\ \sigma_i^k - \sigma_i^{k-1} \end{bmatrix}.
$$

Note that the set-point $p_{\mathrm{s},i}$ can be larger than p_i in practice while $p_{\mathrm{s},i} = p_i$ after convergence of the method we propose in this paper. We define the set Ω as all (p_i, v_i, σ_i), $i = 1 \ldots n$, that satisfy the power constraints, (4) and (7), and the interaction model (5)-(6), given the linearization above.

3.1 Approximate integer programming

The integer constraint on the on/off variables u does not fit into a convex optimization problem. Hence, we relax the constraint,

$$0 \leq u_i \leq 1, \qquad (8)$$

The 10th European Workshop on Advanced Control and Diagnosis (ACD 2012)
Technical University of Denmark, Kgs. Lyngby, Denmark, Nov. 8-9, 2012

and introduce the expression,

$$\eta_{\text{int},i} \le \left(u_i^{k-1}\right)^2 - u_i^{k-1} + \left(2u_i^{k-1} - 1\right)\left(u_i^k - u_i^{k-1}\right), \quad (9)$$

with the right hand side being a linearization of $(u_i^2 - u)$ around the point u_i^{k-1}. We add the term,

$$\varphi_{\text{int}} = \rho_{\text{int}} \sum_{i=1}^{n} \eta_{\text{int},i},$$

where ρ_{int} is a constant weight, to the objective function, penalizing when u_i deviates from 0 or 1. We define the set Ω_{int} as all $(u_i, \eta_{\text{int},i})$, $i = 1 \ldots n$ that satisfy (8)-(9).

As we will demonstrate, this approximation of the integer constraints does not always converge to binary values entirely, but might settle at an intermediate level. When this happen, we choose to run the optimization repeatedly, rounding some of the intermediate on/off variables down to zero using a threshold which we slowly increase until the optimal level is reached.

3.2 Regularization

To avoid oscillations from iteration to iteration we add proximal regularization of the form

$$\varphi_{\text{prox}} = k\rho_{\text{prox}} \left\| \left[p_1, p_2, \ldots, p_n\right]^{k-1} - \left[p_1, p_2, \ldots, p_n\right]^k \right\|_{\infty},$$

where ρ_{prox} is a constant, negative, weight chosen to damp large steps in each iteration. Smaller steps will of course increase the number of iterations required for the sequential convex programming method to converge, but, since we are able to compute each iteration extremely fast and might even have a good guess for warm-starting the algorithm we do not consider this to be a problem. Without proximal regularization oscillatory behavior can occur due to radically different solutions having almost the same result in the objective function.

3.3 Algorithm

Algorithm 1 outlines the method. Variables denoted with a ' $\hat{\cdot}$ ' indicate that this is the approximation we obtain by linearizing in the current iteration.

Algorithm 1 Iterative optimization with black-box model.

Initialize
  v_0, σ_0, $[u_i = 0.5]_{i=1}^n$, $[p_{s,i} = P_{\min}]_{i=1}^n$ and $k = 1$.
Evaluate
  Eq. 1 to find $\left\{p_{w,i}^{k-1}\right\}$ for $i = 1 \ldots n$,
  Eq. 2 to find $\left\{d_i^{k-1}, \sigma_i^{k-1}\right\}$ for $i = 1 \ldots n$
  Eq. 2 $(p_{s,i}^{k-1} + 1)$ to find $\left\{\frac{\Delta}{\Delta p_s}\right\}_i^{k-1}$ for $i = 1 \ldots n$
  Eq. 2 $(v_i^{k-1} + 1)$ to find $\left\{\frac{\Delta}{\Delta v}\right\}_i^{k-1}$ for $i = 1 \ldots n$
  Eq. 2 $(\sigma_i^{k-1} + 1)$ to find $\left\{\frac{\Delta}{\Delta \sigma}\right\}_i^{k-1}$ for $i = 1 \ldots n$.
Solve
  maximize $P_{\text{total}}^k + \varphi_{\text{prox}} + \varphi_{\text{int}}$,
  subject to $(p_i^k, \hat{v}_i^k, \hat{\sigma}_i^k) \in \Omega$, $i = 1 \ldots n$,
     $(\hat{u}_i^k, \hat{\eta}_{\text{int},i}^k) \in \Omega_{\text{int}}$, $i = 1 \ldots n$,
Update
  $p_{s,i}^k = p_i^k$, $u_i^k = \hat{u}_i^k$, $v_i^k = \hat{v}_i^k$, $\sigma_i^k = \hat{\sigma}_i^k$ for , $i = 1 \ldots n$,
  $k = k + 1$
Repeat until convergence.

Note that we do not formulate load reductions explicitly in the optimization problem presented in this paper.

4. TESTS AND RESULTS

As our method does not provide any guarantees in terms of optimality or convergence, we report extensive testing and simulation in this paper. We stress that the proposed method is not fully matured nor is it verified sufficiently. For the scope of this paper, we leave this as open questions.

We use $P_{\min} = 100\text{kW}$ and show simulations with a very small farm (4 turbines in a row) and a rather large farm (49 turbines in a 7×7 square pattern). The topologies are seen in Fig. 6 and Fig. 7, respectively. In all cases we use a wind direction parallel to the rows of turbines (the x-axis). This is not a limitation in the model nor in the method but it makes it more intuitive to validate the results.

4.1 Power

We show the resulting power set-points for the 1×4 wind farm at four different ambient wind speeds in Fig. 8. We benchmark our method against the "greedy" control scheme. The figures show the comparison of the two
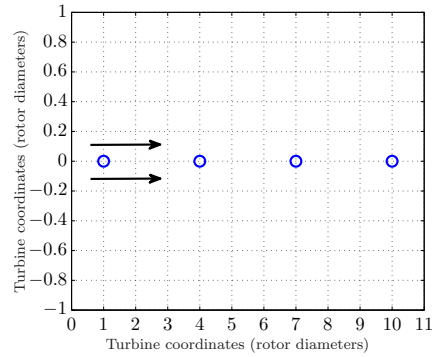

Fig. 6. Topology for small example wind farm (1×4). Arrows indicate the wind direction.
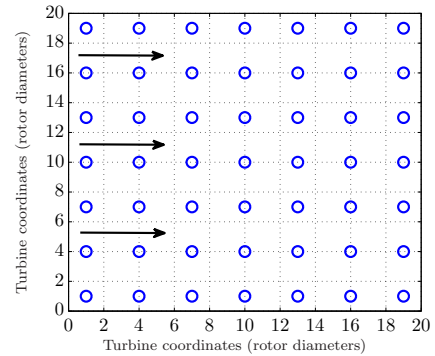

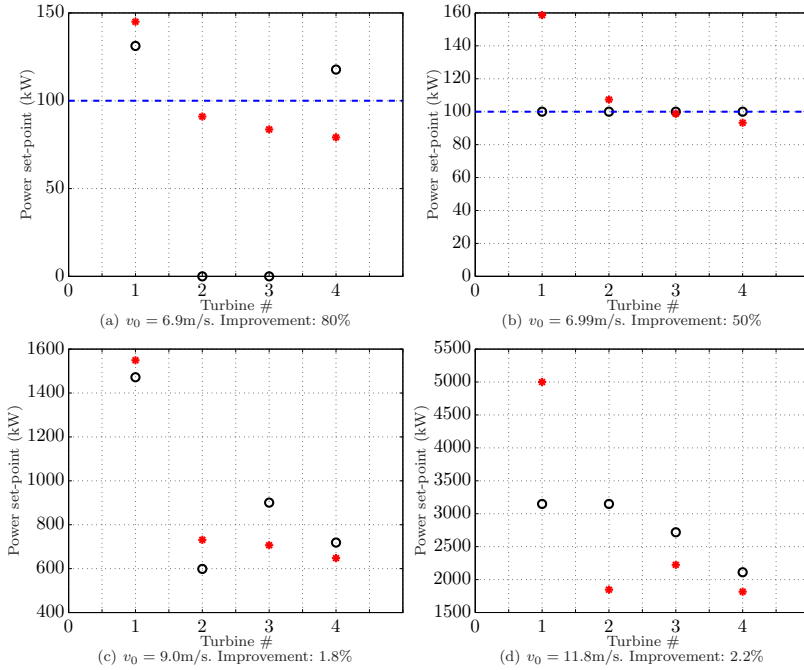Fig. 7. Topology for large example wind farm (7×7). Arrows indicate the wind direction.

Fig. 8. Test of power set-point optimization (blue circles) vs. "greedy", individual turbine control (red stars) for small farm. The dotted blue line is the cut-off ($P_{\min}$).

methods and the differences in P_{total} are reported in the captions. We observe how scenarios with exactly enough wind speed to turn on one more turbine (Fig. 8(a)-8(b)), obviously, are where the farm optimization adds the most benefit (up to 80% increase in power production). Even though they have been left out here, we are able to find situations in which the farm optimization only performs as well as the "greedy", but, in general it seems that typical improvements are in the order of 1.5–2.5%. All results for the 1×4 farm have been validated using a brute-force method to find the optimal solution, as this is doable for such a small number of turbines.

We only report one scenario for the 7×7 farm showing a 2.6% improvement (Fig. 9). In general, we are able to see similar results as for the smaller wind farm, when comparing against the "greedy" strategy. However, a brute-force search for this size of wind farms is not practically possible and we are not able to tell whether a "better" solution from the wind farm optimization (vs. the "greedy" method) is also the "best" achievable solution.

4.2 Integer programming

In Fig. 10 we show two examples of how the relaxed integer variables develop over the iterations of our algorithm. The scenarios correspond to the first two scenarios reported in

Fig. 8. For $v_0 = 6.9$m/s we see how u_2 and u_3 converges to values different from 0 or 1, which is of course not feasible in the real world. (In spite of this, the two turbines with feasible solutions improve the total power output with 51% vs. "greedy" control). Thus, we apply the thresholding technique and round all $u < 0.45$ to zero. Re-running the
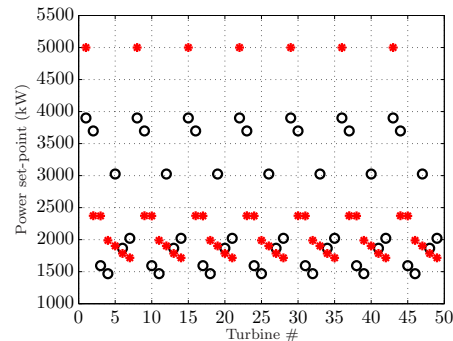

Fig. 9. Test of power set-point optimization (blue circles) vs. "greedy", individual turbine control (red stars) for large farm. $v_0 = 12$m/s. Improvement: 2.6%

Sequential Convex Programming for Power Set-point Optimization in a Wind Farm using Black-box Models, Simple Turbine Interactions, and Integer Variables
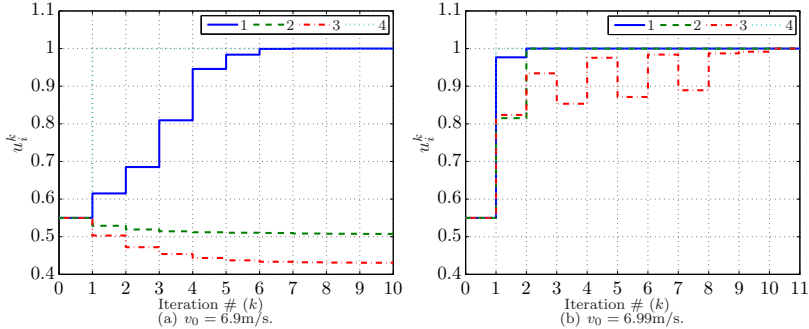
243

Fig. 10. Test illustrating the development of the "integer" variables (first optimization) for the scenarios reported in Fig. 8(a)-8(b).

algorithm with this (turbine number 3 forced off) gives a better result with 60% improvement vs. "greedy" control. Next, we increase to threshold such that all $u < 0.6$ are rounded to zero. With turbines 3 and 4 forced off the resulting power output is now as illustrated in Fig. 8(a) with 80% improvement. We show a scenario ($v_0 = 6.99$m/s) too, where all the on/off variables converge to 1 without thresholding and re-running the algorithm. In practice some logic is needed to decide whether to threshold or not. We have compared the results from our proposed method with mixed-integer programming implemented in CVX (CVX Research, 2012; Grant and Boyd, 2008). However, the computation times observed per iteration are a couple of hundred times longer, even with commercial solvers as `Gurobi` and `Mosek`. Furthermore, when combined with the sequential approximation technique in our algorithm, we saw that the mixed-integer solvers did not always provide the optimal values of the on/off variables.

4.3 Convergence and Computation

Our algorithm usually converges in fewer than 10 iterations in the testing we have performed. Naturally, the regularization parameter ρ_{prox} plays a role in the convergence properties of the method, but, we found it quite easy to tune. Fig. 11 shows an example with $\rho_{\text{prox}} = 0.1$ and ambient wind speed $v_0 = 12$m/s for the 7×7 wind farm. We see how the power levels settle relatively fast. From the figure it is difficult to see all 49 turbines (even though they are in fact there) since the 7 different power set-points found repeat almost identically for the 7 rows with this wind direction.

Recent advances in convex optimization allow for convex QPs to be solved at millisecond and microsecond timescales. We use CVXGEN to generate a custom embedded solver for ultra fast computation of each convex QP in the sequential approach. As an example, CVXGEN transformed the original optimization problem for the 7×7 wind farm into a standard form QP with 345 variables and 1177 constraints, exploiting the sparsity of the interaction matrices W_{d} and W_{t}. Each of these solves in less than $500\mu s$ on a 2.8GHz Intel Core i7.

4.4 Effect on Loads

In general, we observe from testing our method that there is a tendency to even out the power production over the wind farm whereas a "greedy" control most of the time extracts significantly more power from the turbines in the front row. Recall the correlations for tower bending moment from Fig. 5; an increase in power set-point or in turbulence intensity (higher standard deviation or lower mean wind speed) increases the build-up of fatigue loads on the turbines. When a turbine has a high extraction factor ($p_i/P_{\text{w},i}$), obviously, the high power set-point causes more load on that turbine. Furthermore, a high extraction factor leaves less wind speed behind, and adds more turbulence, for the downstream turbines resulting in higher loads per extracted power unit on these turbines as well. Hence, we prefer a more even power production over all turbines in the farm from a load perspective. We could add this explicitly to the cost function in the future to emphasize the effect, but as mentioned, we already see this to some degree as an indirect effect of our method.
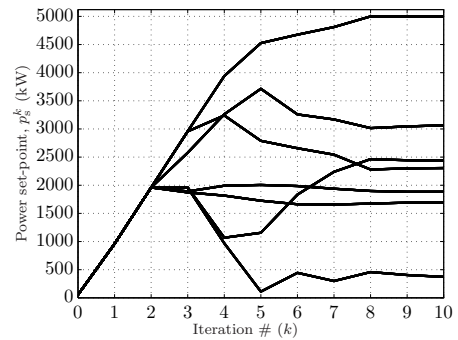

Fig. 11. Illustration of convergence for 7×7 wind farm. $v_0 = 12$m/s.

5. CONCLUSION

In this paper we have presented an approach to power set-point optimization for wind farms. We have based our method on convex optimization, solved iteratively to handle the fact that only black-box models of the farm and turbines are available. We perturbed the model to approximate derivatives and updated these estimates in each iteration. In addition, we proposed a way to solve mixed-integer problems in the same framework. By simulation of a very small and a rather large farm we demonstrated the method and revealed quite good improvements compared to a more naive control scheme. Due to the scale of economics for a large wind farm, such improvements are prone to make a big difference in the yearly revenue.

REFERENCES

Adegas, F.D., Stoustrup, J., and Odgaard, P.F. (2011). Repetitive model predictive approach to individual pitch control of wind turbines. In *IEEE Conference on Decision and Control*, 3664–3670.

Alves, M.J. and Clímaco, J. (2007). A review of interactive methods for multiobjective integer and mixed-integer programming. *European Journal of Operational Research*, 180(1), 99–115.

Boggs, P.T. and Tolle, J.W. (1995). Sequential quadratic programming. *Acta Numerica*, 4, 1–51.

Brand, A.J. and Wagenaar, J.W. (2010a). A quasi-steady wind farm flow model in the context of distributed control of the wind farm. In *European Wind Energy Conference (EWEC 2010)*.

Brand, A.J. and Wagenaar, J.W. (2010b). Validation of a quasi-steady wind farm flow model in the context of distributed control of the wind farm. In *The Science of making Torque from Wind (Torque2010)*.

CVX Research, I. (2012). CVX: Matlab software for disciplined convex programming, version 2.0 beta. http://cvxr.com/cvx.

Dang, D.Q., Wu, S., Wang, Y., and Cai, W. (2010). Model predictive control for maximum power capture of variable speed wind turbines. In *International Power Electronics Conference*, 274–279.

Danish Ministry of Climate, E. and Building (2012). Energy policy report 2012. Technical report, Danish Ministry of Climate, Energy and Building. Denmark. URL http://www.ens.dk/en-US/policy/danish-climate-and-energy-policy/Sider/danish-climate-and-energy-policy.aspx.

Dinh, Q.T., Savorgnan, C., and Diehl, M. (2011). Real-time sequential convex programming for nonlinear model predictive control and application to a hydro-power plant. In *50th IEEE Conference on Decision and Control and European Control Conference (CDC-ECC)*, 5905–5910.

Frandsen, S. (2007). *Turbulence and turbulence-generated structural loading in wind turbine clusters*. Risoe National Lab., Roskilde. Wind Energy Dept., Technical University of Denmark, Kgs. Lyngby (Denmark).

Grant, M. and Boyd, S. (2008). Graph implementations for nonsmooth convex programs. In V. Blondel, S. Boyd, and H. Kimura (eds.), *Recent Advances in Learning and Control*, Lecture Notes in Control and Information Sciences, 95–110. Springer-Verlag Limited.

Grossmann, I.E. (2002). Review of nonlinear mixed-integer and disjunctive programming techniques. *Optimization and Engineering*, 3(3), 227–252.

Grunnet, J.D., Soltani, M., Knudsen, T., Kragelund, M.N., and Bak, T. (2010). Aeolus toolbox for dynamics wind farm model, simulation and control. In *European Wind Energy Conference and Exhibition, EWEC*.

Hammerum, K., Brath, P., and Poulsen, N.K. (2007). A fatigue approach to wind turbine control. *Journal of Physics: Conference Series*, 75.

Hansen, A.D., Sørensen, P., Iov, F., and Blaabjerg, F. (2006). Centralised power control of wind farm with doubly fed induction generators. *Renewable Energy*, 31(7), 935–951.

Hansen, N., Auger, A., Ros, R., Finck, S., and Pošík, P. (2010). Comparing results of 31 algorithms from the black-box optimization benchmarking bbob-2009. In *12th annual conference companion on Genetic and evolutionary computation*, 1689–1696. ACM.

Hau, E. (2006). *Wind turbines: fundamentals, technologies, application, economics*. Springer Verlag.

Henriksen, L.C., Poulsen, N.K., and Hansen, M.H. (2011). Nonlinear model predictive control of a simplified wind turbine. In *18th IFAC World Congress*, 551–556. IFAC.

Hovgaard, T.G., Larsen, L.F.S., Jørgensen, J.B., and Boyd, S. (2012a). Fast nonconvex model predictive control for commercial refrigeration. In *4th IFAC Nonlinear Model Predictive Control Conference*, 514–521. The International Federation of Automatic Control.

Hovgaard, T.G., Larsen, L.F.S., Jørgensen, J.B., and Boyd, S. (2012b). Nonconvex model predictive control for commercial refrigeration. http://www.stanford.edu/~boyd/papers/noncvx_mpc_refr.html.

Johnson, K.E. and Thomas, N. (2009). Wind farm control: Addressing the aerodynamic interaction among wind turbines. In *American Control Conference.*, 2104–2109. IEEE.

Mattingley, J. and Boyd, S. (2012). CVXGEN: a code generator for embedded convex optimization. *Optimization and Engineering*, 13, 1–27.

Pao, L.Y. and Johnson, K.E. (2009). A tutorial on the dynamics and control of wind turbines and wind farms. In *American Control Conference*, 2076–2089. IEEE.

Soleimanzadeh, M., Brand, A.J., and Wisniewski, R. (2011). A wind farm controller for load and power optimization in a farm. In *IEEE International Symposium on Computer-Aided Control System Design (CACSD)*, 1202–1207. IEEE.

Soleimanzadeh, M., Wisniewski, R., and Kanev, S. (2012). An optimization framework for load and power distribution in wind farms. *Journal of Wind Engineering and Industrial Aerodynamics*.

Spudic, V., Jelavic, M., and Baotic, M. (2011). Wind turbine power references in coordinated control of wind farms. *AUTOMATIKA*, 52(2), 82–94.

Steinbuch, M., de Boer, W., Bosgra, O., Peters, S., and Ploeg, J. (1988). Optimal control of wind power plants. *Journal of Wind Engineering and Industrial Aerodynamics*, 27(1), 237–246.

MPC for Wind Power Gradients—Utilizing Forecasts, Rotor Inertia, and Central Energy Storage

MPC for Wind Power Gradients — Utilizing Forecasts, Rotor Inertia, and Central Energy Storage

Tobias Gybel Hovgaard, Lars F. S. Larsen, John Bagterp Jørgensen and Stephen Boyd

Abstract— **We consider the control of a wind power plant, possibly consisting of many individual wind turbines. The goal is to maximize the energy delivered to the power grid under very strict grid requirements to power quality. We define an extremely low power output gradient and demonstrate how decentralized energy storage in the turbines' inertia combined with a central storage unit or deferrable consumers can be utilized to achieve this goal at a minimum cost. We propose a variation on model predictive control to incorporate predictions of wind speed. Due to the aerodynamics of the turbines the model contains nonconvex terms. To handle this nonconvexity, we propose a sequential convex optimization method, which typically converges in fewer than 10 iterations. We demonstrate our method in simulations with various wind scenarios and prices for energy storage. These simulations show substantial improvements in terms of limiting the power ramp rates (disturbance rejection) at the cost of very little power. This capability is critical to help balance and stabilize the future power grid with a large penetration of intermittent renewable energy sources.**

I. Introduction

Today, wind power is the most important renewable energy source. For the years to come, many countries have set goals for further reduced CO_2 emission, increased utilization of renewable energy, and phase out of fossil fuels. In Denmark one of the means to achieve this is to increase the share of wind power to 50% of the electricity consumption by 2020 and to fully cover the energy supply with renewable energy by 2050 [1]. Installing this massive amount of wind turbines introduces several challenges to reliable operation of power systems due to the fluctuating nature of wind power. To mitigate fluctuations, modern wind power plants (WPP) are equipped with variable speed wind turbine (VSWT) technologies, which are interfaced with power electronics converters that are required and designed to fulfil increasingly demanding grid codes (see, *e.g.* [2], [3]).

The Grid Code (GC) is a technical document setting out the rules, responsibilities and procedures governing the operation, maintenance and development of the power system. It is a public document periodically updated with new requirements and it differs from operator to operator. Countries with large amount of wind power have issued dedicated GCs for its connection to transmission and distribution levels, focused mainly on power controllability and power quality [4], [5]. Particularly, Denmark establishes some of the most

T. G. Hovgaard and L. F. S. Larsen are with Vestas Technology R&D, DK-8200 Aarhus N, Denmark. {togho,lfsla}@vestas.com
J. B. Jørgensen is with DTU Compute, Technical University of Denmark, DK-2800 Lyngby, Denmark. jbjo@dtu.dk
S. Boyd is with the Information Systems Laboratory, Department of Electrical Engineering, Stanford University, USA. boyd@stanford.edu

demanding requirements regarding active power control [6]. One of the regulation functions required is a power gradient constraint that limits the maximum rate-of-change of non-commanded variations in the power output from the WPP to the grid. As of today, this constraint is softened if the power production in the WPP drops due to the lack of wind. This is merely out of necessity, and the GCs are expected to tighten further regarding this requirement. Ensuring slow power gradients reduces the risk of instability on the grid, allows the TSO time for counteracting the change, and improves the predictability of power output, enabling the WPP owner to put less conservative bids on the power market.

Energy storage strikes the major problems of wind power and joining energy storage with WPPs to smoothen variations and improve the power quality is not a new idea. In, *e.g.*, [7]–[10] the benefits, economics, and challenges of using different means of storage, *i.e.*, batteries, hydrogen, flywheels etc., in combination with wind power are investigated. [11] uses a Lithium-iron-phosphate battery to achieve power forecast improvement and output power gradient reduction. However, the additional cost of batteries or other energy storages is usually the showstopper, at least as the market is today. In our previous works, we have shown how thermal capacity, *e.g.*, in supermarket refrigeration, can be utilized for flexible power consumption [12], [13]. It is very likely that such techniques (where the capacity is a bi-product of fulfilling another need) can play a major role instead of adding expensive technologies which have storage as their sole purpose. In the rest of this paper, we consider energy storage in general without distinguishing actual storage from flexible power consumption.

Traditionally, the rotor speed of modern wind turbines is controlled for tracking the tip-speed ratio (TSR = angular rotor speed × rotor radius / wind speed) for maximum power extraction, constrained by the maximum rated speed. However, due to the inertia of the rotating masses in the turbine, there is a potential to improve the quality of the power output by actively letting the rotor speed deviate from the optimal setting. This might of course come at a cost of slightly reduced power output. In, *e.g.*, [14], [15] turbine inertia is used for frequency response and power oscillation damping. In addition, a vast amount of works exist that address power optimization, fatigue load reduction and pitch control for individual turbines in the more traditional sense, *e.g.*, [16]–[18]. Some of these take optimization and model predictive control approaches to solve the problems and many rely on a known operating point (*e.g.*, local wind speed and power set-point) for deriving linearized models.

Other works consider the control of large wind farms where the power extracted by upwind turbines reduces the power that is available from the wind and increases the turbulence intensity in the wake reaching other turbines (see, *e.g.*, [19]–[21]).

In [13], we demonstrate the appreciation of a sequential convex programming (SCP) approach [22] for a model predictive control problem, controlling the power consumption for commercial refrigeration with linear dynamics, convex constraints, and a nonconvex objective. Inspired by this, we now turn to the power producers' side of the grid and apply the same technique to a nonlinear wind turbine model. Our method, like sequential quadratic programming (SQP) [23], involves the solution of a sequence of (convex) quadratic programs (QPs), but differs very much in how the QPs are formed. In SQP, an approximation to the Lagrangian of the problem is used; the linearization required in each step can end up dominating the computation [24]. In our SCP method, the convexification step is quite straightforward.

We demonstrate how model predictive control using forecasts of the wind speed can ensure very low power gradients (*e.g.*, less than 5% of the rated power per minute). We do this with a central energy storage added to the WPP and show how we can utilize the inertia in the individual turbines to further improve this and minimize the extra storage capacity needed. Our method gives no guarantee in terms of convergence or optimality but is observed to perform well in practice. [25] uses convex optimization to operate a portfolio of electrical storage devices. In [26], we present a change of variables that renders the problem fully convex and demonstrate efficient closed-loop simulations with real wind data.

II. WIND POWER PLANT

In this section, we describe the dynamic model used for the WPP in the paper. The WPP can have a number of individual wind turbines arranged in a certain geographical topology and one central storage unit. We describe the simplified dynamics of rotational motion, the constraints of the system and the function reflecting the objective of operating the plant.

A. Wind Turbine Model

The WPP in the examples consists of turbines using the NREL 5MW model since this is openly available, but, could easily be substituted with any specific turbine model. The model is described in detail in, *e.g.*, [27], [28]. We simplify the model and derive the system equations as follows. Neglecting the shaft torsion, we describe the turbine itself by two dynamical states, the generator speed, ω_g, in rad/s and the generator torque, T_g, in Nm.

$$\dot{\omega}_g = \frac{1}{I_g + I_r/N^2}\left(\frac{T_r}{N} - T_g\right), \tag{1}$$

$$\dot{T}_g = \frac{1}{\tau_g}\left(T_{g,\text{ref}} - T_g\right), \tag{2}$$

where I_g and I_r are the inertias of generator and rotor respectively, N is the gear ratio, τ_g is the time constant of the generator and $T_{g,\text{ref}}$ is the torque set-point. The torque, T_r, delivered to the rotor by the wind is given by

$$T_r = \frac{1}{2}\rho A C_P(\lambda, \beta)\frac{v^3}{\omega_r},$$

where ρ is air density, A is swept area of the rotor, v is wind speed in m/s, ω_r is angular rotor speed in rad/s, and the coefficient of power, C_P, is a look-up table (see Fig. 1) derived from the geometry of the blades as a function of TSR and blade pitch angle (β) in degrees. TSR is defined as $\lambda = R\omega_r/v$, where R is the rotor radius in m. We use $\omega_r = \omega_g/N$ to eliminate ω_r and describe the power produced in the generator by

$$P_g = \eta_g T_g \omega_g,$$

where η_g is the generator efficiency.

B. Energy Storage Model

We use a simple integrator for illustrating the central energy storage and describe its state-of-charge (Q [J]) in discrete-time by

$$Q(t + T_s) = Q(t) + c(t)T_s, \tag{3}$$

where c is the charge rate in W and t denotes time. We assume that the energy storage is lossless. However, in reality batteries have losses just as, *e.g.*, refrigeration systems increase the heat load, and thereby the power loss, as the temperatures are lowered to store extra cooling energy. A loss term could be modeled as $-\eta_{\text{loss}}Q(t)$ which is added to the equation above, but, as our time-scale for storing energy is in the range of seconds to minutes, we neglect this.

We can now find the power supplied from the WPP to the grid
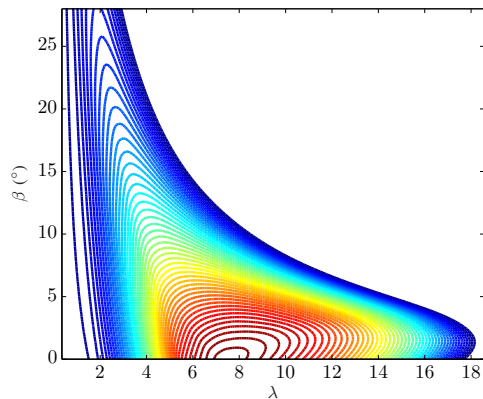
$$P_{\text{grid}} = P_g - c.$$

Fig. 1: Coefficient of power C_P. The peak power coefficient is 0.482.

C. Control

Manipulated variables: Our optimizer manipulates the set-points to the generator torque, $T_{g,ref}$, and the pitch angle, β_{ref}, for each individual turbine in the WPP. Normally, the pitch is controlled by an inner loop exercising a gain-scheduled PI controller. This controller samples up to 100 times faster than our MPC and we set $\beta_{ref} = \beta$ as long as the slew rate limit on β_{ref} is observed. Additionally, we manipulate the charge rate, c, to/from the central energy storage.

Measured variables: The controller bases its decisions on measurements of the rotational speed and generator torque in each turbine, on the known current wind speed, and on the filtered, predicted future values of the latter covering the entire prediction horizon, N_p.

D. Constraints

The extracted power, P_g, must be equal to or less than the available power in the wind, P_w, which is a function of the wind speed, v. The turbine is build for a rated power and when the available power in the wind exceeds this level, the blades gradually pitch out of the wind to keep the extracted power at the rated level and reduce loads on the turbine. Likewise, the extracted power can only follow the available power curve down to a certain level, P_{min}, due to the mechanical design. Thus,

$$P_{min} \leq P_g \leq P_{rated}, \qquad (4)$$

$$P_g \leq P_w(v), \qquad (5)$$

For security reasons, the turbine is turned off for wind speeds above 25m/s. Therefore, $P_w = 0$, and the constraint (4) is not relevant for such high wind speeds.

In addition, four physical constraints are given by the system

$$0° \leq \beta \leq 90°, \qquad (6)$$

$$-8°/s \leq \frac{\beta(t + T_s) - \beta(t)}{T_s} \leq 8°/s, \qquad (7)$$

$$c \leq P_g, \qquad (8)$$

and

$$0 \leq Q \leq \mu P_{rated}, \qquad (9)$$

where we introduce the variable μ which is the maximum needed storage capacity in per unit (pu), *i.e.*, normalized by rated power.

The rotational speed is usually limited by a maximum rated speed, mainly due to too high loads on the turbine at higher speeds. However, since we want to put the turbine inertia in play, we allow for higher speeds and introduce the parameter ω_{os} which is the fraction of the rated maximum speed that we accept as over-speed.

$$\omega_{g,rated,min} \leq \omega_g \leq (1 + \omega_{os})\omega_{g,rated,max}. \qquad (10)$$

The power supplied to the grid P_{grid} must fulfill the power gradient

$$-\Delta pu \leq \frac{P_{grid}(t + T_s) - P_{grid}(t)}{P_{rated}T_s} \leq \Delta pu, \qquad (11)$$

where $\Delta pu \in [0, 1]$ is the grid code for maximum power gradient in per unit with respect to rated power.

In this study, we do not include the wake effects that couple the individual turbines through the downwind wind flow which is affected by the amount of power extracted by upwind turbines. This type of constraint is a focus of our future work.

We define the set Ω as all $(T_{g,ref}, \beta_{ref}, c)$ that satisfy the system dynamics (1)–(3) and the constraints (4)–(11).

E. Cost

We assume in this study that the objective of the WPP is to maximize the average power supplied to the grid. Alternative operating modes such as delta production (keeping a reserve by producing less than possible) or frequency response (reacting on frequency deviations on the grid to support stabilization at nominal grid frequency) are thus not considered. The supplied energy, E, over the period $[T_0, T_{final}]$ is

$$E = \int_{T_0}^{T_{final}} P_{grid} dt.$$

Furthermore, we have a cost on the available storage capacity. For a period $[T_0, T_{final}]$ this is

$$S = \max [\mu]_{T_0}^{T_{final}} c_{storage}.$$

We can consider the storage price, $c_{storage}$, as a tuning parameter or as directly reflecting, *e.g.*, purchase price of batteries divided by their lifetime, a service agreement with a flexible consumer, etc. Thus, S is a cost in the design phase only (or for simulations as we will show here).

F. Nominal Controller

We compare the performance of our proposed method to the solution from the nominal wind turbine control strategy, also defined in the NREL 5MW model. For natural reasons this system is only capable of obeying the power gradient constraint in three cases: 1) When the rate-of-change of the available power in the wind is less than the power gradient constraint. 2) When the available power in the wind only changes from one point to another, where both are above rated power. 3) When sufficiently large amounts of storage is added and its charge/discharge is controlled by some kind of predictive control with knowledge of the future wind speed.

III. MPC CONTROLLER

The WPP is influenced by disturbances from the wind speed which we can predict (with some uncertainty) over a time horizon into the future. The controller must obey certain constraints, while maximizing the power supply and limiting additional costs for storage. Economic MPC can address all these concerns. Whereas the cost function in MPC traditionally penalizes a deviation from a set-point, the proposed economic MPC directly reflects the actual costs of operating the plant. Like in traditional MPC, we implement the controller in a receding horizon manner, where an optimization problem over N_p time steps (the control and prediction horizon) is solved at each step. The

result is an optimal input sequence for the entire horizon, out of which only the first step is implemented. The optimization problem is thus formulated as

$$\begin{aligned} \text{maximize} \quad & E - S, \\ \text{subject to} \quad & (\mathbf{T}_{\mathrm{g,ref}}, \boldsymbol{\beta}_{\mathrm{ref}}, \mathbf{c}) \in \Omega, \end{aligned} \quad (12)$$

where the variables are $T_{\mathrm{g,ref}}$, β_{ref} and c (all functions of time). Instead of (12) we solve a discretized version with N_{p} steps over the time interval $[T_0, T_{\mathrm{final}}]$,

$$\{\mathbf{T}_{\mathrm{g,ref}}, \boldsymbol{\beta}_{\mathrm{ref}}, \mathbf{c}\} = \{T^k_{\mathrm{g,ref}}, \beta^k_{\mathrm{ref}}, c^k\}_{k=0}^{N_{\mathrm{p}}-1}. \quad (13)$$

The MPC feedback law is the first move in (13). The controller uses the initial state as well as predictions of the wind speed for the time interval. The predictions could come from any good sources available, see *e.g.*, [29] where 10-minute ahead predictions are implemented.

A. Sequential convex programming method

As we saw in §II, neither the feasible set Ω nor the cost function term P are fully convex. Instead of using a generic nonlinear optimization tool, we choose to solve the optimization problem iteratively using convex programming, replacing the nonconvex terms with convex approximations. In each iteration, i, we perform a first-order Taylor expansion of the nonconvex parts around the operating point found in iteration $i-1$, estimating the derivatives that involve table look-ups by perturbing the parameters. As the wind speed v is predicted we can use v^3 as input to our model instead. We establish the following linear approximations

$$\hat{T}^i_{\mathrm{r}} = T_{\mathrm{r}}^{\,i-1} + \left[\frac{\Delta T_{\mathrm{r}}}{\Delta \omega_{\mathrm{r}}}, \frac{\Delta T_{\mathrm{r}}}{\Delta C_{\mathrm{P}}}\right]^{i-1} \left[\begin{array}{c} \omega^i_{\mathrm{r}} - \omega^{i-1}_{\mathrm{r}} \\ C^i_{\mathrm{P}} - C^{i-1}_{\mathrm{P}} \end{array}\right],$$

$$\hat{P}^i_{\mathrm{g}} = P_{\mathrm{g}}^{\,i-1} + \left[\frac{\Delta P_{\mathrm{g}}}{\Delta \omega_{\mathrm{g}}}, \frac{\Delta P_{\mathrm{g}}}{\Delta T_{\mathrm{g}}}\right]^{i-1} \left[\begin{array}{c} \omega^i_{\mathrm{g}} - \omega^{i-1}_{\mathrm{g}} \\ T^i_{\mathrm{g}} - T^{i-1}_{\mathrm{g}} \end{array}\right].$$

Thus, in each iteration we solve a convex optimization problem, which can be done very reliably and extremely quickly [30]. While our proposed method gives no theoretical guarantee on the performance, we must remember that the optimization problem is nothing but a heuristic for computing a good control and that the quality of closed-loop control with MPC is generally good without solving each problem accurately.

B. Regularization

We use two different types of regularization in the optimization problem. To avoid oscillations from iteration to iteration, we add proximal regularization of the form

$$\varphi_{\mathrm{prox}} = \rho_{\mathrm{prox}} \sum_{k=0}^{N-1} \|X^k - X^{k,\mathrm{prev}}\|_2^2, \quad (14)$$

for each of the control variables $X = \{T_{\mathrm{g,ref}}, \beta_{\mathrm{ref}}, c\}$. The superscript 'prev' indicates that it is the solution from the previous iteration and ρ_{prox} is a constant weight chosen to damp large steps in each iteration. In addition, we add a

quadratic penalty on the rate-of-change (roc) of the manipulable variables,

$$\varphi_{\mathrm{roc}} = \rho_{\mathrm{roc}} \sum_{k=1}^{N-1} \|X^k - X^{k-1}\|_2^2. \quad (15)$$

This regularization term serves two purposes: It improves the convergence of the sequential programming method, and also discourages rapid changes, which helps reduce oscillations and fatigue loads.

C. Algorithm

Algorithm 1 outlines the method. The term *nominal* refers to the solution obtained from the nominal controller. We use this as a baseline for initializing the algorithm. In MPC, the solution from the previous time step is usually well suited for warm-starting the algorithm.

Algorithm 1 Iterative optimization.

Initialize
  $\{\mathbf{T}^0_{\mathrm{g}}, \mathbf{T}^0_{\mathrm{r}}, \boldsymbol{\omega}^0_{\mathrm{g}}, \boldsymbol{\omega}^0_{\mathrm{r}}, \mathbf{C}^0_{\mathrm{P}}, \mathbf{T}^0_{\mathrm{g,ref}}, \boldsymbol{\beta}^0_{\mathrm{ref}}\} = \{\mathrm{nominal}(v_k)\}_{k=1}^{N_{\mathrm{p}}}$,
  $i = 1$.
Compute
  $\hat{\mathbf{T}}^i_{\mathrm{r}}, \hat{\mathbf{P}}^i_{\mathrm{g}}$ and $\hat{\mathbf{C}}^i_{\mathrm{P}}$, from $\{\mathbf{T}_{\mathrm{g}}, \mathbf{T}_{\mathrm{r}}, \boldsymbol{\omega}_{\mathrm{g}}, \boldsymbol{\omega}_{\mathrm{r}}, \mathbf{C}_{\mathrm{P}}, \mathbf{T}_{\mathrm{g,ref}}, \boldsymbol{\beta}_{\mathrm{ref}}\}^{i-1}$
  and v.
Solve
  maximize $E^i - S^i + \varphi_{\mathrm{prox}} + \varphi_{\mathrm{roc}}$,
  subject to $(\mathbf{T}^i_{\mathrm{g,ref}}, \boldsymbol{\beta}^i_{\mathrm{ref}}, \mathbf{c}) \in \hat{\Omega}$,
Update
  $\{\mathbf{T}^i_{\mathrm{g}}, \mathbf{T}^i_{\mathrm{r}}, \boldsymbol{\omega}^i_{\mathrm{g}}, \boldsymbol{\omega}^i_{\mathrm{r}}, \mathbf{C}^i_{\mathrm{P}}, \mathbf{T}^i_{\mathrm{g,ref}}, \boldsymbol{\beta}^i_{\mathrm{ref}}\}$, and $i = i+1$
Repeat until convergence.

IV. RESULTS

In this paper, we apply the proposed method to a conceptual study limited to only one wind turbine. We implement and solve our controller for different scenarios using CVX [31], [32]. In this section, we report on results with a power gradient constraint as low as 3% of the rated power per minute ($\Delta pu = 5 \cdot 10^{-4}$pu/s) and with an allowed overspeed of 50% above rated speed for short time intervals. We sample with $T_{\mathrm{s}} = 1$s intervals and use a horizon of 5 minutes ($N_{\mathrm{p}} = 300$) in this case. Obviously, a wide range of solutions can be obtained depending on the specific ramp rate of the wind speed, the wind speeds before and after the change occurs, the allowed amount of overspeed and the definition of storage price versus power sales price. In this paper, we give proof-of-concept of the method, using a few selected trajectories, and for the next version of this work, we will derive a more generalized measure of the relation between wind ramp rates, overspeed ratio, power constraint, and storage capacity.

Fig. 2 shows examples of how our proposed method performs in different cases, while satisfying the power gradient constraint. For all four cases shown in the figures, we can calculate the total power delivered to the grid from $t = 0 \ldots 800$s. For the scenario in figures 2(a)–2(b) (wind speed changes from 10m/s to 8m/s), the available power in the wind is below the rated power for the entire interval. Thus,
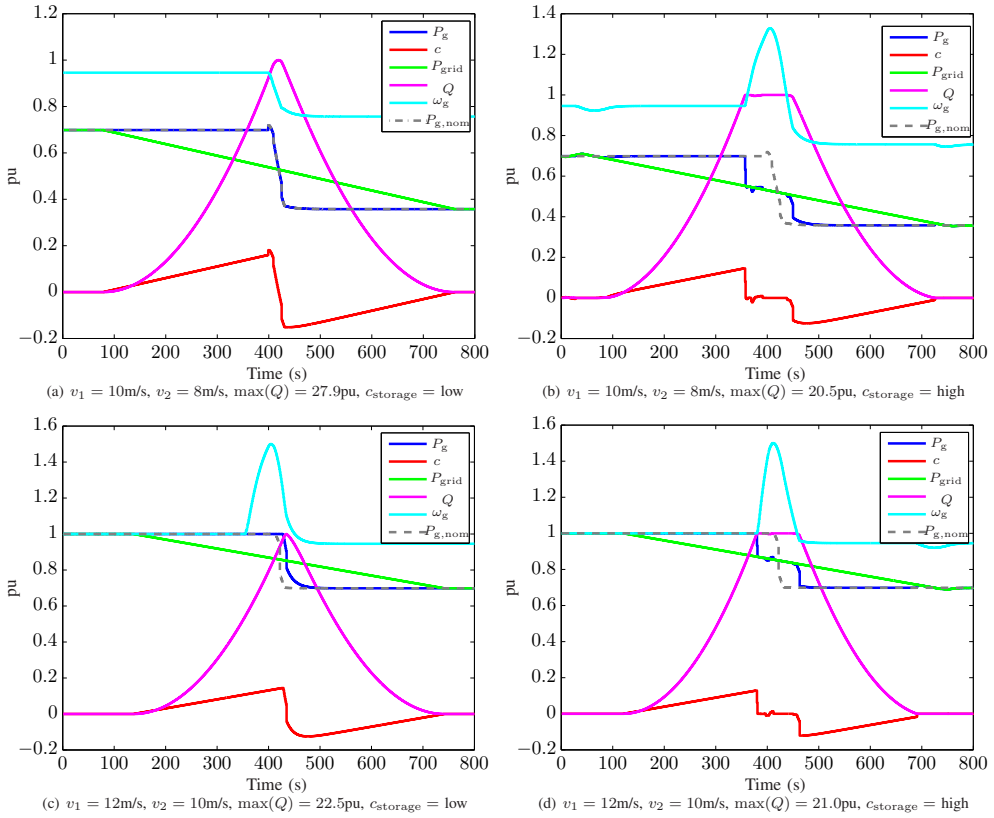
Fig. 2: Test of power gradient satisfaction. We use pu as the unit for all quantities, except the state-of-charge (Q) which is normalized first with respect to maximum storage capacity. In all scenarios we let the wind speed drop from v_1 to v_2 linearly from $t = 400$s to $t = 430$s, and we show cases with high and low storage cost. $P_{\mathrm{g,nom}}$ is the power output from the nominal controller.

no extra power exists for accelerating the rotor beyond rated speed. If central energy storage is relatively cheap (Fig. 2(a)) this is used entirely as a buffer for achieving the commanded power gradient while the turbine behaves exactly as with the nominal controller. In this case, the total amount of energy delivered to the grid is equal to the nominal case too. As the price of energy storage increases the controller trades off the power production that is lost during the phase where the rotor is accelerated, in order to use that kinetic energy during the power ramp to reduce the peak of needed storage capacity. In Fig. 2(b) the storage capacity is reduced by 26.5% at the cost of 1.3% of the energy delivered to the grid, compared to Fig. 2(a). For the scenario in figures 2(c)–2(d) (wind speed changes from 12m/s to 10m/s), the available power in the wind goes from above rated to below rated power. In this case, the rotor can be accelerated to reach the maximum

allowed speed just when the available power in the wind begins to drop. This kinetic energy is used during the power ramp no matter how cheap storage is, as it only adds to the total delivered energy. In Fig. 2(c) the amount of energy delivered to the grid is 1.6% higher than with the nominal controller. When storage cost is increased, the utilization of stored inertia is shifted towards the time when the storage needs peak, to reduce the required additional capacity, and the extra production gained otherwise is now traded off with storage cost. In Fig. 2(d) the energy delivered is just 0.03% less than with the nominal controller while the storage need is reduced by almost 7%.

A. Convergence and Computation

When initialized with the trajectory from the nominal controller, the proposed method generally converges in 5–10 iterations. In MPC, however, the open-loop trajectory

from the previous run of the optimizer, shifted one time-step, is an excellent guess on the next outcome and is well-suited for warm-starting the algorithm. Using this warm start initialization, the method generally just need a couple of iterations to converge.

V. Conclusion

In this paper, we present an approach to power gradient reduction for fulfilling future, tighter grid codes and for improving the quality of power delivered to the grid from wind power plants. We utilize turbine inertia as a resource of distributed energy storage, limited by the rotational speed, in addition to a central storage unit which is associated with an extra cost. Our method is based on convex optimization, solved iteratively to handle the nonconvexity of the aerody-namics. Simulation on realistic models reveal a significant ability to reject the disturbances from fast changes in wind speed, ensuring certain power gradients, while keeping the amount of produced power close to nominal. We can easily trade off lost production versus price of extra energy storage.
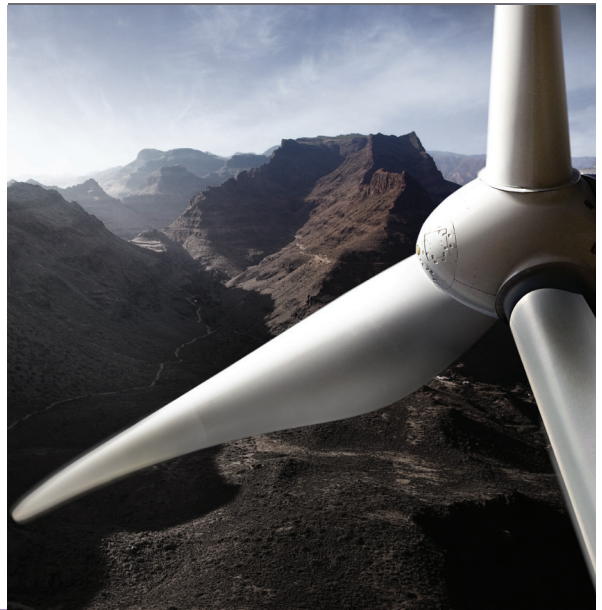
VI. ACKNOWLEDGMENTS

References

[1] Danish Ministry of Climate Energy and Building, "Energy policy report 2012," Tech. Rep., May 2012. [Online]. Available: http://www.ens.dk/en-US/policy/danish-climate-and-energy-policy/Sider/danish-climate-and-energy-policy.aspx

[2] J. Morren, J. Pierik, and S. W. H. de Haan, "Inertial response of variable speed wind turbines," *Electric Power Systems Research*, vol. 76, no. 11, pp. 980–987, 2006.

[3] J. F. Conroy and R. Watson, "Frequency Response Capability of Full Converter Wind Turbine Generators in Comparison to Conventional Generation," *IEEE Transactions on Power Systems*, vol. 23, no. 2, pp. 649–656, may 2008.

[4] F. Iov, A. Hansen, P. Sørensen, and N. Cutululis, "A survey of interconnection requirements for wind power," in *Proc. of the Nordic wind power conference (NWPC)*. Risø National Laboratory, 2007.

[5] B. Singh and S. Singh, "Wind Power Interconnection into the Power System: A Review of Grid Code Requirements," *The Electricity Journal*, vol. 22, no. 5, pp. 54–63, 2009.

[6] Eltra/Elkraft/Energinet.dk, "Regulation TF 3.2.5, Wind turbines connected to grids with voltages above 100 kV — Technical regulation for the properties and the regulation of wind turbines," https://selvbetjening.preprod.energinet.dk/NR/rdonlyres/E4E7A0BA-884F-4E63-A2F0-98EB5BD8D4B4/0/WindTurbinesConnectedtoGridswithVoltageabove100kV.pdf.

[7] M. Korpås and A. T. Holen, "Operation planning of hydrogen storage connected to wind power operating in a power market," *IEEE Transactions on Energy Conversion*, vol. 21, no. 3, pp. 742–749, 2006.

[8] M. Black and G. Strbac, "Value of Bulk Energy Storage for Managing Wind Power Fluctuations," *IEEE Transactions on Energy Conversion*, vol. 22, no. 1, pp. 197–205, march 2007.

[9] D. I. Stroe, A. I. Stan, R. Diosi, R. Teodorescu, and S. J. Andreasen, "Short term energy storage for grid support in wind power applications," in *Proc. of the 13th International Conference on Optimization of Electrical and Electronic Equipment*, 2012, pp. 1012–1021.

[10] C. Budischak, D. A. Sewell, H. Thomson, L. Mach, D. E. Veron, and W. Kempton, "Cost-Minimized Combinations of Wind Power, Solar Power and Electrochemical Storage, Powering the Grid up to 99.9% of the Time," *Journal of Power Sources*, vol. 225, pp. 60–74, 2013.

[11] M. Swierczynski, R. Teodorescu, and P. Rodriguez, "Lifetime investigations of a lithium iron phosphate (LFP) battery system connected to a wind turbine for forecast improvement and output power gradient reduction," in *Proc. of the 15th Battcon Stationary Battery Conference and Trade Show*, 2011, pp. 20.1–20.8.

[12] T. G. Hovgaard, L. F. S. Larsen, K. Edlund, and J. B. Jørgensen, "Model predictive control technologies for efficient and flexible power consumption in refrigeration systems," *Energy*, vol. 44, no. 1, pp. 105 – 116, 2012.

[13] T. G. Hovgaard, L. F. S. Larsen, J. B. Jørgensen, and S. Boyd, "Nonconvex model predictive control for commercial refrigeration," *International Journal of Control*, p. In Press, 2012.

[14] T. Knuppel, J. N. Nielsen, K. H. Jensen, A. Dixon, and J. Østergaard, "Power oscillation damping controller for wind power plant utilizing wind turbine inertia as energy storage," in *Proc. of the IEEE Power and Energy Society General Meeting*, 2011, pp. 1–8.

[15] G. C. Tarnowski, "Coordinated Frequency Control of Wind Turbines in Power Systems with High Wind Power Penetration," Ph.D. dissertation, Technical University of Denmark, 2012.

[16] K. Hammerum, P. Brath, and N. K. Poulsen, "A fatigue approach to wind turbine control," *Journal of Physics: Conference Series*, vol. 75, 2007.

[17] D. Q. Dang, S. Wu, Y. Wang, and W. Cai, "Model Predictive Control for maximum power capture of variable speed wind turbines," in *International Power Electronics Conference*, 2010, pp. 274–279.

[18] L. C. Henriksen, N. K. Poulsen, and M. H. Hansen, "Nonlinear Model Predictive Control of a Simplified Wind Turbine," in *Proc. of the 18th IFAC World Congress*, 2011, pp. 551–556.

[19] M. Soleimanzadeh, R. Wisniewski, and S. Kanev, "An optimization framework for load and power distribution in wind farms," *Journal of Wind Engineering and Industrial Aerodynamics*, vol. 107-108, pp. 256–262, 2012.

[20] V. Spudić, M. Jelavić, and M. Baotić, "Wind turbine power references in coordinated control of wind farms," *Automatika–Journal for Control, Measurement, Electronics, Computing and Communications*, vol. 52, no. 2, pp. 82–94, 2011.

[21] T. G. Hovgaard, L. F. S. Larsen, J. B. Jørgensen, and S. Boyd, "Sequential Convex Programming for Power Set-point Optimization in a Wind Farm using Black-box Models, Simple Turbine Interactions, and Integer Variables," in *Proc. of the 10th European Workshop on Advanced Control and Diagnosis (ACD)*, 2012, pp. 1–8.

[22] S. Boyd, "EE364b, Lecture Slides and Notes: Sequential convex programming," http://www.stanford.edu/class/ee364b/lectures/seq_slides.pdf.

[23] P. T. Boggs and J. W. Tolle, "Sequential Quadratic Programming," *Acta Numerica*, vol. 4, pp. 1–51, 1995.

[24] Q. T. Dinh, C. Savorgnan, and M. Diehl, "Real-time sequential convex programming for nonlinear model predictive control and application to a hydro-power plant," in *Proc. of the 50th IEEE Conference on Decision and Control and European Control Conference (CDC-ECC)*, 2011, pp. 5905–5910.

[25] M. Kraning, Y. Wang, E. Akuiyibo, and S. Boyd, "Operation and Configuration of a Storage Portfolio via Convex Optimization," in *Proc. of the 18th IFAC World Congress*, 2011, pp. 10 487–10 492.

[26] T. G. Hovgaard, S. Boyd, and J. B. Jørgensen, "Model predictive control for wind power gradients," http://www.stanford.edu/~boyd/papers/wind_gradients_cvx.html, 2013.

[27] J. M. Jonkman, S. Butterfield, W. Musial, and G. Scott, *Definition of a 5-MW reference wind turbine for offshore system development*. National Renewable Energy Laboratory, Feb 2009.

[28] J. D. Grunnet, M. Soltani, T. Knudsen, M. N. Kragelund, and T. Bak, "Aeolus Toolbox for Dynamics Wind Farm Model, Simulation and Control," in *Proc. of the European Wind Energy Conference and Exhibition, EWEC*, 2010.

[29] P. Pinson, "Very-short-term probabilistic forecasting of wind power with generalized logit-normal distributions," *Journal of the Royal Statistical Society: Series C (Applied Statistics)*, vol. 61, no. 4, pp. 555–576, 2012.

[30] S. Boyd and L. Vandenberghe, *Convex Optimization*. Cambridge University Press, 2004.

[31] CVX Research, Inc., "CVX: Matlab Software for Disciplined Convex Programming, version 2.0 beta," http://cvxr.com/cvx, Sept. 2012.

[32] M. Grant and S. Boyd, "Graph implementations for nonsmooth convex programs," in *Recent Advances in Learning and Control*, ser. Lecture Notes in Control and Information Sciences, V. Blondel and S. Boyd and H. Kimura, Ed. Springer-Verlag Limited, 2008, pp. 95–110.

[This page intentionally left blank]

In this PhD thesis, we consider problems in the design and implementation of economic model predictive control (MPC) policies for two industrial applications: commercial refrigeration and power production by wind turbines. For the refrigeration systems, the goal is to enable flexible and efficient power consumption, and for the wind turbines, we aim at improving power quality and integrability to the grid. We apply economic MPC and present novel studies on modeling and problem formulations for the industrial applications, means to handle uncertainty in the control problems, and dedicated optimization routines to solve the problems in real-time. We present careful numerical simulations with validated models in realistic scenarios. Our studies reveal a potential for significant savings in operating costs and demonstrate economic MPC combined with novel computation approaches to be a top candidate methodology for handling current and future smart grid challenges.